

UC San Diego

Research Theses and Dissertations

Title

Bromination of Indoles by Vanadium Bromoperoxidase: Products, Selectivity, Mechanism, and Enzyme-Substrate Complex

Permalink

<https://escholarship.org/uc/item/18d9b9tf>

Author

Tschirret-Guth, Richard A.

Publication Date

1996

Peer reviewed

INFORMATION TO USERS

This manuscript has been reproduced from the microfilm master. UMI films the text directly from the original or copy submitted. Thus, some thesis and dissertation copies are in typewriter face, while others may be from any type of computer printer.

The quality of this reproduction is dependent upon the quality of the copy submitted. Broken or indistinct print, colored or poor quality illustrations and photographs, print bleedthrough, substandard margins, and improper alignment can adversely affect reproduction.

In the unlikely event that the author did not send UMI a complete manuscript and there are missing pages, these will be noted. Also, if unauthorized copyright material had to be removed, a note will indicate the deletion.

Oversize materials (e.g., maps, drawings, charts) are reproduced by sectioning the original, beginning at the upper left-hand corner and continuing from left to right in equal sections with small overlaps. Each original is also photographed in one exposure and is included in reduced form at the back of the book.

Photographs included in the original manuscript have been reproduced xerographically in this copy. Higher quality 6" x 9" black and white photographic prints are available for any photographs or illustrations appearing in this copy for an additional charge. Contact UMI directly to order.

UMI

A Bell & Howell Information Company
300 North Zeeb Road, Ann Arbor MI 48106-1346 USA
313/761-4700 800/521-0600

UNIVERSITY OF CALIFORNIA
Santa Barbara

**Bromination of Indoles by Vanadium Bromoperoxidase: Products,
Selectivity, Mechanism, and Enzyme-Substrate Complex.**

A dissertation submitted in the partial satisfaction of the requirements for the
degree of

Doctor in Philosophy

in

Chemistry

by

Richard André Tschirret-Guth

Committee in Charge:

Professor A. Butler, Chairperson

Professor B. Rickborn

Professor W. Kaska

Professor J.T. Gerig

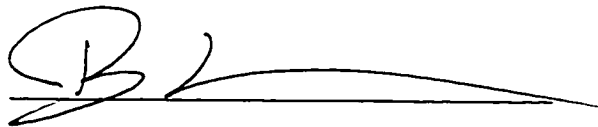
UMI Number: 9704308

UMI Microform 9704308
Copyright 1996, by UMI Company. All rights reserved.

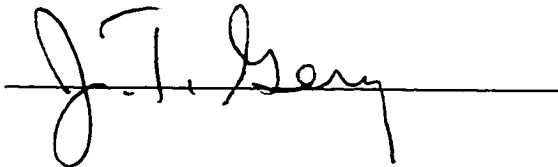
**This microform edition is protected against unauthorized
copying under Title 17, United States Code.**

UMI
300 North Zeeb Road
Ann Arbor, MI 48103

The dissertation of
Richard A. Tschirret-Guth
is approved:



William C. Kaden



John Butler

Committee Chairperson

July 1996

Curriculum Vitae

Education

Ingenieur Chimiste, Ecole Supérieure de Chimie Organique et Minérale, Paris, France, 1988.

D.E.A. Spectrochimie Organique, Université Pierre et Marie Curie, Paris VI, France, 1988.

Maitrise de Chimie, Université Pierre et Marie Curie, Paris VI, France, 1985.

Licence de Chimie, Université Pierre et Marie Curie, Paris VI, France, 1985.

DEUG A, Université Pierre et Marie Curie, Paris VI, France, 1984.

Experience

Postdoctoral Fellow. Department of Pharmaceutical Chemistry, University of California, San Francisco, January 1995 - present

Research Assistant. Department of Chemistry, University of California, Santa Barbara, July 1990 - December 1994.

Teaching Assistant, Department of Chemistry, University of California, Santa Barbara, September 1988 - June 1990.

Trainee, Centre de Recherches des Carrières, Rhône-Poulenc, St. Fons, France, October 1986 - July 1987.

Publications

Tschirret-Guth, R.A. & Butler, A. (1994) *J. Am. Chem. Soc.* 116, 411-412

Vaughn, P.M., Tschirret-Guth, R.A. & Ortiz de Montellano P.R. (1995) *Arch. Biochem. Biophys.* 319, 333-340.

Acknowledgements

I would like to thank California Sea Grant for a Traineeship, as part of projects to Dr. Alison Butler (R/MP-44 and R/MP-53), for partial support of this work.

Abstract

**Bromination of Indoles by Vanadium Bromoperoxidase: Products, Selectivity,
Mechanism, Enzyme-Substrate Complex.**

by

Richard A. Tschirret-Guth

The reactivity of a series of simple substituted indoles in the bromination catalyzed by vanadium bromoperoxidase (V-BrPO) was investigated, and the results were interpreted on the basis of the binding of the substrate to, or near to the active site of the enzyme.

In the presence of bromide and hydrogen peroxide, V-BrPO catalyzed the bromination and the oxidation of simple substituted indoles. The products formed were in agreement with initial attack of the C2-C3 double bond by an oxidized bromine species, and no reaction on the benzene ring was observed. The rearrangement of the bromonium intermediate and the formation of the final products depended of the nature of the substituent. In general, 2-substituted indoles yielded the 3-bromo product whereas the 3-substituted indoles gave the 3-oxo derivative. When indole was used as a substrate, 3-bromoindole, oxindole and indigo were the main products formed. The mechanism of indigo formation was investigated in further details and it was found to occur *via* oxidative coupling of 3-bromoindole and indoxyl and did not require molecular oxygen.

Kinetic studies showed that V-BrPO reacted with indoles preferentially over many others substrates, including monochlorodimedone, phenol red, and

oxidation of a second equivalent of hydrogen peroxide. The reactivity of V-BrPO differed greatly with the reactivity observed for HOBr and strongly suggested binding of indoles to V-BrPO.

The fluorescence of 2-phenylindole was quenched by V-BrPO with a quenching constant (in 100 mM Tris buffer at pH 8.3 and 21 °C) of $1.1 \times 10^5 \text{ M}^{-1}$. The quenching was not consistent with dynamic interactions and was therefore interpreted as being due to static interactions (binding) between 2-phenylindole and V-BrPO. Labeling of V-BrPO with photoreactive 5-azidoindoles resulted in highly specific insertion of the probes in the enzyme and confirmed that indoles bind to V-BrPO.

Table of Contents

	Page
Acknowledgements	iii
Curriculum Vitae	iv
Abstract	v
Table of Content	vii
List of Tables	xi
List of Figures	xii
Abbreviations	xvii
Chapter 1: Introduction	1
Chapter 2: Bromination of Indoles by V-BrPO	17
Introduction	17
Materials and Methods	22
Materials	22
Isolation and Characterization of Products from Enzymatic Reactions	23
Indole	23
1-Methylindole	23
2-Methylindole	26
3-Methylindole	26
1,2-Dimethylindole	27
2-Phenylindole	27
3-Phenylindole	28
3- <i>tert</i> -Butylindole	30
1,3-Di- <i>tert</i> -butylindole	30
Results	31
Bromination of Indole by V-BrPO	31
pH Effect on the Product Selectivity of the Bromination of Indole by V-BrPO and by HOBr	35
Bromination of 3-Bromindole and Oxindole by V-BrPO	37
Bromination of 1-Methylindole by V-BrPO	38
Bromination of 2-Methylindole by V-BrPO	45
Bromination of 3-Methylindole by V-BrPO	47
Bromination of 1,2-Dimethylindole by V-BrPO	49
Bromination of 2-Phenylindole by V-BrPO	50

Bromination of 3-Phenylindole by V-BrPO	52
Bromination of 2- <i>tert</i> -Butylindole by V-BrPO	54
Bromination of 3- <i>tert</i> -Butylindole by V-BrPO	57
Bromination of 1,3-di- <i>tert</i> -Butylindole by V-BrPO	58
Oxidation of Indole and 3-Methylindole by V-BrPO using H ₂ ¹⁸ O ₂	59
Discussion	61
 Chapter 3: Oxidative Coupling of Indole to Indigo by V-BrPO	 69
Introduction	69
Materials and Methods	76
Materials	76
Oxidation of Indole to Indigo by V-BrPO	76
Oxidation of Indoxyl to Indigo by V-BrPO	76
Results	76
Oxidation of Indole to Indigo as a Function of V-BrPO Concentration	78
Influence of Dissolved Dioxygen on the Yield of Indigo	80
Formation of Indigo as a Function of H ₂ O ₂ Concentration	82
Yield of Indigo as a Function of Indole Concentration	85
Oxidation of Indoxyl to Indigo by V-BrPO	86
Indoxyl Concentration dependence on the Oxidation of Indoxyl to Indigo	88
Oxidation of Indoxyl to Indigo by Dioxygen Generating Systems	91
Oxidative Coupling of Indoxyl and 3-Bromoindole to Indigo	92
Discussion	93
 Chapter 4: Substrate Specificity and Reaction Mechanism	 101
Introduction	101
Materials and Methods	104
Materials	104
Hypobromite Solutions	104
Substrate Specificity	104
Dioxygen Measurements	105
Substituent Effect on the Rate of Bromination of Indoles	105
Experimental Reproducibility and Error	105
Results	106
Substrate Specificity	106
Comparison of the Substrate Specificity of V-BrPO	106

and HOBr	108
Comparison of the Rates of Dioxygen Evolution in the Presence of Indoles during Enzymatic and HOBr reactions	110
Effect of $[H_2O_2]$ on K_{app}	114
Effect of $[V-BrPO]$ on K_{app}	115
Substrate Concentration Dependence of the Rate of Bromination of 3-Methylindole	118
$[H_2O_2]$ Dependence on the Rate of Bromination of 3-Methylindole	119
Substituent Effect on the Rate of Bromination	120
Inhibition of V-BrPO by Organic Compounds	123
Discussion	127
Appendix to Chapter 4	132
 Chapter 5: Quenching of the Fluorescence of 2-Phenylindole by V-BrPO	136
Introduction	136
Materials and Methods	142
Materials	142
Fluorescence Measurements	142
Results	143
Quenching of the Fluorescence of 2-Phenylindole by V-BrPO	143
Quenching of the Fluorescence of 2-Phenylindole by Apo-BrPO and Heat-Denatured V-BrPO	148
Viscosity and Temperature Dependence	150
Buffer and pH Dependence	153
Discussion	155
 Chapter 6: Photoaffinity Labeling of V-BrPO with Azidoindoles	159
Introduction	159
Materials and Methods	162
Materials	162
Synthesis of 5-Azido-2-Phenylindole	162
Synthesis of $[^3H]$ 5-Azido-1,2-Dimethylindole	164
Photolysis Experiments	165
Labeling of V-BrPO with $[^3H]$ 5-Azido-1,2-Dimethylindole	165
In-Gel Tryptic Digestion of V-BrPO	166
Tryptic Digestion of V-BrPO	166

	CNBr cleavage of V-BrPO	167
Results		168
	Synthesis and Properties of 5-Azido-2-Phenylindole	168
	HPLC separation of Tryptic Peptides of 5-Azido- 2-Phenylindole-Labeled V-BrPO	171
	Synthesis of [³ H] 5-Azido-1,2-Dimethylindole	173
	Photolysis of [³ H] 5-Azido-1,2-Dimethylindole	175
	Photoaffinity Labeling of V-BrPO with [³ H] 5-Azido-1,2-Dimethylindole	176
	HPLC Separation of CNBr and Tryptic Peptides from V-BrPO Labeled with [³ H] 5-Azido-1,2-Dimethylindole	177
Discussion		181
Appendix		185
References		214

List of Tables

	Page
Table 1.1: Production of Volatile Halogenated Organic Compounds by <i>A. nodosum</i>	14
Table 3.1: Influence of Dissolved O ₂ on the Yield of Indigo	81
Table 3.2: Amount of H ₂ O ₂ Necessary to Carry the Reaction of indole with V-BrPO to Completion	84
Table 3.3: Effect of [Indole] on the Formation of 3-Bromo-indole and Indigo	83
Table 3.4: Effect of [Indoxyl] on the Formation of Indigo	89
Table 3.5: Oxidation of Indoxyl to Indigo using Different Sources of O ₂ .	90
Table 3.6: Formation of Indigo from Indoxyl and/or 3-Bromoindole by V-BrPO	92
Table 4.1: Substrate Specificity of V-BrPO	107
Table 4.2: Variation of K_{app} for 3-Methylindole as a Function of the Rate of HOBr Addition	117
Table 4.3: Rate of Bromination of Substituted Indoles by V-BrPO	121
Table 4.4: Inhibition of O ₂ Production by V-BrPO	123
Table 5.1: Temperature Dependence of the Quenching of the Fluorescence of 2-Phenylindole by V-BrPO	152
Table 5.2: Effect of the Nature of the Buffer on the Quenching of the Fluorescence of 2-Phenylindole by V-BrPO	154
Table 6.1: Percentage of Deuteration as Determined by ¹ H NMR for Each Step of the Synthesis of [² H] 5-Azido-1,2-Dimethylindole	174

List of Figures

	Page
Fig. 1.1: The proposed coordination of vanadium in the active site of V-BrPO from EXAFS	4
Fig. 1.2: General reactivity of V-BrPO with bromide	6
Fig. 1.3: Lewis acid mechanism for the catalytic cycle of V-BrPO	10
Fig. 1.4: Proposed scheme for the biosynthesis of volatile organic compounds from <i>A. nodosum</i> by V-BrPO	13
Fig 1.5: Schematic view of the channel leading to the vanadium binding site of V-CIPO from <i>C. inaequalis</i> .	16
Fig. 2.1: UV/Vis spectra of the bromination of indole by V-BrPO	31
Fig. 2.2: HPLC chromatogram of the bromination of indole by V-BrPO	32
Fig. 2.3: 500 MHz ¹ H NMR spectrum of product 20	35
Fig. 2.4: Effect of the pH on the final product composition of the bromination of indole by V-BrPO	36
Fig. 2.5: Effect of the pH on the final product composition of the reaction of aqueous bromine with indole	37
Fig. 2.6: HPLC chromatograms of the bromination of 1-methylindole by V-BrPO and HOBr	39
Fig. 2.7: ¹ H NMR of a) 1,3-dihydro-1-methyl-3,3-di-(1-methyl-1 <i>H</i> -indol-3-yl)-2 <i>H</i> -indol-2-one (30) and b) 1,2-dihydro-1-methyl-3,3-di-(1-methyl-1 <i>H</i> -indol-3-yl)-3 <i>H</i> -indol-3-one (31)	45
Fig. 2.8: HPLC chromatograms of the bromination of 2-methylindole by V-BrPO and HOBr	46

Fig. 2.9: HPLC chromatograms of the bromination of 3-methylindole by V-BrPO and HOBr	48
Fig. 2.10: HPLC chromatograms of the bromination of 1,2-dimethylindole by V-BrPO and HOBr	50
Fig. 2.11: HPLC chromatograms of the bromination of 2-phenylindole by V-BrPO and HOBr	51
Fig. 2.12: HPLC chromatograms of the bromination of 3-phenylindole by V-BrPO and HOBr	53
Fig. 2.13: HPLC chromatograms of the bromination of 2- <i>tert</i> -butylindole by V-BrPO and HOBr	56
Fig. 2.14: HPLC chromatograms of the bromination of 3- <i>tert</i> -butylindole by V-BrPO and HOBr	57
Fig. 2.15a: EIMS spectrum of indigo (15) isolated from incubation of indole (14) with V-BrPO and ¹⁸ O enriched hydrogen peroxide	59
Fig. 2.15b: EIMS spectrum of 3-methyloxindole (34) isolated from incubation of 3-methylindole (33) with V-BrPO and ¹⁸ O enriched hydrogen peroxide	60
Fig. 3.1: Oxidation of indole to indigo as function of V-BrPO concentration	78
Fig. 3.2: Rate of formation of indigo as a function of V-BrPO concentration	79
Fig. 3.3: Effect of V-BrPO concentration on the final yield of indigo from indole	80
Fig. 3.4: Composition in indole, indigo and dioxygen during the course of the oxidation of indole by V-BrPO	81
Fig. 3.5A: Final composition of reaction of indole with V-BrPO as a function of the ratio [H ₂ O ₂]/[indole] in air saturated buffer	82
Fig. 3.5B: Final composition of reaction of indole with V-BrPO as a	

function of the ratio $[H_2O_2]/[indole]$ in buffer sparged with N_2	83
Fig. 3.6: V-BrPO concentration dependence of the formation of indigo from indoxyl	86
Fig. 3.7: V-BrPO dependence of the maximum rate of V-BrPO-catalyzed oxidation of indoxyl to indigo	87
Fig. 3.8: Effect of V-BrPO concentration on the final yield of indigo from indoxyl	88
Fig. 3.9: Dependence of indoxyl concentration on the uncatalyzed and V-BrPO-catalyzed rates of oxidation of indoxyl to indigo	90
Fig. 4.1: Effect of phenol red and 2-methylindole on the bromination of MCD by V-BrPO	106
Fig. 4.2: Time course of the bromination of phenol red by V-BrPO as a function of 2-methylindole concentration	109
Fig. 4.3: Bromination of phenol red by HOBr as a function of 2-methylindole concentration	110
Fig. 4.4: Dioxygen formation in the presence of 2-methylindole	111
Fig. 4.5: Dioxygen formation in the presence of 3-methylindole	112
Fig. 4.6: Disproportionation of H_2O_2 by HOBr in the presence of 3-methylindole	113
Fig. 4.7: Normalized rates of dioxygen formation by V-BrPO in the presence of 3-methylindole as a function of H_2O_2 concentration	114
Fig. 4.8: Plot of $1/K_{app}$ versus $[H_2O_2]$	115
Fig. 4.9: Normalized rates of dioxygen formation by V-BrPO in the presence of 3-methylindole as a function of V-BrPO concentration	116
Fig. 4.10: Plot of K_{app} versus $[V-BrPO]$	117

Fig. 4.11: Effect of 3-methylindole concentration on the initial rate of 3-methylindole bromination by V-BrPO	118
Fig. 4.12: Effect of H ₂ O ₂ concentration on the initial rate of 3-methylindole bromination by V-BrPO	119
Fig. 4.13: Bromination of substituted indoles by V-BrPO	120
Fig. 4.14: Comparison of the reactivity of V-BrPO with 2- <i>tert</i> -butylindole and 3- <i>tert</i> -butylindole	122
Fig. 4.15: Inhibition of dioxygen formation by benzofuran	124
Fig. 4.16: Effect of benzofuran on the rate of dioxygen formation in the presence of 3-methylindole	125
Fig. 4.17: General reaction mechanisms for the reaction of V-BrPO with indoles	129
Fig. 5.1: Fluorescence of spectrum 2-phenylindole in the absence and presence of V-BrPO	143
Fig. 5.2: Quenching of the fluorescence of 2-phenylindole by V-BrPO and BSA	144
Fig. 5.3: Stern-volmer and modified stern-volmer plots of the quenching of the fluorescence of 2-phenylindole by V-BrPO	145
Fig. 5.4: Quenching of the fluorescence of 2-phenylindole by apo- and heat-denatured V-BrPO	148
Fig. 5.5: Quenching of the fluorescence of 2-phenylindole by V-BrPO as a function of isopropanol concentration	150
Fig. 5.6: Plot of <i>V</i> versus viscosity	151
Fig. 5.7: Plot of <i>V</i> versus pH	153
Fig. 6.1: Fluorescence emission spectrum of 5-azido-2-phenylindole	169

Fig. 6.2: Effect of the irradiation time on the absorption spectrum of 5-azido-2-phenylindole	170
Fig. 6.3: C-18 HPLC profile of the tryptic digests of V-BrPO and V-BrPO following labeling with 5-azido-2-phenylindole	172
Fig. 6.4: ¹ H NMR of [² H] 1,2-dimethylindole	174
Fig. 6.5: Effect of the irradiation time on the absorption spectrum of [³ H] 5-azido-1,2-dimethylindole	175
Fig. 6.6: Absorbance of [³ H] 5-azido-1,2-dimethylindole at 248 nm as a function of duration of photolysis	176
Fig. 6.7: DEAE purification of V-BrPO labeled with [³ H] 5-azido-1,2-dimethylindole	177
Fig. 6.8: C-4 HPLC profile of cyanogen bromide peptides of V-BrPO labeled with [³ H] 5-azido-1,2-dimethylindole	179
Fig. 6.9: C-18 profile of tryptic peptides of V-BrPO labeled with [³ H] 5-azido-1,2-dimethylindole	180
Fig 6.10: Schematic view of the channel leading to the vanadium binding site of V-CIPO from <i>C. inaequalis</i> with the photoactivated 5-azido-2-phenylindole bound to the hydrophobic surface of the channel.	183

Abbreviations

BCA - bicinchoninic acid
BSA - bovine serum albumin
CIPO - chloroperoxidase
ESR - electron spin resonance
EXAFS - extended x-ray absorption fine structure
FeHemeCIPO - Iron heme chloroperoxidase
HPLC - high performance liquid chromatography
IR - infra red spectrophotometry
MCD - monochlorodimedone (5,5-dimethyl-2-chloro-1,3-cyclohexadione)
MES - 2-(N-morpholino)-ethane-sulfonic acid
EIMS - electron impact mass spectrometry
NMR - nuclear magnetic resonance
rel int - relative intensity
SDS-PAGE - sodium dodecylsulfate polyacrylamide gel electrophoresis
Tris - tris(hydroxymethyl)-aminomethane
V-BrPO - vanadium bromoperoxidase
V-CIPO - vanadium chloroperoxidase

Chapter 1

Introduction

Scope of the Dissertation

The vanadium-containing haloperoxidase¹ (V-BrPO) from *Ascophyllum nodosum* belongs to a new class of non-heme haloperoxidases mainly found in marine seaweed (Butler, 1993; Butler & Walker, 1993). Although the exact role of these enzymes has yet to be unambiguously determined, it has been suggested that they are involved in the biosynthesis of halometabolites, including the halogenated indoles. The goal of this dissertation was to investigate the reaction of V-BrPO with simple substituted indoles. A general background on V-BrPO is presented in Chapter 1. Chapter 2 and 3 give an overview of the products formed from these reactions. Kinetic aspects of these reactions were also examined and the results are presented in Chapter 4. Finally, the binding of indoles to V-BrPO was studied using fluorescence quenching (Chapter 5) and photoaffinity labeling (Chapter 6).

¹ Haloperoxidases are the subgroup of peroxidases that catalyze the oxidations of halide ions by hydrogen peroxide. They are generally named after the most electronegative halide they can oxidize: Chloroperoxidases (ClPO) can oxidize chloride, bromide, and iodide, bromo-peroxidases (BrPO) oxidize bromide and iodide, and iodoperoxidases (IPO) oxidize only iodide.

Background

V-BrPO was first discovered by Vilter and co-workers (Vilter et al., 1983) while they were looking for peroxidase activity in Phaeophyceae (brown algae). The enzyme was found to catalyze the oxidation of iodide by H_2O_2 , the iodide dependant peroxidation of o-dianisidine (Vilter et al., 1983), and the peroxidative bromination of monochlorodimedone (MCD) (Vilter, 1983a). Unlike all haloperoxidases previously isolated, this enzyme did not present any Soret absorption band typical of heme-containing proteins (Vilter, 1983b). Furthermore, it was completely deactivated when dialyzed against EDTA in phosphate buffer at pH 3.8 and could only be reactivated by addition of vanadium(V). All other metals used (including Mo^{VI} , Fe^{II} , Fe^{III} and Cr^{VI}) did not restore more than 13 % of the activity (Vilter, 1984). It was subsequently shown that the native protein contained vanadium (de Boer et al., 1986). Thus, it was evident that this was a non-heme, vanadium dependent bromoperoxidase.

V-BrPO is an acidic ($pI = 4$) glycoprotein (Krenn et al., 1989). Its molecular weight was first reported, based on gel-exclusion HPLC, to be 90 kDa (Vilter, 1983; de Boer et al., 1986). It was reported later that, under non-reducing SDS-PAGE, the observed molecular weight was 97 kDa (Krenn, et al., 1989), while under reducing conditions, SDS-PAGE indicated a molecular weight of 67 kDa (Everett, 1990; Wever et al., 1988a). Ultracentrifugation experiments showed that V-BrPO had a molecular weight of 97 kDa and a sedimentation

coefficient of 6.96 S that is unusually high for a protein of this mass, suggesting that V-BrPO is a very compact molecule (Tromp et al., 1990).

V-BrPO contains 16 cysteine residues that all participate in the formation of disulfide bridges (Tromp et al., 1990). The circular dichroism spectrum in the far ultraviolet region at pH 7.5 in 10 mM phosphate buffer showed typical bands for a helical protein. The data were consistent with a structure consisting of 74 % α -helix, 26 % random coil and no β -sheet (Tromp et al., 1990). The content and nature of the sugars attached to V-BrPO have not yet been determined. The amino acid sequence and the three-dimensional structure of V-BrPO have not yet been resolved.

Two different isoenzymes of V-BrPO have been isolated from *A. nodosum*. The locations of those two different enzymes were determined by activity staining of cross-sections of algal parts. The most abundant one (V-BrPO I) was located inside the thallus, particularly around the conceptacles (fruiting bodies) of the alga (Krenn et al., 1989). The other one (V-BrPO II) was found on the surface of the thallus, and could be extracted by simply washing the alga with the extraction buffer (Krenn et al., 1989). Both enzymes have similar specific activities, isoelectric points, amino acid analysis and antigenic response but have different carbohydrate compositions, and could be separated based on their affinity for Concanavalin A (ConA). Only V-BrPO II was retained on ConA, whereas V-BrPO I eluted in the void volume (Krenn, et al., 1989; Everett, 1990). V-BrPO II had a slightly higher molecular weight (67 kDa) than V-BrPO I (65 kDa), as determined by SDS-PAGE.

As isolated, V-BrPO contains about 0.4 mole of vanadium per mole of enzyme (de Boer et al., 1988). By incubating V-BrPO with excess vanadate in 0.1 M Tris buffer pH 8.3, the ratio of vanadium to enzyme can be increased to 1, with a concomitant increase of activity (Vilter, 1984). The dissociation constant of the protein-vanadium complex was 55 nM (at pH 8.5) and rapidly increased at lower pH (Tromp et al., 1990). This value reasonably corresponds with the concentration of vanadium in seawater, 20-35 nM (Collier, 1984) and explains why V-BrPO, as isolated, does not contain equimolar amounts of vanadium. The data indicated that the binding of vanadate is prevented by the protonation of a group with a pKa higher than 8.5 (Tromp et al., 1990). The active-site vanadium can be removed by incubating V-BrPO in 0.1 M phosphate-citrate buffer pH 3.8 containing EDTA to form the apoenzyme (apo-BrPO) (Vilter, 1984). It was also determined that phosphate is necessary and sufficient in order to efficiently remove the vanadium (Soedjak, 1991; Soedjak & Butler, 1991). Phosphate is a structural analog of vanadate and probably competes with vanadium on the active site of the enzyme. However, inactivation can be protected by H₂O₂ (Soedjak et al., 1991). Reconstitution of the native enzyme from apo-BrPO and vanadate was also inhibited by phosphate (de Boer et al., 1986a; Tromp et al., 1990), arsenate (Tromp et al., 1990) and molybdate (de Boer et al., 1988a) with inhibition constants of 60, 120 and 98 μM, respectively, and by the metallofluoric compounds AlF₄⁻ and BeF₄²⁻ (Tromp et al., 1991).

The structure of the active site is still not unambiguously known. From extended X-ray absorption fine structures (EXAFS) and X-ray absorption near-edge structure (XANES) spectra analysis the vanadium site is believed to be a distorted octahedron coordinated by a single oxide ligand at 1.61 Å, three unknown light-atom donors at 2.11 Å and two nitrogen donors, possibly from two histidines residues, at 2.11 Å (Figure 1.1) (Hormes et al., 1988; Arber et al., 1989). Those results are confirmed by EPR spectroscopy of the reduced enzyme²

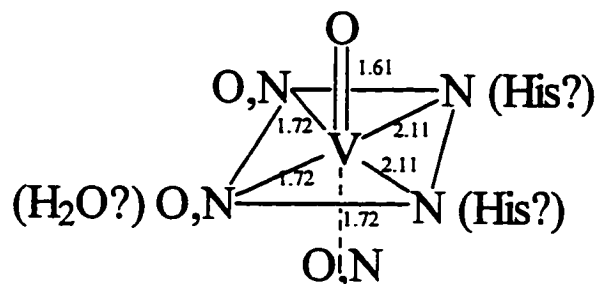


Figure 1.1: The proposed coordination of vanadium in the active site of V-BrPO from EXAFS (Butler & Walker, 1993).

(de Boer et al., 1986a,b). The EPR data suggested that in the reduced enzyme the vanadium ion is in a ligand field containing 6 to 8 oxygen and/or nitrogen donor atoms, including an axial terminal ligand (de Boer et al., 1988a) and a molecule of water. The EPR signal was pH dependant and indicated the involvement of a functional group with an apparent pKa of 5.4. It is suggested that protonation of a histidine or aspartate/glutamate residue near the metal is involved. The presence of nitrogen atoms in the equatorial plane of the vanadyl cation was further

² The vanadium in native V-BrPO is in the +5 oxidation state and is therefore EPR silent. Reduction with dithionite produces V(IV)O-BrPO that is paramagnetic.

confirmed by comparison of the electron spin echo envelope modulation (ESEEM) spectra of the reduced enzyme to those of a number of model compounds (de Boer et al., 1988b). EPR studies of other oxo-vanadium (IV)-imidazole model compounds also suggested that in the reduced enzyme the vanadium is coordinated by at least one imidazole-type nitrogen donor (Calviou et al., 1989).

Reactivity. V-BrPO catalyzes peroxidative halogenation reactions (Vilter, 1984; Wever et al., 1985) and the halide-dependant disproportionation of hydrogen peroxide (Everett & Butler, 1989; Soedjak & Butler, 1990) (Figure 1.2). The first step of those reactions is the formation from hydrogen peroxide and a halogen ion of a two-electron-oxidized halogen species intermediate ("Br⁺"). This

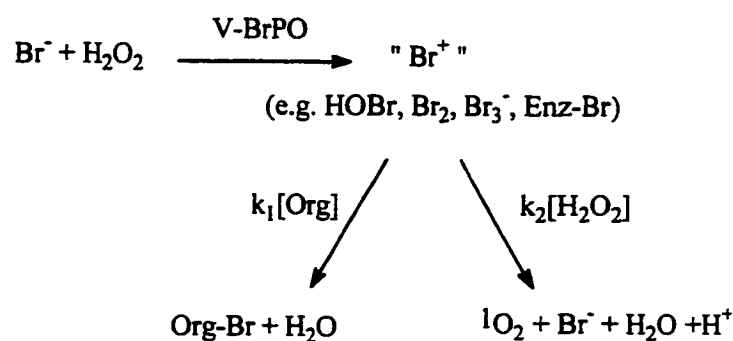


Figure 1.2: General reactivity of V-BrPO with bromide.

intermediate can subsequently halogenate a suitable organic substrate or, in the absence of such a substrate, react with a second molecule of hydrogen peroxide to form dioxygen (Everett & Butler, 1989). When bromide is used, the dioxygen formed is in the singlet excited state ($^1\text{O}_2$, $^1\Delta_g$) as detected by the characteristic

near infrared emission at 1268 nm (Everett et al., 1990a). Contrary to FeHeme-CIPO and other haloperoxidases, V-BrPO is not deactivated by the singlet oxygen formed, even after multiple turnovers. It has also been established that the oxygen atoms in the dioxygen formed during the bromide-assisted disproportionation of hydrogen peroxide come from the same molecule of hydrogen peroxide (Soedjak et al., 1995), consistent with $^1\text{O}_2$ production.

V-BrPO can also use acyl peroxides (i.e. peracetic acid, *m*-chloroperbenzoic acid) instead of hydrogen peroxide to catalyze the bromination of a variety of organic substrates (Soedjak & Butler, 1990). In the absence of an organic substrate no dioxygen is formed since oxidized bromine species are unable to oxidize acyl peroxide in the time frame of the enzymatic reaction. V-BrPO does not use alkyl peroxide as oxidizing agents due, probably, to their inability to bind to the active site of the enzyme.

The specific activity³ of V-BrPO from *A. nodosum* is 170-360 U/mg (1 U = 1 μmole of MCD/min) under standard assay conditions: 0.1 M phosphate buffer pH 6.5, 0.1 M Br^- , 2 mM H_2O_2 , 50 μM MCD and 0.2 M Na_2SO_4 . In the absence of MCD, the activity of V-BrPO can also be determined by monitoring the formation of dioxygen. It was found that the rate of MCD bromination and the rate of disproportionation of hydrogen peroxide in absence of an organic substrate are the same, supporting the proposed mechanism in which the same reactive intermediate (" Br^+ ") is common to both reactions and is formed in a rate limiting

³Haloperoxidases are generally assayed by following the halogenation at the 2 position of monochlorodimedone (MCD, 2-chloro-1,3-dimedone) spectrophotometrically at 290 nm, which monitors the loss of the enol form of MCD ($\Delta\epsilon = 20,000 \text{ M}^{-1}\text{cm}^{-1}$).

step (Everett & Butler, 1989). Furthermore, the sum of $k_1[\text{MCD}]$ and $k_2[\text{H}_2\text{O}_2]$ in the presence of MCD is equal to $k_2[\text{H}_2\text{O}_2]$ in the absence of MCD, indicating that $k_1[\text{MCD}]$ is competitive with $k_2[\text{H}_2\text{O}_2]$ (Soedjak et al., 1995).

Extensive steady-state analysis of the bromination of MCD and the dioxygen formation catalyzed by V-BrPO have shown that the formation of the reactive intermediate from hydrogen peroxide and bromide follows a bi-bi ping-pong type mechanism (Everett et al., 1990b; de Boer & Wever, 1988c). At pH 5.25 the K_m for hydrogen peroxide and bromide were 284 μM and 10.5 mM, respectively (Everett et al. 1990b). It is not clear from the kinetic data which substrate is binding first. However, the binding of H_2O_2 was observed by optical spectroscopy: The near ultraviolet and visible spectrum of V-BrPO contains a protein peak at 280 nm, and a shoulder at 315 nm (that is absent in the apoenzyme). Upon addition of hydrogen peroxide a decrease in absorption from 300 nm to 340 nm is observed. When bromide is added to the reaction mixture, the original spectrum returns and the native enzyme is recovered (Tromp et al., 1990), showing that hydrogen peroxide could be binding first to the enzyme, followed by bromide. A pH study showed that V-BrPO must first be deprotonated before binding of hydrogen peroxide (de Boer & Wever, 1988c). The functional group controlling the binding of hydrogen peroxide has a pKa of 5.7 and, in agreement with the results obtained using EPR spectroscopy (see above), was ascribed to be a histidine residue.

V-BrPO is inhibited by hydrogen peroxide, bromide, chloride, fluoride and azide. The inhibition of V-BrPO by hydrogen peroxide is noncompetitive with

respect to bromide and increases with increasing pH (Soedjak et al., 1995). The data showed that an ionizable group with a pKa between 6.5 and 7 is involved in the inhibition. Inhibition by bromide was first reported as competitive (de Boer & Wever, 1988). It was later shown that bromide inhibition is noncompetitive and pH dependent with a maximum at pH 5-5.5 (Everett et al., 1990b). Chloride was found to be a competitive inhibitor with respect to bromide (Soedjak, 1991). Inhibition of V-BrPO by fluoride is reversible and competitive with respect to hydrogen peroxide and uncompetitive with respect to bromide (Everett et al., 1990b). V-BrPO was inhibited by azide by a mechanism-based inactivation which irreversibly deactivated the enzyme (Everett, 1990; Soedjak, 1991). Inactivation occurs only in the presence of hydrogen peroxide and azide, and is protected by the presence of bromide and thiocyanate.

As for the heme-containing chloroperoxidase from *C. fumago* (FeHeme-CIPO), the exact nature of the halogenating intermediate in V-BrPO-catalyzed halogenation reactions (Figure 1.2 is a topic of much interest and speculation. The main controversy relies on whether the oxidized bromine intermediate is enzyme bound or freely diffusible. Under conditions that reduce the reaction of HOBr/Br₂/Br₃⁻ with H₂O₂ to form dioxygen (pH 5, 300 μM H₂O₂, 100 mM Br⁻) (Kanofsky, 1984) the formation of Br₃⁻ was observed during the initial portion of the reaction (de Boer & Wever, 1988). Under identical conditions, the rate of production of the oxidized bromine species was equal to the rate of bromination of MCD. The authors also compared the rate of bromination of MCD, 5-phenylbarbituric acid, 2-thiouracil and *trans*-4-hydroxycinnamic acid, and found

them to be equal. It was then suggested that the reactive intermediate in V-BrPO catalyzed reactions was free $\text{HOBr}/\text{Br}_2/\text{Br}_3^-$. However, it can be argued that the conditions used to detect tribromide (i.e. low pH, low H_2O_2 , and high Br^-) favored its formation, and did not correspond to physiological conditions. In addition the organic compounds used as substrates are probably not the natural substrate(s) and the identical rates of bromination observed may only indicate that in all cases the rate limiting step was the formation of the brominating intermediate.

It was found recently that V-BrPO is also able to catalyze chlorination reactions and chloride assisted disproportionation of hydrogen peroxide (Soedjak & Butler, 1990). The reactivity of V-BrPO with chloride was not detected earlier because of a very low specific activity (0.46 U/mg) and a fairly high K_m for chloride (344 mM at pH 5).

The absence of an EPR signal in the resting state of V-BrPO established that the active-site-vanadium was in the +5 oxidation state. No EPR signals were produced upon addition of bromide or incubation with hydrogen peroxide or under turnover conditions. However, upon reduction of the vanadium in V-BrPO by dithionite, the enzyme is deactivated and produces an EPR signal consistent with formation of a vanadium (IV) derivative ligated to the enzyme as a vanadyl cation (VO^{2+}) (de Boer et al., 1986a,b). Since no change in the oxidation state of the vanadium (V) in the active site has been detected during turnover, it has been suggested that vanadium could act as a Lewis acid catalyst and be used only as a binding site for hydrogen peroxide and bromide (Figure 1.3) (Butler &

Walker, 1993). Although less likely, the vanadium could also be used as an electron transfer catalyst, cycling between V(V) and V(III).

Stability. V-BrPO is a unusually stable enzyme. It is not deactivated after several

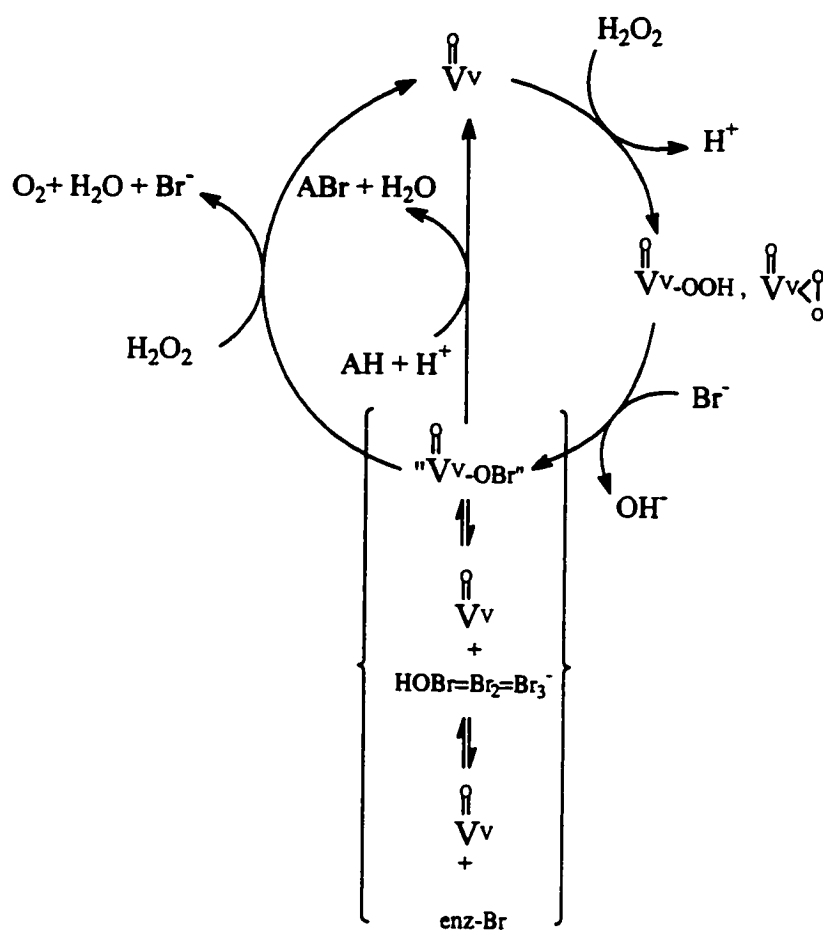


Figure 1.3: Lewis acid mechanism for the catalytic cycle of V-BrPO.

hours at 50 °C, and its T_m (the midpoint of the thermal denaturation curve) is 72 °C (Wever et al., 1985; Tromp et al. 1990). V-BrPO was not fully denatured when incubated in 4 M guanidine hydrochloride, and its secondary structure was

not affected upon incubation with 4 % sodium dodecyl sulphate (Tromp et al., 1990). As mentioned above, V-BrPO is not deactivated by oxidized bromine species or singlet oxygen and retains full activity for weeks under turnover conditions (de Boer et al., 1987; Everett et al., 1990a). V-BrPO is also exceptionally stable in several organic solvents: The enzyme did not lose its activity upon incubation in 60 % acetone, 60 % ethanol, 60 % methanol or a mixture of 47 % butanol and 40 % ethanol in water for more than one month (de Boer et al., 1987a,b). Such a stability greatly enhances the applicability of V-BrPO for organic synthesis.

Biological function. The role of V-BrPO in *A. nodosum* has not been determined yet. Based on the observation that phloroglucinol (1,3,5-tri-hydroxyphenol), a compound found in abundance in *A. nodosum*, reversibly inhibits the bromination of MCD (Butler et al., 1990), it has been suggested that V-BrPO is involved in the polymerization of phloroglucinol to phlorotannins. Those tannins may be produced to protect the alga against herbivorous predation (Geiselman & MacConnell, 1981). On the other hand, it has been well documented that *A. nodosum* produces large quantities of volatile halogenated organic compounds (Table 1.1). Those compounds could originate from halogenation of β -ketoacids by V-BrPO followed by non-enzymatic hydrolysis (Figure 1.4). This hypothesis has already been tested using a bromoperoxidase isolated from a red marine alga producing similar halogenated compounds, *Bonnemaisonia hamifera*, and 3-ketooctanoic acid as a substrate (Theiller et al., 1978). The main products were identified as tribromomethane, dibromomethane and 1-bromopentane. From a

similar experiment carried with a bromoperoxidase from the green alga *Penicillus capitatus*, tribromomethane, 1-bromo-2-heptanone, 1,1-dibromo-2-heptanone and 1,1,1-tribromo-2-heptanone were isolated as the main products (Beissner et al., 1981).

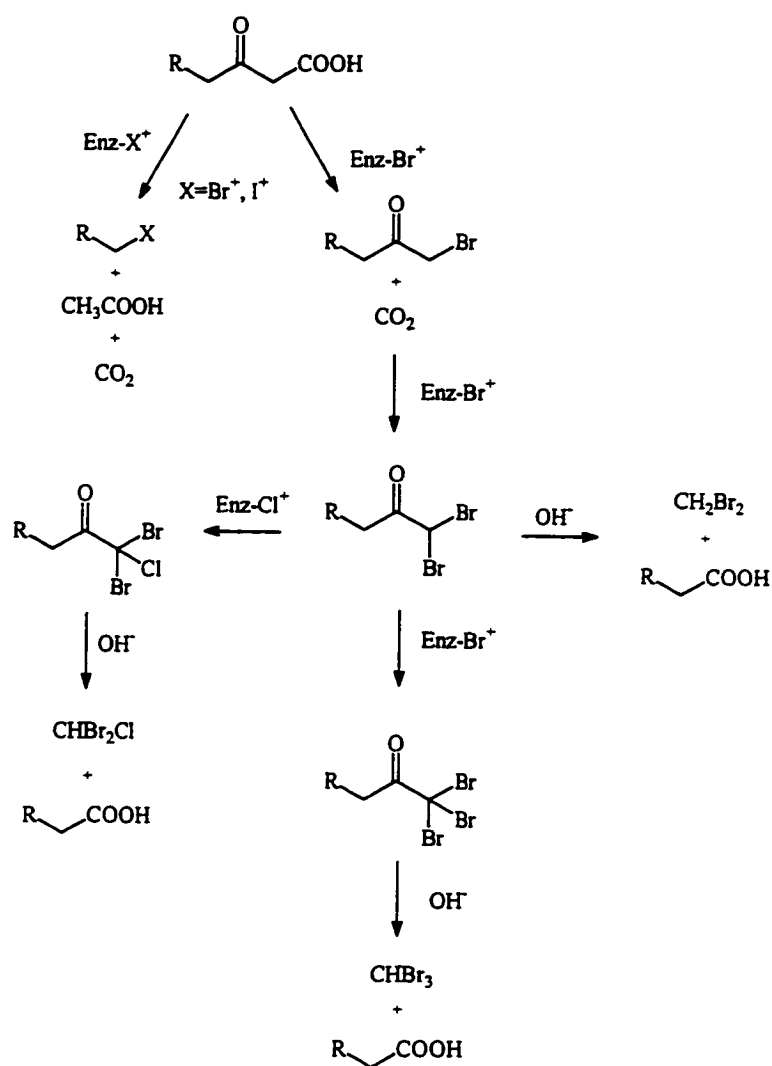


Figure 1.4: Proposed scheme for biosynthesis of volatile halogenated organic compounds of *A. nodosum* by V-BrPO (adapted from Theiller et al., 1978 and Beissner et al., 1981).

Table 1.1: Production of volatile halogenated organic compounds by *A. nodosum*.

	Mean composition ^a	Mean rate of release ^b
Isopropyl bromide	12	-
1-bromopropane	7	-
Methyl iodide	n.d.	-
Ethyl iodide	18	-
Isopropyl iodide	25	-
1-iodopropane	240	-
1-iodobutane	3	-
1-iodopentane	25	-
1-iodohexane	11	-
CH ₂ Br ₂	18	680
CHBrCl ₂	7	-
CHBr ₂ Cl	280	1,100
CH ₂ I ₂	4	-
CHBr ₃	520	4,500
CHBr ₂ I	2	-

^a(Gschwend et al., 1985; Newman & Gschwend, 1987). ^b(Gschwend et al., 1985)

Since the discovery of V-BrPO from *A. nodosum*, many new non-heme, vanadium-containing haloperoxidases have been reported (Butler, 1993), all but one having been isolated from marine sources (Butler & Walker, 1993). Although it appears that in most cases they have similar molecular masses, amino acid composition and EPR signals (which indicate that the vanadium is identically ligated in the protein) (Wever & Krenn, 1990), they differ largely in reactivity. For instance, V-BrPO from *A. nodosum* and V-BrPO from *Fucus distichus* have brominating specific activities of 1730 U/mg and 1500 U/mg and K_m for bromide of 10.5 mM and 0.90 mM, respectively (Soedjak & Butler, 1991). Also, V-BrPO from *A. nodosum* and V-ClPO from *Curvularia inaequalis* have chlorinating specific activities of 0.46 U/mg and 7.5 U/mg and K_m for chloride

of 344 mM and 0.25 mM, respectively (Soedjak & Butler, 1990; van Schijndel et al., 1993). Such differences have not been explained yet, but could be due to small variations in the tertiary structure around the prosthetic group.

Vanadium Chloroperoxidase from Curvularia Inaequalis. Recently, the primary sequence (Simonns et al., 1995) and the X-ray structure (Messerschmidt & Wever, 1996) of the V-CIPO secreted by the fungus *C. inaequalis* have been determined. The crystal structure of V-CIPO showed that the vanadium was situated at the bottom of a channel formed of two distinct contiguous halves (Messerschmidt & Wever, 1996). One half is mostly hydrophobic with several proline and phenylalanine side-chain residues, whereas the other half has marked hydrophilic properties due to main chain carbonyls and polar residues such as Asp292, Arg360 and Arg490 (Figure 1.5). The vanadium is in the center of a trigonal pyramid with three oxygens in the trigonal plane, one oxygen at the apex of the pyramid, and the N^{ε2} of His496 as the fifth ligand.

Although not involved in vanadium coordination, the imidazole ring of His404 was found to be located near the active site vanadium (Figure 1.5). It has been suggested, therefore, that His404 may play an important role in catalysis since binding of hydrogen peroxide was inhibited when a group with a pK_a > 5 was protonated (van Schindell et al., 1994). Analogous results were also found for V-BrPO that suggested that deprotonation of a residue with a pK_a of 5.7 was necessary before hydrogen peroxide could bind (de Boer & Wever, 1988c).

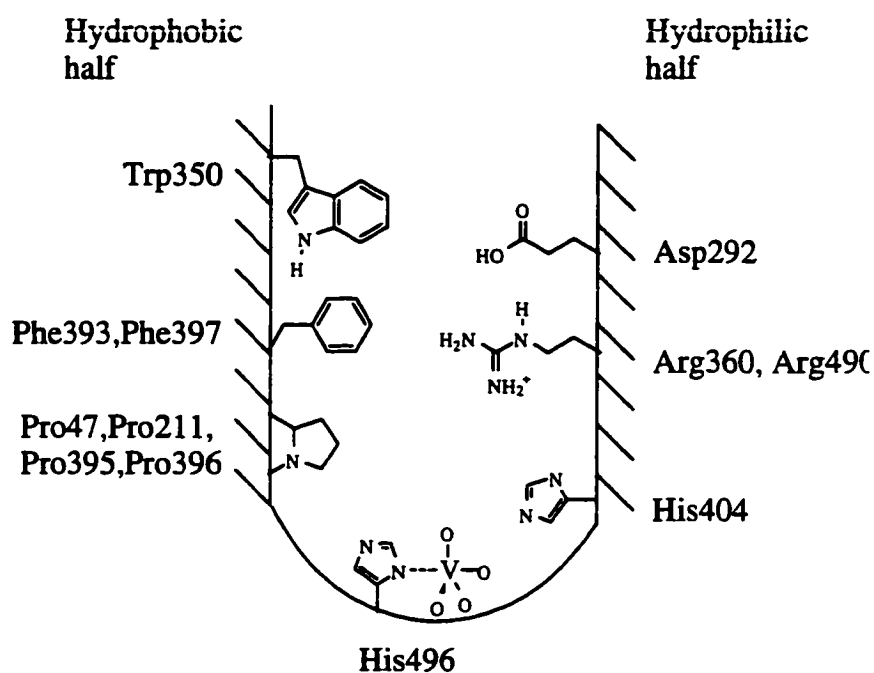


Figure 1.5: Schematic view of the channel leading to the vanadium binding site of V-CIPO from *C. inaequalis* (adapted from Messerschmidt & Wever, 1996).

Partial sequence comparison between V-BrPO and V-CIPO revealed regions of high similarities. All the active site residues that interact with the vanadate cofactor (His-496, Gly-403, Arg-360, Arg-490 and Ser 402) are conserved with the exception of Lys-353 that was substituted with an asparagine in V-BrPO. However, this substitution still allows for hydrogen bonding to vanadate. These observations suggested that the metal binding sites in both enzymes and overall protein structure should be similar (Messerschmidt & Wever, 1996).

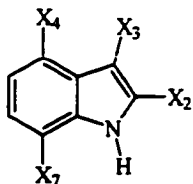
Chapter 2

Bromination of Indoles by Vanadium-Bromoperoxidase

Introduction

Marine algae are an extraordinary source of halogenated secondary metabolites, including monoterpenes, sesquiterpenes, non-terpenoid C₁₅ acetogenins, phenols, and indoles, that are generally distinctive to the genus. Although biochemists have long evoked the possible role of haloperoxidases, the biogenesis of these metabolites still remains obscure.

Although not as widespread as halogenated sesquiterpenes, halogenated indoles have been found in large amounts in several algae. The red alga *Rhodophyllis membranacea* Harvey was found to contain a complicated mixture of polyhalogenated indoles (Brennan & Erickson, 1978). All identified indoles (1a-j) are substituted in position 2 and 3. Furthermore, all compounds have a substituent in position 4 or 7, or both. But this substitution pattern is not general since unidentified compounds with five or six halogen atoms were also characterized by mass spectrometry: Br₅ (two isomers), Br₄Cl (two isomers), Br₃Cl₂ (two isomers), Br₂Cl₃ (two isomers), Br₆, Br₅Cl, Br₄Cl₂, Br₃Cl₃. In addition to the identified structures, the following tetra- and trihalogenated indoles could be seen in the mass spectra: Br₄, Br₃Cl, Br₂Cl₂, Br₂Cl, BrCl₃, BrCl₂ and Cl₃. The number of different structures is overwhelming and seems to point to a nearly total scrambling of the possible chloro and bromo substitution patterns.

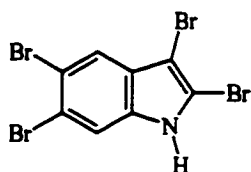
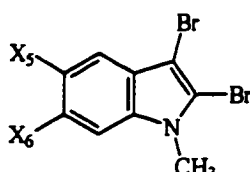


1a-j

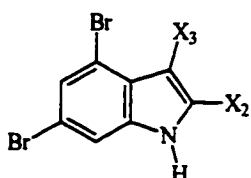
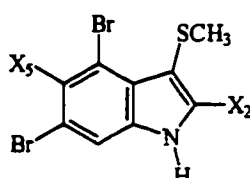
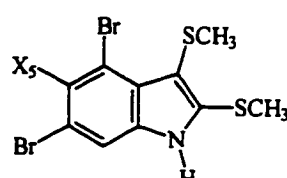
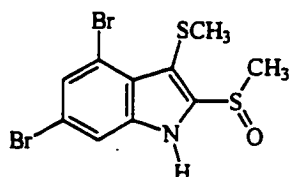
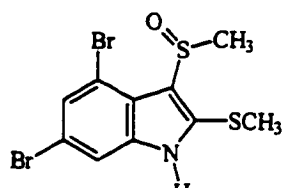
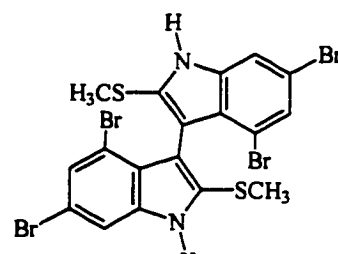
- | | |
|------------------------------------------------------------|-----------------------------------------------------------------------------------|
| a $X_2 = X_3 = X_7 = \text{Cl}, X_4 = \text{H}$ | f $X_2 = X_3 = X_4 = X_7 = \text{Cl}$ |
| b $X_2 = X_3 = \text{Cl}, X_7 = \text{Br}, X_4 = \text{H}$ | g $X_2 = X_3 = \text{Cl}, X_4 = \text{Br}(\text{Cl}), X_7 = \text{Cl}(\text{Br})$ |
| c $X_2 = X_7 = \text{Br}, X_3 = \text{Cl}, X_4 = \text{H}$ | h $X_2 = X_3 = \text{Cl}, X_4 = X_7 = \text{Br}$ |
| d $X_2 = X_3 = X_7 = \text{Br}, X_4 = \text{H}$ | i $X_4 = X_7 = \text{Br}, X_2 = \text{Br}(\text{Cl}), X_3 = \text{Cl}(\text{Br})$ |
| e $X_2 = X_3 = X_4 = \text{Cl}, X_7 = \text{H}$ | j $X_2 = X_3 = X_4 = X_7 = \text{Br}$ |

The red alga *Laurencia brongniartii* is exceptional in that the usual metabolites of the genus (i.e. terpenoids) are missing and that it contains polybromoindoles instead. From a Caribbean collection (Carter et al. 1978), a brominated indole (**2a**) and three brominated methylindoles (**3a-c**) were isolated in copious amounts: 0.039 %, 0.038 %, 0.006 % and 0.010 % of the wet weight, respectively. Positions 2, 3, 5 and 6 seem to be the favored bromination sites for these metabolites. Taiwanese and Okinawan samples of *L. brongniartii* also contained polybrominated indoles, but their structures were different from the ones isolated from the Caribbean alga (Sun, 1983; Tanaka et al. 1988; Tanaka et al., 1989). Besides simple brominated indoles (**4a-b**), several interesting new sulfur-containing brominated indoles were identified: thiomethylindoles (**5a-c**, **6a-b**), sulfoxides (**7**, **8**) and a biindole (**9**). The presence of thiomethylindoles in a *Laurencia* species is of special interest in view of the fact that related compounds have been found in marine invertebrates. Tyrian purple (6-6'-dibromoindigotin), a dye produced by a number of marine mollusks and also by an acorn worm, is presumably derived from α -thiomethylindolic precursors (Prota, 1980) (See also Chapter 3, Introduction).

a) Caribbean collection.

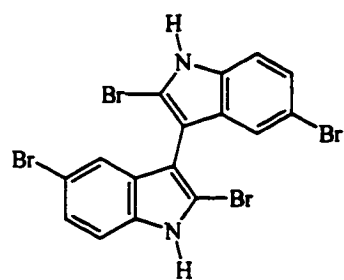
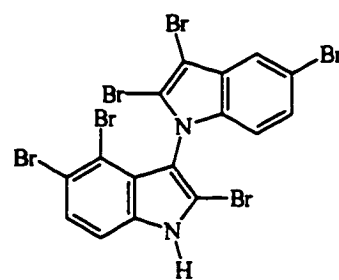
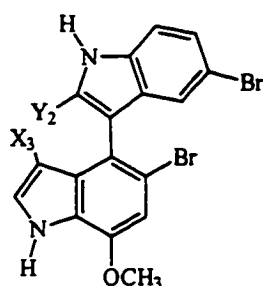
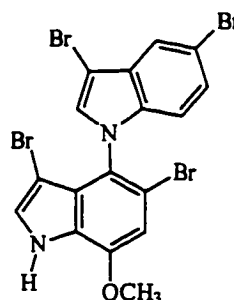
**2a****3a-c**a $X_5 = \text{H}, X_6 = \text{Br}$ b $X_5 = \text{Br}, X_6 = \text{H}$ c $X_5 = X_6 = \text{Br}$

b) Taiwanese and Okinawan collections.

**4a-b**a $X_2 = \text{Br}, X_3 = \text{H}$ b $X_2 = X_3 = \text{Br}$ **5a-c**a $X_2 = X_5 = \text{H}$ b $X_2 = \text{Br}, X_5 = \text{H}$ c $X_2 = X_5 = \text{Br}$ **6a-b**a $X_5 = \text{H}$ b $X_5 = \text{Br}$ **7****8****9**

Six unprecedented biindoles have been isolated from the blue-green alga *Rivularia firma* Womersley (Norton and Wells, 1982). Structures were solved using information obtained from ^{13}C - ^1H NMR coupling constants and ^{13}C NMR spin-lattice relaxation data. Compounds 11-13 were optically active and belong to a very small class of natural products that are chiral only because of restricted

rotation within the molecule. The absolute configurations of **11** and **12c** were established as R and S, respectively, by single-crystal X-ray analysis (Blount et al., 1983).

**10****11****12a-c****13**

- a $X_3 = \text{H}$, $Y_2 = \text{Br}$
 b $X_3 = \text{Br}$, $Y_2 = \text{H}$
 c $X_3 = Y_2 = \text{Br}$

Although the function of halogenated indoles *in vivo* has not yet been established, some of them are biologically active: **1a-j** are all antifungal, **2a** showed antimicrobial and antitumoral activities, and **12c** is an antiinflammatory agent.

Only a few examples of the reactivity of haloperoxidases with indoles have been reported: In the presence of hydrogen peroxide and in the absence of a halide ion, FeHeme-CIPO reacts with indole to form oxindole as the major product (Corbett & Chipko, 1979). The optimal pH was 4.6, consistent with other halogen-independent oxidation reactions of FeHeme-CIPO (Thomas et al. 1970a). Trace amounts (2 % by weight) of intensely colored pigments, including indigo, were detected in large scale reactions. The reaction kinetics were first-order with respect to indole up to 8 mM. It was also found that hydrogen peroxide inhibited the reaction at concentrations above 0.5 mM. 2-Methylindole was not a substrate for FeHeme-CIPO, but strongly inhibited indole oxidation. In addition, 1-methylindole was a poor substrate and a weak inhibitor of indole oxidation. In 1986 Wiesner and co-workers isolated a new CIPO from *Pseudomonas pyrocinia* (Wiesner et al., 1986). It was reported to react with indole to form 7-chloroindole and a monobromo indole (the exact position of the bromine atom on the indole ring was not reported).

Materials and Methods

Materials. V-BrPO was isolated from *Ascophyllum nodosum* collected in Holland as described previously (Wever et al., 1985; Everett, 1990). Indole, 1-methylindole, 2-methylindole, 3-methylindole, 1,2-dimethylindole and 2-oxindole were obtained from Aldrich (Milwaukee, MI). β -D-Indoxylglucose and β -glucosidase were purchased from Sigma Chemical Co. (St. Louis, MO). 3-Bromoindole and 3-bromo-2-methylindole were prepared by bromination of indole and 2-methylindole in DMF (Bocchius & Palla, 1982). 2-Phenylindole and 2-*tert*-butylindole were prepared by a modified Madelung indole synthesis (Houlihan et al., 1981). 3-Phenylindole was prepared by Fisher indole synthesis. 3-*tert*-Butylindole and 1,3-di-*tert*-butylindole were prepared by alkylation of indolylmagnesium chloride with *tert*-butylchloride (Smith & Waters, 1961). $^{18}\text{O}_2$ was purchased from Isotech (Miamisburg, OH). $\text{H}_2^{18}\text{O}_2$ was prepared by the method developed by Sitter and Turner (1985). Preparative thin-layer chromatography was carried out on 20 x 20 cm plates coated with 2 mm of silica gel 60 PF-254 (EM Reagents). Zones were visualized by irradiation at 254 nm. Analytical HPLC was carried out on a Waters System with Waters 510 pumps and Waters 484 UV detector using a Val-U-Pak HP, 25 cm x 4.6 mm column (Regis, Morton Grove, IL), or a Spherisorb S5 ODS2 25 cm x 4.6 mm column (Phase Sep, Norwalk, Ct). The gradients are given in the main text. Preparative-HPLC was carried out with an Econosil C-18 10 μm , 25 cm x 10 mm column (Alltech, Deerfield, IL) with a linear gradient water-acetonitrile at 2 or 3 mL/min; 0 to 5 min, 0 % acetonitrile, 5 to 60 min, 0-100 % acetonitrile. Fractions were collected

every minute. Proton NMR spectra were obtained at 500 MHz and at 300 MHz on General Electric GN-500 and GN-300 instruments. Infra-red spectra were obtained on a Perkin-Elmer 1330 infrared spectrophotometer. Mass spectra were measured with a VG70-250HF double sector mass spectrometer. UV-Vis spectra were obtained on a Hewlett-Packard HP8452A diode-array spectrophotometer.

Isolation and Characterization of Products from Enzymatic Reactions.

Indole. Indole (**14**) (41.2 mg, 0.349 mmol) was dissolved in 20 mL of ethanol and added to 80 mL of a solution of 100 mM sodium phosphate (pH 6.5) and 100 mM KBr. H₂O₂ (36.7 μ L, 9.8 M, 0.359 mmol) and V-BrPO (58.3 μ L, 18.7 μ M, 1.1 nmol) were added and the mixture was left overnight. A dark blue precipitate formed and was collected by filtration. It was washed with water and dried *in vacuo* to yield indigo (**15**) as a blue powder (17.3 mg, 37 %). Electron impact mass spectrometry (EIMS) *m/z* (relative intensity (rel int)) 262 (M⁺, base), 234 (18), 131 (10), 104 (30), 76 (27). The filtrate was analyzed by HPLC. Two major products were found. They were identified as 3-bromoindole (**16**) (39 %) and 1,3-dihydro-2*H*-indol-2-one (oxindole) (**17**) (8 %) by co-injection with authentic compounds.

1-Methylindole. 1-Methylindole (**22**) (40.2 mg, 0.306 mmol) was dissolved in 60 mL of ethanol and added to 240 mL of a solution of 100 mM sodium phosphate (pH 6.00) and 50 mM KBr. H₂O₂ (68 μ L, 9.7 M, 0.658 mmol) and V-BrPO (60 μ L, 61 μ M, 3.7 nmol) were added, and the reaction was allowed to sit for 4 h. The solution turned cloudy and green. The reaction mixture was then extracted 3 times with ethyl acetate. The organic phases were combined,

dried over MgSO_4 , and evaporated to give a green oily residue (34.1 mg). The residue was a mixture of products and was separated using preparative reverse-phase HPLC. The fractions collected were analyzed by NMR. Fractions [33-37] gave 4.9 mg of a mixture of 2 products that were further separated by HPLC to give 1,3-dihydro-3-hydroxy-1-methyl-2*H*-indol-2-one (**23**) (2.1 mg, 4 %): ^1H NMR (CDCl_3 , 500 MHz) δ 3.17 (s, 3H), 5.03 (s, 1H), 6.81 (d, $J = 7.5$ Hz, 1H), 7.08 (t, $J = 7.5$ Hz, 1H), 7.32 (t, $J = 7.5$ Hz, 1H), 7.43 (d, $J = 7.5$ Hz); IR (KBr) ν 3300, 2930, 2830, 1700, 1618, 1470, 1390, 1099, 764; EIMS m/z (rel int) 163 (M^+ , 71), 147 (43), 118 (71), 106 (base); and 1*H*-indole-2,3-dione (1-methylisatin) (**24**) (2.4 mg, 5 %): ^1H NMR (CDCl_3 , 500 MHz) δ 3.23 (s, 3H), 6.87 (d, $J = 7.5$ Hz, 1H), 7.11 (t, $J = 7.5$ Hz, 1H), 7.58 (t, $J = 7.5$ Hz, 1H), 7.58 (d, $J = 7.5$ Hz, 1H); IR (KBr) ν 1780, 1615, 1475, 1335, 1100, 765; EIMS m/z (rel int) 161 (M^+ , 92), 133 (47), 104 (base). Fractions [38-39] yielded 1,3-dihydro-1-methyl-2*H*-indol-2-one (**25**) (0.8 mg, 2 %): ^1H NMR (CDCl_3 , 500 MHz) δ 3.19 (s, 3H), 3.50 (s, 2H), 6.80 (d, $J = 8$ Hz, 1H), 7.02 (t, $J = 7.5$ Hz, 1H), 7.23 (d, $J = 7.5$ Hz, 1H), 7.26 (t, $J = 8$ Hz, 1H); IR (KBr) ν 3400, 2910, 1705, 1610, 1420, 1375, 1350, 1260, 1095, 1020, 805, 755; EIMS m/z (rel int) 147 (M^+ , base) 118 (93). Fractions [40-42] gave 1,3-dihydro-3-ethoxy-1-methyl-2*H*-indol-2-one (**26**) (0.6 mg, 1%): ^1H NMR (CDCl_3 , 500 MHz) δ 1.25 (t, $J = 7.5$ Hz, 3H), 3.15 (s, 3H), 3.66 (dq, $J = 7.5$ Hz and $J = 8.7$ Hz, 1H), 3.86 (dq, $J = 7.5$ Hz and $J = 8.7$ Hz, 1H), 4.88 (s, 1H), 6.78 (d, $J = 7.5$ Hz, 1H), 7.06 (t, $J = 7$ Hz, 1H), 7.31 (t, $J = 7.5$ Hz, 1H), 7.37 (d, $J = 7$ Hz, 1H); IR (KBr) ν 3420, 2930, 1715, 1615 1470, 1375, 1350, 1115, 1095, 755; EIMS m/z (rel int), 191 (M^+ , 15), 147 (base), 134 (41), 118 (41). Fractions [48-52] gave 1,3-dihydro-1-methyl-3-(1-methyl-1*H*-indol-3-yl)-2*H*-

indol-2-one (**28**) (1.0 mg, 2 %): $^1\text{H NMR}$ (CDCl_3 , 500 MHz) δ 3.28 (s, 3H), 3.72 (s, 3H), 6.90 (d, $J = 7.5$ Hz, 1H), 6.94 (s, 1H), 6.99 (t, $J = 7.5$ Hz, 1H), 7.19 (t, $J = 8$ Hz, 1H), 7.24 (m, 3H), 7.30 (t, $J = 7.5$ Hz, 1H); IR (KBr) ν 3440, 2940, 2870, 1720, 1615, 1475, 1380, 1350, 745; EIMS m/z (rel int) 276 (M^+ , base), 247 (83), 162 (25). Fractions [59-60] gave 3-bromo-1-methylindole (**27**) (8.2 mg, 13 %): $^1\text{H NMR}$ (CDCl_3 , 500 MHz) δ 3.76 (s, 3H), 7.06 (s, 1H), 7.18 (t, $J = 7.5$ Hz, 1H), 7.24 (t, $J = 7.5$ Hz, 1H), 7.28 (d, $J = 7.5$ Hz, 1H), 7.56 (d, $J = 7.5$ Hz, 1H); IR (neat, NaCl) ν 3130, 3075, 2940, 1475, 1330, 1250, 955, 750; EIMS m/z (rel int) 211/209 (M^+ , 99/base), 130 (34). Fraction [61] contained 1,3-dihydro-1-methyl-3,3-di-(1-methyl-1*H*-indol-3-yl)-2*H*-indol-2-one (**30**) (1.0 mg, 3 %): $^1\text{H NMR}$ (CDCl_3 , 500 MHz) δ 3.31 (s, 3H), 3.66 (s, 6H), 6.81 (s, 2H), 6.89 (t, $J = 8$ Hz, 2H), 6.95 (d, $J = 7.5$ Hz, 1H), 6.98 (t, $J = 7.5$ Hz, 1H), 7.12 (t, $J = 8$ Hz, 2H), 7.23 (d, $J = 8$ Hz, 2H), 7.26 (t, $J = 8$ Hz, 2H), 7.29 (t, $J = 7.5$ Hz, 1H), 7.41 (d, $J = 7.5$ Hz, 1H); IR (KBr) ν 3400, 2925, 2860, 1718, 1610, 1470, 1375, 1175, 1135, 1090, 745; EIMS m/z (rel int) 405 (M^+ , base), 376 (91), 247 (66). Fraction [62] gave 1,2-dihydro-1-methyl-3,3-di-(1-methyl-1*H*-indol-3-yl)-3*H*-indol-3-one (**31**) (0.7 mg, 2 %): $^1\text{H NMR}$ (CDCl_3 , 500 MHz) δ 2.94 (s, 3H), 3.70 (s, 6H), 6.72 (t, $J = 7.5$ Hz, 1H), 6.80 (d, $J = 7.5$ Hz, 2H), 6.94 (t, $J = 7.5$ Hz, 2H), 6.97 (s, 2H), 7.16 (t, $J = 7.5$ Hz, 2H), 7.27 (d, $J = 8$ Hz, 2H), 7.33 (d, $J = 8$ Hz, 2H), 7.52 (t, $J = 7.5$ Hz, 1H), 7.64 (d, $J = 7.5$ Hz, 1H); IR (KBr) ν 3400, 2925, 2860, 1718, 1610, 1470, 1375, 1175, 1135, 1090, 745; CIMS (CH_4) m/z (rel int) 406 ($\text{M}^+ + 1$, 28), 405 (M^+ , 34), 275 (base). Fractions [64-67] gave 3-bromo-2-methyl-2-(1-methyl-1*H*-indol-3-yl)-1*H*-indole (**29**) (2.6 mg, 5%): $^1\text{H NMR}$ (CDCl_3 , 500 MHz) δ 3.61 (s, 3H), 3.85 (s, 3H), 7.12 (t, $J = 7.5$ Hz, 1H), 7.16 (t, $J = 7.5$ Hz, 1H), 7.23 (m,

2H), 7.25 (s, 1H), 7.30 (d, $J = 8$ Hz, 1H), 7.36 (d, $J = 8$ Hz, 1H), 7.42 (d, $J = 8$ Hz, 1H), 7.54 (d, $J = 8$ Hz, 1H); IR (KBr) ν 2920, 1465, 1225, 745; EIMS m/z (rel int) 340/338 (M^+ , 97/base), 260 (49).

2-Methylindole. 2-Methylindole (**32**) (260 mg, 1.98 mmol) was dissolved in 200 mL of ethanol and added to 800 mL of a solution of 100 mM sodium phosphate (pH 6.00) and 100 mM KBr. H_2O_2 (204 μ L, 9.6 M, 1.95 mmol) and V-BrPO (300 μ L, 6.6 μ M, 1.98 nmol) were added. The solution turned cloudy and was allowed to stand for 20 h at room temperature. The solution was then extracted with ethyl acetate. The organic layers were combined, dried over $MgSO_4$ and evaporated to dryness to give a yellow oil that slowly crystallized. The solid was recrystallized with methanol/water to give 3-bromo-2-methylindole (**33**) (267 mg, 64 %): 1H NMR ($CDCl_3$, 500 MHz) δ 2.42 (s, 3H), 7.04 (t, $J = 7.5$ Hz, 1H), 7.08 (t, $J = 7.5$, 1H), 7.25 (d, $J = 7.5$ Hz, 1H), 7.33 (d, $J = 7.5$ Hz, 1H), 7.99 (s, 1H); EIMS m/z (rel int) 211/209 (M^+ , 97/base), 130 (91).

3-Methylindole. 3-Methylindole (**34**) (189 mg, 1.44 mmol) was dissolved in 200 mL of ethanol and added to 1800 mL of a solution of 100 mM sodium phosphate (pH 6.00) and 100 mM KBr. H_2O_2 (200 μ L, 9.8 M, 1.96 mmol) and V-BrPO (500 μ L, 9.0 μ M, 4.5 nmol) were added and the reaction allowed to proceed for 2 h. The solution was then extracted 3 times with ethyl acetate. The organic layers were combined, dried over $MgSO_4$ and evaporated to dryness to give 1,3-dihydro-3-methyl-2*H*-indol-2-one (**35**) as a yellow oil that slowly crystallized (200 mg, 69 %): 1H NMR ($CDCl_3$, 500 MHz) δ 1.51 (d, $J = 7.8$ Hz, 3H), 3.47 (q, $J = 7.8$ Hz, 1H), 6.80 (d, $J = 7.2$ Hz, 1H), 7.08 (t, $J = 7.2$ Hz, 1H), 7.2 (m, 2H); EIMS m/z (rel int) 147 (M^+ , base), 119 (82), 118 (53).

1,2-Dimethylindole. 1,2-Dimethylindole (**37**) (291 mg, 2.01 mmol) was dissolved in 200 mL of ethanol and poured into 800 mL of a solution of 100 mM phosphate buffer (pH 6.00) and 100 mM KBr. H_2O_2 (204 μL , 9.6 M, 1.95 mmol) and V-BrPO (300 μL , 6.6 μM , 1.98 nmol) were added successively and the solution was allowed to stand at room temperature for 24 h. The product crystallized as thin, short needles. The ethanol was then removed by evaporation under vacuum. The product was collected by filtration, washed with water and dried under vacuum to give 3-bromo-1,2-dimethylindole (**38**) as a pale yellow solid (319 mg, 72 %): ^1H NMR (CDCl_3 , 500 MHz) δ 2.44 (s, 3H), 3.68 (s, 3H), 7.15 (t, $J = 7.5$ Hz, 1H), 7.20 (t, $J = 7.5$ Hz, 1H), 7.25 (d, $J = 7.5$ Hz, 1H), 7.48 (d, $J = 7.5$ Hz, 1H); EIMS m/z (rel int) 225/223 (M^+ , 96/base), 144 (67), 115 (21).

2-Phenylindole. 2-Phenylindole (**39**) (19.9 mg, 0.103 mmol) was dissolved in 40 mL of ethanol and added to a solution (60 mL) of 100 mM sodium phosphate (pH 5.91) and 55.7 mM KBr. H_2O_2 (15 μL , 10.3 M, 0.154 mmol) and V-BrPO (50 μL , 7.7 μM , 0.38 nmol) were added successively. The mixture was allowed to react for 12 h and then extracted 3 times with ethyl acetate. The organic layers were combined, dried over MgSO_4 and evaporated to a yellowish solid. TLC analysis showed two products that were separated by preparative TLC eluted with a 90:10 hexanes:ethyl acetate solvent system. The major product was washed from the silica with methanol. The methanol was evaporated to give 3-bromo-2-phenylindole (**40**) as a faint yellow solid (11.1 mg, 39 %): ^1H NMR (CDCl_3 , 500 MHz) δ 7.22 (t, $J = 7.5$ Hz, 1H), 7.24 (t, $J = 7.5$ Hz, 1H), 7.26 (t, $J = 7.5$ Hz, 1H), 7.38 (d, $J = 7.5$ Hz, 1H), 7.43 (d, $J = 7.5$ Hz, 2H), 7.49 (t, $J = 7.5$ Hz,

2H), 7.62 (d, $J = 7.5$ Hz, 1H), 7.82 (d, $J = 7.5$ Hz, 2H), 8.32 (s, 1H); EIMS m/z (rel int) 273/271 (M^+ , 98/base), 192 (87).

3-Phenylindole. 3-Phenylindole (**42**) (96.6 mg, 0.500 mmol) was dissolved in 150 mL of ethanol and added to 200 mL of a solution of 100 mM sodium phosphate (pH 6.45) and 60 mM of KBr. H_2O_2 (55 μ L, 10.4 M, 0.572 mmol) and V-BrPO (40 μ L, 61.5 μ M, 2.5 nmol) were added. The reaction was carried overnight at room temperature. The reaction mixture was then concentrated to *ca.* 200 mL and extracted 3 times with ether. The organic layers were combined, dried over $MgSO_4$ and concentrated to an oily residue (140.9 mg). The residue was placed on top of a 3 cm x 18 cm column of silica gel packed in hexanes and eluted with a gradient hexanes into ethyl acetate into methanol (500 mL each). After a 250 mL were eluted, 49 fractions (20 mL each) were collected. The fractions were analyzed by TLC, combined according to content and further purified by preparative reverse phase HPLC, when necessary. Fractions [11-19] were combined and gave 2-bromo-3-phenylindole (**43**) (8.1 mg, 6%): 1H NMR ($CDCl_3$, 500 MHz) δ 7.13 (t, $J = 7.5$ Hz, 1H), 7.21 (t, $J = 8$ Hz, 1H), 7.33 (d, $J = 8$ Hz, 1H), 7.34 (t, $J = 7.5$ Hz, 1H), 7.47 (t, $J = 7.5$ Hz, 2H), 7.62 (d, $J = 8$ Hz, 2H), 7.71 (d, $J = 7.5$ Hz, 1H), 8.19 (s, 1H); IR (KBr) ν 3380, 3050, 1600, 1440, 1410, 1340, 1250, 770, 740, 695; EIMS m/z (rel int) 273/271 (M^+ , 97/base), 192 (24), 190 (26), 165 (36). Fractions [20-26] were combined and gave 3,3'-diphenyl-2,2'-bi-1*H*-indole (**44**) (21.7 mg, 24 %): 1H NMR ($CDCl_3$, 500 MHz) δ 7.10 (t, $J = 7.5$ Hz, 2H), 7.15 (t, $J = 7.5$ Hz, 2H), 7.16 (d, $J = 7.5$ Hz, 2H), 7.40 (d, $J = 7.5$ Hz, 2H), 7.47 (t, $J = 7.5$ Hz, 4H), 7.60 (d, $J = 7.5$ Hz, 4H), 7.62 (d, $J = 7.5$ Hz, 2H), 8.01 (s, 2H); IR (KBr) ν 3420, 3325, 3020, 1590, 1440,

1240, 740, 690; EIMS m/z (rel int) 385 (M^+ , 31), 384 (base), 306 (13), 153 (12); and 3-phenyl-2-(3-phenyl-3*H*-indol-2-yl)-1*H*-indole (**45**) (12.0 mg, 13 %): ^1H NMR (CDCl_3 , 500 MHz) δ 4.95 (s, 1H), 6.71 (d, $J = 8 = 7.5$ Hz, 1H), 7.17 (d, $J = 8$ Hz, 2H), 7.18 (t, $J = 8$ Hz, 1H), 7.19 (t, $J = 7.5$ Hz, 2H), 7.22 (t, $J = 7.5$ Hz, 1H), 7.28 (d, $J = 8$ Hz, 2H), 7.42 (t, $J = 7.5$ Hz, 1H), 7.82 (s, 1H), 8.10 (d, $J = 7.5$ Hz, 1H), 8.15 (d, $J = 7.5$ Hz, 1H); IR (KBr) ν 3380, 3030, 1590, 1430, 1330, 1245, 1245, 740, 690; EIMS m/z (rel int) 384 (M^+ , base), 307 (33), 193 (55). Fractions [27-29] gave 3-phenyl-2-(3-ethoxy-3-phenyl-3*H*-indol-2-yl)-1*H*-indole (**46**) (2.5 mg, 3 %): ^1H NMR (CDCl_3 , 500 MHz) δ 1.12 (t, $J = 7$ Hz, 3H), 3.64 (dq, $J = 10$ and $J = 7$ Hz, 1H), 4.12 (dq, $J = 10$ and $J = 7$ Hz, 1H), 6.92 (m, 3H), 7.05 (t, $J = 7.5$ Hz, 1H), 7.08 (d, $J = 7.5$ Hz, 1H), 7.16 (m, 5H), 7.26 (s, 5H), 7.29 (d, $J = 8$ Hz, 1H), 7.33 (d, $J = 7.5$ Hz, 1H), 7.37 (d, $J = 8$ Hz, 1H), 7.88 (s, 1H); IR (KBr) ν 3400, 3050, 2920, 1580, 1310, 1030, 740, 695; EIMS m/z (rel int) 428 (M^+ , 93), 399 (87), 351 (base). Fractions [47-48] gave 1,3-dihydro-3-hydroxy-3-phenyl-2*H*-indol-2-one (**47**) (2,8 mg, 3 %): ^1H NMR (Acetone- d_6 , 500 MHz) δ 5.49 (s, 1H), 6.96 (d, $J = 7.5$ Hz, 1H), 6.98 (t, $J = 7.5$ Hz, 1H), 7.16 (d, $J = 7.0$ Hz, 1H), 7.24 (t, $J = 7.0$ Hz, 1H), 7.25 (d, $J = 7.0$ Hz, 1H), 7.29 (t, $J = 7.5$ Hz, 2H), 7.40 (d, $J = 7.5$ Hz, 2H), 9.34 (s, 1H); IR (KBr) ν 3410, 3150, 1680, 1600, 1450, 1150, 1050; EIMS m/z (rel int) 225 (M^+ , 33), 209 (60), 197 (92), 196 (base), 180 (79); and 1,3-dihydro-3-ethoxy-3-phenyl-2*H*-indol-2-one (**48**) (8.8 mg, 7 %): ^1H NMR (CDCl_3 , 500 MHz) δ 1.24 (t, $J = 7$ Hz, 3H), 3.32 (dq, $J = 7$ and $J = 7$ Hz, 1H), 3.47 (dq, $J = 7$ and $J = 7$ Hz, 1H), 6.91 (d, $J = 8$ Hz, 1H), 7.07 (t, $J = 7.5$ Hz, 1H), 7.21 (d, $J = 7.5$ Hz, 1H), 7.80 (m, 4H), 7.39 (d, $J = 7.5$ Hz, 2H), 8.45 (s, 1H);

IR (KBr) ν 3190, 1700, 1610, 1450, 1205, 1175, 1105, 1070, 740; EIMS m/z (rel int) 253 (M^+ , 8), 224 (73), 209 (73), 196 (base), 180 (57).

3-tert-Butylindole. **3-tert-Butylindole (50)** (20.1 mg, 0.116 mmol) was dissolved in 10 mL of ethanol and added to a solution (90 mL) of 100 mM sodium phosphate (pH 5.91) and 55.7 mM of KBr. H_2O_2 (18 μ L, 10.3 M, 0.185 mmol) and V-BrPO (100 μ L, 7.69 μ M, 0.77 nmol) were added successively and the reaction allowed to stand at room temperature for 1h. The reaction mixture was then extracted three times with ethyl acetate. The organic layers were combined, dried over $MgSO_4$ and evaporated to give 1,3-dihydro-3-*tert*-butyl-2*H*-indol-2-one (**51**) as a faint yellow solid (20.0 mg, 91 %): 1H NMR ($CDCl_3$, 500 MHz) δ 1.13 (s, 9H), 3.30 (s, 1H), 6.86 (d, $J = 7.5$ Hz, 1H), 6.98 (t, $J = 7.5$ Hz, 1H), 7.20 (t, $J = 7.5$ Hz, 1H), 7.30 (d, $J = 7.5$ Hz, 1H), 8.36 (s, 1H).

1,3-Di-tert-butylindole. **1,3-Di-tert-Butylindole (53)** (28.4 mg, 0.112 mmol) was dissolved in 10 mL of ethanol and added to a solution (90 mL) of 100 mM sodium phosphate (pH 5.91) and 55.7 mM of KBr. H_2O_2 (18 μ L, 10.3 M, 0.185 mmol) and V-BrPO (100 μ L, 7.69 μ M, 0.77 nmol) were added successively and the reaction allowed to stand at room temperature for 1h. The reaction mixture was then extracted three times with ethyl acetate. The organic layers were combined, dried over $MgSO_4$ and evaporated to give 1,3-dihydro-1,3-di-*tert*-butyl-2*H*-indol-2-one (**54**) as a faint yellow solid (25.7 mg, 84%): 1H NMR ($CDCl_3$, 500 MHz) δ 1.08 (s, 9H), 1.70 (s, 9H), 2.92 (s, 1H) 6.94 (t, $J = 7.5$ Hz, 1H), 7.20 (m, 2H), 7.26 (d, $J = 7.5$ Hz, 1H).

Results

Bromination of Indole by V-BrPO. When indole (14) was incubated with bromide, hydrogen peroxide and V-BrPO at pH 6.5, a rapid change in the UV spectrum of the reaction mixture was observed (Figure 2.1). In the first 6 min of the reaction, the original absorption peak of 14 at 278 nm decreased and shifted to a higher wavelength (281 nm) with concomitant appearance of peaks at 380 nm and 660 nm. After this period, the peaks at 380 nm and 660 nm continued to increase, whereas the peak at 281 nm rapidly decreased, indicating consecutive reactions.

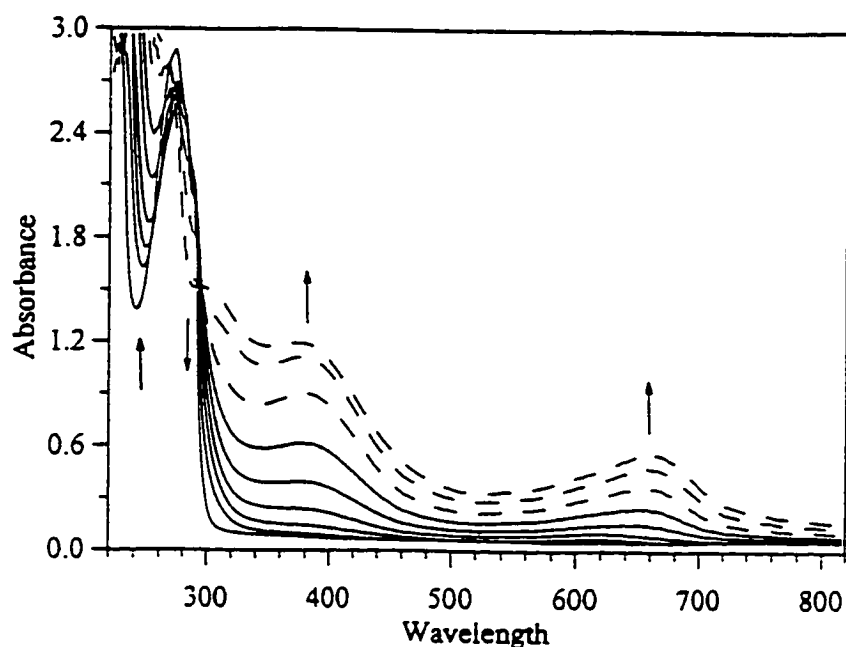
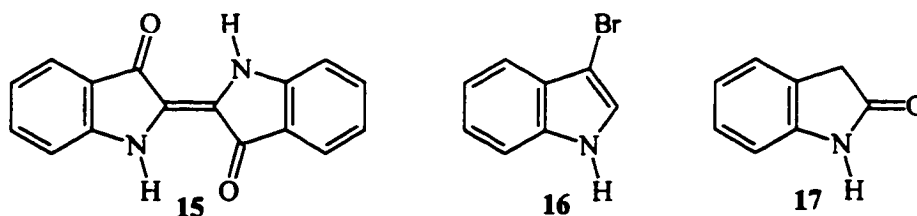


Figure 2.1: UV/Vis spectra of the bromination of indole (14) by V-BrPO. Conditions: 100 mM sodium phosphate, pH 6.5, 50 mM KBr, 10 % ethanol, 1.3 mM indole, 2.8 mM H₂O₂ and 11.7 nM V-BrPO. Spectra were recorded every 2 min.



Upon completion, the reaction yielded a blue precipitate and a yellow supernatant. Mass spectrometry analysis of the precipitate gave a molecular ion with $m/z = 262$, consistent with the blue dye indigo (15). In addition, the TLC R_f of the precipitate coincided with authentic 15. HPLC of the supernatant showed

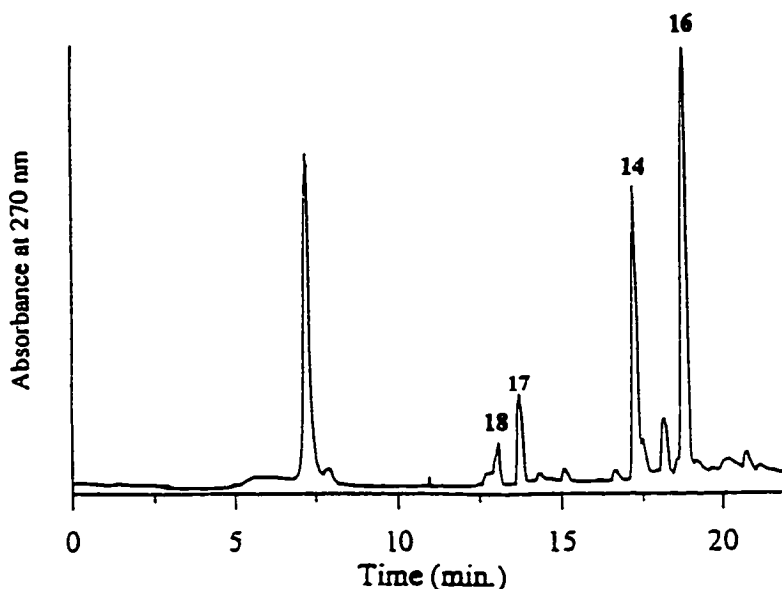
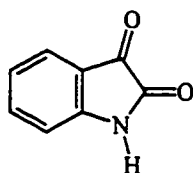


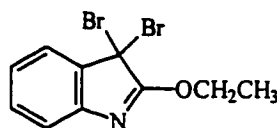
Figure 2.2: HPLC chromatogram of the bromination of indole (14) by V-BrPO. Conditions: 100 mM sodium phosphate, pH 6.35, 100 mM KBr, 20 % ethanol, 3.53 mM 14, 3.66 mM H_2O_2 and 12 nM V-BrPO. After 24 h a 10 μ L aliquot was injected on a Regis C-18 Val-U-Pak HP column with a gradient of acetonitrile (B) into water (A): 0-2.5 min (0 % B), 2.5-3.0 min (0-50 % B), 3.0-8.0 min (50 % B), 8.0-8.5 min (50-80 % B) 8.5-22 min (80 % B). Detection was at $\lambda = 270$ nm.

the presence of several additional products (Figure 2.2). Analysis of the crude ethyl acetate extract of the filtrate indicated the presence of 2 major compounds with molecular ion peaks at m/z 133 and 197/195 identified as 1,3-dihydro-2*H*-indol-2-one (oxindole) (**16**) and 3-bromoindole (**17**), respectively, by HPLC co-injections with reference compounds.

Three other products were isolated in trace amounts (< 1%) from the filtrate after fractionation of the ethyl acetate extract by RP(C-18)-HPLC. The first one had a molecular ion peak at m/z 148 and was identified as 1*H*-indole-2,3-dione (isatin) (**18**) by HPLC co-injection with an authentic sample. The EIMS spectrum of the second compound had molecular ion peaks at m/z 321, 319, and 317 with relative intensities of 1.6, 3.6, and 1.5, respectively, corresponding to a molecular formula of $C_{10}H_9Br_2NO$. The 1H NMR spectrum included signals at δ 1.50 (t, 3H, $J = 7.5$ Hz) and 4.60 (d, 2H, $J = 7.5$ Hz) revealing the presence of a CH_3CH_2O - group, and four additional aromatic protons at d 7.16 (t, 1H, $J = 7.5$ Hz), 7.22 (d, 1H, $J = 7.5$ Hz), 7.27 (t, 1H, $J = 7.5$ Hz) and 7.53 (d, 1H, $J = 7.5$ Hz). The IR spectrum was characterized by the absence of any N-H stretch (e.g. 3300-3500 cm^{-1}) and the presence of a strong absorption band at 1734 cm^{-1} indicating the presence of an imine or an oxazole group. The spectroscopic data were consistent with 3,3-dibromo-2-ethoxy-3*H*-indole (**19**).



18



19

The molecular ion peak of the third compound (**20**) had an exact mass of 248.0537 corresponding to the molecular formulas $C_{15}H_8N_2O_2$ (248.0585), $C_{16}H_{10}NO_2$ (248.0712), or $C_{16}H_{12}N_2O$ (248.0949) and indicated that this product was a bi-indole. The 1H MNR spectrum showed the presence of 8 distinct aromatic C-H protons (Figure 2.3). The signal splitting patterns indicated that there was no indole ring N-H protons (also confirmed by the absence, in the IR spectrum, of any sharp band between 3300 and 3500 cm^{-1} , typical for indolic N-H stretch frequencies) and that the benzene ring portions of the molecule were unsubstituted. The IR spectrum displayed strong bands at 1735, 1690, and 1592 cm^{-1} that could be attributed to an $\alpha\beta$ unsaturated carbonyl in a 5 membered ring and, possibly, two different imine functions, respectively. The presence of these functions was further supported by ^{13}C NMR resonances at 182, 158 and 146 ppm. In addition, the carbon spectrum included 12 other peaks (a total of 15) all with chemical shifts above 115 ppm. All the data at hand seemed to agree with the molecular formula $C_{15}H_8N_2O_2$. The formula has an unsaturation number of 13 that likely accounts for 4 ring structures and 9 double bonds. Keeping in mind the structure of the parent compound indole, only a limited set of structures can be derived that fit this formula (**20a&b**). However, neither structure appears to be satisfactory: Structure **20a** includes benzoxazole and indolone functions, and although the ^{13}C NMR of **20** agrees with the chemical shifts observed for benzoxazole (Benassi et al., 1986) 2-phenylindolone (Adams et al., 1986) the formation of **20a** under the reaction conditions used is unlikely. On the other hand, structure **20b** is expected to be fairly unstable which stands in contrast with

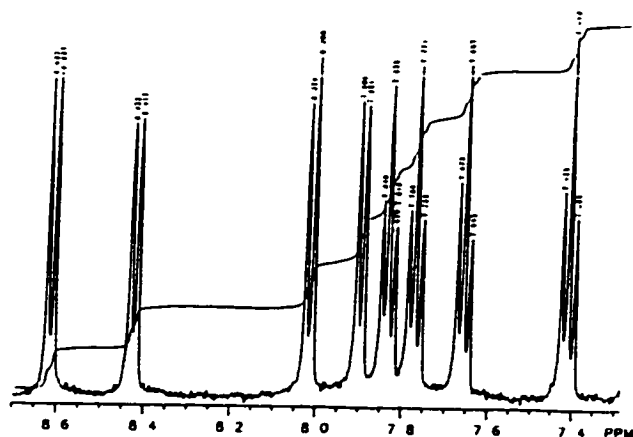
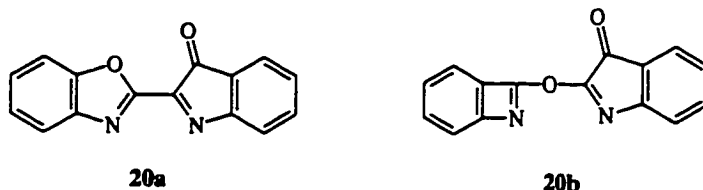


Figure 2.3: 500 MHz ^1H NMR spectrum of product **20**.

what was observed for the product isolated. Apparently, more work is required to fully characterize product **20**.



The yields in indigo (**15**), 3-bromoindole (**16**) and oxindole (**17**), which were the three main products of the reaction of indole with V-BrPO, were highly dependent on the reaction conditions (see below and Chapter 3). However, under conditions comprising 100 mM sodium phosphate pH 6.5, 50 mM potassium bromide, 20 % ethanol, 3.49 mM indole, 3.59 mM hydrogen peroxide and 11 nM V-BrPO, indigo (**15**), 3-bromoindole (**16**), and oxindole (**17**) were obtained in 37 %, 39 % and 8 % yield, respectively.

pH Effect on the Product Selectivity of the Bromination of Indole by V-BrPO and by HOBr. The selectivity¹ in indigo (**15**), 3-bromoindole (**16**), and oxindole (**17**) formed during the reaction of V-BrPO with indole (**14**) depended on

¹ The selectivity is defined as the ratio $\frac{\text{Yield (in \%)}}{\text{Substrate Consumed (in \%)}} \times 100$.

mainly formed at low pH and the amount produced decreased as the pH was increased. Indigo (**15**) was only produced between pH 5.5 and 7.5, with a maximum at pH 6.5.

When aqueous bromine was used as a brominating agent, indigo (**15**), 3-bromoindole (**16**), and oxindole (**17**) were also formed, but in much lesser amount (Figure 2.5), and from pH 4 to pH 7 they accounted for only 15-18 % of the products formed (the alternative products have not been characterized). In

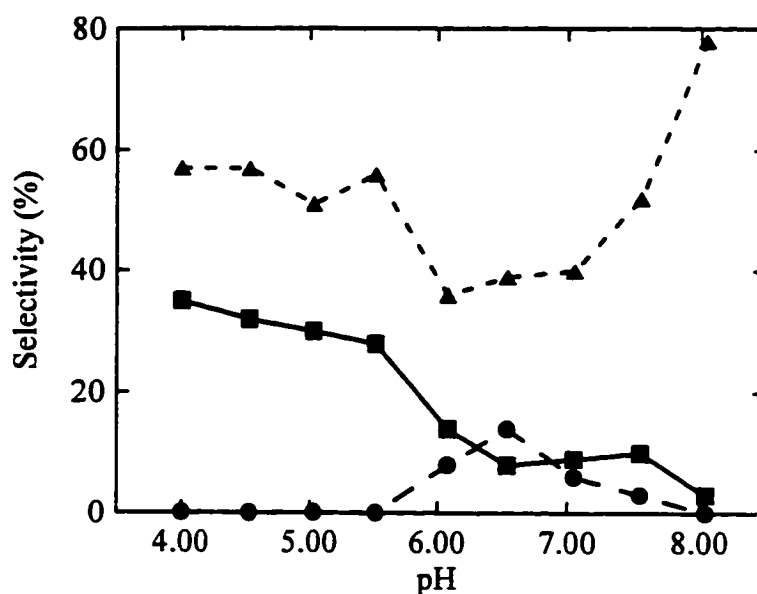


Figure 2.4: Effect of pH on the final product composition of the bromination of indole (**14**) with V-BrPO. Conditions: 100 mM sodium citrate (pH 4.0-5.5) or 100 mM sodium phosphate (pH 6.0-8.0), 50 mM potassium bromide, 10 % ethanol, 1.02 mM **14**, 1.15 mM H_2O_2 and 8.5 nM V-BrPO; (●) Indigo (**15**); (▲) 3-bromoindole (**16**); (■) oxindole (**17**).

contrast to V-BrPO, aqueous bromine did not produce 3-bromoindole (**16**) at low pH, and only traces of indigo (**15**) were formed throughout the pH range.

However, the selectivity of enzymatic and chemical reactions were similar at pH 8.0.

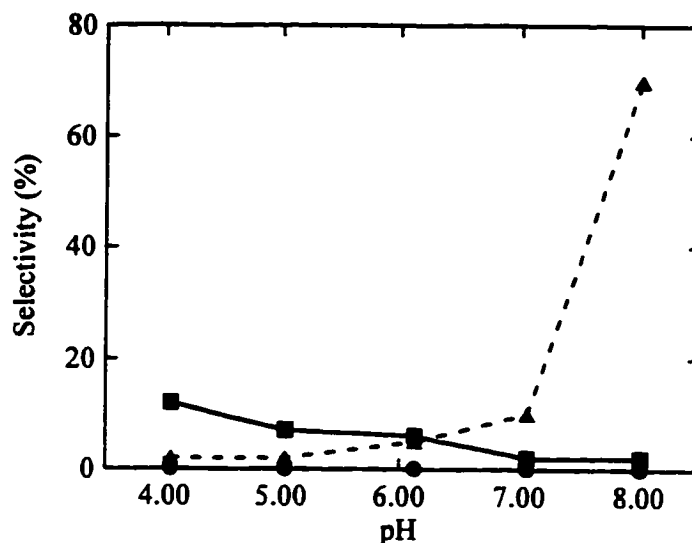
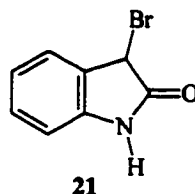


Figure 2.5: Effect of pH on the final product composition of the reaction of aqueous bromine with indole (14). Conditions: 100 mM sodium citrate (pH 4.0-5.0) or 100 mM sodium phosphate (pH 6.0-8.0), 50 mM potassium bromide, 10 % ethanol and 1.02 mM 14. Br₂ (200 mM in 200 mM sodium phosphate pH 8.1) was added equimolar with indole. (●) Indigo (15); (▲) 3-bromoindole (16); (■) oxindole (17).

Bromination of 3-Bromoindole and Oxindole with V-BrPO. V-BrPO also catalyzes a reaction with 3-bromoindole (16). Upon incubation of 16 with V-BrPO and one equivalent of hydrogen peroxide in 100 mM phosphate buffer at pH 6.5 containing 50 mM KBr, several products were formed, of which only isatin (19) (4 %) and 3-bromo-1,3-dihydro-2H-indol-2-one (21) (14 %) were identified. V-BrPO did not catalyze any reaction with oxindole (17) under these conditions.

(19) (4 %) and 3-bromo-1,3-dihydro-2*H*-indol-2-one (21) (14 %) were identified. V-BrPO did not catalyze any reaction with oxindole (17) under these conditions.



Bromination of 1-Methylindole with V-BrPO. Incubation of 1-methylindole (22) with V-BrPO and 1.1 equivalent of hydrogen peroxide resulted in almost quantitative conversion of the substrate, and formation of multiple products (Figure 2.6b). Most of these products had shorter retention times than 22, indicating that they were more polar in nature and suggesting that they are oxygenated products, rather than brominated. Incubation of 22 with 2 or 3 equivalents of hydrogen peroxide resulted in disappearance of some the initial products of the reaction (Figure 2.6c&d; r.t. 1.8 min and r.t. 2.2 min), and appearance of new ones (r.t. 2.6 min and r.t. 3.3 min). In contrast, the HPLC traces obtained for the reaction of 22 with 1, 2 or 3 equivalents of HOBr were different from the ones observed with V-BrPO under similar conditions (Figure 2.6e-f), and only one major product was formed (r.t. 1.8 min).

In order to determine the structures of the products, 40.2 mg (0.306 mmol) of 22 were incubated with V-BrPO in the presence of 0.658 mmol of hydrogen peroxide. After completion of the reaction, the products were extracted with ethyl acetate and separated by reverse phase semi-preparative HPLC. Eight different compounds (23-30) were isolated and characterized by EIMS, ¹H NMR and IR spectroscopy.

The most polar compounds, 1,3-dihydro-3-hydroxy-1-methyl-2*H*-indol-2-one (**23a**) (or its tautomer 1,2-dihydro-2-hydroxy-1-methyl-3*H*-indol-3-one (**23b**)) and 1-methyl-1*H*-indole-2,3-dione (**24**) were initially isolated as a mixture. The

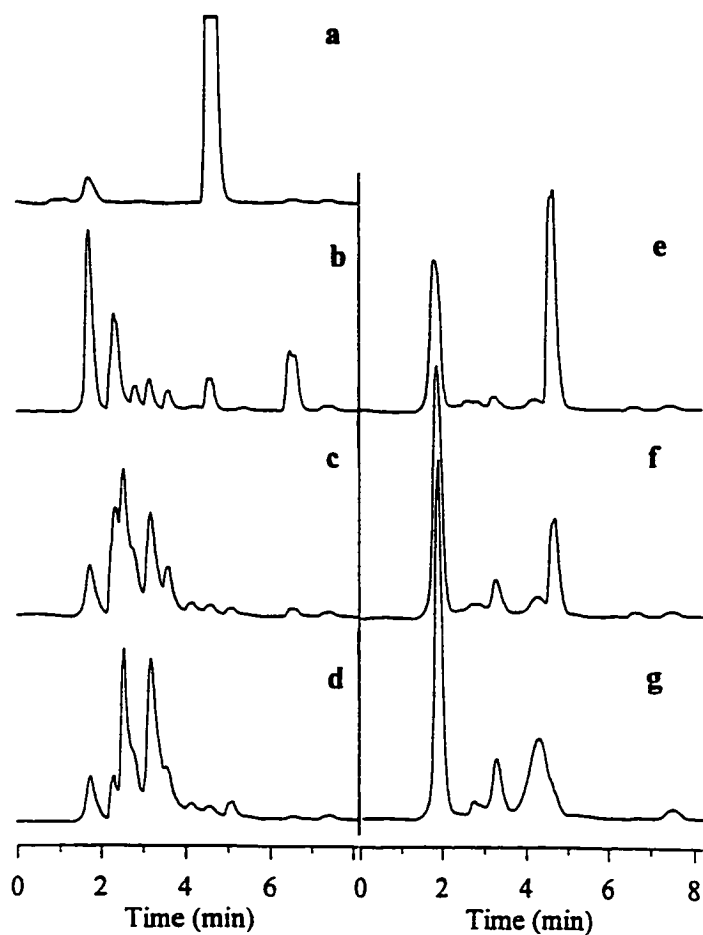
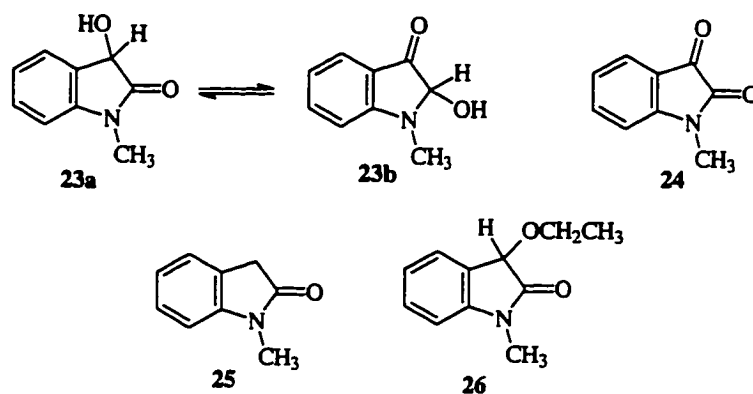


Figure 2.6: HPLC chromatograms of the bromination of 1-methylindole (**22**) by V-BrPO (b,c,d) and HOBr (e,f,g). Conditions: 100 mM sodium phosphate pH 6.5, 100 mM KBr, 20 % ethanol, 1.00 mM 1-methylindole; a) 1-Methylindole (**22**); b) 29.6 nM V-BrPO and 1.13 mM H₂O₂; c) 29.6 nM V-BrPO and 2.26 mM H₂O₂; d) 29.6 nM V-BrPO and 3.39 mM H₂O₂; e) 1.04 mM HOBr; f) 2.08 mM HOBr; g) 3.12 mM HOBr. Reaction times were 1h. Aliquots (20 μ L) of each reaction mixture were then injected on a Spherisorb S5 ODS 2 column eluted with acetonitrile-water (70:30) at 1.2 mL/min. Detection was at $\lambda = 270$ nm.

two compounds were then further separated by HPLC and obtained in 4 % and 5 % yields, respectively. EIMS of **23** showed a molecular ion at m/z 163, in agreement with a structure comprising a 1-methylindole moiety and two additional oxygen atoms ($C_9H_9NO_2$). The four coupled aromatic protons observed in the NMR spectrum, δ 6.81 (d, $J = 7.5$ Hz, 1H), 7.08 (t, $J = 7.5$ Hz, 1H), 7.32 (t, $J = 7.5$ Hz, 1H), 7.43 (d, $J = 7.5$ Hz) indicated that the benzene ring was not substituted. The single proton at δ 5.03 (s, 1H) and the IR absorption bands at 3300 cm^{-1} established the secondary hydroxyl group. The presence of the carbonyl group was confirmed by the IR absorption at 1700 cm^{-1} .

Compound **24** had a EIMS molecular ion at m/z 161 and a base peak at m/z 104 accounting for the loss of a C_2H_3NO fragment. ^1H NMR analysis established

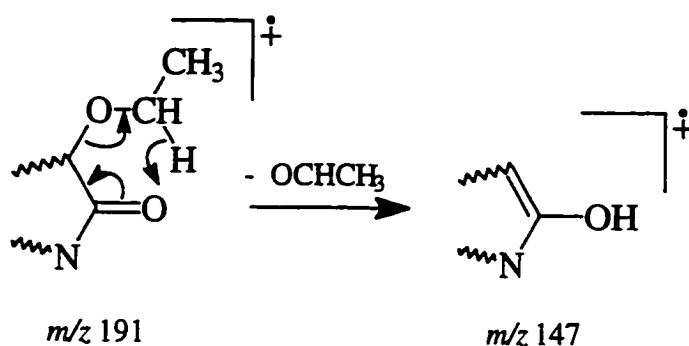


the presence of 4 aromatic protons at δ 6.87 (d, $J = 7.5$ Hz, 1H), 7.11 (t, $J = 7.5$ Hz, 1H), 7.58 (t, $J = 7.5$ Hz, 1H), 7.58 (d, $J = 7.5$ Hz, 1H). The presence of two carbonyl functions was evident from the strong IR absorption at 1780 cm^{-1} . Open chain 1,2-diketones generally have bands at $1730\text{--}1710\text{ cm}^{-1}$, but when included in

a 5-membered ring they are forced into a *s-cis* configuration that raises the absorption frequency by *ca.* 50 cm^{-1} .

1,3-dihydro-1-methyl-2*H*-indol-2-one (**25**) was isolated in 2 % yield. Its structure was established on the basis of its EIMS molecular ion at m/z 147, the presence of a strong IR absorption band at 1705 cm^{-1} , characteristic of 5-membered ring lactams, and the ^1H NMR signals at δ 3.19 (s, 3H), 3.50 (s, 2H).

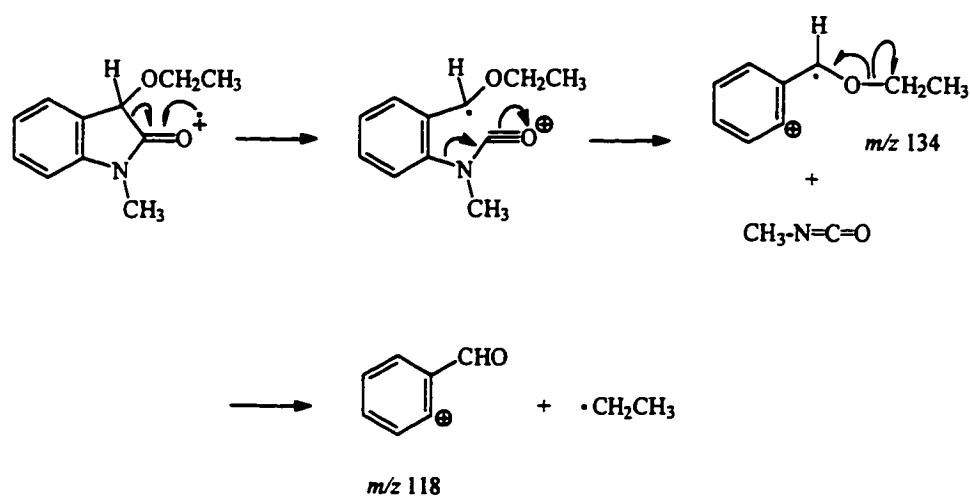
The next product isolated was 1,3-dihydro-3-ethoxy-1-methyl-2*H*-indol-2-one (**26**) (1%). The EIMS included a weak molecular ion at m/z 191 (15), a base fragment at m/z 147, and two fragmentation ions at m/z 134 (41) and 118 (41). The base ion indicated loss of a $\text{C}_2\text{H}_4\text{O}$ fragment that was due to a primary rearrangement fragmentation typical for carbonyl compounds having a γ -hydrogen (Scheme 2.1). The two other ions observed were attributed to successive losses of CH_3NCO and C_2H_5 fragments and established the relative positions of the carbonyl and ethoxy functions (Scheme 2.2). The presence of those two groups was further confirmed by the ^1H NMR resonances at δ 1.25 (t, $J = 7.5$ Hz, 3H, $\text{CH}_3\text{CH}_2\text{O}$ -), 3.66 (dq, $J = 7.5$ Hz and $J = 8.7$ Hz, 1H), 3.86 (dq, $J = 7.5$ Hz and J



Scheme 2.1

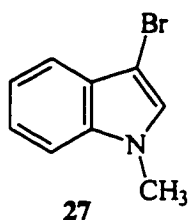
= 8.7 Hz, 1H) and the strong IR absorption bands at 1715 cm^{-1} (C=O) and 1115 cm^{-1} (C-O).

The major product isolated from the bromination of 1-methylindole by V-

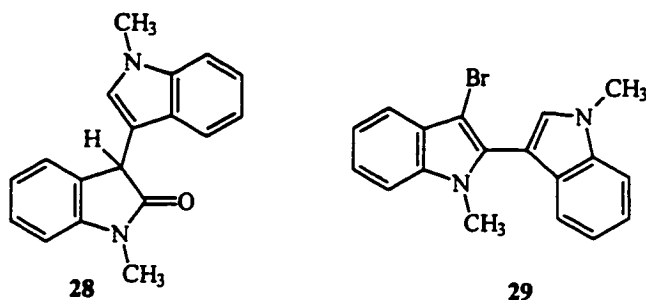


Scheme 2.2

BrPO, under the 2/1 H_2O_2 /1-methylindole conditions, was 3-bromo-1-methylindole (**27**) (13 %). EIMS of **27** showed molecular ion peaks at m/z 211 and 209 split into a 1:1 ratio and a fragmentation ion at m/z 130 due to loss of a bromine atom. The ^1H NMR spectrum was identical to the one obtained for an authentic sample of **27**.

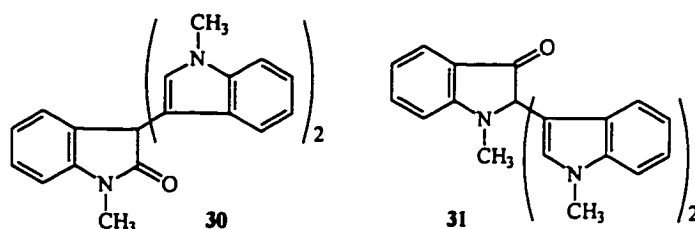


1,3-Dihydro-1-methyl-3-(1-methyl-1*H*-indol-3-yl)-2*H*-indol-2-one (**28**) was obtained in 2 % yield. The EIMS spectrum had a molecular ion at m/z 276 consistent with the molecular formula $C_{18}H_{16}N_2O$ and clearly indicated that **28** was a coupling product. The 1H NMR spectrum showed two different methyl signals at δ 3.28 (s, 3H), and δ 3.72 (s, 3H), a methine proton, at δ 3.87 (s, 1H) and nine aromatic protons at δ 6.90 (d, $J = 7.5$ Hz, 1H), 6.94 (s, 1H), 6.99 (t, $J = 7.5$ Hz, 1H), 7.19 (t, $J = 8$ Hz, 1H), 7.24 (m, 4H) and 7.30 (t, $J = 7.5$ Hz, 1H). The aromatic protons indicated that the indole units were not linked *via* the benzene rings. The singlet at 6.94 ppm was likely due to a proton situated at the C-2 of one of the indole rings and suggested strongly that this indole unit was substituted at the C-3 position. The strong IR absorption band at 1720 cm^{-1} indicated the presence of a carbonyl included in a 5 membered ring, possibly a lactam. The methyl signal at 3.28 ppm was consistent with the carbonyl being adjacent to the nitrogen bearing the methyl group and confirmed the presence of a lactam functionality.



The brominated biindole **29** was isolated in 5 % yield. The presence of the bromine atom was confirmed by EIMS. The molecular ion peak was at m/z 340 and 338 in a 1:1 ratio. In addition, a fragmentation ion at m/z 260 was consistent with loss of a bromine atom. The 1H NMR included eight benzene protons and a

singlet at δ 7.25 (1H) indicating that the bromine atom as well as the indole-indole linkage were on the pyrrole rings. The chemical shift of the singlet suggested strongly that the proton was located on one of the C-2 positions (C-3 protons generally appear at higher fields, between δ 6.50 and δ 6.80 (Bocchi & Palla, 1984)). Consequently, the indole-indole linkage had to be either 2,3' or 3,3'. The 3,3' linkage was eliminated on the basis of the facts that direct coupling of two indoles at the 3 position is highly unfavorable and that 3-bromo-1-methylindole (27) has been shown to couple with 1-methylindole (22) to form the 2,3'-biindole (Bocchi & Palla, 1984).



The condensation product **30** and its isomer **31** were isolated in 3 % and 2 % yields, respectively. Both compounds had an identical molecular ion peak at m/z 405, consistent with the molecular formula of $C_{27}H_{23}N_3O$. The IR spectra of **30** and **31** were almost identical, and included a strong absorption band at *ca.* 1720 cm^{-1} indicating the presence of a carbonyl group. The 1H NMR spectra of **30** and **31** revealed that both compounds were formed from three indole units, of which two were equivalent (Figure 2.7). The single indole group of each compound had one methyl group and four aromatic protons, indicating that the two other units were attached to the same carbon atom (either C-2 or C-3), with the carbonyl function residing on the remaining carbon. The indole methyl group of the single

indole unit bearing the carbonyl group of compound **30** and compound **31** had a chemical shift of δ 3.31 and 2.94, respectively. It was concluded that **30** had the carbonyl at the C-2 position, whereas the carbonyl of **31** was located on the C-3 position.

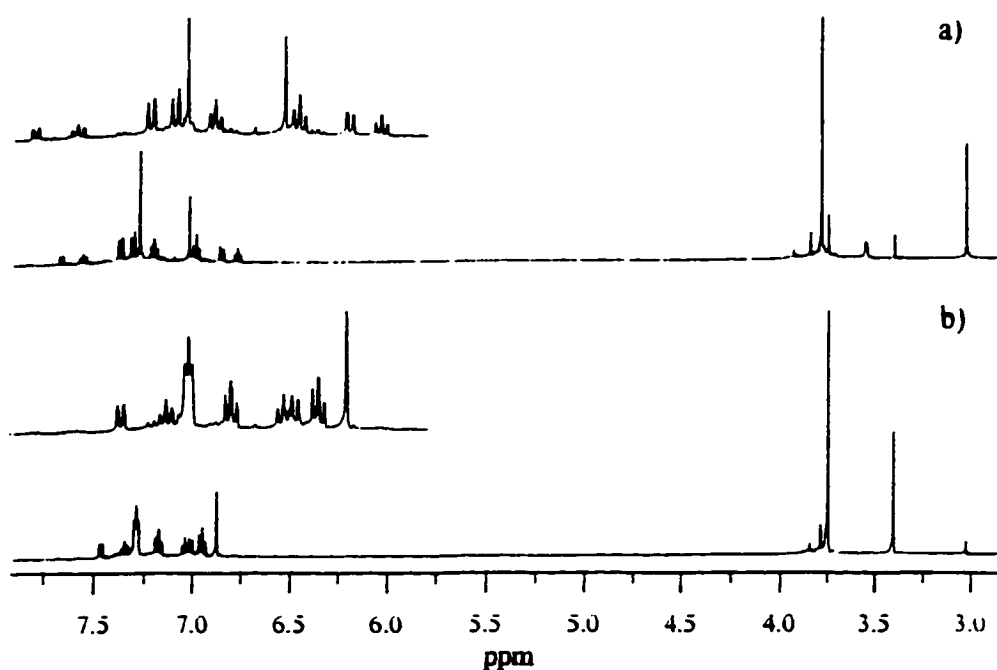


Figure 2.7: ¹H NMR of a) **30** and b) **31**.

Bromination of 2-Methylindole by V-BrPO. When 2-methylindole (**32**) was incubated with V-BrPO and one equivalent of hydrogen peroxide, **32** was almost quantitatively converted to a single product (Figure 2.8b). Bromination of **32** with one equivalent of HOBr gave similar results (Figure 2.8c). The product

was first identified as 3-bromo-2-methylindole (**33**) by HPLC co-injection with an authentic sample of **33**. The structure of **33** was confirmed by isolating **33**, in 67 % yield, from an incubation of **32** (1.98 mmol) with V-BrPO and hydrogen peroxide (1.95 mmol). The ^1H NMR spectrum of **33** was consistent with the loss of the C-3 proton of **32**, and the EIMS showed a molecular ion peaks at m/z 211 and 209 (split into a 1:1 ratio) and a fragmentation ion at m/z 130 due to the loss of a bromine atom.

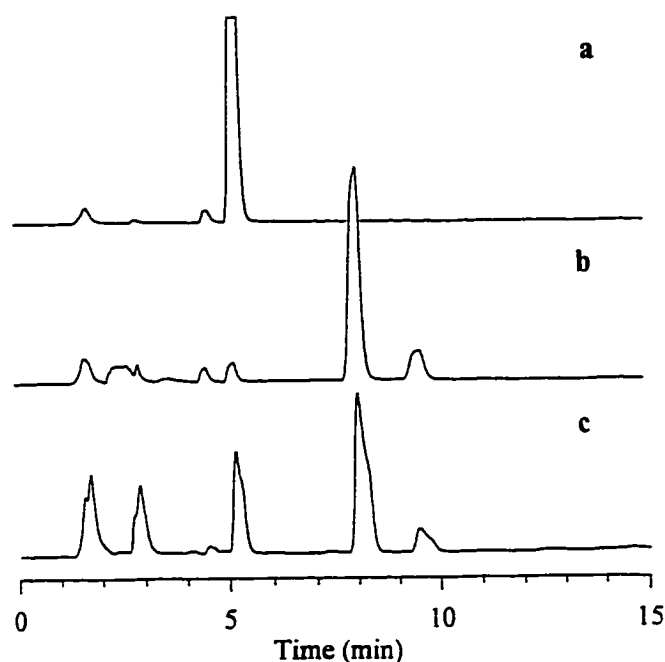
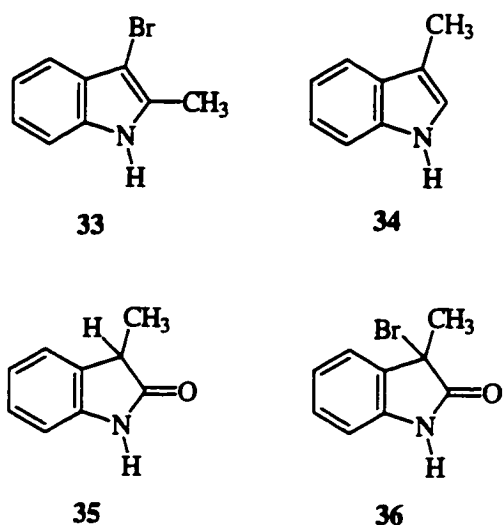


Figure 2.8: HPLC chromatograms of the bromination of 2-methylindole (**32**) by V-BrPO (b) and HOBr (c). Conditions: 100 mM sodium phosphate pH 6.5, 100 mM KBr, 20 % ethanol, 1.07 mM 1-methylindole; a) 2-Methylindole (**32**); b) 29.6 nM V-BrPO and 1.13 mM H_2O_2 ; c) 1.04 mM HOBr. Reaction times were 1h. Aliquots (20 μL) of each reaction mixture were then injected on a Spherisorb S5 ODS 2 column eluted with acetonitrile-water (70:30) at 1.2 mL/min. Detection was at $\lambda = 270$ nm.



Bromination of 3-Methylindole by V-BrPO. HPLC analysis of an incubation of 3-methylindole (**34**) with V-BrPO and one equivalent of hydrogen peroxide showed that the reaction yielded one major product, 1,3-dihydro-3-methyl-2*H*-indol-2-one (**35**), with a retention time of 3.0 min (Figure 2.9d). No further products were formed upon incubation with excess hydrogen peroxide (two or three equivalents), suggesting that V-BrPO did not react with the initial product formed (Figure 2.9c&d). Reaction of **34** with one equivalent of HOBr also gave quantitative conversion of **34** to **35** (Figure 2.9e). However, reaction of **34** with two equivalents of HOBr resulted in disappearance of **35** and formation of a new product with a retention time of 3.9 min (Figure 2.9f). Although this product has not been characterized in this study, the previously published data on bromination of **34** and **35** suggest strongly that it is 3-bromo-1,3-dihydro-3-methyl-2*H*-indol-2-one (**36**) (Hinman & Bauman, 1963).

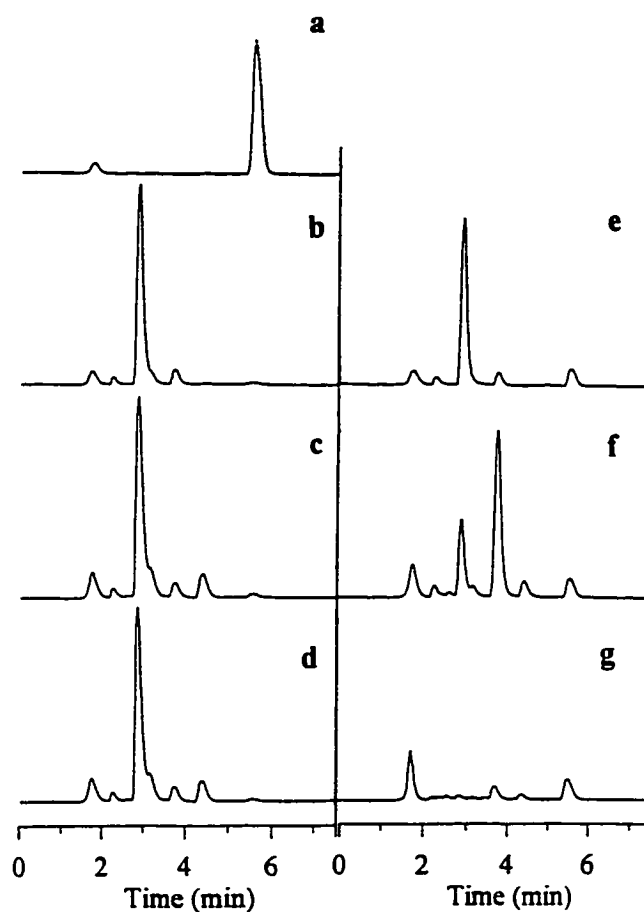
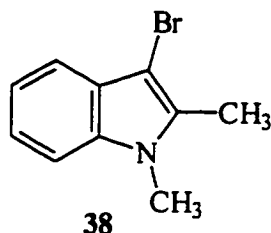


Figure 2.9: HPLC chromatograms of the bromination of 3-methylindole (**34**) with V-BrPO (b,c,d) and with HOBr (e,f,g). Conditions: 100 mM sodium phosphate pH 6.5, 100 mM KBr, 20 % ethanol, 1.00 mM **34**; a) 3-Methylindole (**34**); b) 29.6 nM V-BrPO and 1.13 mM H₂O₂; c) 29.6 nM V-BrPO and 2.26 mM H₂O₂; d) 29.6 nM V-BrPO and 3.39 mM H₂O₂; e) 1.04 mM HOBr; f) 2.08 mM HOBr; g) 3.12 mM HOBr. Reaction times were 1h. Aliquots (20 μ L) of each reaction mixture were then injected on a Spherisorb S5 ODS 2 column eluted with acetonitrile-water (70:30) at 1.2 mL/min. Detection was at $\lambda = 270$ nm.

The product **35** was isolated in 69 % yield from an incubation of **34** (1.44 mmol) with V-BrPO and hydrogen peroxide (1.96 mmol). EIMS of **35** showed a

molecular ion peak at m/z 147, corresponding to a molecular formula of C_9H_9NO , and a fragmentation ion at m/z 119 ($M^+ - 28$), indicating the loss of either C_2H_4 or CO. The 1H NMR displayed the signal due to a methyl group at δ 1.51 (d, $J = 7.8$ Hz, 3H) coupled to a methine proton at δ 3.47 (q, $J = 7.8$ Hz, 1H), consistent with 3-methyl-2-oxindole (**35**).

1,2-Dimethylindole. Bromination of 1,2-dimethylindole (**37**) by V-BrPO with one equivalent of hydrogen peroxide gave one major product (**38**) (Figure 2.10b). When the reaction was carried out with two equivalents of hydrogen peroxide, the initial product was also consumed to form several unidentified products (Figure 2.10c). In contrast, bromination of **37** with HOBr (one or two equivalents) produced only traces of **38** (Figure 2.10d&e). Isolation of the product of an incubation of **37** (2.01 mmol) with V-BrPO and hydrogen peroxide (1.95 mmol) gave 3-bromo-1,2-dimethylindole (**38**) in 72 %. The EIMS spectrum of **38** included molecular ions peaks at m/z 225 and 223 split into a 1:1 ratio, and fragmentation ions at m/z 144 and 115 attributed to loss of a bromine atom and subsequent loss of a CH_3N fragment, respectively. The 1H NMR spectrum showed two methyl groups at δ 2.44 (s, 3H) and 3.68 (s, 3H) and four aromatic protons at δ 7.15 (t, $J = 7.5$ Hz, 1H), 7.20 (t, $J = 7.5$ Hz, 1H), 7.25 (d, $J = 7.5$ Hz, 1H), 7.48 (d, $J = 7.5$ Hz, 1H), and clearly indicated that the bromine was located on the C-3 position.



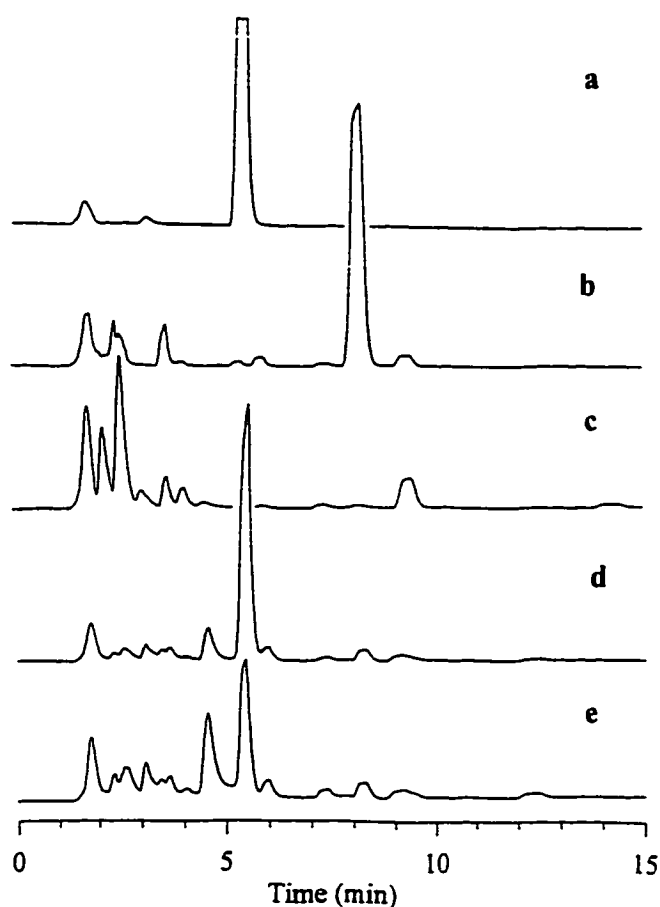


Figure 2.10: HPLC chromatograms of the bromination of 1,2-dimethylindole (**37**) with V-BrPO (b,c) and with HOBr (d,e). Conditions: 100 mM sodium phosphate pH 6.5, 100 mM KBr, 20 % ethanol, 1.00 mM **37**; a) 1,2-Dimethylindole (**37**); b) 29.6 nM V-BrPO and 1.13 mM H₂O₂; c) 29.6 nM V-BrPO and 2.26 mM H₂O₂; d) 1.04 mM HOBr; e) 2.08 mM HOBr. Reaction times were 1h. Aliquots (20 μ L) of each reaction mixture were then injected on a Spherisorb S5 ODS 2 column eluted with acetonitrile-water (80:20) at 1.2 mL/min. Detection was at $\lambda = 270$ nm.

2-Phenylindole. Figure 2.11b&c shows the HPLC analysis of the bromination of 2-phenylindole (**39**) by V-BrPO with one and two equivalents of hydrogen peroxide. When one equivalent of hydrogen peroxide was used, 2-

phenylindole was converted to a single product (**40**) (Figure 2.11b) that was further converted to a second product (**41**) upon addition of a second equivalent of hydrogen peroxide (Figure 2.11c). Bromination of **39** with HOBr gave the same HPLC profile (Figure 2.11d).

The initial product was 3-bromo-2-phenylindole (**40**) and was isolated in 39 % yield from a reaction containing hydrogen peroxide in a molar excess with

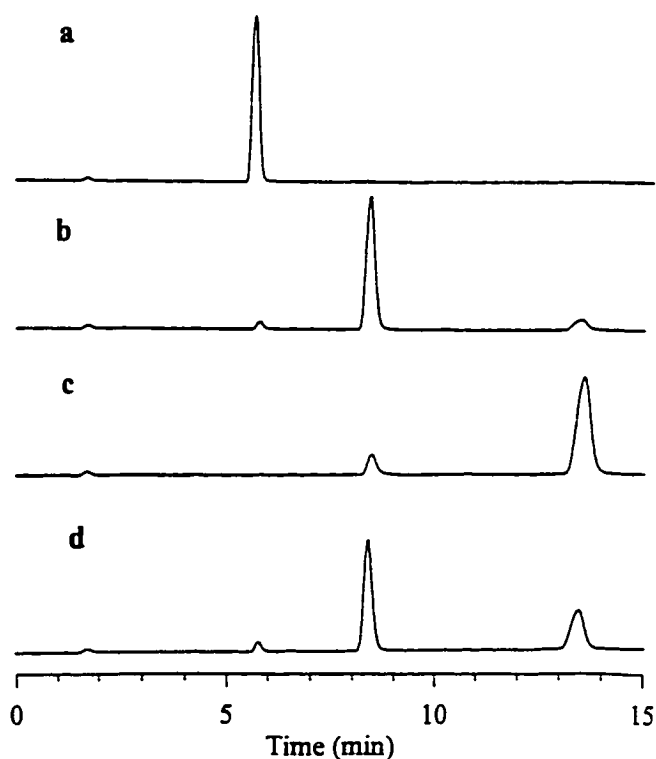
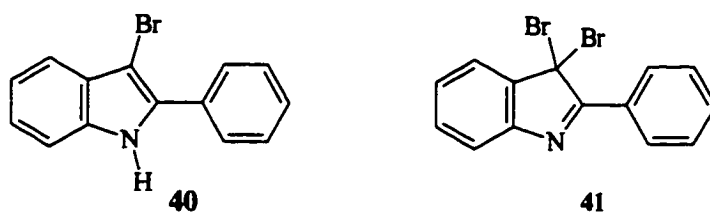


Figure 2.11: HPLC chromatograms of the bromination of 2-phenylindole (**39**) by V-BrPO. Conditions: 100 mM sodium phosphate pH 6.5, 100 mM KBr, 20 % ethanol, 1.00 mM **39**; a) 2-Phenylindole (**39**); b) 29.6 nM V-BrPO and 1.13 mM H₂O₂ ; c) 29.6 nM V-BrPO and 2.26 mM H₂O₂; d) 1.25 mM HOBr. Reaction times were 1h. Aliquots (20 μ L) of each reaction mixture were then injected on a Spherisorb S5 ODS 2 column eluted with acetonitrile-water (80:20) at 1.2 mL/min. Detection was at $\lambda = 310$ nm.

respect to **39** of 1.5. The EIMS spectrum of **40** had a molecular ion peak at m/z 273 and 271 split in a 1:1 ratio and indicated the presence of a bromine atom. The ^1H NMR spectrum indicated that the C-3 proton had been substituted. The product of the subsequent bromination of **40** had EIMS molecular ion peak(s) at m/z 353, 351 and 349 in a 1:2:1 ratio indicating the presence of two bromine atoms. The structure of this compound could not be unambiguously determined. Earlier work on the chlorination of **39** by sodium hypochlorite (NaOCl) suggest, however, that this compound could be 3,3-dibromo-2-phenyl-3*H*-indole (**41**) (De Rosa et al., 1981).



Bromination of 3-Phenylindole by V-BrPO. HPLC analysis of the incubation of 3-phenylindole (**42**) with V-BrPO and with one equivalent of hydrogen peroxide indicated the production of several products (Figure 2.12b). Addition of excess hydrogen peroxide did not appear to greatly modify the number and nature of the products formed (Figure 2.12c). Bromination of **42** with two equivalents of HOBr appeared to produce the same products (Figure 2.12d). In order to determine the structure of the products formed by the enzymatic reaction, the reaction was carried out on a large scale (0.50 mmol of **42** and 0.57 mmol of hydrogen peroxide) and extracted with ethyl acetate upon completion. Silica gel chromatography of the extract gave six different products.

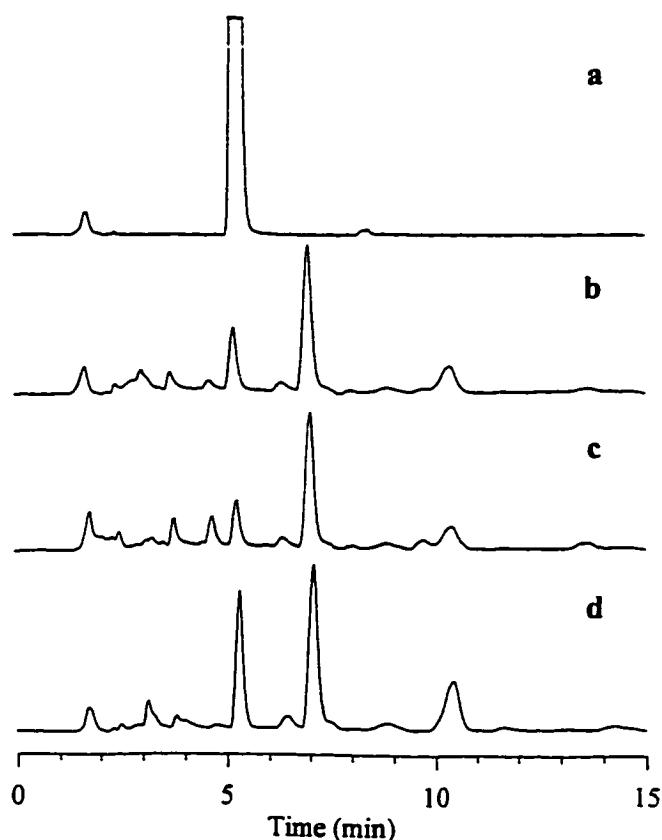
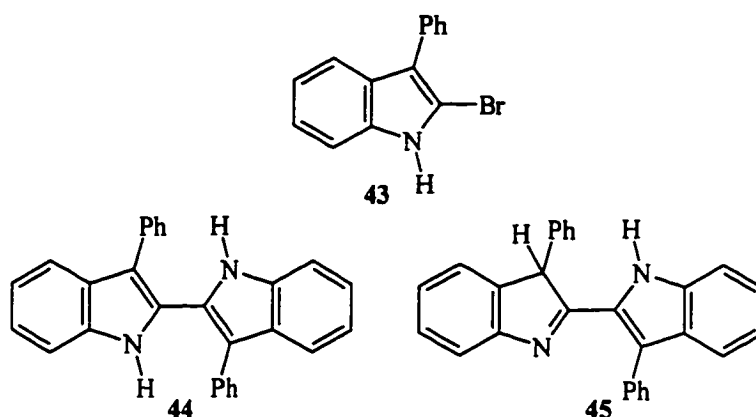


Figure 2.12: HPLC chromatograms of the bromination of 3-phenylindole (**42**) with V-BrPO (b,c) and with HOBr (d). Conditions: 100 mM sodium phosphate pH 6.5, 100 mM KBr, 20 % ethanol, 1.00 mM **42**; a) 3-Phenylindole (**42**); b) 29.6 nM V-BrPO and 1.13 mM H₂O₂; c) 29.6 nM V-BrPO and 2.26 mM H₂O₂; d) HOBr 1.04 mM. Reaction times were 1h. Aliquots (20 μ L) of each reaction mixture were then injected on a Spherisorb S5 ODS 2 column eluted with acetonitrile-water (80:20) at 1.2 mL/min. Detection was at $\lambda = 310$ nm.

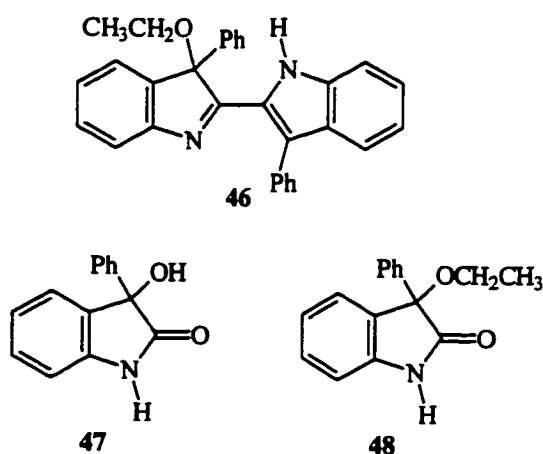
2-Bromo-3-phenylindole (**43**) was isolated in 6 % yield. Its EIMS spectrum showed molecular ion peaks at m/z 273 and 271 in a 1:1 ratio and a fragmentation ion at m/z 192 arising from the loss of a bromine atom. The ¹H NMR spectrum indicated the presence of the indole N-H proton at δ 8.19 (s, 1H),

confirmed by the sharp IR absorption band observed at 3380 cm^{-1} , and the absence of the C-2 proton resonance. The ^1H NMR spectrum of **43** was clearly distinct from the spectrum obtained with its positional isomer **41**.

The major products identified were 3,3'-diphenyl-2,2'-bi-1*H*-indole (**44**) (24 %) and its isomer 3-phenyl-2-(3-phenyl-3*H*-indol-2-yl)-1*H*-indole (**45**) (13 %). Both compounds were characterized by EIMS molecular ion peaks at m/z 384 consistent with molecular formulas of $\text{C}_{28}\text{H}_{20}\text{N}_2$. The ^1H NMR spectrum of **44** consisted of 8 distinct aromatic signals accounting for 10x2 protons and indicated that the compound was a symmetric dimer. The presence of 2 indole protons at δ 8.01 (s, 2H) and the absence of any C-2 proton resonance indicated also that the presence of a 2,2' linkage between indole units. The ^1H NMR spectrum of **45**, on the other hand, showed 18 different resonances accounting for 20 protons and included a methine proton at δ 4.95 (s, 1H) and only one single indole N-H proton at δ 8.15 (s, 1H). The IR spectrum had a strong absorption band at 1520 cm^{-1} consistent with the presence, in **45**, of an imine function that explained the loss of one indole proton observed in the ^1H NMR spectrum..



The next compound identified was 3-phenyl-2-(3-ethoxy-3-phenyl-3*H*-indol-2-yl)-1*H*-indole (**46**). The EIMS of **46** had a molecular ion peak at m/z 428, in agreement with a molecular formula of $C_{30}H_{24}N_2O$, and two fragmentation ions at m/z 399 and 351 consistent with the loss of a C_2H_5 and a C_6H_5 (phenyl) group, respectively. The 1H NMR spectrum had signals at δ 1.12 (t, $J = 7$ Hz, 3H), 3.64 (dq, $J = 10$ and $J = 7$ Hz, 1H), 4.12 (dq, $J = 10$ and $J = 7$ Hz, 1H) characteristic of an ethoxy group containing two magnetically unequivalent methylene protons. In addition, the presence of a single indole proton at δ 7.88 (s, 1H) and the IR absorption band observed at 1580 cm^{-1} confirmed the 2,2' linkage, and the presence of a imine function.



1,3-dihydro-3-hydroxy-3-phenyl-2*H*-indol-2-one (**47**) and 1,3-dihydro-3-ethoxy-3-phenyl-2*H*-indol-2-one (**48**) were obtained in 3% and 7 % yield, respectively. The EIMS of **47** had a molecular ion peak at m/z 225 consistent with a molecular formula of $C_{14}H_{11}NO_2$. The two main fragmentation ions were observed at m/z 197 and m/z 196 and accounted for loss of CO and CHO, indicating the presence of a carbonyl group. In addition, the IR carbonyl

stretching frequency observed at 1680 cm^{-1} , typical for a lactam in a 5-member ring, and the down field shift of the N-H resonance signal at 9.34 ppm further indicated that the carbonyl was located on the C-2 position. The EIMS of **48** had a molecular ion peak at m/z 253 consistent with a molecular formula of $\text{C}_{16}\text{H}_{15}\text{NO}_2$. The a lactam function was confirmed by the IR band at 1700 cm^{-1} .

Bromination of 2-tert-Butylindole by V-BrPO. Incubation of 2-tert-butylindole (**49**) with V-BrPO and one equivalent of hydrogen peroxide gave one

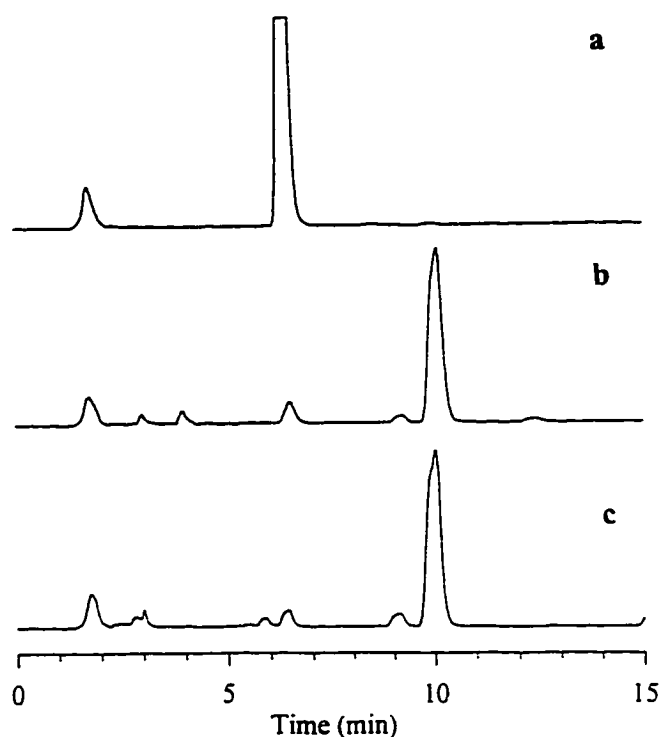


Figure 2.13: HPLC chromatograms of the bromination of 2-*tert*-butylindole (**49**) by V-BrPO (b) and HOBr (c). Conditions: 100 mM sodium phosphate pH 6.5, 100 mM KBr, 20 % ethanol, 1.07 mM **49**; a) 2-*tert*-Butylindole (**49**); b) 29.6 nM V-BrPO and 1.13 mM H_2O_2 ; c) 1.04 mM HOBr. Reaction times were 1h. Aliquots (20 μL) of each reaction mixture were then injected on a Spherisorb S5 ODS 2 column eluted with acetonitrile-water (80:20) at 1.2 mL/min. Detection was at $\lambda = 270\text{ nm}$.

main product (Figure 2.13b). Bromination of **49** with one equivalent of HOBr gave the same result (Figure 2.13c). The product was unstable under the isolation procedure and could not be identified.

Bromination of 3-tert-Butylindole by V-BrPO. Incubation of 3-tert-butylindole (**50**) with V-BrPO and 1 equivalent of hydrogen peroxide gave one

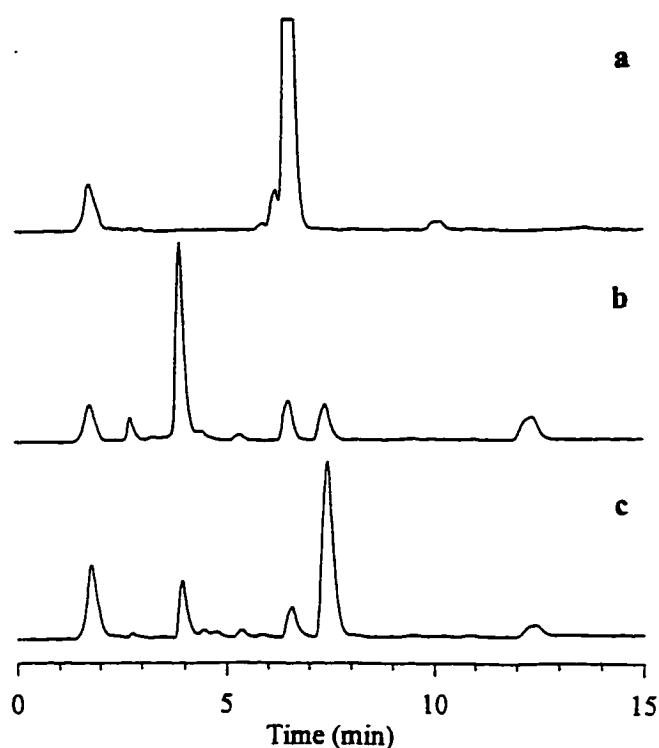
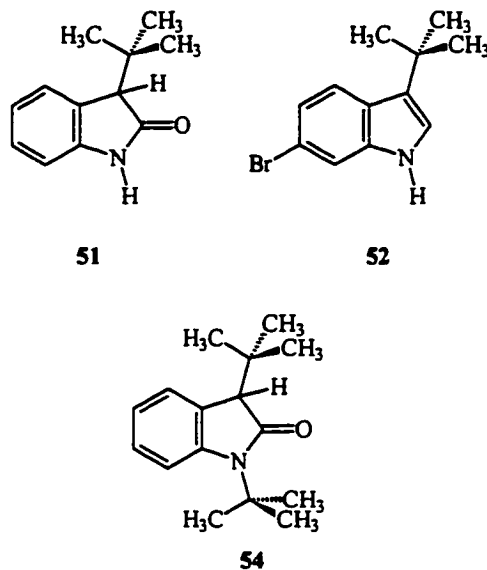


Figure 2.14: HPLC chromatograms of the bromination of 3-tert-butylindole (**50**) by V-BrPO (b) and HOBr (c). Conditions: 100 mM sodium phosphate pH 6.5, 100 mM KBr, 20 % ethanol, 1.07 mM **50**; a) 3-tert-Butylindole (**50**); b) 29.6 nM V-BrPO and 1.13 mM H₂O₂; c) 1.04 mM HOBr. Reaction times were 1h. Aliquots (20 μ L) of each reaction mixture were then injected on a Spherisorb S5 ODS 2 column eluted with acetonitrile-water (80:20) at 1.2 mL/min. Detection was at $\lambda = 270$ nm.

major product (Figure 2.14b). Isolation of the product gave 1,3-dihydro-3-*tert*-butyl-2*H*-indol-2-one (**51**) in 91 % yield. The ^1H NMR spectrum of **51** included a methine proton at δ 3.30 (s, 1H) respectively, adjacent to a carbonyl function, identical to the one found in the literature (Hino et al., 1977). In contrast, **51** was a minor product when **50** was brominated using one equivalent of HOBr (Figure 2.14c).² The major product, eluting with a retention time of 7.6 min was not identified, but a previous study on the bromination of **50** suggested that it was 6-bromo-3-*tert*-butylindole (**52**).



Bromination 1,3-Di-tert-Butylindole by V-BrPO. 1,3-Bi-*tert*-butylindole (**53**) was brominated by V-BrPO and gave 1,3-dihydro-3-hydroxy-1,3-di-*tert*-butyl-2*H*-indol-2-one (**54**) in 84 % yield. The ^1H NMR spectrum of **54** included

²This result is to be taken with caution. Gretchen Meister and Michelle Testor have found that, in their hands, the reaction of 3-*tert*-butylindole with V-BrPO or with HOBr gave the same product, as determined by HPLC analysis. This product as yet to be unambiguously identified.

a methine proton at δ 2.92 (s, 1H), adjacent to a carbonyl function, identical to the one found in the literature (Hino et al., 1977).

Bromination of Indole and 3-Methylindole by V-BrPO using $H_2^{18}O_2$
Indole and 3-methylindole were brominated by V-BrPO using 99 % ^{18}O enriched hydrogen peroxide, and the oxygenated products (indigo (15) and 3-methyl-2-oxindole (17)) rapidly isolated in order to minimize loss of ^{18}O by exchange with water. EIMS analysis of the products showed molecular ion peak at m/z 262 and 147 for 15 and 17, respectively (Fig. 2.15a&b) and absence of molecular ion peaks at m/z 266 (and/or 264) and 149.

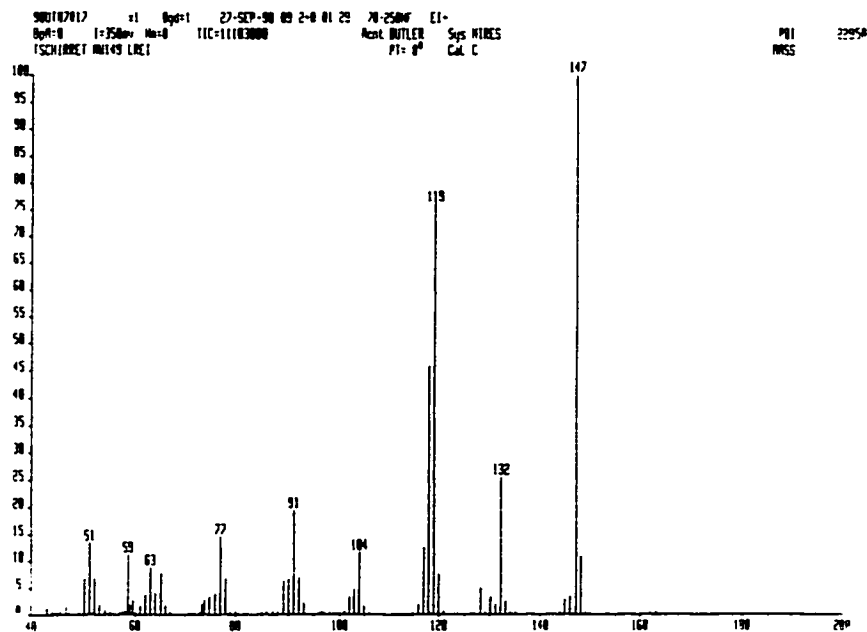


Figure 2.15a: EIMS spectrum of 15 isolated from incubation of 14 with V-BrPO and ^{18}O enriched hydrogen peroxide.

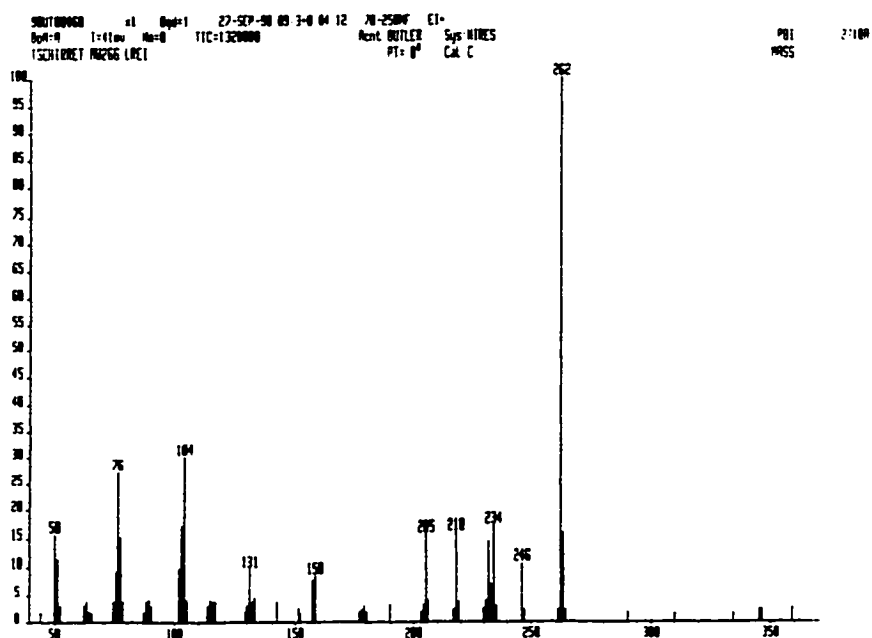
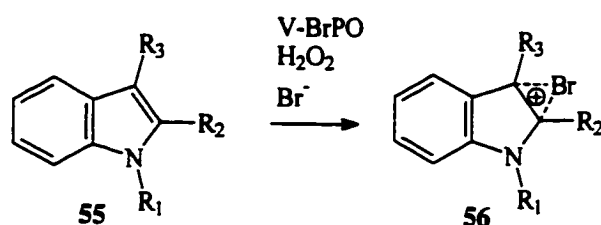


Figure 2.15b: EIMS spectrum of **34** isolated from incubation of **33** with V-BrPO and ^{18}O enriched hydrogen peroxide.

Discussion

V-BrPO was found to react efficiently with alkyl and aryl indoles. The products observed were consistent with a mechanism including a rapid initial pre-equilibrium in which the electrophilic brominating species (Br^+ , Br_2 , Br_3^- , or Enz-Br) attacks the indole molecule at the electron rich double bond of the pyrrole ring (De Fabrizio, 1968) (Scheme 2.3). The fate of the resulting bromoindolinium cation (**56**) depended on the position and nature of the substituents.

The major products isolated from the bromination of indole (**14**) by V-



Scheme 2.3.

BrPO were indigo (**15**), 3-bromoindole (**16**) and oxindole (**17**) (The mechanism of formation of indigo is presented in more detail in Chapter 3). The oxidation state of indigo indicates clearly that indigo is not a primary product of the reaction but that it is the product of further oxidation steps after the initial bromination. Although indoxyl has not been detected in the course of the reaction, there is strong evidence that it is formed initially, and that it is a precursor of indigo (see Chapter 3). The formation of 3-bromoindole **16** and oxindole **17** is in agreement with all previous reports that stressed the competition between substitution

(mainly at the C-3) and oxidation at the C-2 position in the course of the bromination reaction of indoles in aqueous media with various halogenating reagents (Hinman & Bauman, 1963; Da Settimo & Nannipieri, 1970; Da Settimo et al., 1977). Although oxindole (**17**) likely arises from the conversion of the postulated bromonium intermediate **56** ($R_1=R_2=R_3=H$) (tautomeric with a 3-bromo-indolonium ion), *via* its hydrated form it may also be produced by the hydrolysis of 3-bromoindole since it has been shown that 3-haloindoles are converted to oxindoles under acidic conditions (Weissgerber, 1913).

The pH dependence of the product selectivity of the bromination of indole by V-BrPO and aqueous bromine were markedly different (Fig. 2.6 & 2.7). In each case, the product selectivity observed appeared to depend not only on the fate of the bromonium intermediate **56** ($R_1=R_2=R_3=H$) as a function of the pH but also on the relative composition of the brominating species in the media at the given pH. Indeed, aqueous bromine solutions are complex mixtures of Br_2 , Br_3^- , HOBr, BrO^- , and unreactive Br^- , for which the concentrations depend on the pH and bromide concentration (Ziderman, 1972; Palou, 1994).³ From pH 4 to 7, 3-bromoindole and 2-oxindole accounted for only *ca.* 15 % of the products formed from the reaction of indole with aqueous bromine⁴ (Fig. 2.7). In contrast, at pH 8 3-bromoindole became the major product formed (*ca.* 70 % of the product formed). Earlier studies on indole halogenation have shown that loss of the

³ At an initial concentration of Br_2 of 1 mM, hypobromous is the predominant species from pH= 5 to pH=8, whereas Br_2/Br_3^- is the main component at pH<5. At pH=8 BrO^- accounts for *ca.* 90 % of the composition.

⁴ Those reactions gave complex mixtures of product of which only **16** and **17** could be identified. It appears that in acidic conditions, bromination of indole with equimolar amount of bromine does not generally give definite products (Da Settimo et al., 1977)

proton from the haloindolinium cation **56** ($R_1=R_2=R_3=H$) was a slow process (De Fabrizio, 1968) since there was a strong isotope effect on the overall reaction rate when the C-3 proton was replaced with deuterium. In addition, bromination of indole in acetic acid with 1:1 or 3:1 mole ratio of bromine with respect to indole did not yield definite products (Da Settimo et al., 1967; Da Settimo et al., 1977).⁵ On the other hand, bromination of indole in dimethylformamide with 1:1 mole ratio of bromine gave 3-bromoindole quantitatively (Bocchi & Palla, 1982). The difference was attributed to the mildly basic character of dimethylformamide that played an essential role, promoting hydrogen abstraction and trapping the hydrobromic acid produced during the reaction. Those results are consistent with the pH dependence for the bromination of indole by aqueous bromine, but they do not explain the selectivity observed for the V-BrPO catalyzed reaction and raise questions about the possible role of the enzyme during bromination. On the one hand, the nature of the brominating intermediate formed by V-BrPO may resemble hypobromite and therefore form 3-bromoindole throughout the pH range investigated (i.e. pH 4 to 8). This would require that the indole be positioned in proximity to the active site of V-BrPO in order to react with the active species before it can equilibrate with other bromine species, according to the pH of the buffer. On the other hand, if bromination occurs in close proximity to, or inside the enzyme, loss of proton from the bromoindolinium cation **56** ($R_1=R_2=R_3=H$) formed can be reasonably promoted by a nearby basic residue such as the carboxylates of aspartates or glutamates, still present in large amounts in the

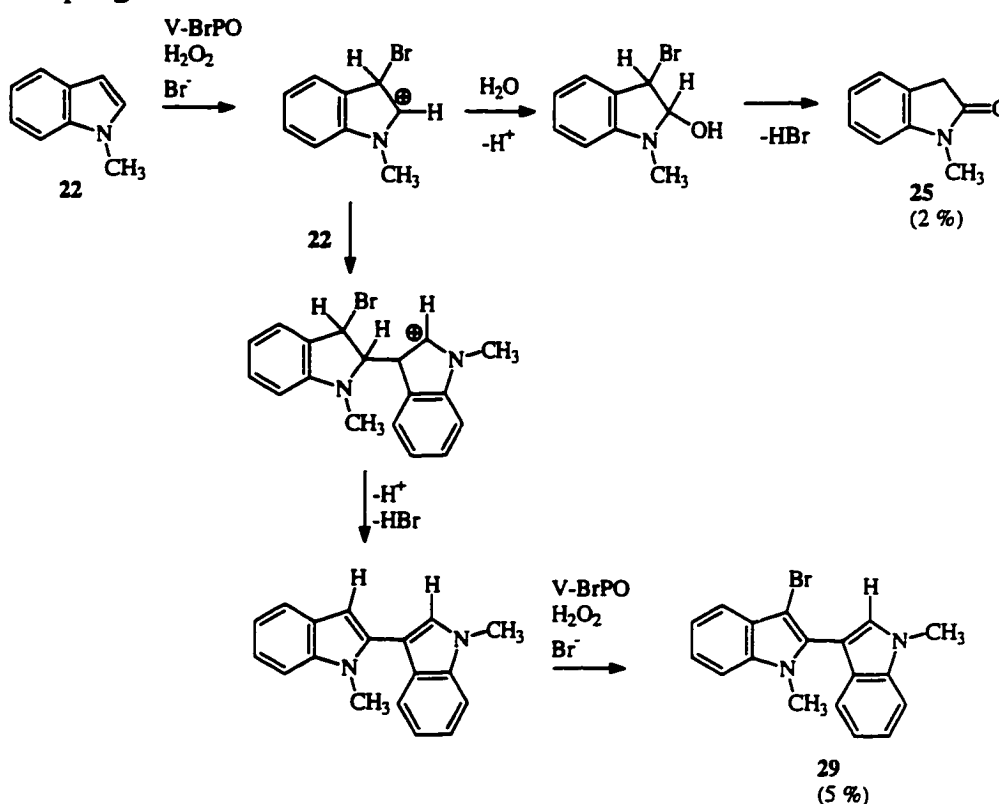
⁵ However, when the mole ratio was increased to 5:1 2,3,5,6-tetrabromoindole was isolated in 8.8 % yield.

protein, even at pH 4. Interestingly, both mechanisms suggest interactions between indole and V-BrPO.

The reaction of V-BrPO with other substituted biindoles presented some interesting synthetic and mechanistic aspects. Bromination of 2-methylindole (32), 3-methylindole (34), and 1,2-dimethylindole (37) by V-BrPO, using one equivalent of hydrogen peroxide with respect to the substrates, gave 3-bromo-2-methylindole (33), 1,3-dihydro-3-methyl-2*H*-indol-2-one (35), and 3-bromo-1,2-dimethylindole (36), respectively, in high yields. Those results are in agreement with bromination of these substrate by Br₂ or NBS in aqueous solvents (Hinman & Bauman, 1964a&b). However, unlike Br₂ or NBS, V-BrPO failed to brominate 35. The difference in reactivity observed is due to (a) the lesser reactivity of the oxindole towards bromination and (b) the presence, in the V-BrPO reaction, of competing hydrogen peroxide that probably reacts more rapidly with the brominating intermediate to form dioxygen (see also Chapt. 4 on the competition between organic substrates and hydrogen peroxide).

The bromination of 1-methylindole (22) yielded eight different compounds, including two biindoles and two triindoles. 3-Bromo--2-methyl-2-(1-methyl-1*H*-indol-3-yl)-1*H*-indole (29) was new and was the product of successive bromination, coupling, and second bromination steps (Scheme 2.4). The 2,3' linkage was consistent with other reports describing the reaction of 3-bromo-1-methylindole (27) with 1-methylindole (22) in dry dichloromethane, in the presence of protic acid such as HBr, to form the 2,3'-biindole (Bocchi & Palla, 1984). Reaction of 1-methylindole (22) with bromide in tetrahydrofuran:dioxane gave also the same biindole (Kunori, 1962). It was surprising that even in

water/ethanol media nucleophilic attack of the bromoindolinium cation **57** ($R_1=CH_3$, $R_2=R_3=H$) by 1-methylindole (to form the biindole (**29**)) was as favored as attack by water (to form 1,3-dihydro-1-methyl-2*H*-indol-2-one (**25**)) (Scheme 2.4). It is conceivable that V-BrPO may be able to hold several molecules of substrate in proximity to each other by simple hydrophobic interactions and thus favor coupling reactions.

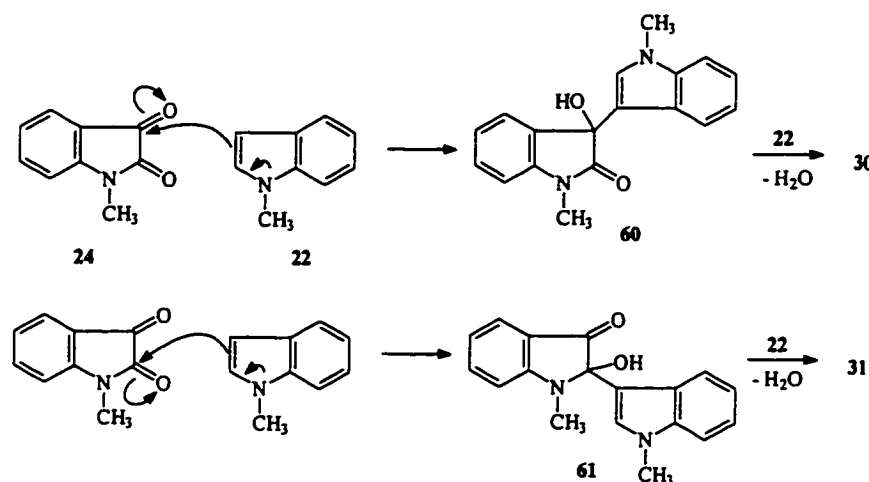


Scheme 2.4.

Compounds **30** and **31** are likely the products of the condensation of 1-methylindole (**22**) with 1-methylisatin (**24**) via **60** and **61** (Scheme 2.5) (Bergman & Eklund, 1980). The condensations occur by nucleophile attack of one the carbonyls of **24** by the electron rich C-3 of 1-methylindole (**22**), and subsequent

nucleophilic substitution of the hydroxides of **60** and **61**, resulting in 3,2',2" and 2,2',2" linkages for **30** and **31**, respectively.

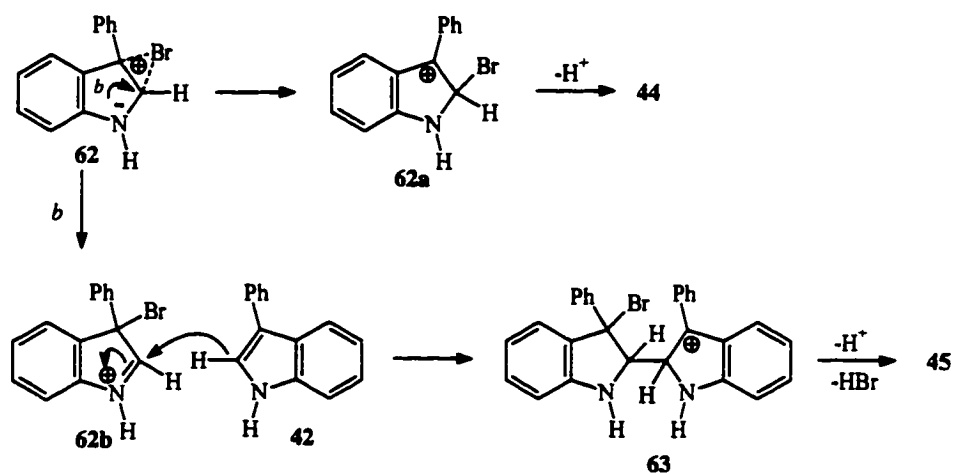
It is of interest that bromination of 3-phenylindole (**42**) by V-BrPO yielded mainly 2,2' coupling products. This stands in contrast to a previous report that



Scheme 2.5.

showed that bromination of 3-phenylindole under various conditions (NBS/AcOH, Br₂/Et₂O and NBS/CCl₄) did not yield any coupling products (Hino et al., 1974). The difference is even more striking if one considers that the concentration of 3-phenylindole (**42**) for the V-BrPO catalyzed reaction was 1.4 mM compared to 120 to 250 mM for the chemical brominations. One would expect that at high substrate concentrations the formation of coupling products would be more favorable. The 2,2' linkage is formed by nucleophilic attack of the 3-bromoindolinium cation (**62**) by 3-phenylindole (**42**) (Scheme 2.6). However, this route is somewhat unexpected since the tautomeric form (**62a**) appears a

priori to be more stable than (62b) due to the additional resonance forms possible. In addition, it is also surprising that 3-phenylindole seems to be a better nucleophile than water or ethanol in this case (water and ethanol are both present in a 2×10^4 fold excess with respect to 3-phenylindole). It is not clear why V-BrPO favors coupling reactions for 3-phenylindole but, as suggested in the case of 1-methylindole, the enzyme structure may be actively involved in the coupling step by bringing the monomers in proximity to each other.



Scheme 2.6.

It has been established that steric hindrance at the C-3 position of indoles inhibits bromonium ion attack and promotes bromination on the benzene nucleus. Bromination of 3-*tert*-butylindole (50) with NBS in acetic acid yielded a mixture of 1,3-dihydro-3-*tert*-butyl-2*H*-indol-2-one (51) (24 %), 6-bromo-3-*tert*-butylindole (52) (22 %) and starting material (47 %), and bromination of 1,3-di-

tert-butylindole (**53**) gave brominated 1,3-di-*tert*-butylindole⁶ (30 %), 1,3-dihydro-1,3-di-*tert*-butyl-2*H*-indol-2-one (**54**) (5 %) and starting material (26 %) (Hino et al., 1977). Surprisingly, bromination of 3-*tert*-butylindole (**50**) and 1,3-di-*tert*-butylindole (**53**) by V-BrPO gave the corresponding oxindoles almost quantitatively. It is not clear why V-BrPO would favor the initial attack of the bromonium ion at the C-3 position and subsequent hydration at the C-2 position in spite of the presence of bulky substituents, such as the *tert*-butyl group, at the C-3 and the N-1 positions. These results may be rationalized by a potential binding of indole to V-BrPO. In such a case it is not unreasonable to have the benzene nucleus of the substrate interacting with the enzyme, and in so doing preventing access for the bromonium ion and thus inhibiting bromination on the benzene nucleus.

Incubation of indole with V-BrPO and H₂¹⁸O₂ yielded unlabeled indigo (Figure 2.15a). The combined reaction time and product isolation time were less than 40 min. Although the rate of oxygen atom exchange of indigo in water has not been reported to this date, the data available suggest that complete exchange was not likely to occur during the aforementioned time (Oshima et al., 1965). Therefore, the oxygen atoms in indigo did not come from hydrogen peroxide, but from water. This result confirms that the initial step is formation of the bromoindolinium cation **56**.

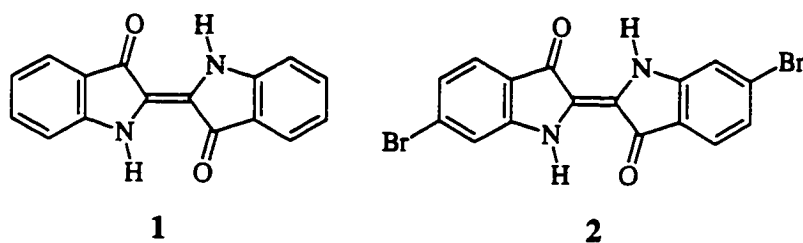
⁶ The exact position of the bromine atom was not clearly stated, but it was suggested that it corresponded to a mixture of the 5- and 6-bromo isomers (Hino et al., 1977).

Chapter 3

Oxidative Coupling of Indole to Indigo by V-BrPO

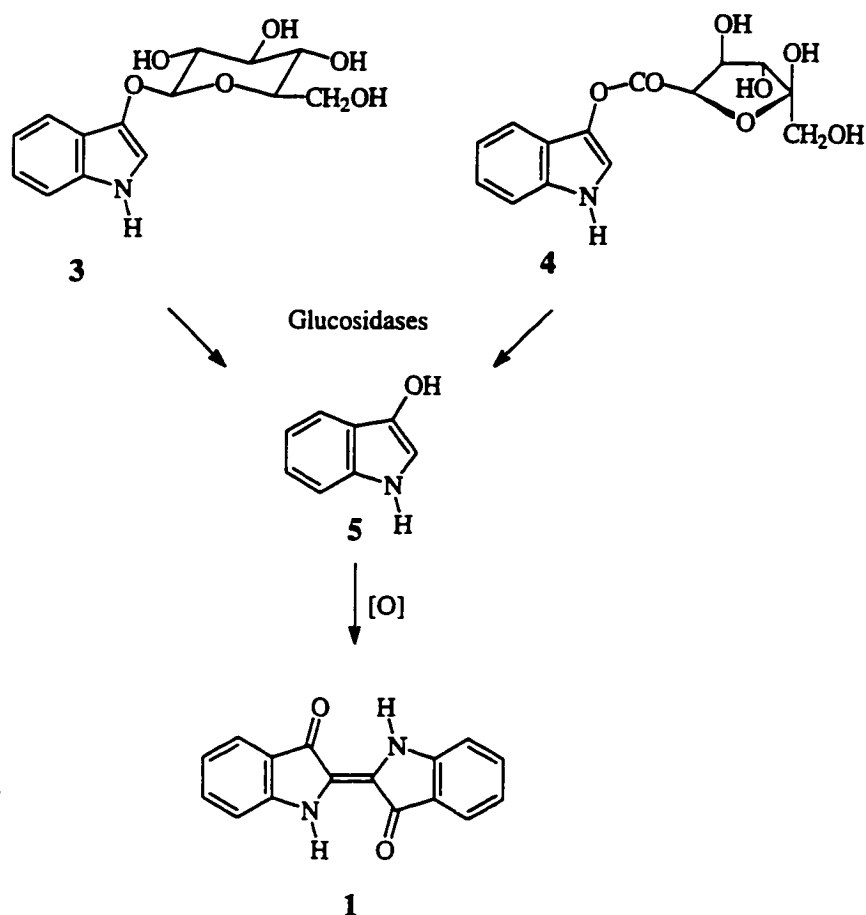
Introduction

Indigo (1) and Tyrian Purple (6,6'-dibromindigotin) (2) are among the most ancient of dyes. Although a large amount of information is available on natural indigo, the place and date of discovery of the dye have not yet been determined. With the exception of certain animals, including the mollusc *Murex trunculus*, indigo was exclusively obtained from plants. Indigo-bearing plants have been grown in many parts of the world since antiquity: examples include *Isatis tinctoria* in Northern Europe and *Indigofera* in Asia (Clark et al., 1993). The structure of indigo was finally determined by Baeyer (von Baeyer, 1883), and the first patent for making synthetic indigo was deposited in 1888 (von Baeyer, 1888). The subsequent commercial process for indigo synthesis developed by "Badische Anilin und Soda Fabrik" in 1890 (Heuman, 1890) led to the collapse of the agricultural production of indigo worldwide.



The leaves of the indigo plants do not actually contain indigo but, rather, indican (indoxyl-3- β -D-glucoside) (3) or isatan B (indoxyl-5-ketogluconate) (4)

(Schraudolf, 1968). By action of β -glucosidases on indican or isatan B, indoxyl (5) is liberated and subsequent air oxidation yields indigo (Scheme 3.1). It was recently found that the precursor of indican and isatan B in indigo producing plants is indole and not tryptophan (Xia & Zenk, 1992), as originally postulated (Maier et al., 1990).

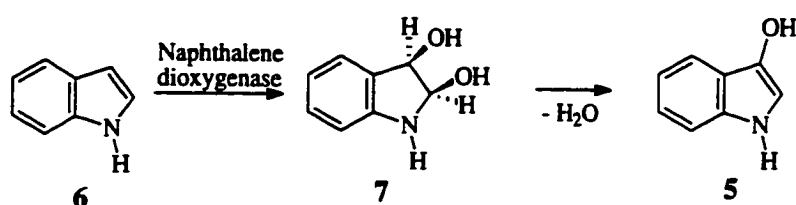


Scheme 3.1: Production of natural indigo

At this time, the mechanism by which these plants oxidize indole at the 3-position to form indoxyl and simultaneously protect this highly unstable intermediate from

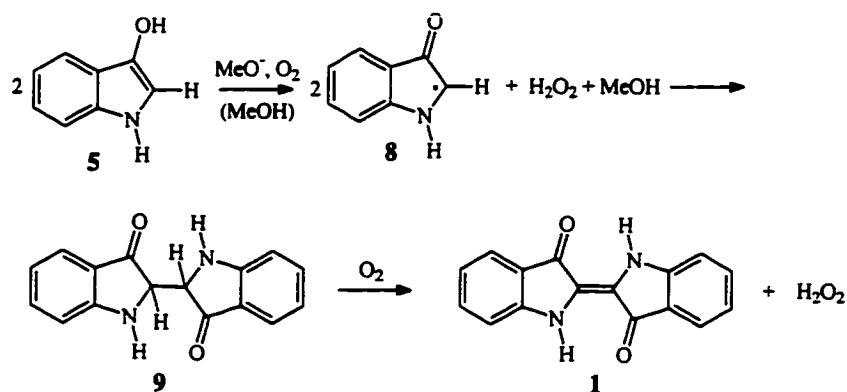
spontaneous oxidation to indigo by glucosylation or by addition of 5-ketogluconate is still unknown.

Enzymatic conversions of indole to indigo in bacteria utilize either toluene monooxygenase, in recombinant *E. coli* (Mermod et al., 1986), or indole-3-hydroxylase, in *P. indoloxidans* (Oshima et al., 1965), which convert indole to indoxyl. In addition, naphthalene dioxygenase expressed in *E. coli* oxidizes indole (6) to the *cis*-indole-2,3-dihydrodiol (7) which, after spontaneous loss of water, gives indoxyl (Scheme 3.2) (Ensley et al. 1983).



Scheme 3.2: Indoxyl synthesis by naphthalene dioxygenase.

The mechanism of conversion of indoxyl to indigo has been the object of many speculations (Madelung & Siefert, 1924; Cotson & Holt, 1958). Oxidation of indoxyl (5) to the indoxyl radical (8) by dioxygen, in basic methanol solution, followed by coupling to leucoindigo (9), and further oxidation of leucoindigo to indigo by dioxygen was supported by ESR spectroscopy (Russell & Kaupp, 1969) and by the fact that conversion of indoxyl to indigo required 2 moles of dioxygen per mole of indigo formed (Scheme 3.3). The overall reaction also releases 2 moles of hydrogen peroxide per mole of indigo formed. This mechanism is also considered to be the most probable one in aqueous solution (Cotson & Holt,

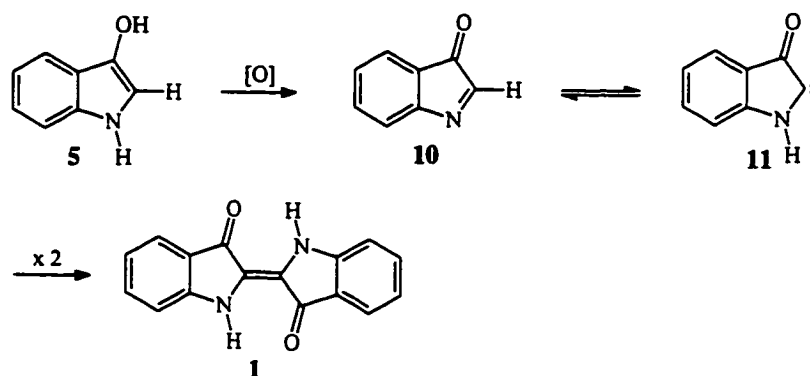


Scheme 3.3

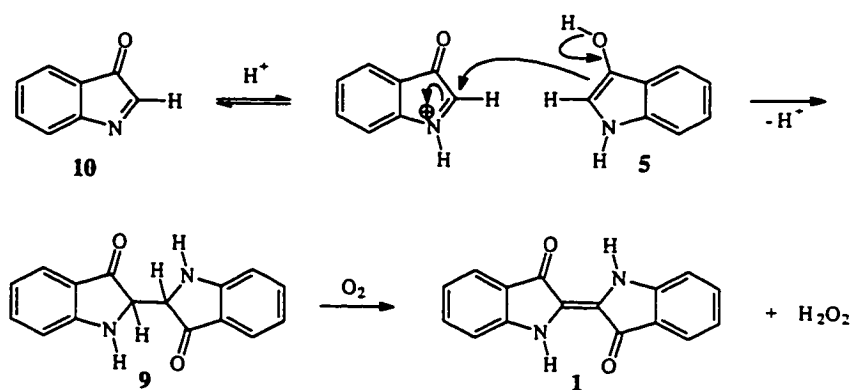
1958). Unlike indigo, leucoindigo (**9**) is almost colourless and is highly soluble in water. The rate of dioxygen consumption during the oxidation of leucoindigo to indigo is extremely fast and the reaction is most likely diffusion limited. On the other hand the oxidation of indoxyl (**5**) proceeds at a more moderate rate (Russell & Kaupp, 1969) and is thus the rate limiting step in the full oxidation of indoxyl to indigo. It has been reported that in dioxygen saturated buffer at 20 °C (the dioxygen concentration was maintained constant at 1.38 mM by a continuous supply of dioxygen) the reaction was first order with respect to indoxyl in the range of 50 to 500 μM , and had a pseudo first order rate constant of *ca.* $0.347 \times 10^{-3} \text{ s}^{-1}$ at pH 6.5 that increased to *ca.* $5.56 \times 10^{-3} \text{ s}^{-1}$ at pH 8.5 (Cotson & Holt, 1958). The observed dependence of the oxidation rate upon pH is consistent with the fact that the enolate form of **5** is the reactive species.

It has also been speculated that indoxyl (**5**) can be oxidized to indolone (**10**), which in turn might couple to form indigo (**1**) *via* its tautomeric carbene (**11**) (Scheme 3.4) (Madelung & Siegert, 1926). The indolone **10** has not been detected

so far, but it can be reasonably postulated as an intermediate in a number of indigo-forming reactions, such as the reduction of 2-chloroindolone with various reducing agents (von Bayer, 1879), the treatment of 2-anilinoindoxyl with base or acid (Pummerer & Göttler, 1910), or the reaction of *o*-nitrobenzaldehyde with acetone in basic solution (Tanascu & Georgescu, 1932). Coupling of indolone with indoxyl was also suggested as a possible mechanism since the presence of indoxyl in indolone generating reactions favored the formation of indigo (Scheme 3.5) (Wahl & Bagard, 1910).

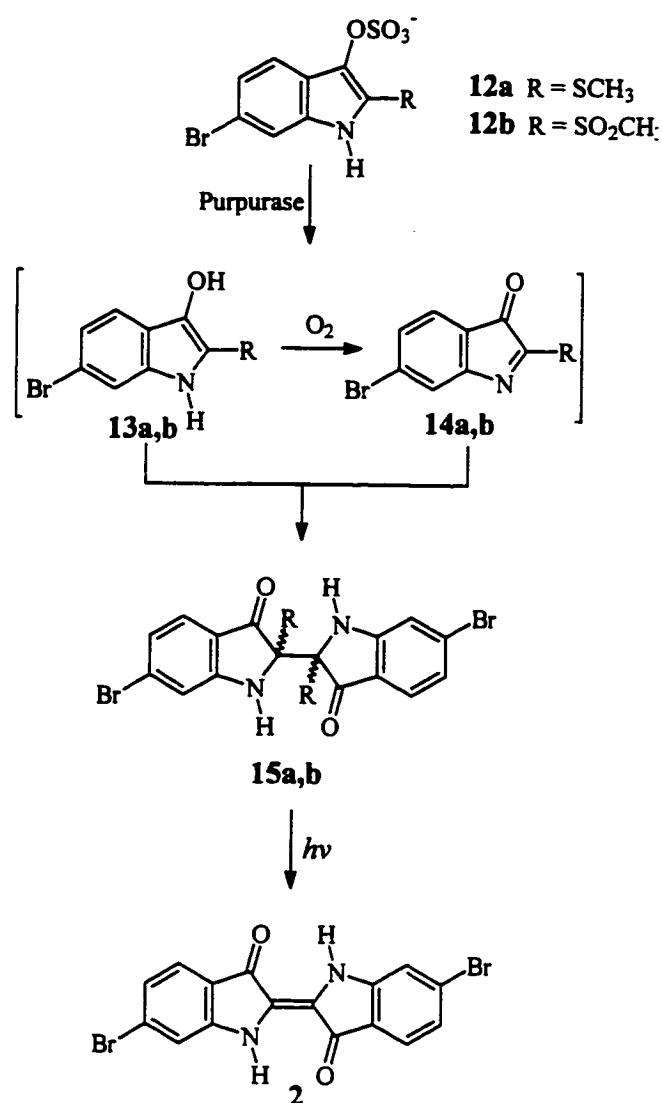


Scheme 3.4



Scheme 3.5

Unlike indigo, Tyrian Purple (**2**) is exclusively derived from animal sources, viz. mollusks, especially *Purpura haemostoma*, *Murex trunculus*, *Murex brandaris*, and *Purpura lapillus* (Govern & Michel, 1990). But, as is the case for indigo, it is not itself present in the mollusk. The chemistry of the conversion of the dye precursors has been shown to be similar for many of the mollusks that yield Tyrian Purple (Scheme 3.6) (Baker, 1974).



Scheme 3.6

The sulfate esters of 6-bromo-2-methylthioindoxyl (tyrindoxyl sulfate) (12a) and 6-bromo-2-methyl sulfonylindoxyl (12b) are enzymatically hydrolyzed by purpurase, followed by air oxidation, to form Tyriverdin (14a) and its methyl sulfonyl analog (14b), respectively. The latter are then converted to Tyrian Purple by a photooxidative process evolving odiferous sulfur compounds (*i.e.* mercaptans in the case of 14a) (Michel & McGovern, 1987).

It has been shown in Chapter 2 that, in the presence of bromide and hydrogen peroxide, the vanadium-containing bromoperoxidase from *A. nodosum* reacts with indole to form 3-bromoindole, oxindole and indigo as the main products. It was further determined that indigo was only produced between pH 5.5 and 7.5. In the present chapter, the V-BrPO-catalyzed formation of indigo is be examined in further detail, with particular emphasis on the mechanism of the reaction and on the nature of the intermediate(s) involved.

Materials and Methods

Materials. V-BrPO was isolated from *Ascophyllum nodosum* collected in Holland as described previously (Wever et al., 1985; Everett, 1990). Protein concentrations were determined using bicinchononic acid (BCA) protein assay (Pierce). Indole was obtained from Aldrich (Milwaukee, MI). Hydrogen peroxide was purchased from Fisher and standardized with sodium thiosulfate. β -D-Indoxylglucose and β -glucosidase were purchased from Sigma Chemical Co. (St. Louis, MO). UV-Vis spectra were recorded on a Hewlett-Packard HP8452a diode-array spectrophotometer. Levels of dioxygen and rates of dioxygen formation were measured with a Yellow Spring Instrument dioxygen probe (YSI 5331) and monitor (YSI 5300). When necessary, dioxygen was removed by sparging the reaction medium with nitrogen gas.

Oxidation of Indole to Indigo by V-BrPO. Indole (0.25 to 2 mM) was incubated with V-BrPO (2 to 500 nM), H₂O₂ (0.25 to 8 mM), in 100 mM phosphate buffer pH 6.5 containing 50 mM KBr and 10 % ethanol. The appearance of indigo was followed by UV-Vis spectrophotometry at $\lambda = 680$ nm. Yields of indigo were obtained by gravimetry (Yield of indigo = (2 x moles of indigo/moles of indole) x 100. Indole and 3-bromoindole were quantitated by HPLC (see Chapter 2).

Oxidation of Indoxyl to Indigo by V-BrPO. Indoxyl was prepared in situ by treating β -D-indoxyl glucose (1.0 or 2.0 mM) with β -glucosidase (.76 units/mL) in a solution of sodium phosphate (100 mM, pH 5.00), potassium bromide (50 mM) and 10 % ethanol. The appearance of indoxyl was followed by

UV-Vis spectrophotometry at $\lambda = 380$ nm. Upon completion of the reaction, the pH was raised to 6.5 using 2 N NaOH. The solution was used directly or rapidly frozen in liquid N₂. The presence of glucosidase did not interfere with the subsequent V-BrPO catalyzed reaction.¹ The appearance of indigo was monitored at $\lambda = 680$ nm, and yields² were determined, as above, by gravimetry.

¹ Removal of the glucosidase by ultrafiltration did not have any effect on the V-BrPO reaction.

² Yields of indigo were calculated using the following equation:

$$\text{Yield of indigo (\%)} = \frac{(\text{moles of indigo formed}) \times 2}{\text{initial moles of indole}} \times 100$$

Results

Oxidation of Indole to Indigo as a Function of V-BrPO Concentration.

Oxidation of indole to indigo by V-BrPO shows a marked lag phase (Figure 3.1).

The lag time is shorter when the concentration of V-BrPO is increased from 1.5

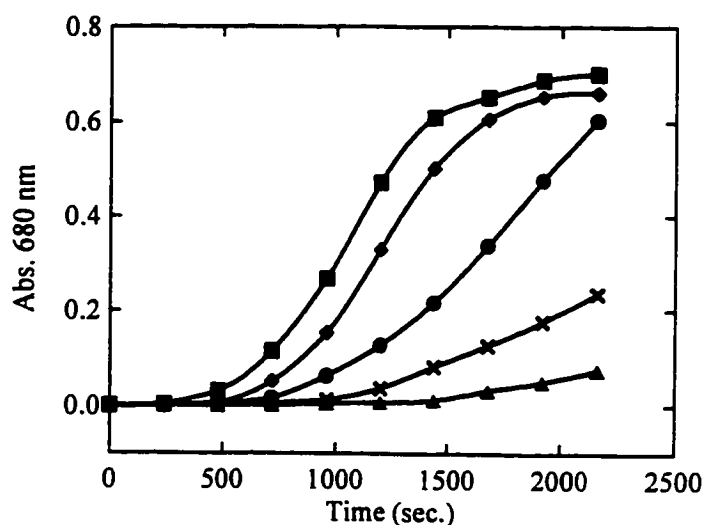


Figure 3.1: Oxidation of indole to indigo as a function of V-BrPO concentration. The appearance of indigo was followed at $\lambda = 680$ nm as a function of [V-BrPO]: (▲) 1.5 nM; (x) 2.9 nM; (●) 4.4 nM; (◆) 7.4 nM; (■) 8.8 nM. Conditions: 100 mM sodium phosphate, pH 6.35, 10 % ethanol, 50 mM potassium bromide, 1.30 mM indole and 2.8 mM H_2O_2 .

nM to 8.8 nM. This result indicates that indigo is not a primary product of the reaction, and that another event (or other events), such as the formation of a sufficient amount of an intermediate, must occur before indigo formation. The maximum rate of appearance of indigo after the lag phase is dependent on the concentration of V-BrPO (Figure 3.2). At low enzyme concentration (1-5 nM) the maximum rate of production of indigo is proportional to the amount of V-BrPO

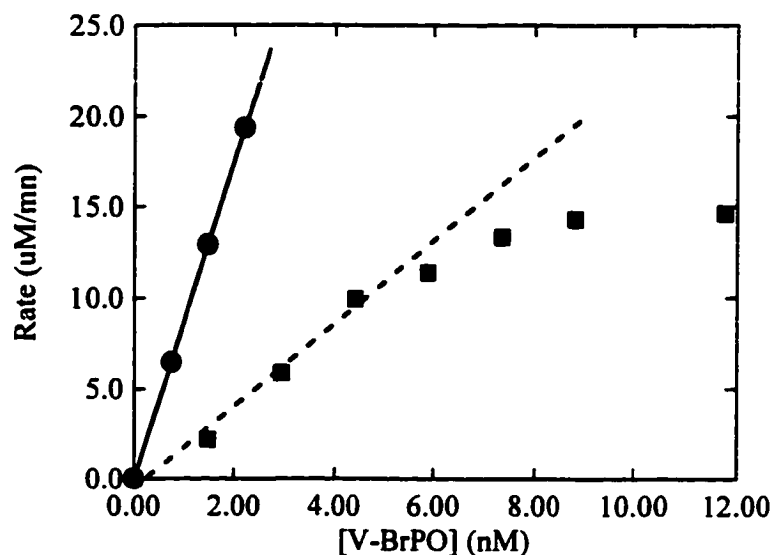


Figure 3.2: Rate of formation of indigo as a function of V-BrPO concentration; (■) Maximum rate of production of indigo versus V-BrPO concentration from figure 3.1; (●) Estimated enzymatic turnover rate. Conditions: 100 mM sodium phosphate (pH 6.35), 10 % ethanol, 50 mM potassium bromide, 1.30 mM indole and 2.8 mM H₂O₂.

added. However, the rate of indigo formation is well below (*ca.* 25 %) the estimated turnover rate³ for the bromination of MCD.

At higher enzyme concentration, however, there is departure from this linear behavior, and the rate of appearance of indigo levels off at V-BrPO concentrations above 9 nM. This rate saturation is associated with the fact that there is a rapid drop in the yield of indigo formation at V-BrPO concentrations above 10 nM (Figure 3.3). Below 10 nM V-BrPO, the yield of indigo reaches 50 %, but at 367 nM V-BrPO, it is close to 0 %. At 367 mM V-BrPO, the reaction produces many different products. Some of those products are highly colored, but efforts to identify them were not successful.

³ The turnover rate was estimated from the specific activity of V-BrPO as determined by MCD assay.

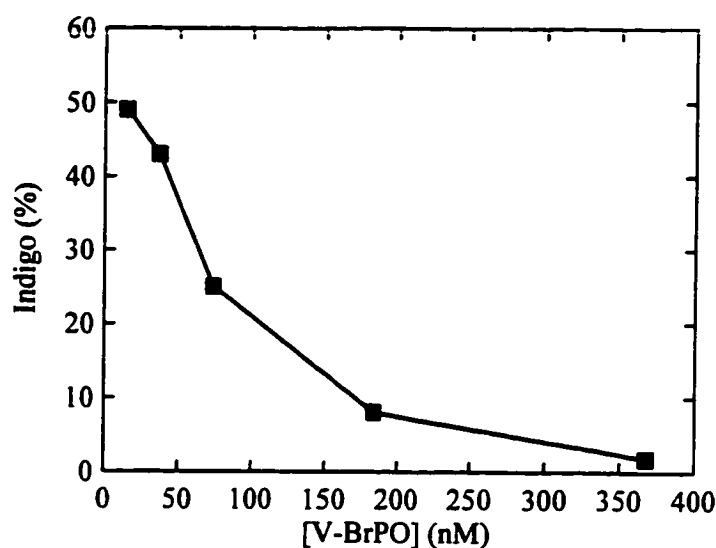


Figure 3.3: Effect of V-BrPO concentration on the final yield of indigo from indole. Conditions: 100 mM sodium phosphate, pH 6.5, 10 % ethanol, 50 mM potassium bromide, 2.10 mM indole, 5.35 mM H₂O₂ and 15 - 367 nM V-BrPO.

Influence of Dissolved Dioxygen of the Yield of Indigo. Concurrent dioxygen consumption and indigo formation suggests that dioxygen may be involved in the formation of indigo (Figure 3.4). However, the rate of dioxygen disappearance measured at 2000 sec (0.9 μ M/min) is much lower than the rate of indigo formation at the same time point (8.8 μ M/min). In addition, oxidation of indole by V-BrPO in air saturated buffer or dinitrogen sparged buffer give the same yield of indigo (Table 3.1) indicating that, although dissolved dioxygen is consumed during the reaction, it is at most only partially involved in the production of indigo. Indoles are fairly sensitive to oxidation by molecular dioxygen (Beer et al., 1950), possibly accounting for the observed loss of dioxygen. In addition, it was observed that the yield of indigo drops when air is

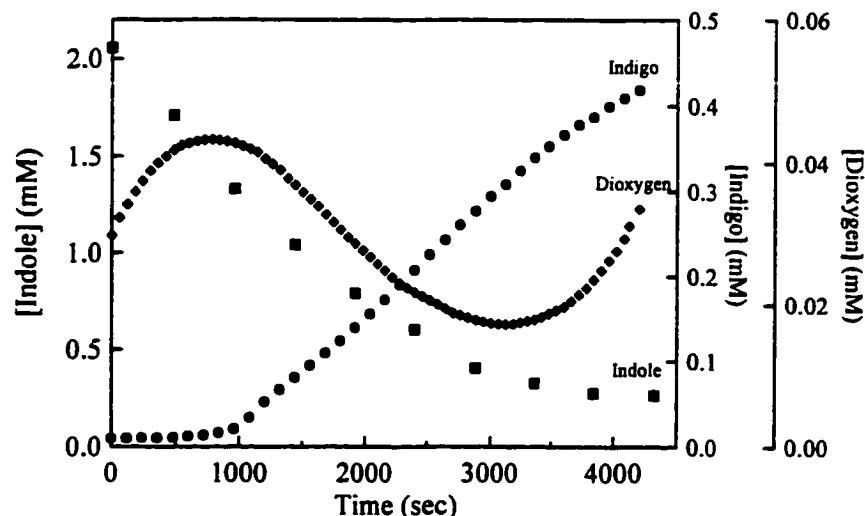


Figure 3.4: Composition in indole, indigo and dioxygen during the course of the oxidation of indole by V-BrPO. Indole (■), indigo (●), dioxygen (◆). Reaction conditions: 100 mM sodium phosphate, pH 6.5, 50 mM potassium bromide, 10 % ethanol, 8 mM H₂O₂, 2.10 mM indole and 3.7 nM V-BrPO. Indole was determined by HPLC with the method outlined in Fig. 2.2, and a predetermined calibration curve.

continuously supplied to the reaction buffer (Table 3.1). This drop can be attributed to the fact that, in aqueous solutions, indigo forms colloidal suspensions that render it more susceptible to oxidation by air (Cotson & Holt, 1958).

Table 3.1: Influence of Dissolved O₂ on the Yield of Indigo. ^a

Reaction conditions	[O ₂] initial (μM)	[O ₂] final (μM)	Indigo (%)
Air saturated. Flask open to air.	240	199	34
Air saturated. Flask closed to air.	240	30	34
Sparged with N ₂ . Flask closed to air.	17	22	34
Continuous air bubbling.	240	n.d. ^b	20

^a Conditions: 100 mM sodium phosphate (pH 6.5), 50 mM potassium bromide, 10 % ethanol, 2.05 mM indole, 2.59 mM H₂O₂ and 7.4 nM V-BrPO. Reaction times 24 h.

^bn.d. : not determined.

Formation of Indigo as Function of Hydrogen Peroxide Concentration. In order to determine whether molecular oxygen or hydrogen peroxide is used to complete the oxidation of indole to indigo, the formation of indigo as a function of the hydrogen peroxide concentration was examined, in the presence and in the absence of dioxygen (Figure 3.5A & Figure 3.5B).⁴ As already noted in Table 3.1, the presence or absence of dioxygen does not affect the yield of indigo. In contrast, the concentration of hydrogen peroxide present relative to the initial

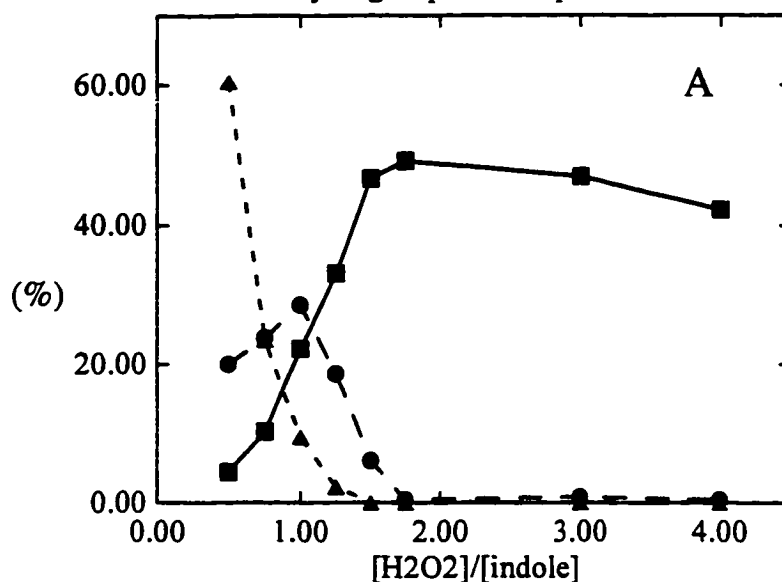


Figure 3.5A: Final composition of the reaction of indole with V-BrPO versus the ratio $[\text{H}_2\text{O}_2]/[\text{indole}]$ in air saturated buffer ($\text{O}_2 \sim 240 \mu\text{M}$); Conditions: 100 mM sodium phosphate (pH 6.5), 10 % ethanol, 50 mM potassium bromide, 2.10 mM indole, 1.05 - 8.80 mM H_2O_2 and 5.6 nM V-BrPO. (▲) Indole; (●) 3-bromoindole; (■) indigo.

concentration of indole critically controls the yields of indigo obtained. At an equimolar ratio of hydrogen peroxide to indole, indole is more than 90 %

⁴ 3-Bromoindole is included in Fig. 3.5 because it is also a substrate for V-BrPO.

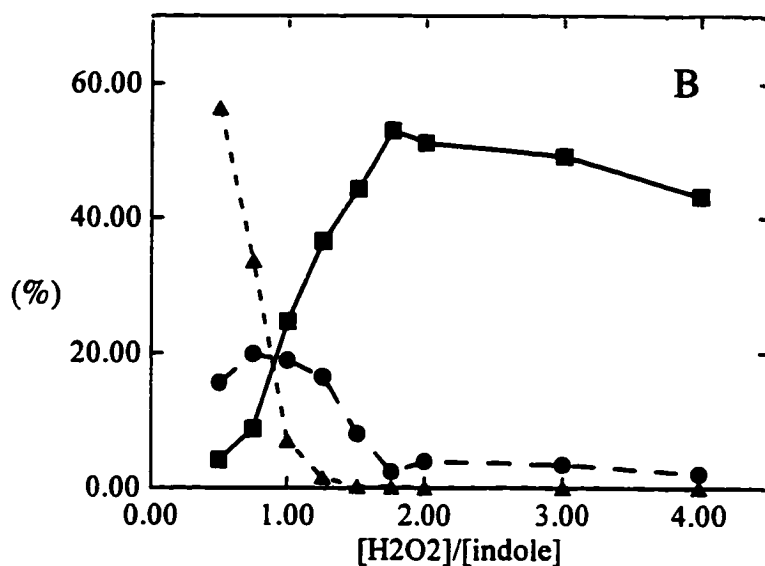


Figure 3.5B: Final composition of the reaction of indole with V-BrPO versus the ratio $[H_2O_2]/[indole]$ in buffer sparged with N_2 (Final O_2 concentration $\sim 17 \mu M$). Conditions: 100 mM sodium phosphate (pH 6.5), 10 % ethanol, 50 mM potassium bromide, 2.10 mM indole, 1.05 - 8.80 mM H_2O_2 and 5.6 nM V-BrPO. (▲) Indole; (●) 3-bromoindole; (■) indigo.

consumed, but the yield of indigo is only *ca.* 25 %. Another 0.75 equivalent of hydrogen peroxide is necessary to maximize the yield of indigo to *ca.* 50 %. However, the yield appears to drop when the concentration of hydrogen peroxide is further increased (i.e. $[H_2O_2]/[indole] > 1.75$). This drop is possibly due to the formation of singlet dioxygen following indole consumption (Figure 3.4), which is likely to oxidize indigo.

The 3-bromoindole formed during the reaction is also consumed upon addition of increasing amounts of hydrogen peroxide (Figure 3.5A & Figure 3.5B). Interestingly, 3-bromoindole is almost fully consumed at a $[H_2O_2]/[indole]$ ratio 1.75, the same ratio at which indigo reaches its maximum yield.

Since it appears that dissolved dioxygen is not involved in the production of indigo, hydrogen peroxide must be the only oxidant used. Inventory of the amount of hydrogen peroxide required to react with indole and 3-bromoindole, and to form indigo at a ratio $[\text{H}_2\text{O}_2]/[\text{indole}]$ equal to 1.4, reveals that the peroxide necessary to carry out these reactions exceeds the actual amount of hydrogen peroxide supplied to the reaction, by 52 μmoles (Table 3.2). This amount is almost equal to the amount of hydrogen peroxide used to consume 3-bromoindole. These observations suggest that 3-bromoindole may be involved in the formation of indigo (see below).

Table 3.2: Amount of H_2O_2 Necessary to Carry the Reaction of Indole with V-BrPO to Completion (based on the final yields of substrate and products).^a

		(μmoles)	H_2O_2 consumed (μmoles)
Indole:	Initial:	209	
	Final:	1	208
3-Bromoindole:	Formed:	75	
	Final:	17	58
Indigo:	Formed:	48	96 ^b
Total H_2O_2 consumed:			362
H_2O_2 added:			310

^aFrom the data in figure 3.5B at $[\text{H}_2\text{O}_2]/[\text{indole}]=1.41$. ^bOxidation of indole to indigo is an 8 e⁻ process and requires 4 moles of H_2O_2 per mole of indigo. The first 2 moles are included in the amount of H_2O_2 used to consume indole formed.

Yield of Indigo as a Function of Indole Concentration. The yield of indigo depends on the initial concentration of indole, and increases with increasing indole concentration (Table 3.3). This is not unexpected since the formation of indigo requires the coupling of two precursors and is favored at higher concentrations.

Table 3.3: Effect of [Indole] on the Production of 3-Bromoindole and Indigo. ^a

[Indole] initial (mM)	Indole consumed (%)	Yield of 3-bromo- indole (%)	Rate of appearance of indigo ($\mu\text{M}/\text{min}$)	Yield of Indigo (%)
2.05	98	14	8.84	32
1.03	99	1	9.20	21
0.51	100	0	8.98	13
0.26	100	0	1.76	3

^a Conditions: 100 mM sodium phosphate (pH 6.5), 50 mM potassium bromide, 10 % ethanol and 7.4 nM V-BrPO. In all cases $[\text{H}_2\text{O}_2]/[\text{indole}] = 1.24$.

The rate of appearance of indigo does not correlate with the yields of indigo formed. At high indole concentration, the rate of indigo formation drops, while the yield of indigo increases. This is most likely due to the fact that indole acts also as an inhibitor of V-BrPO (see Chapter 4). The final yield of 3-bromoindole is also affected by the the initial concentration of indole, and no 3-bromoindole is detected at indole concentrations below 1 mM. This drop in the yield of 3-bromoindole accompanying the drop in indigo yield suggests that the

excess hydrogen peroxide not required for the formation of indigo is used to consume 3-bromoindole instead.

Oxidation of Indoxyl to Indigo by V-BrPO. In order to determine whether indoxyl is an intermediate in the oxidative coupling of indole to indigo by V-BrPO, the reactivity of indoxyl with V-BrPO was investigated. As observed with indole, V-BrPO catalyzes the coupling of indoxyl to indigo (Figure 3.6). At pH 6.35 and initial indoxyl concentration of 1.1 mM, the rate of indigo formation is *ca.* 5.5 $\mu\text{M}/\text{min}$. Addition of 1.8 nM of V-BrPO increases the overall rate to 9.0 $\mu\text{M}/\text{min}$, indicating that the V-BrPO catalyzed reaction occurs at 3.5 $\mu\text{M}/\text{min}$. Although the V-BrPO catalyzed oxidation of indoxyl to indigo does not show a

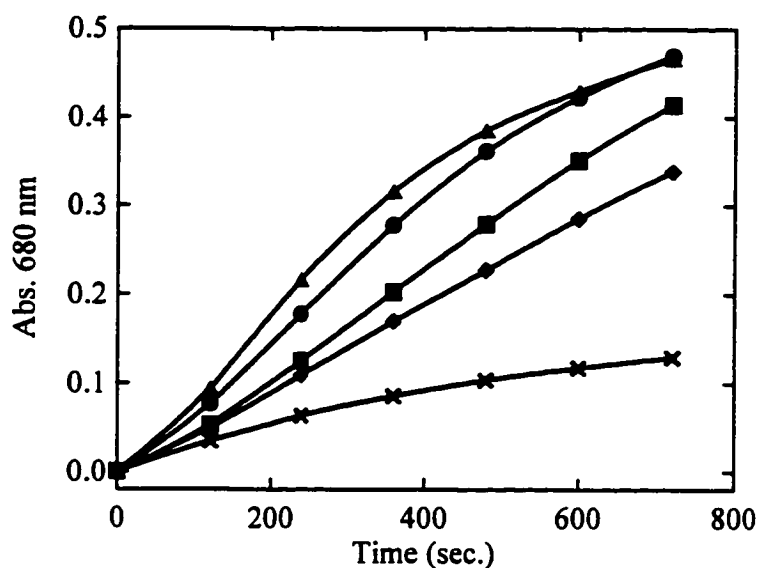


Figure 3.6: V-BrPO concentration dependence of the formation of indigo from indoxyl. The appearance of indigo was followed at $\lambda = 680$ nm as a function of $[\text{V-BrPO}]$; (x) 0 nM; (◆) 1.8 nM; (■) 3.5 nM; (●) 7.0 nM; (▲) 14.0 nM. Conditions: 100 mM sodium phosphate (pH 6.35), 10 % ethanol, 50 mM potassium bromide, 1.10 mM indoxyl and 2.08 mM H_2O_2 .

pronounced lag phase, as is the case for indole (Figure 3.1), there is still a small lag period. This lag phase is not observed in the uncatalyzed reaction and suggests that the V-BrPO catalyzed reaction may occur *via* a different mechanism.

The rate of the V-BrPO catalyzed oxidation of indoxyl to indigo is not proportional to the enzyme concentration (Figure 3.7). Similar to the indole reaction, the rate of indigo appearance maximizes at a V-BrPO concentration of *ca.* 15 nM, and then drops off at higher enzyme concentrations. This drop in the rate of indigo production is accompanied by a marked reduction in the final yields obtained (Figure 3.8), from almost 100 % at low enzyme concentrations (0-10 nM) to 60 % at concentrations above 100 nM. The similarities observed between

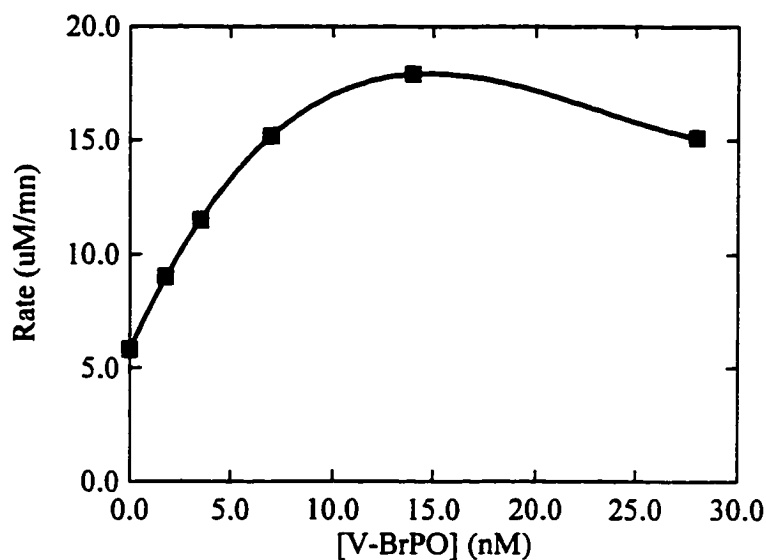


Figure 3.7: V-BrPO concentration dependence of the maximum rate of the V-BrPO catalyzed oxidation of indoxyl to indigo. Reaction conditions: 100 mM sodium phosphate (pH 6.35), 10 % ethanol, 50 mM potassium bromide, 1.10 mM indoxyl and 2.08 mM H₂O₂.

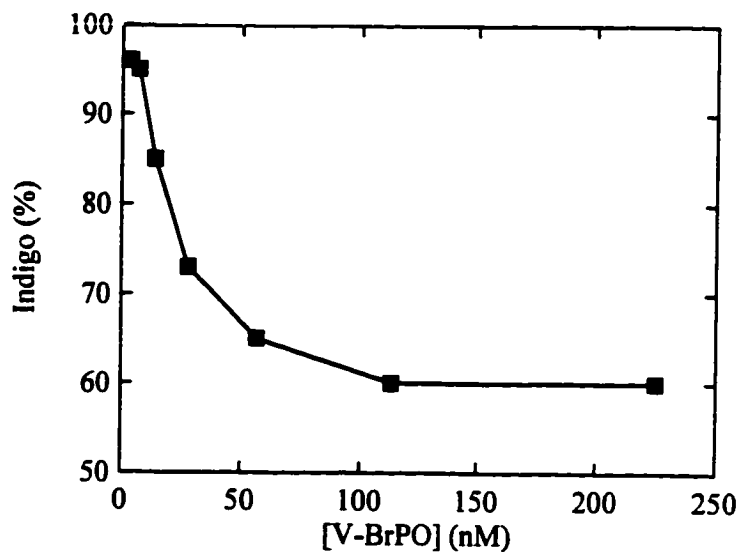


Figure 3.8: Effect of the V-BrPO concentration on the final yield of indigo from indoxyl. Conditions: 100 mM sodium phosphate, pH 6.5, 10 % ethanol, 50 mM potassium bromide, 1.10 mM indole, 2.08 mM H₂O₂ and 0 - 225 nM V-BrPO.

the indole and indoxyl systems strongly suggest that indoxyl is involved in the pathway of oxidation of indole to indigo by V-BrPO.

Indoxyl Concentration Dependence on the Oxidation of Indoxyl to Indigo.

The uncatalyzed oxidation of indoxyl to indigo was first order with respect to indoxyl with $k_1 = 0.059 \times 10^{-3} \text{ s}^{-1}$ (Table 3.4 & Figure 3.9). A previous report, however, indicated a first order rate constant of $0.347 \times 10^{-3} \text{ s}^{-1}$ under identical indoxyl concentrations and pH (Cotson & Holt, 1958). The difference is due to the fact that the present study was carried out in air saturated buffer that had a dioxygen concentration of *ca.* 240 μM , whereas the earlier investigation was

Table 3.4: Effect of [Indoxyl] on the Production of Indigo.^a

[Indoxyl] (mM)	Uncatalyzed reaction			V-BrPO catalyzed reaction ^b	
	Rate of disappear- ance of O ₂ ($\mu\text{M}/\text{min}$)	Rate of appearance of indigo ($\mu\text{M}/\text{min}$)	Yield of indigo 24 h (2 months) (%)	Rate of production of O ₂ ($\mu\text{M}/\text{min}$)	Rate of appearance of indigo ($\mu\text{M}/\text{min}$)
2.07	15.2	7.4	53 (92)	0	31.5
1.03	8.6	4.3	37 (61)	4.1	21.5
0.52	4.1	2.0	20 (40)	16.9	12.7
0.26	2.0	0.9	11 (20)	28.7	4.2
0	-	-	-	61.5	-

^a Conditions: 100 mM sodium phosphate (pH 6.5), 50 mM potassium bromide, 10 % ethanol. ^b [H₂O₂] = 8.0 mM, [V-BrPO] = 7.4 nM; The solutions were sparged with N₂ prior to addition of V-BrPO.

performed in dioxygen saturated buffer that contains 1.38 mM of dioxygen (YSI 5300 Biological Oxygen Monitor Instruction Manual). Examination of these results indicates that the oxidation of indoxyl to indigo by dioxygen is first order in both indoxyl and dioxygen, with a second order rate constant of *ca.* $250 \times 10^{-9} \text{ M}^{-1}\text{s}^{-1}$. Also in accordance with previous observations (Cotson & Holt, 1958; Russell & Kaup, 1958) and the mechanism presented in Scheme 3.3, the rate of dioxygen consumption was twice the rate of indigo formation, confirming that 2 moles of dioxygen are required to produce 1 mole of indigo.

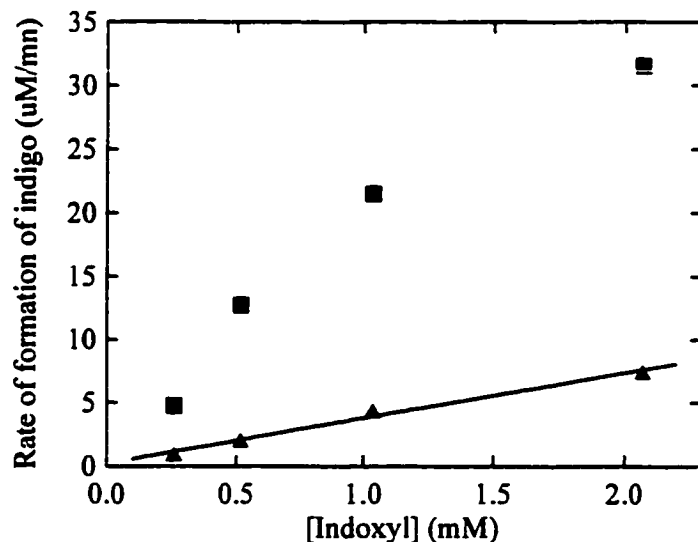


Figure 3.9: Dependence of indoxyl concentration on the uncatalyzed and V-BrPO catalyzed rates of oxidation of indoxyl to indigo. Conditions: 100 mM sodium phosphate, pH 6.5, 50 mM potassium bromide, 10 % ethanol, 8 mM H_2O_2 . (▲), uncatalyzed reaction (no V-BrPO); (■), 7.5 nM V-BrPO.

The results obtained for the V-BrPO catalyzed reaction were different and the rate of indigo formation seems to follow a saturation behavior with respect to indoxyl concentration (Figure 3.9). At an indoxyl concentration of 2 mM, dioxygen is not produced, and the rate of indigo formation is twice the rate of dioxygen evolution measured in the absence of indoxyl (Table 3.4). However, at lower indoxyl concentrations, dioxygen and indigo production do not entirely account for the enzymatic turnover. At 1.03, 0.52, and 0.26 mM of indoxyl, the sum of the rate of dioxygen formation and twice the rate of indigo production are equal to 47, 42, and 37 $\mu\text{M}/\text{min}$, respectively, all below the rate of dioxygen production in the absence of indoxyl (61 $\mu\text{M}/\text{min}$). These results suggest that at lower concentrations, the coupling reaction becomes unfavorable, and indoxyl is converted into other products than indigo.

Oxidation of Indoxyl to Indigo by Dioxygen Generating Systems. In order to assess whether V-BrPO itself is involved in the catalysis of the oxidative coupling of indoxyl to indigo, or if the rate enhancement is only due to the dioxygen provided by the bromide-assisted disproportionation of hydrogen peroxide catalyzed by V-BrPO, V-BrPO was compared to other systems that produce dioxygen (Table 3.5). Neither the system catalase/H₂O₂, nor the system HOBr/H₂O₂ substantially enhance the rate of indigo production, unlike V-BrPO. In both cases, the rate of dioxygen production is only modestly reduced in the presence of indoxyl, whereas it is turned off for V-BrPO.

Table 3.5: Oxidation of Indoxyl to Indigo using Different Sources of O₂.^{a,b}

O ₂ source	Rate of appearance of O ₂ in the absence of indoxyl (μM/min)	Rate of appearance of O ₂ in the presence of indoxyl (μM/min)	Rate of appearance of indigo (μM/min)
None	-	-	1.0
HOBr/H ₂ O ₂ ^c	45.5	44.0	low ^f
Catalase/H ₂ O ₂ ^d	57.0	54.6	4.0
V-BrPO/H ₂ O ₂ /Br ^e	61.5	0	31.5

^a Reactions conditions: 100 mM sodium phosphate, 50 mM potassium bromide, 10 % ethanol, 2.07 mM indoxyl and 8.00 mM H₂O₂, and were degassed with N₂ before use.

^b Indoxyl was generated *in situ* as described in the Materials and Methods section.

^cHOBr (17.9 mM in 200 mM NaOH) was added at a rate of 49.7 μM/min. ^d [Catalase] = 0.4 Units/mL. ^e [V-BrPO] = 7.4 nM. ^f The rate of appearance of indigo could not be measured spectrophotometrically, but the color of the solution remained only faint blue throughout the assay, indicating that indigo was not produced.

Oxidative Coupling of Indoxyl and 3-Bromoindole to Indigo. As mentioned above, it appears that disappearance of 3-bromoindole occurs simultaneously with indigo production during the oxidation of indole by V-BrPO (Figure 3.5A & Figure 3.5B). 3-Bromoindole alone is not converted to indigo when treated with V-BrPO (Table 3.6). However, in the presence of an equimolar amount of indoxyl, it undergoes coupling to form indigo. The amount of indigo formed is almost double the amount formed when indoxyl is used alone.

Table 3.6: Formation of Indigo from Indoxyl and/or 3-Bromoindole by V-BrPO.^a

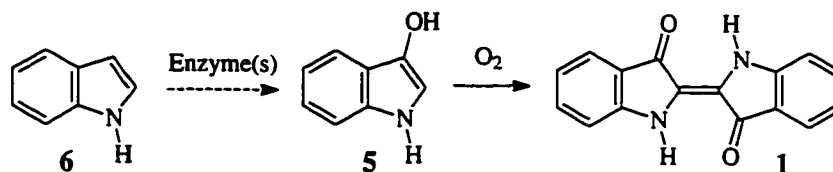
Indoxyl (μ moles)	3-Bromoindole (μ moles)	Indigo formed (μ moles)
40.3 ^b	0	13.3
0 ^b	43.5	0
40.3 ^c	43.5	25.2

^aReaction conditions: 100 mM sodium phosphate pH 6.67, 50 mM potassium bromide, 10 % ethanol, substrate(s), 8 mM H₂O₂ and 7.5 nM V-BrPO. ^b20 mL total volume. ^c 40 mL total volume. Reaction times were 13 h.

Discussion

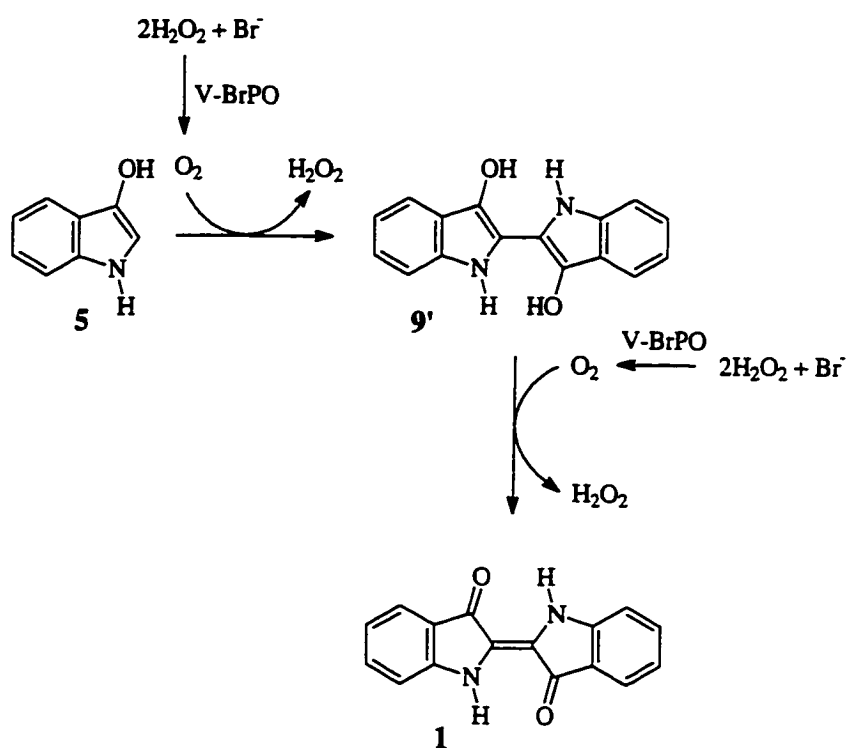
V-BrPO catalyzes the oxidative coupling of indole to indigo (Figure 3.1). This is the first report on a halide-assisted production of indigo by a haloperoxidase. Indigo had been detected earlier, in trace amounts, in the FeHeme-CIPO catalyzed oxidation of indole, but this reaction was carried out in the absence of any halide (Corbett & Chipko, 1979). The main product of the FeHeme-CIPO-catalyzed reaction was oxindole, and indigo was only observed as a minor product in large scale preparations. In contrast, the yields in indigo obtained with V-BrPO were close to 50 % at low V-BrPO concentrations (below 8-10 nM) and when hydrogen peroxide was added in a molar excess of at least 1.4 with respect to indole (Figure 3.3 and Figure 3.5A). Thus, the V-BrPO catalyzed reaction is a new biosynthetic route for the formation of indigo.

Contrary to all previous reports on enzymatic production of indigo (i.e. Mermod & al., 1986; Cotson & Holt, 1958) V-BrPO does not require dioxygen to complete the reaction (Table 3.1), and requires only excess hydrogen peroxide as an oxidant (Figure 3.5A). In all these reports, indoxyl was the only intermediate produced enzymatically and the subsequent oxidation of indoxyl to indigo was purely "chemical" and necessitated a supply of dioxygen (Scheme 3.7).



Scheme 3.7.

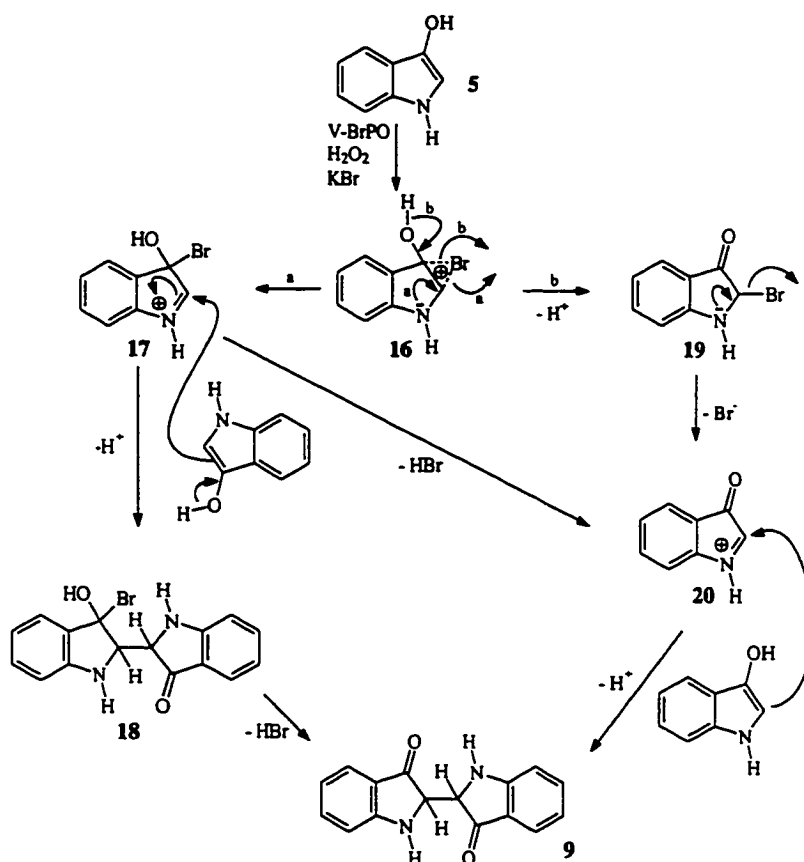
It was also found that V-BrPO catalyzes the formation of indigo from indoxyl (Figure 3.6). Enzymatic catalysis of the oxidative coupling of indoxyl had not been reported before and, the mechanism of this new reaction was of particular interest, since it was a potential step in the V-BrPO catalyzed formation of indigo from indole. As expected, oxidation of indoxyl to indigo by V-BrPO requires two enzymatic turnovers per molecule of indigo formed (Table 3.4), equating to a net 4-electron oxidation process. A possible reaction scheme has V-BrPO acting only as a mere supplier of the dioxygen necessary to oxidize indoxyl (5) to leucoindigo (represented in its enol form (9')) and leucoindigo to indigo (1) (Scheme 3.8). Both steps produce 1 mole of hydrogen peroxide that can be



Scheme 3.8.

recycled by V-BrPO. Although in agreement with the accepted mechanism of indoxyl oxidation, this mechanism is not supported by the observation that other systems, adjusted to produce dioxygen at similar rate as V-BrPO, such as catalase/H₂O₂ and HOBr/H₂O₂, failed to substantially increase the rate of indigo formation (Table 3.4). However, the dioxygen formed from the V-BrPO catalyzed disproportionation cannot be entirely ruled out as the oxidant in the reaction. V-BrPO may be directly involved in binding indoxyl and, in so doing, catalyzing the reaction between dioxygen and indoxyl.

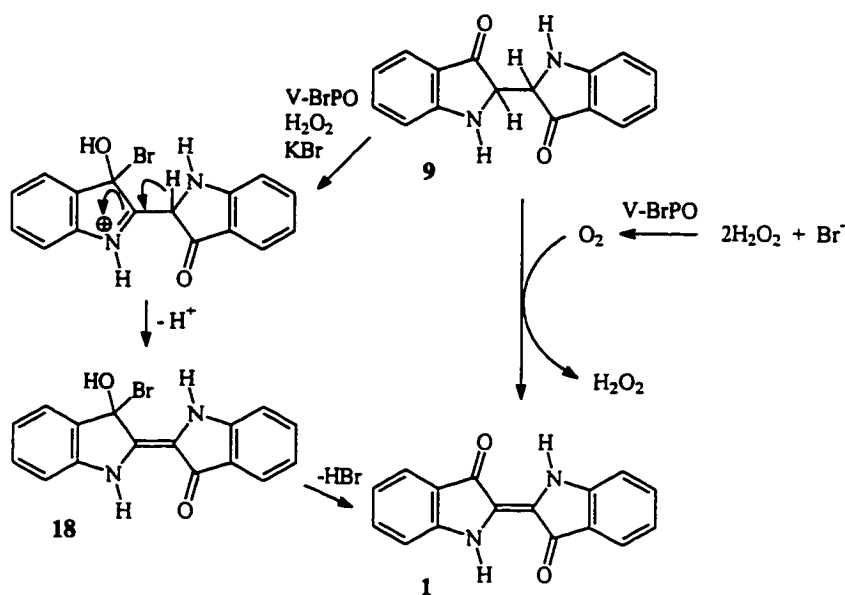
Oxidation of indoxyl to indigo could also occur *via* bromination of indoxyl (Scheme 3.9). The following intermolecular displacement of the bromonium



Scheme 3.9.

intermediate **16** by either the lone pair of the nitrogen or of the dioxygen gives protonated indolones **17** and **20** (see also Scheme 3.4) that can undergo nucleophilic addition of a second molecule of indoxyl to yield leucoindigo. This mechanism offers an explanation for the decrease in the yields of indigo observed as the V-BrPO concentration is increased (Figure 3.8). At low V-BrPO concentrations, the indolones formed initially are still in the presence of substantial amounts of indoxyl, and coupling can occur. At high V-BrPO concentrations however, all indoxyl might be rapidly converted to indolone at which point it would no longer be available for coupling. The indolones are then converted to non-indigo products.

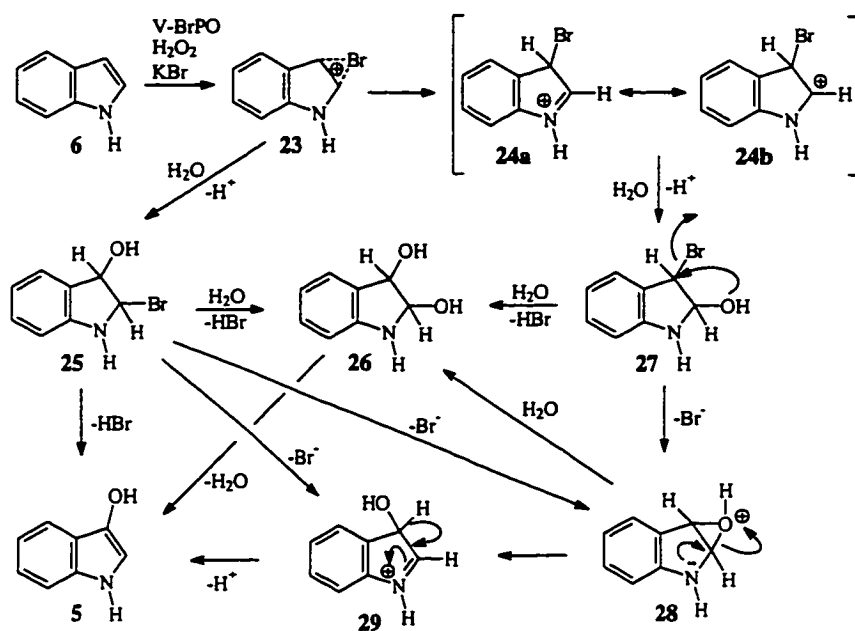
Oxidation of leucoindigo (**9**) to indigo by (1) dioxygen is extremely rapid and its rate is probably diffusion-limited (Russell & Kaupp, 1969). It is therefore not possible to determine whether leucoindigo is directly brominated by V-BrPO



Scheme 3.10

or oxidized by the dioxygen formed by V-BrPO (Scheme 3.10). In the former route, the bromonium ion intermediate formed first loses a proton. The following net loss of HBr is likely to occur *via* displacement of bromide catalyzed by water (or hydroxide).

In view of these results, indoxyl (**5**) is a probable intermediate in the oxidative coupling of indole to indigo by V-BrPO. It can be generated *via* several pathways (Scheme 3.11). After initial bromination of indole, nucleophilic attack by water at either the C-2 or the C-3 positions gives the two isomeric bromohydrins **25** and **27**, respectively. Since 3-bromoindole and oxindole are the other main products isolated (besides indigo, see Chapter 2), attack of water at the C-3 is probably minimal, and indoxyl (**5**) is formed mainly from rearrangement of bromohydrin **27**. A possible pathway could involve the formation of a highly unstable protonated α -amino epoxide (**28**) that would readily open, and form



Scheme 3.11

indoxyl after loss of a proton. Alternatively, the same bromohydrin could be converted to the diol **26** that would easily lose water to form indoxyl (Ensley et al. 1983; Scheme 3.2).

Chemical oxidation of indoxyl to indigo by dioxygen is probably not involved (or only at low levels) since, at low V-BrPO, the rate of indigo production is proportional to the concentration of V-BrPO added and since the rates observed exceed 10 $\mu\text{M}/\text{min}$ at enzyme concentrations above 5 nM (Figure 3.2). The estimated maximum rate of indigo appearance from dioxygen oxidation of indoxyl under similar conditions would not exceed 2.3 $\mu\text{M}/\text{min}$.⁵ In addition, the rates of indigo appearance would be independent of the concentration in V-BrPO.

Oxidation of indole to indigo is an 8-electron process and therefore requires consumption of 4 moles of hydrogen peroxide per mole of indigo formed. It was found that at a ratio $[\text{H}_2\text{O}_2]:[\text{indole}]$ equal to 1.4, and in the absence of dioxygen, the amount of hydrogen peroxide added did not correlate with the sum of the peroxide necessary to react with indole plus the peroxide used to react with the 3-bromoindole formed and the peroxide required to form indigo (assuming that indoxyl is the only intermediate in the reaction) (Table 3.2). This observation indicates that indoxyl cannot be the only intermediate in the formation of indigo. In addition, the fact that the excess hydrogen peroxide required is almost equal to the amount of hydrogen peroxide used to react with 3-bromoindole and that V-

⁵ Under the conditions detailed in Figure 3.2, the maximum amount of indoxyl formed would not exceed 650 μM . Dioxygen concentration can also be estimated at *ca.* 240 μM .

BrPO catalyzes the coupling of 3-bromoindole with indoxyl to form indigo (Table 3.6) suggest that 3-bromoindole is directly involved in the formation of indigo.

In conclusion, it appears that there are several routes possible in the V-BrPO catalyzed oxidation of indole to indigo (Scheme 3.12). The first bromination step produces 3-bromoindole and indoxyl. It also produces 2-oxindole -see Chapter 2-, which is not directly involved in the formation of indigo. Indoxyl can then be oxidized either by bromination by V-BrPO or by V-BrPO produced dioxygen to form leucoindigo (**9**) (see also Scheme 3.10). Alternatively, 3-bromoindole can be brominated a second time by V-BPO. The dibromoindole cation (**31**) may undergo nucleophilic attack by indoxyl to give the 3,3-dibromo-3'-oxo-2,2'-bi-1*H*-indole **32**. Subsequent hydrolysis of **32** yields leucoindigo (**9**). As mentioned earlier (Scheme 3.10), there are then two possible routes for oxidizing leucoindigo to indigo, both involving V-BrPO.

Chapter 4

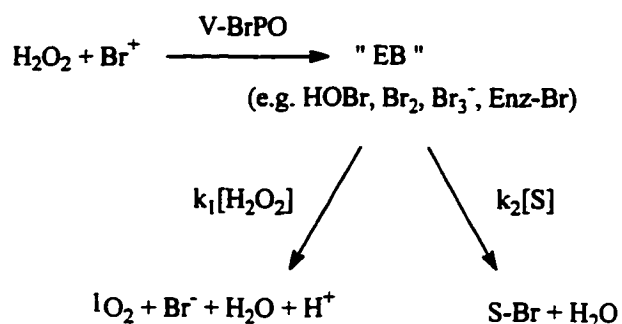
Substrate Specificity and Reaction Mechanism

Introduction

The vanadium-containing bromoperoxidase (V-BrPO) from the brown seaweed *Ascophyllum nodosum* was the first non-heme haloperoxidase to be isolated (Vilter et al., 1983). Since then, several other vanadium containing bromoperoxidases have been isolated from marine sources, including the red seaweed *Corallina pilulifera* (Itoh et al., 1985; Itoh et al., 1986). It was originally reported that certain species of Rhodophyta were producing non-heme iron bromoperoxidases (Itoh et al., 1985). However, it has been demonstrated since that the activity was due to a small amount of vanadium present in these enzymes, and that the activity could be fully restored by addition of vanadate (Everett et al., 1990).

V-BrPO catalyzes peroxidative halogenation reactions as well as the halide assisted disproportionation of hydrogen peroxide. The reaction mechanism of V-BrPO has been the object of intensive studies (de Boer & Wever, 1988; Everett et al., 1990a; Everett et al., 1990b; Soedjak et al., 1995). The majority of the information obtained so far point to a reaction scheme in which hydrogen peroxide reacts first with V-BrPO and forms an enzyme-hydrogen peroxide complex. In the next step, bromide reacts with the complex and an enzyme-bound bromonium complex ("EB") is produced (Scheme 4.1). Next, the intermediate

either reacts with an suitable substrate, or, in the absence of such a substrate, reacts with a second equivalent of hydrogen peroxide to produce dioxygen and water.



Scheme 4.1.

The exact nature of the intermediate complex "EB" still remains an open question. It has not been unambiguously determined yet whether the intermediate remains an enzyme bound species or if it decays to give back the native enzyme and a free oxidized bromine moiety (i.e. Br_2 , Br_3^- , HOBr or BrO^-). Alternatively, the fate of the intermediate may depend on the reaction conditions or on the nature of the organic substrate. Earlier studies have shown that, in the absence of substrate, tribromide can be detected (de Boer & Wever, 1988). However, the conditions used (i.e. high bromide and low pH) favor the production of tribromide and do not necessarily reflect the activity under physiological conditions. Others have observed differences between the reactivity of V-BrPO and the reactivity of HOBr towards monochlorodimedone, cytosine and phenol and have suggested that bromination of organic substrates occurs at the active site of V-BrPO and involves an enzyme-bound intermediate (Itoh et al., 1987). However, the same

authors were unable to detect any difference between the regioselectivity and the stereospecificity of the enzymatic reaction and the chemical bromination using HOBr (Itoh et al., 1988).

It has been shown in Chapter 2 that the regioselectivity of the bromination of indoles by V-BrPO is not always identical to the one observed in the chemical reaction with HOBr. Bromination of 3-*tert*-butylindole by V-BrPO gives 3-*tert*-butyloxindole almost quantitatively, whereas bromination with HOBr gives predominantly a different product (possibly 5- or 6-bromo-3-*tert*-butylindole). Likewise the highly sterically hindered 1,3-di-*tert*-butylindole was quantitatively converted to the corresponding 2-oxindole by V-BrPO suggesting that the enzymatic bromination strictly occurs at the C-2/C-3 double bond and that bromination on the benzene ring is somehow prohibited. The difference observed in the regioselectivity of the enzymatic and chemical bromination suggests that V-BrPO binds indole in such a way that access of the brominating intermediate to the benzene nucleus is restricted and redirected to the C-2/C-3 double bond.

In this chapter, substrate specificity and kinetic assays have been used in order to further examine the existence of an enzyme-substrate complex during the bromination of indoles by V-BrPO.

Materials and Methods

Materials. V-BrPO was purified as described previously (Everett, 1990). Protein concentrations were determined using the bicinchononic acid protein assay (Pierce). The concentration of hydrogen peroxide was determined spectrophotometrically by the formation of triiodide (Cotton & Dunford, 1973). All reagents were purchased from Aldrich or prepared as described in Chapter 2. Spectrophotometric measurements were collected either on a Kontron double-beam Uvikon 860 spectrophotometer or on a Hewlett-Packard diode-array HP8452 spectrophotometer.

Hypobromite Solutions. Hypobromite solutions were prepared by dilution of bromine vapors into 0.07 N sodium hydroxide. The final concentration of hypobromite in solution was determined spectrophotometrically by oxidation of iodide to triiodide: Aliquots of the hypobromite solution were added to 100 mM potassium iodide in 100 mM acetate buffer at pH 4.5. The amount of triiodide formed was determined from the absorbance of the solution at 353 nm using $\epsilon = 26,000 \text{ M}^{-1}\text{cm}^{-1}$.

Substrate Specificity. The relative specificity of V-BrPO was determined using monochlorodimedone (MCD) as a reference substrate. The initial change in absorbance at 290 nm (ΔA) was monitored for the reaction of V-BrPO with a) MCD alone (ΔA_a), b) the competing substrate alone (ΔA_b), c) an equimolar mixture of MCD and the competing substrate (ΔA_c). The relative percent of MCD being brominated during the competitive reaction was estimated using equation 4.1:

$$MCD(\%) = 100 \times \frac{\Delta A_c - \Delta A_b}{\Delta A_a - \Delta A_b} \quad (4.1)$$

Dioxygen Measurements. Rates of dioxygen formation were measured with a yellow Spring Instrument (YSI) oxygen probe (YSI 5331) and monitor (YSI 5300). The reaction mixtures were sparged with nitrogen gas prior to initiation. The reactions were initiated by addition of V-BrPO or by introduction of HOBr *via* a syringe fitted on a syringe pump.

Substituent Effect on the Rate of Indoles Bromination. The rates of bromination of 3-methylindole, 3-phenylindole, 3-*tert*-butylindole, 2-*tert*-butylindole, and 1,3-di-*tert*-butylindole were determined by following the loss in absorbance at 281 nm, 267 nm, 280 nm, 272 nm, and 291 nm, respectively, and using experimentally determined molar absorption coefficients of 4037 M⁻¹cm⁻¹, 8687 M⁻¹cm⁻¹, 3336 M⁻¹cm⁻¹, 5602 M⁻¹cm⁻¹, and 3194 M⁻¹cm⁻¹, respectively.

Data Fitting. All data fitting was done using GRAPHER™ for Windows or IGORpro™ for Macintosh. Plots of $r(O_2)/r(O_2)_0$ *versus* [substrate] were fitted to equation $y = 1/(a+bx)$.

Experimental reproducibility and error. Unless otherwise mentioned all data reported are the results of a single experiment. The errors on dioxygen evolution measurements can be estimated to be no more than 5 %. The results are, however, not always reliable, and great care must be taken during experimental setup and procedure. The membrane of the probe must be intact and fairly new. Care must be taken when the solutions are sparged with dinitrogen in order not to lose reaction buffer since this would affect (increase) the concentrations of all the reagents added later on.

Results

Substrate Specificity. Monochlorodimedone has been the substrate of choice for most of the mechanistic investigations on V-BrPO found in the literature (de Boer & Wever, 1988; Everett et al., 1990a; Everett et al., 1990b). Figure 4.1 shows the bromination of monochlorodimedone in the absence or presence of phenol red and in the absence or presence of 2-methylindole.¹ The presence of phenol red does not affect the bromination of monochlorodimedone

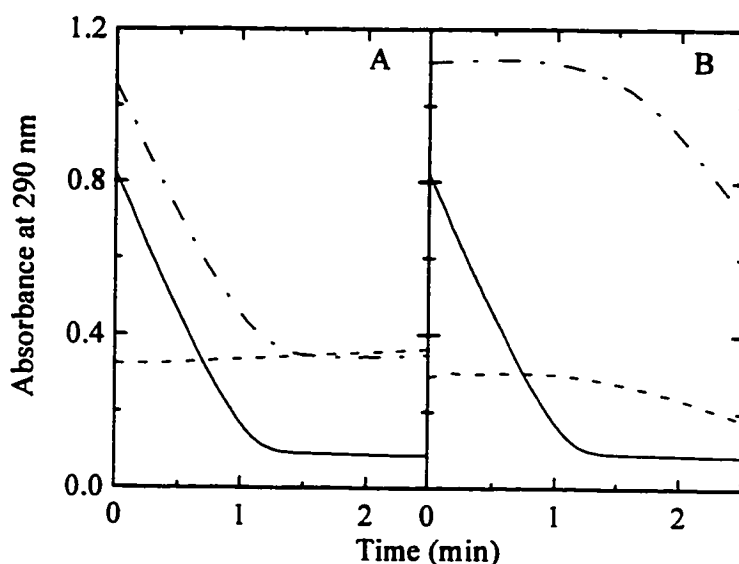


Figure 4.1: Effect of phenol red (A) and 2-methylindole (B) on the bromination of monochlorodimedone (MCD) by V-BrPO. Reactions conditions: 100 mM sodium phosphate pH 6.50, 50 mM potassium bromide, 10 % ethanol, 970 μM H₂O₂ and 4.3 nM V-BrPO with the following substrate concentration: Panel A: (—) 50 μM MCD, (- - -) 50 μM phenol red, (-.-) 50 μM MCD and 50 μM phenol red; Panel B: (—) 50 μM MCD, (- - -) 50 μM 2-methylindole, (-.-) 50 μM MCD and 50 μM 2-methylindole.

¹ Bromination of phenol red by V-BrPO gives tetrabromophenol blue; bromination of 2-methylindole gives 3-bromo-2-methylindole (See Chapter 2).

and the rate of monochlorodimedone bromination in the absence and presence of phenol red are almost equal, indicating that monochlorodimedone is preferentially brominated by V-BrPO (Figure 4.1A). 2-Methylindole, on the other hand appears to be a much better substrate than monochlorodimedone (Figure 4.1B) since monochlorodimedone is not brominated in the presence of an equimolar amount of 2-methylindole.

Table 4.1: Substrate Specificity of V-BrPO. *a, b*

Competing substrate ^c	MCD reacted (%)	Competing substrate	MCD reacted (%)
Cytosine	99.0	Indole-3-methanol	47.6
<i>trans</i> -Cinnamic acid	98.9	Indole-3-acetic acid	47.2
Phenol red	97.4	Farnesol	46.6
Indole-3-acrylic acid	62.0	Indole	33.1
5-Aminoindole	60.1	3-Methylindole	32.9
Indoxyl- β -D-glucoside	59.8	5-Hydroxyindole	23.8
1,3,5-Trimethoxybenzene	57.0	2-Phenylindole	18.9
		2- <i>tert</i> -Butylindole	5.8
		2-Methylindole	0.5

^a Reaction conditions: 100 mM sodium phosphate, 50 mM potassium bromide, 10 % ethanol, 970 μ M H₂O₂, 50 μ M MCD, 50 μ M competing substrate and 2 nM V-BrPO.

^b As determined according to equation 4.1 in the "Materials and Methods" section.

^c The bromination of indole, 2-phenylindole 3-methylindole, 3-methylindole and 2-*tert*-butylindole by V-BrPO is examined in Chapters 2 & 3. Cytosine and 1,3,5-trimethoxybenzene are brominated to 5-bromocytosine and 2-bromo-1,3,5-trimethoxybenzene (Soedjak & Butler, 1990). Farnesol is converted to the terminal bromohydrin (McAdara, 1991). The products formed from reaction of V-BrPO with *trans*-cinnamic acid, indole-3-acrylic acid, 5-aminoindole, indoxyl- β -D-glucoside, indole-3-methanol, and indole-3-acetic acid have not been characterized yet.

The extent of monochlorodimedone bromination by V-BrPO in the presence of an equimolar competing substrate is given in Table 4.1. The data show that V-BrPO has a broad substrate specificity but, more importantly, they show that monochlorodimedone is not the best suited substrate for V-BrPO. With the exception of indole-3-acrylic acid, 5-amino-indole and indoxyl- β -D-glucoside, all indoles tested are better substrates than monochlorodimedone. On the other hand, cytosine, *trans*-cinnamic acid and phenol red were found to be very poor substrates when compared to monochlorodimedone.

Comparison of the Substrate Specificity of V-BrPO and HOBr. If free molecular bromine or hypobromite were the brominating species in the V-BrPO catalyzed reaction, then the substrate specificity should be identical with that of chemical bromination reaction. If, however, the brominating species is an enzyme-bound intermediate or if there is binding of the substrate to the enzyme, then the substrate specificity could be quite different from that of the chemical bromination.

In a mixture of 2-methylindole and phenol red, V-BrPO preferentially brominates 2-methylindole, as shown by the lag phase observed in the appearance of bromophenol blue ($\lambda_{\text{max}}=596$ nm) (Figure 4.2). The lag phase increases with increasing concentration of 2-methylindole, but the rate of bromophenol blue appearance following the lag phase remains independent of the 2-methylindole concentration.

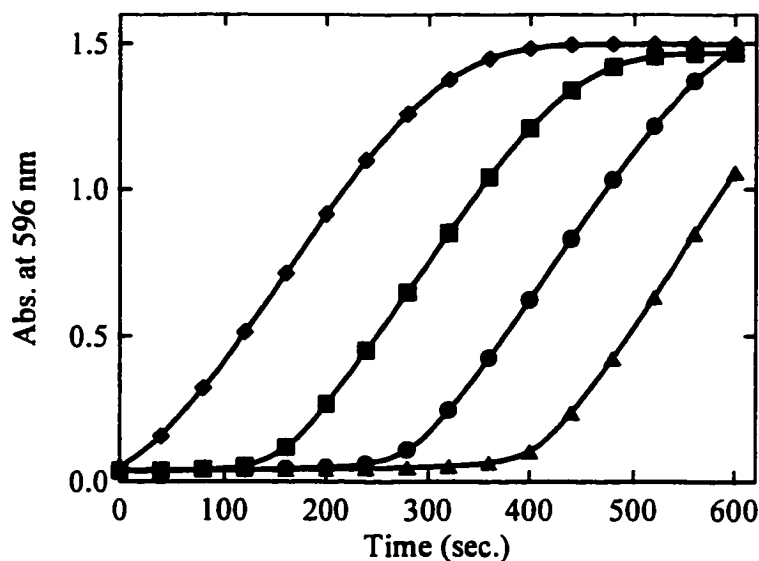


Figure 4.2: Time course of the bromination of phenol red by V-BrPO as a function of 2-methylindole concentration. Concentration of 2-methylindole: (◆), 0 μM ; (■), 28.8 μM ; (●), 57.6 μM ; (▲), 86.4 μM . Reaction conditions: 100 mM sodium phosphate pH 6.5, 50 mM potassium bromide, 20 % ethanol, 416 μM H_2O_2 , 25.3 μM phenol red and 2.5 nM V-BrPO.

In contrast, no lag phase is observed in the competitive bromination of 2-methylindole and phenol red by HOBr (Figure 4.3). Under these conditions, bromination of 2-methylindole and phenol red occur concomitantly. An increase in the concentration of 2-methylindole results in a decrease in the appearance of tetrabromophenol blue. The differential reactivity observed between V-BrPO and HOBr suggest that "free" (or enzyme-released) BrO^- is not the active brominating species in the V-BrPO-catalyzed bromination of 2-methylindole.

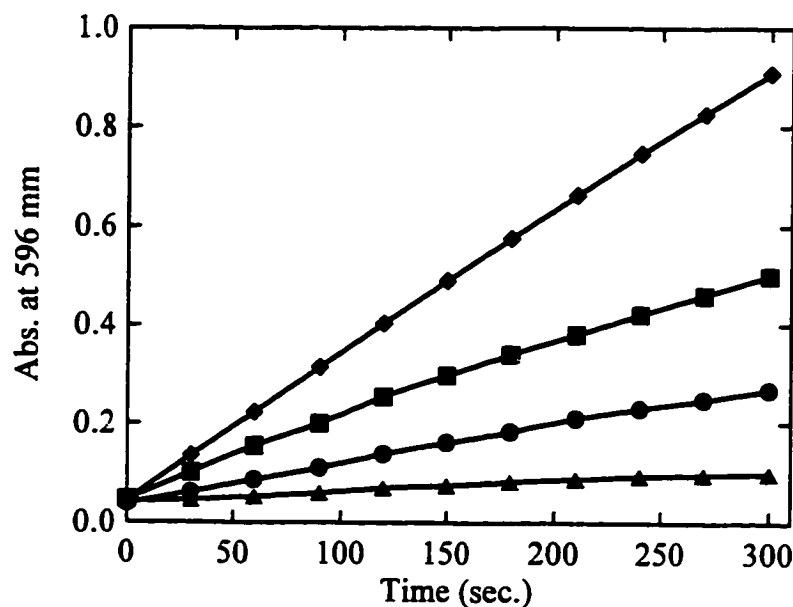


Figure 4.3: Bromination of phenol red by HOBr as a function of 2-methylindole concentration. Concentration of 2-methylindole: (◆), 0 μM ; (■), 28.8 μM ; (●), 57.6 μM ; (▲), 86.4 μM . Reaction conditions: 100 mM sodium phosphate pH 6.5, 50 mM potassium bromide, 20 % ethanol and 25.3 μM phenol red. Ten aliquots of 10 μL each of a 3.63 mM HOBr stock solution were added successively at 30-sec intervals to the initial 1 mL reaction, and the absorbance at 596 nm was measured 20 sec after each addition.

Comparison of the Rates of Dioxygen Evolution in the Presence of Indoles during Enzymatic and HOBr Reactions. According to scheme 4.1, the active species formed by reaction of V-BrPO, hydrogen peroxide and bromide can react either with a suitable (organic) substrate or with a second equivalent of hydrogen peroxide to form dioxygen. It is known that HOBr oxidizes hydrogen peroxide to yield dioxygen as well (Kanofsky, 1984). If the reaction intermediate for V-BrPO catalyzed is consistent with "free" HOBr, then the enzymatic and the chemical

reactions of HOBr in the presence of an organic substrate should show identical rates of dioxygen evolution. The chemical bromination reaction was compared to the enzyme catalyzed reaction by adjusting the rate of HOBr addition to match the activity of V-BrPO and by measuring the rate of dioxygen formation during the addition, in the presence of increasing amounts of organic substrate.

As shown in Figure 4.4 and Figure 4.5, the normalized rate of dioxygen formation (i.e. $r(\text{O}_2)/r(\text{O}_2)_0$, where $r(\text{O}_2)_0$ is the initial rate of dioxygen formation in the absence of organic substrate) in the presence of 2-methylindole (Figure 4.4)

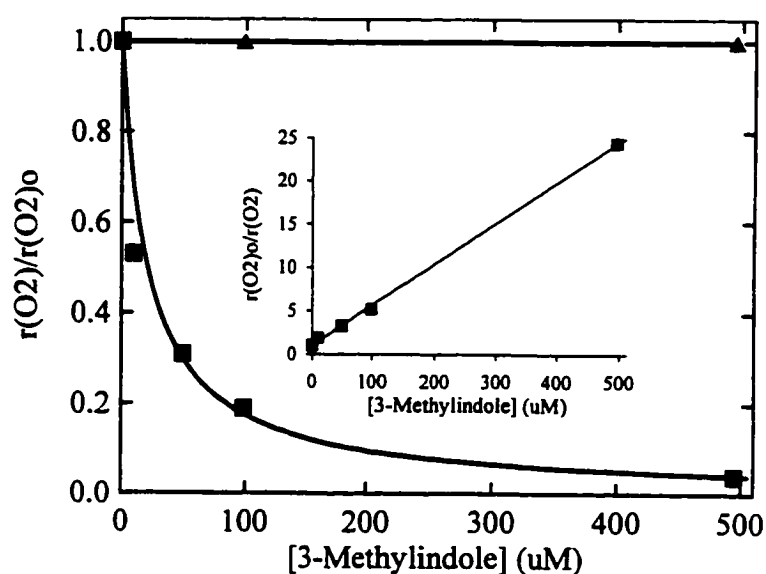


Figure 4.5: Dioxygen formation in the presence of 3-methylindole. (■), V-BrPO; (▲) HOBr. Conditions 100mM sodium phosphate pH 6.5, 50 mM potassium bromide, 10 % ethanol and H_2O_2 40 mM. In the enzyme reaction V-BrPO was 2 nM; under these conditions and in the absence of 3-methylindole, the rate of dioxygen formation was $9.7 \mu\text{M}/\text{min}$. In the HOBr reaction, HOBr was added by syringe pump at a rate of $5.7 \mu\text{M}/\text{min}$.

or 3-methylindole (Figure 4.5) decreases as the concentration of substrate is increased. By comparison, the normalized rate of dioxygen formation from the oxidation of hydrogen peroxide by HOBr in the presence of 2-methylindole or 3-methylindole remained constant as the concentration of substrate was increased (Figure 4.4 & 4.5).

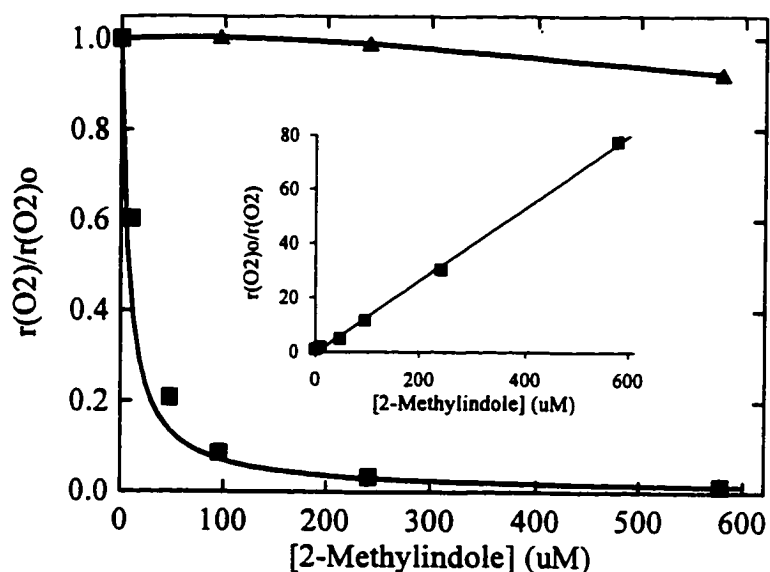


Figure 4.4: Dioxygen formation in the presence of 2-methylindole. (■), V-BrPO; (▲) HOBr. Conditions 100mM sodium phosphate pH 6.5, 50 mM potassium bromide, 20 % ethanol and H_2O_2 10 mM. In the enzyme reaction V-BrPO was 9.7 nM; under these conditions and in the absence of 2-methylindole, the rate of dioxygen formation was 49 $\mu M/min$. In the HOBr reaction, HOBr was added by syringe pump at a rate of 31 $\mu M/min$.

The plot of the inverse of the normalized rate of dioxygen formation *versus* the substrate concentration is linear (Figure 4.4 & 4.5, Inserts) and follows equation 4.2:

$$\frac{r(O_2)_0}{r(O_2)} = 1 + K_{app}[S] \quad (4.2)$$

where K_{app} for 2-methylindole is $1.33 \times 10^5 \text{ M}^{-1}$ and K_{app} for 3-methylindole is $0.46 \times 10^5 \text{ M}^{-1}$. The meaning of K_{app} will be discussed below.

The oxidation of hydrogen peroxide by HOBr in the presence of 3-methylindole also follows the relationship given by equation 4.2 but this behavior is only detected at quite low hydrogen peroxide concentration (e.g., $250 \mu\text{M}$) (Figure 4.6). In this case K_{app} for 3-methylindole is $0.025 \times 10^5 \text{ M}^{-1}$.

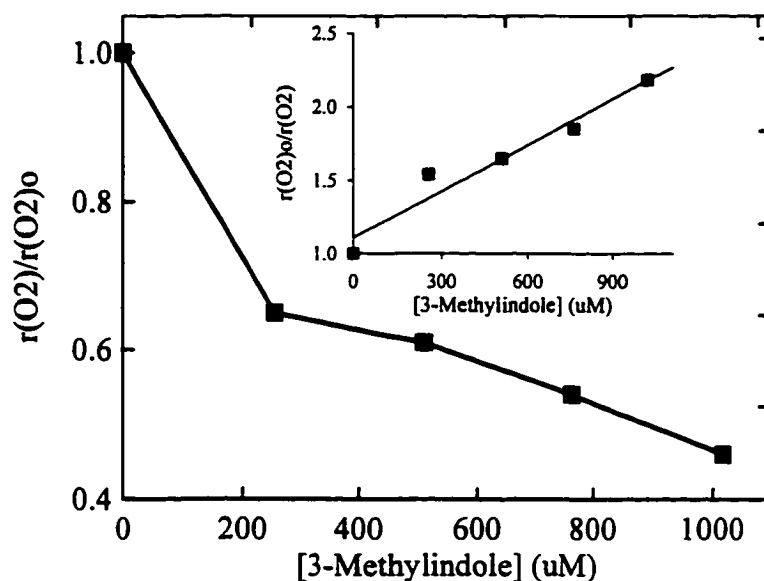


Figure 4.6: Oxidation of H_2O_2 by HOBr in the presence of 3-methylindole. Reaction conditions: 100 mM sodium phosphate pH 6.5, 50 mM potassium bromide, 20 % ethanol and $250 \mu\text{M}$ H_2O_2 . HOBr was added at a rate of $5.7 \mu\text{M}/\text{min}$.

Effect of hydrogen peroxide concentration on K_{app} . The rate of the V-BrPO-catalyzed bromide assisted disproportionation of hydrogen peroxide in the presence of 3-methylindole depends on the concentration of hydrogen peroxide (Figure 4.7).

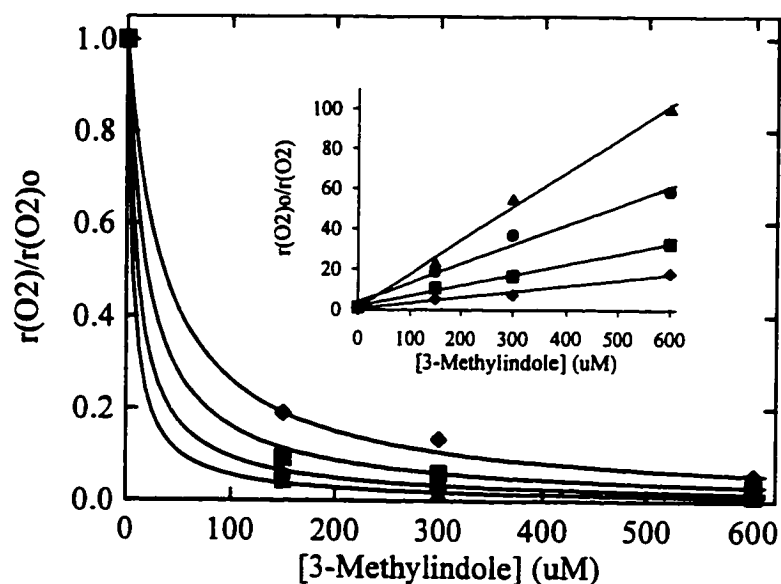


Figure 4.7: Normalized rate of dioxygen formation by V-BrPO in the presence of 3-methylindole, as a function of hydrogen peroxide concentration. Reaction conditions: 100 mM sodium phosphate pH 6.5, 50 mM potassium bromide, 20 % ethanol, 2.1 nM V-BrPO. H_2O_2 : (◆), 100 mM; (■), 50 mM; (●), 25 mM; (▲), 12.5 mM. Insert: Plot of the inverse of the normalized rate of dioxygen formation *versus* 3-methylindole concentration.

The plot of the inverse of the normalized rate of dioxygen production as a function of 3-methylindole is linear at all hydrogen peroxide concentrations investigated and follows equation 4.2 (Figure 4.7, Insert). It was found that the

plot of $1/K_{app}$ versus $[H_2O_2]$ is linear for V-BrPO (Figure 4.8), but does not intersect the origin. It was fitted by equation 4.3:

$$\frac{1}{K_{app}} = 3.4 \pm 0.4 \times 10^{-4} [H_2O_2] + 1.8 \pm 0.2 \times 10^{-6} \quad (4.3)$$

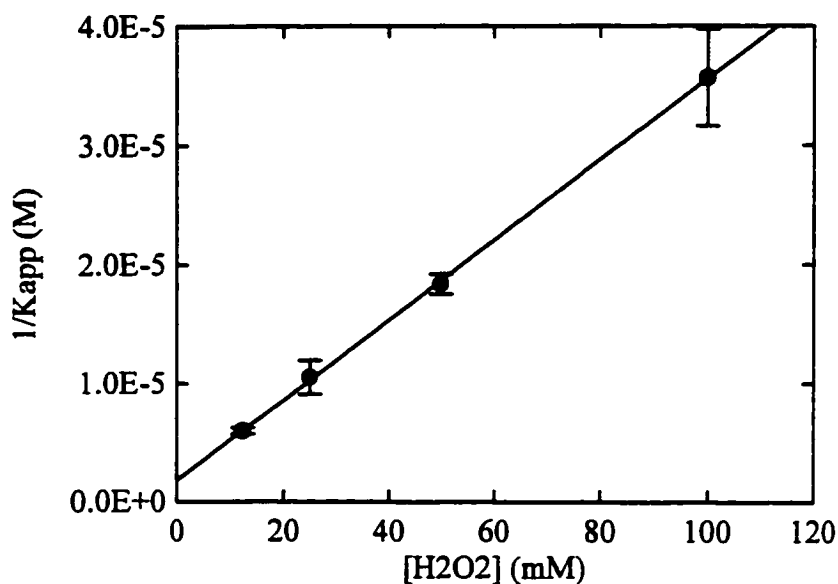


Figure 4.8: Plot of $1/K_{app}$ versus $[H_2O_2]$. Results were obtained from data in Figure 4.7.

V-BrPO Concentration Dependence of K_{app} . It can be argued that the difference observed between K_{app} determined for V-BrPO and K_{app} determined for HOBr is due to microscopic dissimilarity between the two systems. Although HOBr is introduced to the reaction mixture at a rate adjusted to match the activity of the enzyme, the concentration of HOBr at the point of injection is still very high. In order to address that question, the rate of dioxygen formation in the

presence of 2-methylindole was measured as a function of the concentration in V-BrPO (Figure 4.9). It was found that the magnitude of K_{app} depends on the concentration of V-BrPO and that K_{app} increases with increasing V-BrPO concentration (Figure 4.10). K_{app} appears to follow a "saturation behavior" with respect to the concentration in enzyme. At high V-BrPO concentration, K_{app} tends toward a limiting value of $K_{app,max}$. The value of $K_{app,max}$ can be determined from the intercept of the plot of $1/K_{app}$ versus $1/[V-BrPO]$ (Figure 4.10, Insert) and $K_{app,max} = 7.69 \times 10^4 \text{ M}^{-1}$ for 2-methylindole.

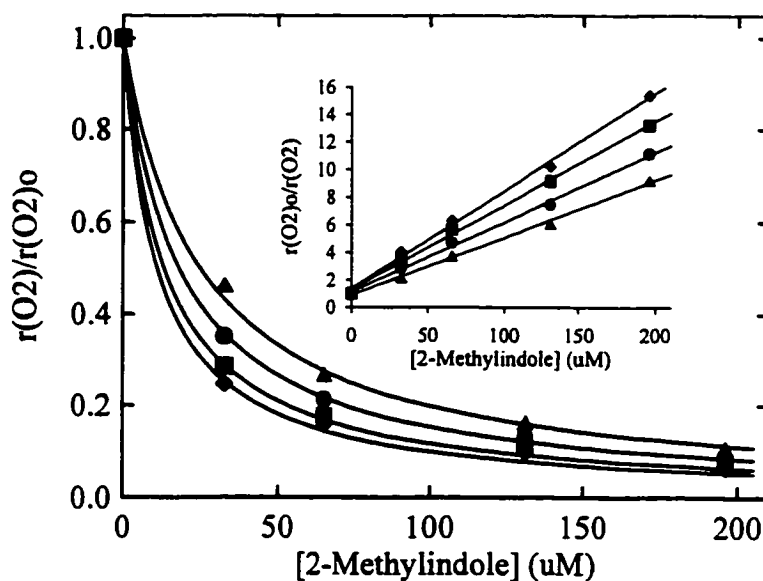


Figure 4.9: Normalized rate of dioxygen production in the presence of 2-methylindole as a function of V-BrPO concentration. Reaction conditions: 100 mM sodium phosphate pH 6.5, 50 mM potassium bromide, 20 % ethanol, 10 M H_2O_2 . V-BrPO : (\blacklozenge), 9.0 nM; (\blacksquare), 2.45 nM; (\bullet), 1.22 nM; (\blacktriangle), 0.82 nM. Insert: Plot of the inverse of the normalized rate of dioxygen formation.

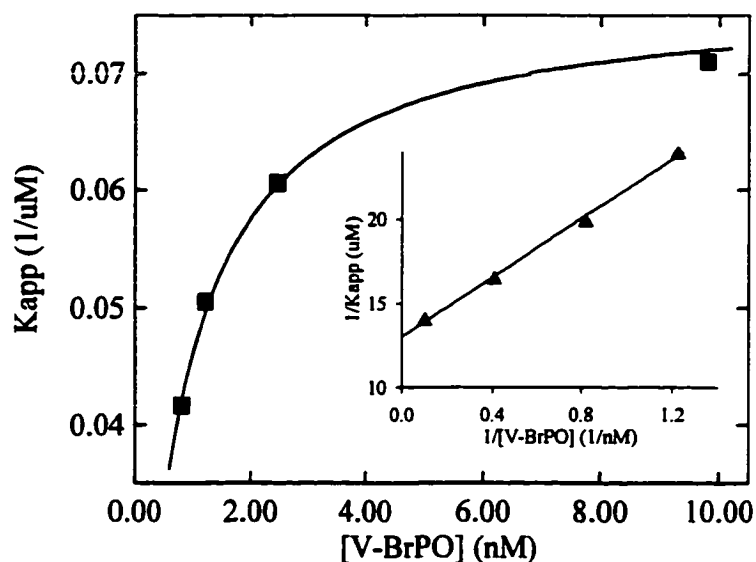


Figure 4.10: Plot of K_{app} versus $[V-BrPO]$.

In contrast, the rate of HOBr addition has no effect on the magnitude of K_{app} for the chemical brominating system (Table 4.2). These data further indicate that the bromination reaction of the enzyme is not due to HOBr released into the reaction mixture.

Table 4.2: Variation of K_{app} for 3-Methylindole as a Function of the Rate of HOBr Addition.

Rate of addition of HOBr ($\mu\text{M}/\text{min}$)	K_{app} (M^{-1})
5.75	2.50×10^3
19.09	2.56×10^3
74.09	2.52×10^3

Reaction conditions: 100 mM sodium phosphate, pH 6.5, 50 mM potassium bromide, 10 % ethanol, 250 μM H_2O_2 , 0-1 mM 3-methylindole. HOBr (6.90 mM) was added *via* syringe pump.

Substrate Concentration Dependence of the Oxidation of 3-Methylindole by V-BrPO. The oxidation of 3-methylindole by V-BrPO to form 3-methyl-2-oxindole can be conveniently followed by monitoring the loss of absorbance of 3-methylindole at $\lambda=281$ nm. The rate of the reaction was computed using $\Delta\varepsilon = 4037 \text{ M}^{-1} \text{ cm}^{-1}$. The substrate-concentration dependence experiment was conducted using 3-methylindole concentrations between 50 μM and 1 mM at various hydrogen peroxide concentrations. The results presented in Figure 4.11 indicate the rate of bromination of 3-methylindole depends only slightly on the concentration of 3-methylindole over the range studied. It can be seen that the concentration effects are independent of the concentration of hydrogen peroxide. At concentrations of 3-methylindole below 200 μM , the rate of the reaction

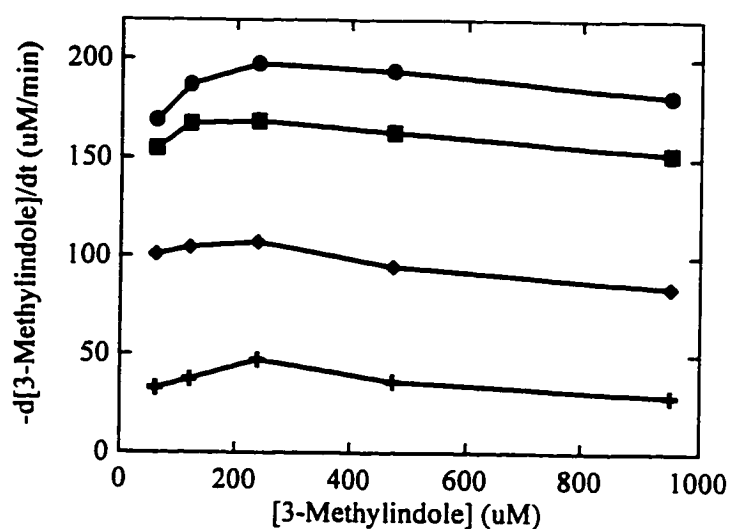


Figure 4.11: Effect of 3-methylindole concentration on the initial rate of bromination of 3-methylindole by V-BrPO. Conditions: 100 mM sodium phosphate pH 6.0, 50 mM potassium bromide, 10 % ethanol, 37 nM V-BrPO, and (+) 50 μM , (◆) 200 μM , (■) 800 μM , or (●) 3.2 mM H_2O_2 .

increases with increasing substrate concentration. Although the changes in the rate observed are fairly small they may indicate the end of a substrate saturation curve. The rate of 3-methylindole drops slightly at 3-methylindole concentrations above 200 μM . This drop suggests substrate inhibition at those concentrations.

Hydrogen peroxide concentration dependence. The rate of 3-methylindole oxidation depends on the concentration of hydrogen peroxide (Figure 4.12). The initial reaction velocity reaches a maximum at a hydrogen peroxide concentration of *ca.* 3.2 mM and decreases at higher hydrogen peroxide concentrations. At low hydrogen peroxide concentration ($[\text{H}_2\text{O}_2] < 3.2 \text{ mM}$) the

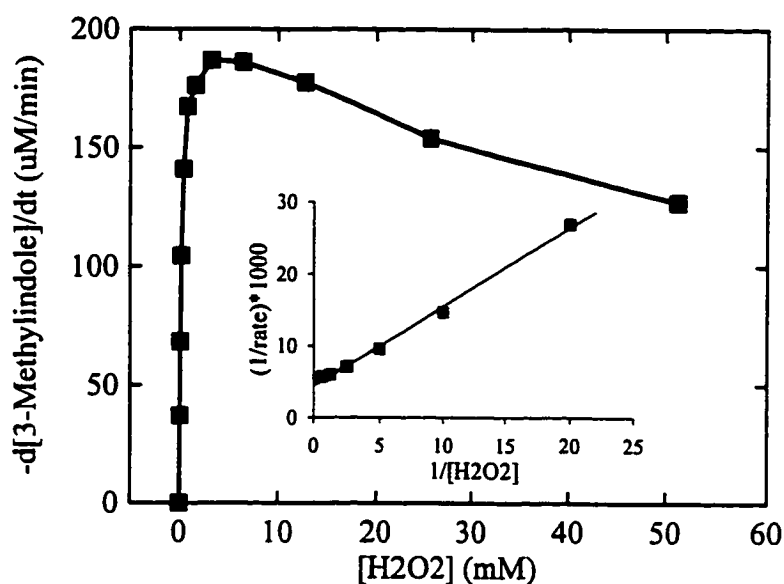


Figure 4.12: Effect of H_2O_2 concentration on the initial rate of oxidation of 3-methylindole by V-BrPO. Conditions: 100 mM sodium phosphate pH 6.00, 50 mM potassium bromide, 10 % ethanol, 37 nM V-BrPO and 120 μM H_2O_2 .

data could be fitted to a rectangular hyperbola consistent with the Michaelis-Menten kinetic equation (Figure 4.12, insert):

$$v = -\frac{d([3\text{-Methylindole}])}{dt} = \frac{V_{\max} [H_2O_2]}{K_M^{H_2O_2} + [H_2O_2]} \quad (4.4)$$

$K_M^{H_2O_2}$ and V_{\max} were found to be $250 \pm 17 \mu\text{M}$ and $226 \pm 21 \mu\text{M}/\text{min}$, respectively.

Substituent Effect on the Rate of Bromination. It was determined in Chapter 2 that bromination of indole catalyzed by V-BrPO occurred exclusively on C-2/C-3 double bond. It was of interest to see whether the presence of substituents on that bond affects the rate of bromination of indoles. Figure 4.13 and Table 4.3 show

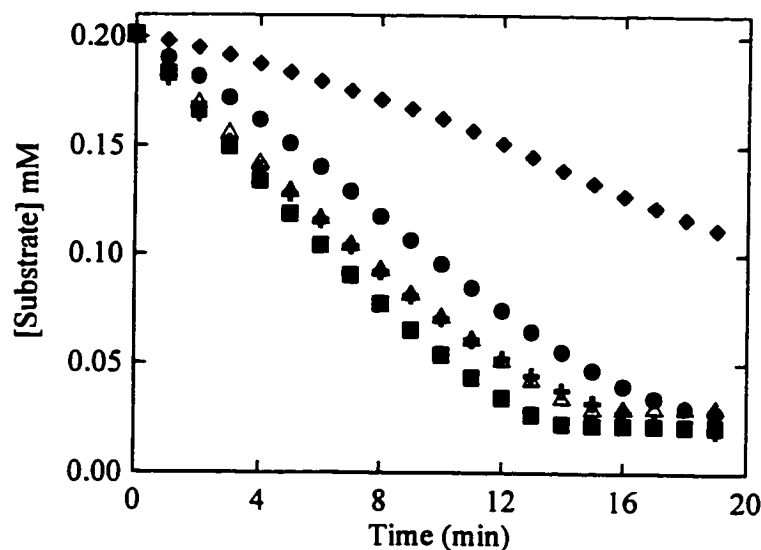


Figure 4.13: Bromination of substituted indoles by V-BrPO. (+), 3-Phenylindole; (▲), 3-methylindole; (■), 3-*tert*-butylindole; (●), 1,3-di-*tert*-butylindole (◆), 2-*tert*-butylindole. Conditions: 100 mM sodium phosphate, pH 6.50, 50 mM potassium bromide, 20 % ethanol, 2 nM V-BrPO, 0.20 mM substrate, and 0.22 mM H_2O_2 .

that the initial rate ($t < 1$ min) of indole bromination decreases as a function of the

substituent, in the following order: 3-phenylindole \approx 3-*tert*-butylindole > 3-methylindole > 1,3-di-*tert*-butylindole \gg 2-*tert*-butylindole. A lag phase is observed for 2-*tert*-butylindole and, to a lesser extent, 1,3-di-*tert*-butylindole. The cause of this lag phase is not known but it could be due to initial substrate inhibition. As the substrate is consumed, the concentration of inhibitor decreases, and an increase in the rate of the reaction is observed.

Table 4.3: Rate of Bromination of Substituted Indole by V-BrPO.

Substrate	Initial rate of substrate bromination ^a ($\mu\text{M}/\text{min}$)	Initial rate of dioxygen production ^b ($\mu\text{M}/\text{min}$)
3-Phenylindole	17.7	0.03
3- <i>tert</i> -Butylindole	17.4	0
3-Methylindole	14.9	0
1,3-Di- <i>tert</i> -butylindole	9.5	0
2- <i>tert</i> -Butylindole	2.7	0

^a Calculated from the data in Figure 4.13 for $t < 1 \text{ min}$. ^b The rate of dioxygen production in the absence of substrate is $10.1 \pm 0.6 \mu\text{M}/\text{min}$.

Dioxygen production is turned off during the bromination of all indoles used (Table 4.3), but the rates of bromination of the indoles do not match the rate of dioxygen production in the absence of any substrate. In the case of 3-phenylindole, 3-*tert*-butylindole, and 3-methylindole, the rate of substrate bromination is greater than the rate of dioxygen production in the absence of

substrate. The rate of 2-*tert*-butylindole was, however, lower than the rate of dioxygen production in absence of substrate.

The initial rate of bromination of 2-*tert*-butylindole is only 25 % of the initial rate of bromination of 3-*tert*-butylindole (Figure 4.14A). It is expected in a competition experiment with both substrates present in equimolar amounts, that 3-*tert*-butylindole would be favorably brominated over 2-*tert*-butylindole. Figure 4.14B shows that the opposite is observed, and that 2-*tert*-butylindole is preferentially brominated over 3-*tert*-butylindole.

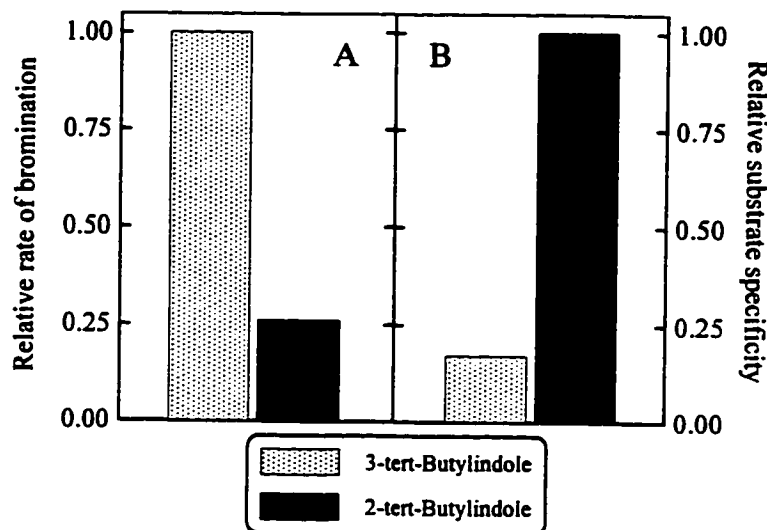


Figure 4.14: Comparison between the reactivity of V-BrPO with 2-*tert*-butylindole and 3-*tert*-butylindole. Panel A: Relative rates of substrate bromination measured in separate assays (Data from table 4.3). Panel B: Relative amount of substrate being brominated in competition experiment: Conditions: 100 mM sodium phosphate, 50 mM potassium bromide, 20 % ethanol, 200 μM H_2O_2 , 2.0 nM V-BrPO, 208 μM 2-*tert*-butylindole, and 204 μM 3-*tert*-butylindole.

Inhibition of V-BrPO by organic compounds. Since it was observed that bromination of 3-methylindole appeared to be inhibited at high substrate

concentrations (Figure 4.1) it was of interest to see if V-BrPO could be inhibited by organic compounds structurally related to indole. Table 4.4 gives the rate of dioxygen production observed in the presence of different compounds that are not brominated by V-BrPO. 3-Nitroindole and benzimidazole do not inhibit V-BrPO whereas benzofuran and 2-*tert*-butylbenzofuran clearly inhibit dioxygen production. Inhibition by 3-*tert*-butylbenzofuran appears to be weaker than the two other benzofurans tested.

Table 4.4: Effect of 3-Nitroindole, Benzofurans, and Benzimidazole on the Production of Dioxygen by V-BrPO.

Compound Tested	Rate of O ₂ production in the absence of compound (μM/min) ^a	[Compound] (mM)	Rate of O ₂ production in the presence of compound (μM/min)
3-Nitroindole	9.36	0.217	9.44
Benzofuran	11.73	1.348	9.22
3- <i>tert</i> -Butylbenzofuran	11.73	1.343	10.49
2- <i>tert</i> -Butylbenzofuran	11.73	1.280	8.51
Benzimidazole	11.67	1.130	10.25
		5.440	10.74

Reaction conditions: 100 mM sodium phosphate, 50 mM potassium bromide, pH 5.95 10 % ethanol, 0.101 mM H₂O₂, 2nM V-BrPO. ^a The variations observed in this column are due to the fact that different batches of V-BrPO were used.

Inhibition of dioxygen production by 2-*tert*-butylbenzofuran and 3-*tert*-butylbenzofuran could not be investigated in greater detail due to the poor miscibility of those compounds with water. Only the inhibition by benzofuran was further studied. The double reciprocal plot of the rate of dioxygen formation *versus* the hydrogen peroxide concentration at various benzofuran concentrations is shown in Figure 4.15. The effect of benzofuran generates a competitive pattern with respect to hydrogen peroxide. However, the plot of the slope of each linear fit as a function of the corresponding benzofuran concentration does not produce a straight line (Figure 4.15, insert). The departure from the generally observed linear behavior is most likely due to the poor miscibility of benzofuran in 20 %

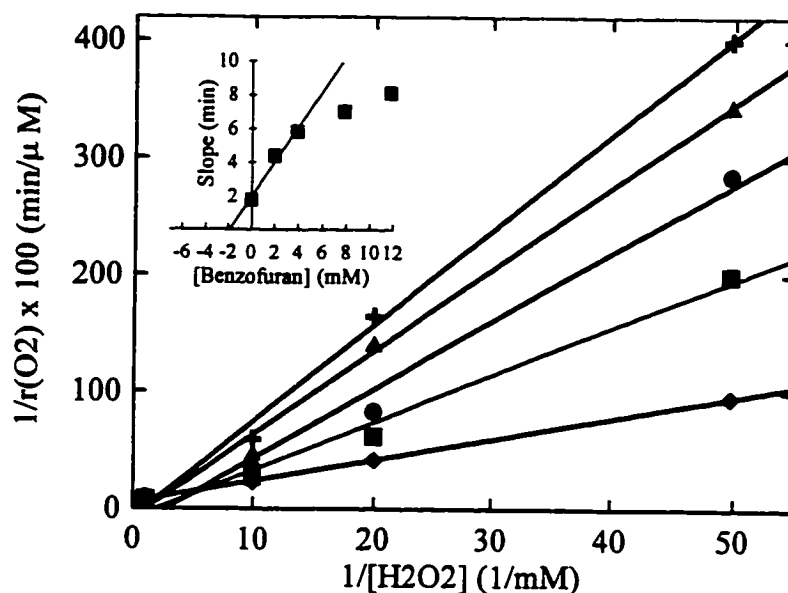


Figure 4.15: Inhibition of dioxygen production by benzofuran. Benzofuran: (\blacklozenge), 0 mM; (\blacksquare), 2.0 mM; (\bullet), 3.9 mM; (\blacktriangle), 7.8 mM; ($+$), 11.8 mM. Conditions: 100 mM sodium phosphate pH 6.5, 50 mM potassium bromide, 20 % ethanol, and 2.0 nM-BrPO.

ethanol at concentrations above 4 mM.² A value of the inhibition constant (K_i) for benzofuran was estimated to be *ca.* 1.4 mM by using only the first three data points and calculating the x-axis intercept of the corresponding linear fit.

The fact that benzofuran is a competitive inhibitor with respect to hydrogen peroxide suggests that binding of benzofuran must occur near to the active site of V-BrPO and in so doing prevent access of hydrogen peroxide to the vanadium center. If bromination of indole(s) occurs outside of the protein, then benzofuran should not alter the relative reactivity of V-BrPO towards indole and

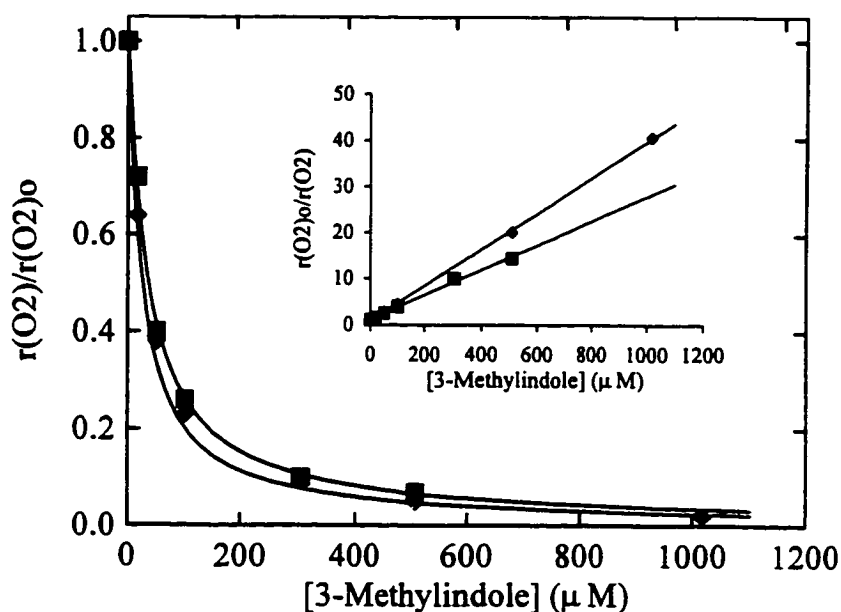


Figure 4.16: Effect of benzofuran on the rate of dioxygen formation in the presence of 3-methylindole. Benzofuran: (\blacklozenge), 0 mM; (\blacksquare), 14.7 mM. Conditions: 100 mM sodium phosphate pH 6.0, 50 mM potassium bromide, 20 % ethanol, 25.1 mM H_2O_2 , 2.9 nM V-BrPO.

² At concentrations of benzofuran above 4 mM solutions become increasingly cloudy. The actual concentration of benzofuran in the aqueous solution was not determined.

hydrogen peroxide. However, the data in Figure 4.16 show that in the presence of benzofuran, more dioxygen is produced indicating that the affinity of the oxidizing (brominating) intermediate generated by V-BrPO towards hydrogen peroxide has been increased. This result more likely reflects competitive binding between 3-methylindole and benzofuran. The observed binding constant for 3-methylindole, as determined from the slope of the linear fit (Figure 4.16, insert) was determined to be $3.89 \times 10^4 \text{ M}^{-1}$ in the absence of benzofuran and $2.74 \times 10^4 \text{ M}^{-1}$ in the presence of a nominal benzofuran concentration of 14.7 mM.

Discussion

Although the reactivity of V-BrPO has been extensively investigated, the details of the final bromination step are still topics of considerable controversies. The data presented in this chapter show that indoles are good substrates for V-BrPO and that they can be used as mechanistic probes for the study of the mechanism of action of V-BrPO. In addition, the results of this study indicate that the bromination of indoles is not consistent with bromination *via* freely diffusible oxidized bromine species (i.e. $\text{Br}_2=\text{Br}_3^-=\text{HOBr}=\text{BrO}^-$), and that V-BrPO is directly involved during the bromine transfer step.

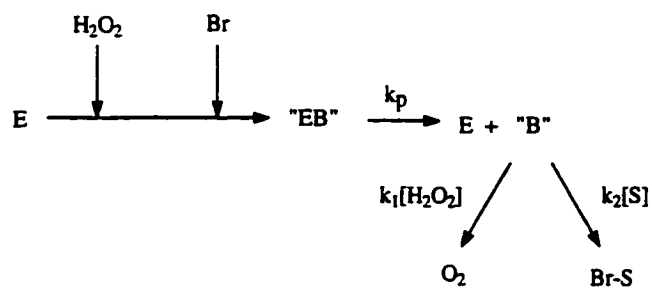
It was reported in earlier studies that MCD, *trans*-cinnamic acid, phenol red, and barbituric acids are suitable substrates for V-BrPO (Wever et al. 1985; de Boer et al., 1987a; Franssen et al., 1988). However, it appears that MCD, *trans*-cinnamic acid, and phenol red are poor substrates when compared to indoles (Table 4.1). Thus, mechanistic investigations carried out with these substrates may not give an accurate description of all the steps involved in V-BrPO-catalyzed bromination reactions. The dramatic difference in substrate specificity between the enzymatic and the nonenzymatic competitive reaction with 2-methylindole and phenol red (Figure 4.2 & 4.3) suggest that the brominating intermediate in the case of 2-methylindole is not a free bromine species and the mechanism of bromination may be more complex than the one given in Scheme 4.1.

The three mechanisms considered to be good candidates for the V-BrPO catalyzed bromination reaction are given in Figure 4.17. All three mechanisms

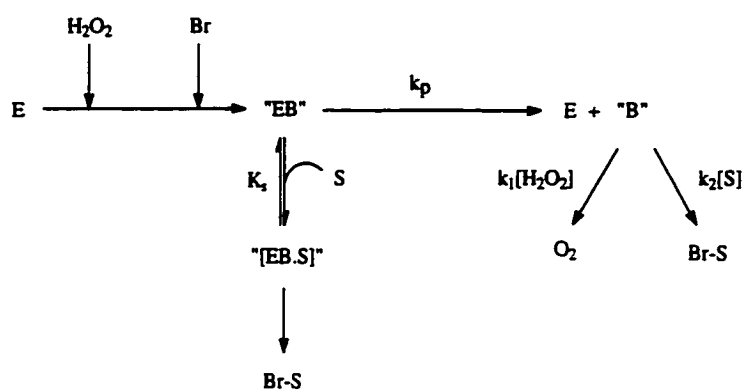
involve the formation of an enzyme-bound intermediate EB, generated by the reaction of V-BrPO with hydrogen peroxide and bromide. Mechanism A involves dissociation of EB to give the native enzyme and the halogenating species B. The nature of B is most likely consistent with molecular bromine or free hypobromous acid. Mechanism B adds an alternate route for substrate bromination *via* substrate binding to V-BrPO. The substrate is shown to bind to EB for simplification. The data presented in Chapter 5 & 6 suggest that, in fact, binding of the substrate to V-BrPO readily occurs with the native enzyme, and does not require addition of peroxide and/or bromide. Mechanism C further adds binding of hydrogen peroxide to EB. Binding of hydrogen peroxide, shown here to be competitive with the substrate, cannot be detected by standard kinetic measurements (i.e. by measuring the rate of dioxygen formation), since even in the absence of binding, reaction of an oxidized bromine species with hydrogen peroxide to form dioxygen will occur. Under the conditions used throughout in this study for the enzymatic reaction (i.e $[H_2O_2] \gg [Substrate]$) all three mechanisms predict behavior conforming to equation 4.2. Each mechanism, however is characterized by a different definition for K_{app} (See Appendix I for the derivation of the equation for each mechanism).

For mechanism A:
$$K_{app} = \frac{k_2}{k_1[H_2O_2]} \quad (4.5)$$

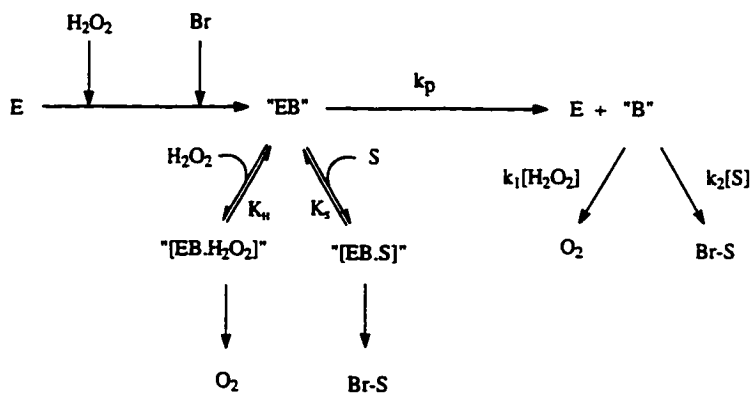
For mechanism B:
$$K_{app} = K_S \quad (4.6)$$



Mechanism A



Mechanism B



Mechanism C

Figure 4.17: General reaction mechanisms for the reaction of indoles with V-BrPO.

For mechanism C:
$$K_{app} = \frac{K_S}{1 + K_H[H_2O_2]} \quad (4.7)$$

As a result, the plot of $1/K_{app}$ versus $[H_2O_2]$ should allow distinction between mechanisms. For mechanism B, $1/K_{app}$ is expected to be independent of $[H_2O_2]$, whereas for both mechanisms A and C the plot $1/K_{app}$ versus $[H_2O_2]$ is expected to be linear. Mechanisms A and C can be differentiated since for mechanism A the plot will intersect the origin.

When 3-methylindole is used as substrate, the plot of $1/K_{app}$ versus $[H_2O_2]$ for the V-BrPO reaction is linear but does not intersect the axis origin (Figure 4.8) and therefore points to mechanism C as a possible reaction mechanism for V-BrPO. Fit of the data to equation 4.7 gives $K_S = 5.6 \pm 0.6 \times 10^5 \text{ M}^{-1}$ ($K_{d,S} = 1.8 \pm 0.2 \text{ }\mu\text{M}$) and $K_H = 189 \pm 48 \text{ M}^{-1}$ ($K_{d,H} = 5.2 \pm 0.9 \text{ mM}$).

The differences in the dioxygen formation rates between the enzymatic and the chemical reactions in the presence of 2-methylindole or 3-methylindole further shows that the V-BrPO-catalyzed bromination of these substrates does not depend on the release of molecular bromine or hypobromite ion into the reaction mixture as predicted by mechanism A (Figure 4.4 & 4.5). However, it has been shown that when monochlorodimedone is used as substrate, the bromination of monochlorodimedone ($k_2[\text{MCD}]$) is competitive with the oxidation of hydrogen peroxide ($k_1[\text{H}_2\text{O}_2]$), since the sum $k_1[\text{H}_2\text{O}_2] + k_2[\text{MCD}]$ is equal to the rate of dioxygen formation in the absence of MCD (Everett et al., 1990b; Soedjak, 1991, Soedjak et al., 1995). In addition, the kinetic parameters for monochlorodimedone bromination and dioxygen formation are identical and

indicate that the reaction occur *via* a common intermediate which is produced in a rate limiting step (Everett et al., 1990b). These data suggest that bromination of MCD follows mechanism A since mechanisms B and C both involve more than one brominating intermediate. Thus, the exact path of the reaction appears to depend on the structure of the substrate. The competitive behavior observed for the MCD/H₂O₂ system is not observed in the case of indoles, and the rates of 3-phenylindole, 3-*tert*-butylindole and 3-methylindole bromination are higher than the rate of dioxygen production in the absence of any substrate (Table 4.3). Furthermore, in the case of 2-*tert*-butylindole, the sum of the rate of substrate bromination (2.7 $\mu\text{M}/\text{min}$) and the rate of dioxygen formation (0 $\mu\text{M}/\text{min}$) do not equal the rate of dioxygen production in the absence of substrate (10.1 $\mu\text{M}/\text{min}$), and strongly suggest that bromination of 2-*tert*-butylindole and formation of dioxygen do not occur *via* the same intermediate.

The formation of dioxygen by V-BrPO is inhibited by benzofuran. The inhibition pattern observed indicates that benzofuran binds V-BrPO competitively with respect to hydrogen peroxide (Figure 4.16). In addition, the presence of benzofuran induces a drop in the K_{app} for 3-methylindole (Figure 4.17). In the light of mechanism C, this result suggests that binding of benzofuran to V-BrPO prevents binding of 3-methylindole and therefore favors release of the brominating intermediate (molecular bromine or hypobromous acid) outside of the protein. Under the conditions used (i.e. $[\text{H}_2\text{O}_2] \gg [3\text{-methylindole}]$) this intermediate reacts predominantly with hydrogen peroxide to form dioxygen and thus, decreases the value of K_{app} .

Appendix to Chapter 4

Derivation of equation 4.2 for mechanisms A, B, and C (Figure 4.17).

Mechanism A

In mechanism A, the fully dissociated intermediate "B" is the only reactive species. It is formed from dissociation of the enzyme-bound intermediate "EB" and consumed by reaction with hydrogen peroxide or by reaction with an halogen acceptor (S).

The rate of dioxygen production is given by

$$r(O_2) = k_1[B][H_2O_2] \quad (A.1)$$

From the hypothesis that the intermediate B is in steady state, one can write that

$$r(B) = k_p[EB] - k_1[B][H_2O_2] - k_2[B][S] = 0 \quad (A.2)$$

and

$$[B] = \frac{k_p[EB]}{k_1[H_2O_2] + k_2[S]} \quad (A.3)$$

The rate of dioxygen production becomes

$$r(O_2) = \frac{k_1 k_p [EB][H_2O_2]}{k_1[H_2O_2] + k_2[S]} \quad (A.4)$$

The rate of dioxygen production in the absence of substrate is given by

$$r(O_2)_0 = \frac{k_1 k_p [EB][H_2O_2]}{k_1[H_2O_2]} \quad (A.5)$$

From equations A.4 and A.5,

$$\frac{r(O_2)}{r(O_2)_0} = \frac{k_1[H_2O_2]}{k_1[H_2O_2] + k_2[S]} \quad (A.6)$$

and

$$\frac{r(O_2)_0}{r(O_2)} = 1 + \frac{k_2[S]}{k_1[H_2O_2]} \quad (\text{A.7})$$

or

$$\frac{r(O_2)_0}{r(O_2)} = 1 + K_{app}[S] \quad (\text{A.8})$$

Mechanism B

In mechanism B, the substrate can bind to the enzyme-bound intermediate "EB" and form a complex "[EB.S]" prior to bromine atom transfer.

$$K_s = \frac{[EB.S]}{[EB][S]} \quad (\text{B.1})$$

The derivation is accomplished for conditions in which $[H_2O_2] \gg [S]$, and "B" reacts in an HOBr-like fashion. Thus, it is assumed that "B" will only react with hydrogen peroxide.

It is also assumed that "free" "EB" ("EB" that has no S bound) will dissociate to give "B" and that k_p is not a rate limiting step, therefore the rate of dioxygen production is proportional to the concentration of "EB":

$$r(O_2) \propto [EB] \quad (\text{B.2})$$

The rate of dioxygen production in the absence of substrate can be given by:

$$r(O_2)_0 \propto [EB] + [EB.S] \quad (\text{B.3})$$

The ratio of the rate of dioxygen production in the absence of substrate over the rate of dioxygen production in the presence of substrate becomes:

$$\frac{r(O_2)_0}{r(O_2)} = \frac{[EB] + [EB.S]}{[EB]} \quad (\text{B.4})$$

and

$$\frac{r(O_2)_0}{r(O_2)} = 1 + \frac{[EB.S]}{[EB]} \quad (\text{B.5})$$

By plugging in equation B.1, equation B.5 becomes:

$$\frac{r(O_2)_0}{r(O_2)} = 1 + K_S[S] \quad (\text{B.6})$$

Mechanism C

Mechanism C is an extension of mechanism B in which hydrogen peroxide can also bind to "EB":

$$K_H = \frac{[EB.H_2O_2]}{[EB][H_2O_2]} \quad (\text{C.1})$$

By assuming that the rate limiting step lies prior to "EB", the rate of dioxygen production is given by:

$$r(O_2) \propto [EB] + [EB.H_2O_2] \quad (\text{C.2})$$

and the rate of dioxygen formation in the absence of S is given by equation C.3.

$$r(O_2)_0 \propto [EB] + [EB.H_2O_2] + [EB.S] \quad (\text{C.3})$$

Using a similar derivation to the one used for mechanism B gives:

$$\frac{r(O_2)_0}{r(O_2)} = \frac{[EB] + [EB.H_2O_2] + [EB.S]}{[EB] + [EB.H_2O_2]} \quad (\text{C.4})$$

And:

$$\frac{r(O_2)_0}{r(O_2)} = 1 + \frac{[EB.S]}{[EB] + [EB.H_2O_2]} \quad (\text{C.5})$$

Including equations B.1 and C.1 yields:

$$\frac{r(O_2)_0}{r(O_2)} = 1 + \frac{K_S[EB][S]}{[EB] + K_H[EB][H_2O_2]} \quad (\text{C.6})$$

And:

$$\frac{\kappa(O_2)_0}{\kappa(O_2)} = 1 + \frac{K_s[S]}{1 + K_H[H_2O_2]} \quad (C.7)$$

Chapter 5

Quenching of the Fluorescence of 2-Phenylindole by Vanadium-Bromoperoxidase

Introduction

The mechanism of halogen transfer from various vanadium containing bromoperoxidases (V-BrPO) to halogenation substrates has been the object of several investigations (Itoh et al. 1987a&b; de Boer & Wever, 1988; Everett & Butler, 1989; Everett et al., 1990b, Soedjak & Butler, 1990). Those studies have heavily relied on kinetic and substrate specificity experiments as well as comparisons between enzymatic and non-enzymatic reactions in order to determinate whether the transfer was direct (involving a enzyme bound intermediate) or if it required the intermediacy of an of a non-enzymatic agent, such as Br₂ or HOBr. In no case, however, have the interactions between the enzyme and the halogenated substrates been investigated. A direct physico-chemical determination of substrate binding would undoubtedly aid in the elucidation of the mechanism of action of V-BrPO.

In Chapter 4, it has been shown that V-BrPO selectively brominates indoles over a variety of other substrates and that its reactivity differs from "free" hypobromous acid, suggesting that V-BrPO can bind indoles. In this chapter, the

fluorescence properties of indoles have been used to further investigate their binding to V-BrPO.

Fluorescence of Indoles. The fluorescence and fluorescence quenching of the indole moiety have been extensively studied (Creed, 1984). Investigations were mainly directed to obtain information about the excited state behavior and the location of tryptophan units in biological systems. In addition, the fluorescence spectroscopy of tryptophan has been widely used to study the structure, dynamics, and interactions of proteins in solutions, the solvent exposure of amino acid side chains, protein conformation, rotational diffusion of proteins, and distances between sites on a protein (Lakowicz, 1983; Badea & Brand, 1979; Beecham & Brand, 1985; Eftink, 1991a). However, there are no examples in the literature describing the use of fluorescence spectroscopy to investigate the binding of indoles to proteins, probably because the excitation and emission spectra of most indoles in their neutral form overlap with the spectra of proteins, rendering the data difficult to extract (Bidges & Williams, 1968).

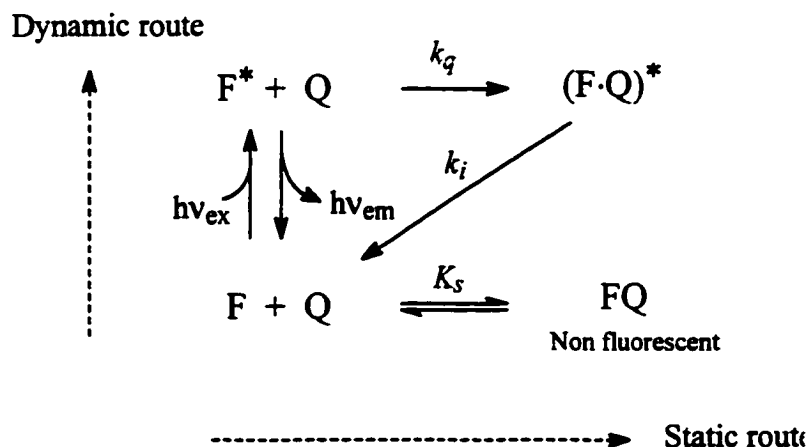
Fluorescence Quenching. Fluorescence quenching reactions have been primarily used to obtain topographical information about proteins and are determined by the accessibility of the fluorescent probe to the quencher. Fluorescence quenching can be the result of a variety of different processes, including excited state reactions, energy transfer, complex formation and collisional quenching, the latter two being the most predominant when studying the interactions between a substrate and a protein. The quenching resulting from collisional encounters between the fluorophore and the quencher is often referred

to as dynamic quenching, whereas the quenching resulting from formation of a complex between the fluorophore and the quencher is generally referred to as static quenching (Lakowicz, 1983).

Dynamic and static quenching are extremely useful because both necessitate molecular contact between the fluorophore and the quencher. In the case of dynamic quenching, the quencher must diffuse to the fluorophore during the lifetime of the excited state. On the other hand, static quenching requires the formation of a non-fluorescing complex between the fluorophore and the quencher. For example, the solvent accessibility of tryptophan residues in proteins has been widely studied by using fluorescence quenching by iodide and this method has been used to separate internal and external tryptophan residues in lysozyme (Lehrer, 1971). It is also a powerful tool for monitoring conformational changes in a protein, since the accessibility of the fluorophore to the quencher may vary with shifts in the tertiary structure of the protein (Eftink, 1991).

The quenching of an excited state by a quencher can be described by the reaction scheme in Scheme 5.1. After excitation, the fluorophore F^* may collide with a quencher Q, with a bimolecular quenching rate constant k_q , to form an excited-state complex $(F \cdot Q)^*$. The complex will then undergo an internal quenching reaction with a rate constant k_i . This type of collisional quenching of fluorescence can be described by the Stern-Volmer equation:

$$\frac{F_0}{F} = 1 + K_D[Q] \quad (5.1)$$



Scheme 5.1

In this equation F_0 and F are the fluorescence intensities in the absence and presence of quencher, respectively, and K_D is the Stern-Volmer quenching constant. K_D is related to the bimolecular quenching constant, k_q , by equation 5.2, where τ_0 is the lifetime of the fluorophore in the absence of quencher.

$$K_D = k_q \tau_0 \quad (5.2)$$

The bimolecular quenching constant k_q , in turn, is related to the collisional frequency, k_0 , by an efficiency coefficient γ :

$$k_q = \gamma k_0 \quad (5.3)$$

Quenching can also occur as a result of the formation of a non-fluorescent complex between the fluorophore and the quencher. When this complex absorbs

light, it immediately returns to the ground state without emitting a photon. This quenching mechanism is described by an equation similar to equation 5.1:

$$\frac{F_0}{F} = 1 + K_s[Q] \quad (5.4)$$

In the case of static quenching, the Stern-Volmer constant, K_s , is equal to the association constant (or the inverse of the dissociation constant, K_d) for the formation of the non-fluorescent complex (Lakowicz, 1983):

$$K_s = \frac{1}{K_d} = \frac{[FQ]}{[F][Q]} \quad (5.5)$$

In some cases, however, fluorescence quenching cannot be described by one mechanism alone, and the total degree of quenching is a product of a dynamic and a static term:

$$\frac{F_0}{F} = (1 + K_d[Q])(1 + K_s[Q]) \quad (5.6)$$

According to this equation, plots of F_0/F versus $[Q]$ (Stern-Volmer plots) have an upward curvature (Eftink et al., 1987). The dynamic portion of the overall quenching can generally be determined by fluorescence lifetime measurements. Ground-state complexation forms a non-fluorescent complex and affects the lifetime of the remaining "free" fluorophore. On the other hand, dynamic quenching of the fluorescence of excited fluorophores requires collision between

the fluorophore and the quencher during the lifetime of the excited species. The net result is a reduced lifetime of the excited state of the fluorophore.

In this chapter, 2-phenylindole has been used as a probe to investigate the binding of organic substrates to V-BrPO. 2-Phenylindole is not only a good substrate for V-BrPO, but its fluorescence properties (λ_{ex} and λ_{em}) are also distinct from the fluorescence properties of V-BrPO. Those characteristics make 2-phenylindole an attractive tool for the study of its interactions with the protein.

Materials and Methods

Materials. V-BrPO was purified as described previously (Everett, 1990). Protein concentrations were determined by bicinchononic acid (BCA) protein assay (Pierce). Apo-V-BrPO was prepared by incubating V-BrPO in 100 mM phosphate buffer at pH 4.5 containing 1 mM EDTA for 24 h. 2-Phenylindole was prepared according to the method of Houlihan and co-workers (Houlihan al. 1981).

Fluorescence Measurements. All fluorescence measurements were performed on a Perkin-Elmer LS 50 luminescence spectrophotometer utilizing a xenon lamp. Conditions, unless otherwise noted, were 0.56 μ M 2-phenylindole in 1.0 or 1.7 mL of 100 mM Tris buffer, pH 8.3, in a 1-cm quartz cuvette at 25 °C. 2-Phenylindole was excited at 314 nm or 330 nm and the emission was followed at 364 nm. Excitation and emission slit widths were 2.5 nm and 3.0 nm respectively. Titrants were added by successive additions of 10 to 20 μ L aliquots. Fluorescence emissions were then measured with an integration time of 5 to 10 sec. Corrections for slight dilutions were applied when necessary.

Results

Quenching of the Fluorescence of 2-Phenylindole by V-BrPO. When excited at 314 nm, 2-phenylindole presented a broad emission spectrum from 330 nm to 430 nm with a maximum at 364 nm and a small shoulder at 348 nm (Figure 5.1, Spectrum a). Addition of 4 equivalents of V-BrPO, resulted in a drop in the

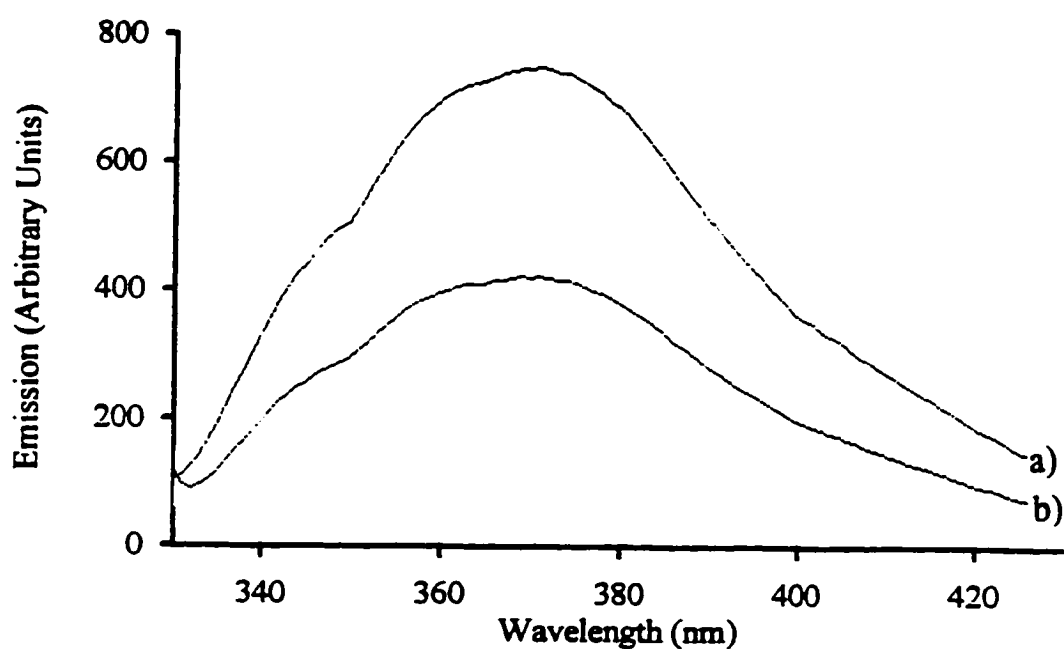


Figure 5.1: Fluorescence spectrum of 2-phenylindole in the absence and the presence of V-BrPO. a) 0 μM V-BrPO , b) 2.0 μM V-BrPO (uncorrected for dilution). Conditions: 100 mM Tris buffer, pH 8.3, 1 % ethanol and 0.56 μM 2-phenylindole in a total volume of 2.8 mL. For b) 350 μL of V-BrPO (18 μM) were added to the mixture at once.

fluorescence intensity of *ca.* 40 % (Figure 5.1, Spectrum b). Correction for dilution indicated a net decrease in fluorescence intensity of 32 %. The addition

of V-BrPO had no discernable effect on the shape and maximum of the 2-phenylindole fluorescence envelope.

Figure 5.2 shows the decrease in 2-phenylindole fluorescence as a function of V-BrPO concentration. Addition of V-BrPO to a concentration of 5.5 μM (10 equivalents) was sufficient to quench 50 % of the initial fluorescence intensity. In a control experiment, bovine serum albumin (BSA), a protein similar to V-BrPO in size and molecular weight, did not quench the fluorescence of 2-phenylindole (Figure 5.2).

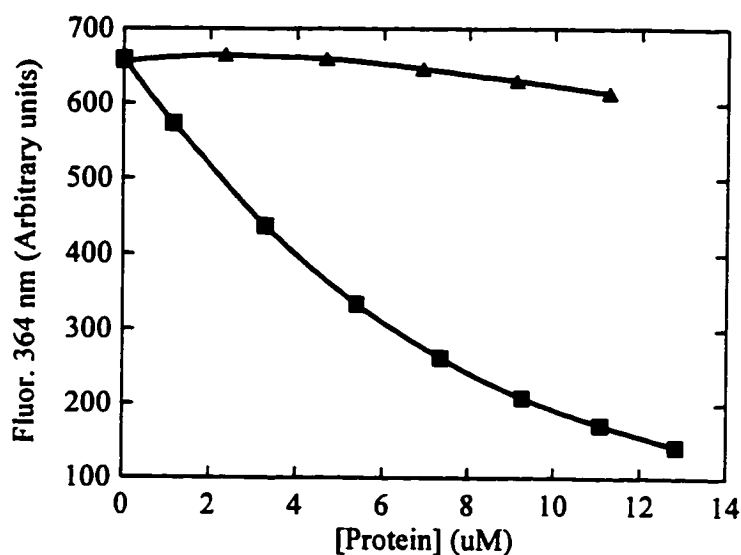


Figure 5.2: Quenching of the fluorescence of 2-phenylindole by V-BrPO and BSA. ■, V-BrPO; ▲, BSA. The experiments were carried out at 21 °C by addition of 20 μL aliquots of a 97 μM V-BrPO stock solution or 20 μL aliquots of a 202 μM BSA stock solution to 1.7 mL of 0.57 μM 2-phenylindole in 0.1 M Tris buffer, pH 8.13.

The plot of F_0/F versus V-BrPO concentration had a marked upward curvature (Figure 5.3A) and did not satisfy the requirement of the Stern-Volmer

equation. Such an upward curvature is generally attributed to concomitant dynamic and static quenching mechanisms as described by equation 5.6.

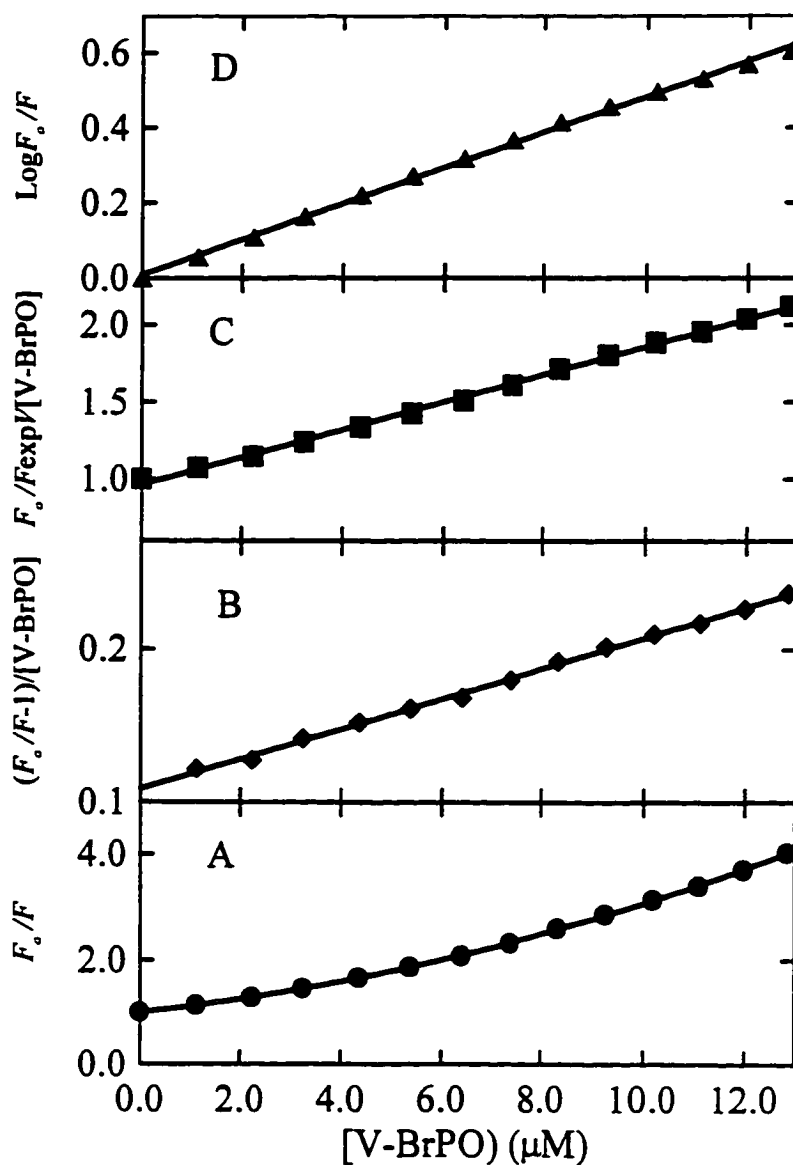


Figure 5.3: Stern-Volmer and modified Stern-Volmer plots of the quenching of the fluorescence of 2-phenylindole by V-BrPO. A: F_0/F vs. $[\text{V-BrPO}]$; B: $(F_0/F - 1)/[\text{V-BrPO}]$ vs. $[\text{V-BrPO}]$; C: $F_0/F_{\text{exp}}V[\text{V-BrPO}]$ vs. $[\text{V-BrPO}]$, $V=0.05$; D: $\text{Log} F_0/F$ vs. $[\text{V-BrPO}]$.

It is predicted from equation 5.6 that plots of $(F_0/F - 1)/[Q]$ against $[Q]$ (here $Q = \text{V-BrPO}$) should give a straight line, and that the K_S and K_D values can be determined from the intercept and the slope of the line. Figure 5.3B shows that the actual plot for the 2-phenylindole/V-BrPO system appears to fit well into that relationship. However, trying to solve equation 5.6 for K_S and K_D failed to accommodate the data and only gave imaginary numbers (Eftink & Ghiron, 1977).

Other models have been used that explain positive deviations from the Stern-Volmer equation (Frank & Vavilov, 1931; Boaz & Rollefson, 1950; Nemzek & Ware, 1975). They all employ the same modification of the Stern-Volmer equation:

$$\frac{F_0}{F_0 - F} = 1 + K_s[Q] \quad (5.7)$$

where V is a static quenching constant that has a different significance for each model: In the "Sphere of Action" model, it has been suggested that instantaneous quenching can occur randomly within a sphere of action of volume $1000V/N (= 4\pi r^3/3)$ and radius r surrounding a fluorophore at the time of excitation (Frank & Vavilov, 1931). In the "Dark Complex" model, instantaneous quenching occurs following excitation of the ground state complex ($F \cdots Q_n$). This complex is defined somewhat loosely, and no true physical contact is necessary; the fluorophore need only be close to the quencher. The association constant for such a complex is V (Boaz & Rollefson, 1950; Nemzek & Ware, 1975).

The data were re-analyzed according to equation 5.7, by plotting $F_0/F \exp(V[\text{V-BrPO}])$ vs. $[\text{V-BrPO}]$ and varying V until a linear plot was obtained ($\rho > 0.99$) (Figure 5.3C). The dynamic (K_D) and static (V) terms were determined

to be $8.9 \times 10^4 \text{ M}^{-1}$ and $5.0 \times 10^4 \text{ M}^{-1}$, respectively. From the value of V obtained, the radius (r) of the active volume around 2-phenylindole can be calculated to be *ca.* 27 Å. Although there are no data available on the shape and dimensions of V-BrPO, an estimation using the data available for V-CIPO from *C. inaequalis* gives a molecular radius of 27 to 40 Å (Messerschmidt & Wever, 1996). This value obtained for r is then in agreement with the value of 30-43 Å which can be estimated for the sum of the molecular radii of 2-phenylindole and V-BrPO. On the other hand, the value obtained for K_D is unusually high for a dynamic process: Assuming that the lifetime of the singlet excited state of 2-phenylindole is *ca.* 10 ns (Eftink, 1991a), the calculated bimolecular quenching constant for the dynamic portion, k_q , is *ca.* $8.9 \times 10^{12} \text{ M}^{-1}\text{s}^{-1}$. Such a constant would necessitate an unacceptable collisional frequency k_0 equal to or above $8.9 \times 10^{12} \text{ M}^{-1}\text{s}^{-1}$, which is almost three orders of magnitude above the limit for diffusion controlled processes ($10^{10} \text{ M}^{-1}\text{s}^{-1}$). This observation indicates that the dynamic quenching pathways for the fluorescence of 2-phenylindole by V-BrPO are negligible, and that the equation

$$\frac{F_0}{F} = e^{V[\text{V-BrPO}]} \quad (5.8)$$

can be used to describe the quenching phenomenon.

In agreement with equation 5.8, the plot of $\text{Log}(F_0/F)$ versus [V-BrPO] is linear (Figure 5.3D), and the static constant V is $1.1 \times 10^5 \text{ M}^{-1}$. The radius of the active volume calculated from V using the "Sphere of Action" model is *ca.* 34 Å. This value is within the range of the estimated sum of the molecular radii of the

quencher and the fluorophore, and suggested strongly that there is molecular contact between V-BrPO and 2-phenylindole at the exact time that 2-phenylindole is excited.

Quenching of 2-phenylindole by apo-BrPO and heat denatured V-BrPO. Apo-BrPO and heat-denatured V-BrPO also quenched the fluorescence of 2-phenylindole (Figure 5.4). The static quenching constant V for apo-V-BrPO was

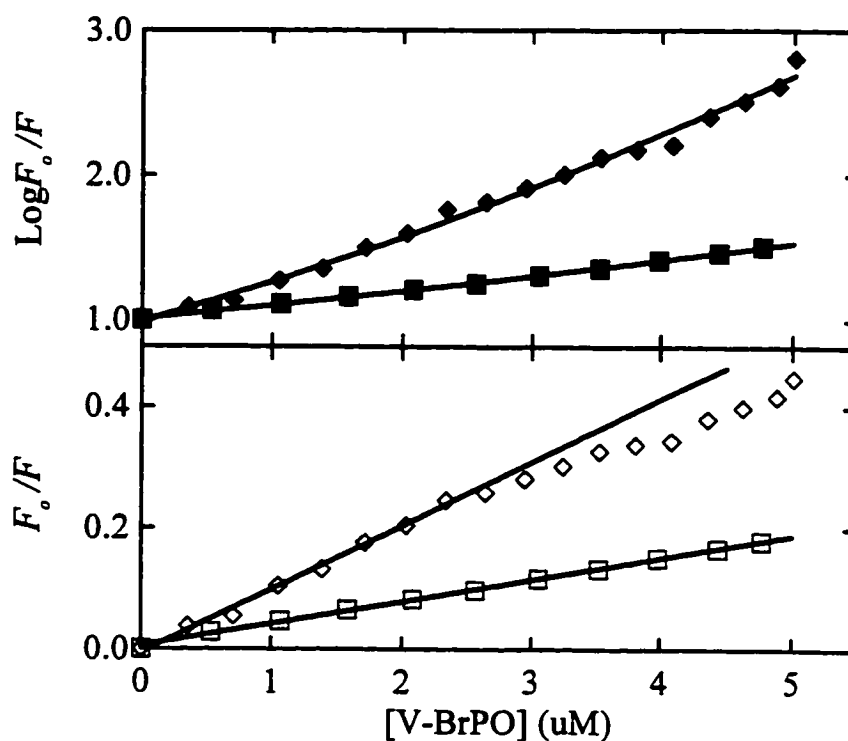


Figure 5.4: Quenching of the fluorescence of 2-phenylindole with apo- (■, □) and heat denatured- (◆, ◇) V-BrPO. Closed symbols represents the normal Stern-Volmer plot; open symbols represents the modified plot from Eq. 5.8. Conditions: 2-phenylindole 0.57 μM , Tris-HCl 100 mM pH 8.3, $T=21\text{ }^\circ\text{C}$.

calculated using eq. 5.8 and amounted to *ca.* $0.36 \times 10^5 \text{ M}^{-1}$. This value is the same order of magnitude to the one obtained for native V-BrPO and indicates that the active site-bound vanadium is not required for binding of 2-phenylindole to V-BrPO. The drop in the static quenching constant observed shows that removal of the vanadium may slightly lower the affinity of V-BrPO for 2-phenylindole due to structural changes in the protein. Alternatively, this drop could be due to a less efficient quenching mechanism after removal of the active-site vanadium since transition metals have been shown to readily quench the fluorescence of aromatic systems (Varnes et al., 1972).

The Stern-Volmer plot of the heat-denatured enzyme was not as well behaved as the ones obtained for the native and apo enzyme. This can be attributed to heterogeneity in the protein solution after denaturation as well as to a change in the viscosity of the solution at higher protein concentrations (see below for the viscosity dependence on the fluorescence quenching). The data were fitted to equation 5.8 and the static quenching constant was estimated from the initial portion of the curve. The value obtained ($V = 2.61 \times 10^5 \text{ M}^{-1}$) was more than twice the value obtained for native V-BrPO and suggested that heat-denatured V-BrPO had a greater affinity for 2-phenylindole than native V-BrPO. It is not clear, at this time why heat-denatured V-BrPO would bind 2-phenylindole more tightly. If binding of 2-phenylindole to native V-BrPO does not require a complex tertiary enzymatic architecture, and if, even after denaturation, the portion of the enzyme that is responsible for quenching is still fairly intact, binding of 2-phenylindole may still occur. On the other hand, denaturation may greatly affect the structure of V-BrPO and expose previously buried lipophilic groups susceptible to

interactions with 2-phenylindole. In this case, the cause of quenching by native and heat denatured V-BrPO may be quite different, and the similar values obtained for V only fortuitous.

Viscosity and temperature dependence. The viscosity and temperature dependence of quenching reactions have been used to provide insights regarding the structure and the dynamics of the quenching system (Eftink & Ghiron, 1978; Eftink & Hagaman, 1987). The viscosity dependence of the quenching of the

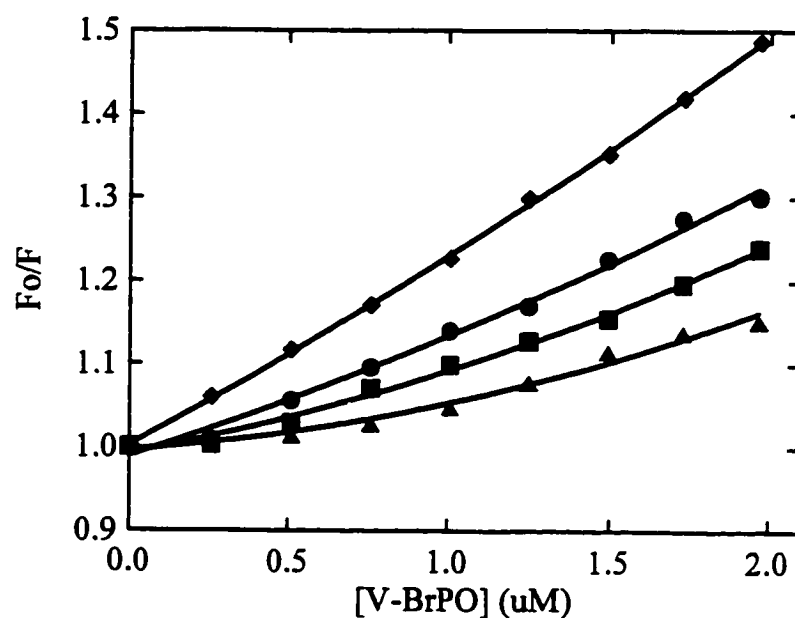


Figure 5.5: Quenching of the fluorescence of 2-phenylindole by V-BrPO as a function of isopropanol concentration: \blacklozenge , 0 %; \blacksquare , 30 %; \blacktriangle , 60 %; \bullet , 90 %. Experiments were carried at 21 °C by addition of 10 μL aliquots of a 44 μM V-BrPO solution to 1.7 mL of 0.57 μM 2-phenylindole in (0.1 M Tris buffer pH 8.3)/isopropanol mixture

fluorescence of 2-phenylindole by V-BrPO in isopropanol-water mixture at 23 °C is shown in Figure 5.5 & 5.6. The static quenching constant V was calculated

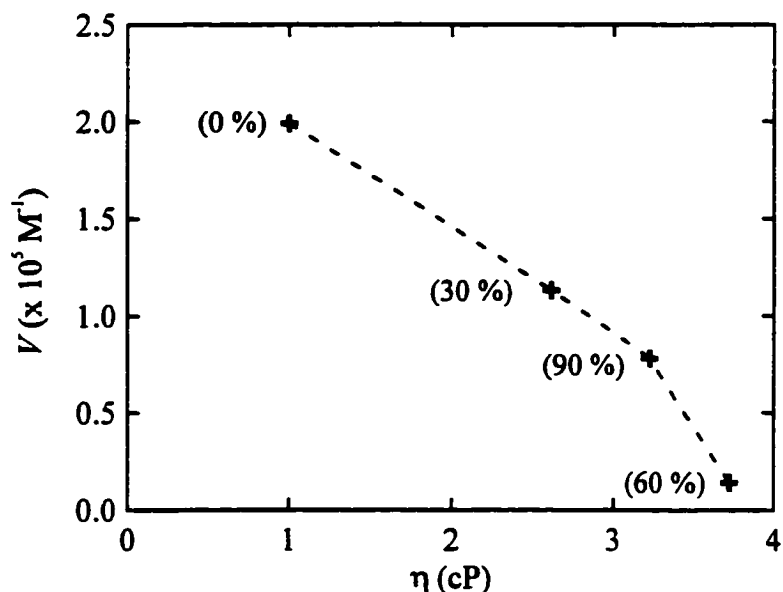


Figure 5.6: Plot of V versus viscosity. Experiments were carried out at 21 °C in Tris buffer/isopropanol mixtures. The number in parenthesis indicate the percentage of isopropanol in the buffer. The bulk viscosity η was obtained from volume 67 of the Handbook of Chemistry and Physics (Chemical Rubber Co.)

from equation 5.8. It was found that V decreased with increasing viscosity and that for $\eta < 3$ cP the viscosity dependence seemed to follow a linear relationship, $V = a\eta + b$.

This result was surprising since quenching reactions involving formation of a complex are not expected to be influenced by the bulk viscosity of the medium (Eftink, 1991). However, if for quenching to occur, 2-phenylindole needs to take a path through part of the protein to reach its binding site, the effect seen could be attributed to changes in the accessibility to the quenching site due to the increased viscosity. The motion of 2-phenylindole through the V-BrPO matrix would be facilitated by fluctuations in the structures of the protein that

would lead to formation of free volume elements and that would allow for the stepwise inward movement of 2-phenylindole (Weber, 1975). A change in the bulk viscosity of the medium could reduce fluctuations in the protein and account for the decrease in V observed. In addition, changes in the nature of the solvent is also likely to affect the stability of the [2-phenylindole-V-BrPO] complex and therefore the variations in V observed may not be due to changes in the bulk viscosity only.

The static quenching constant V was also affected by the temperature (Table 5.1). True temperature dependence could not be determined due to parallel changes of the viscosity along with the temperature. However, the slight decrease in V with increasing temperature was consistent with destabilization of the [V-BrPO-2-phenylindole] complex at higher temperature.

Table 5.1: Temperature Dependence of the Quenching of the Fluorescence of 2-Phenylindole by V-BrPO .

Temperature (°C)	Viscosity ^a (cP)	V (x 10 ⁵ M ⁻¹)
4	1.567	1.19
24	0.911	1.11 ^b
44	0.607	1.07
54	0.516	1.01

^aValues obtained from Volume 67 of the Handbook of Chemistry and Physics (Chemical Rubber Co.). ^bThe value obtained for V appears to differ slightly from the one obtained in Fig. 5.6. This discrepancy was likely due to the fact that two different batches of enzyme with different specific activities were used.

Buffer and pH dependence. The quenching of the fluorescence of 2-phenylindole by V-BrPO was determined using different buffers at various pH. The static binding constant V was calculated using equation 5.8 (Fig. 5.7 and Table 5.2). The binding constant was found to depend not only on the pH of the solution, but also on the nature of the buffer used. Binding of 2-phenylindole was favored at low pH for citrate buffer ($V \approx 22.15 \times \text{pH}^{-1.65}$) (Fig. 5.5). The pH dependence in Tris or bis-Tris buffer was similar, only slightly shifted ($V \approx 30.37 \times \text{pH}^{-1.62}$). This pH profile does not correspond to the pH profile determined for the bromination of monochlorodimedone (MCD) that presented a maximum at pH 4.5 to 7.0, depending on the concentration of bromide and/or hydrogen peroxide (Wever et al., 1985).

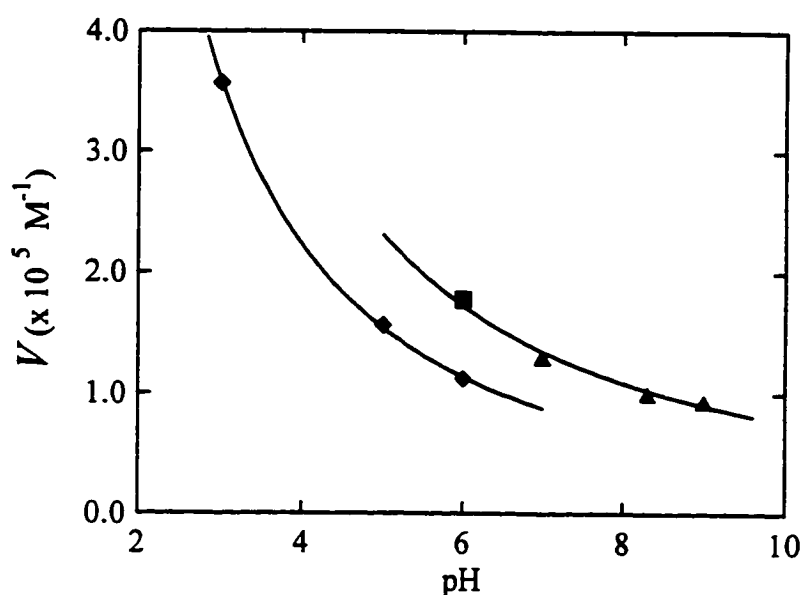


Figure 5.7: pH dependence of the quenching of the fluorescence of 2-phenylindole by V-BrPO. Experiments were carried out at 21 °C: ◆, 0.1 M citrate; ▲, 0.1 M Tris; ■, 0.1 M bis-Tris.

A comparison of the quenching of 2-phenylindole by V-BrPO in citrate, MES, phosphate, and bis-Tris showed that the nature of the buffer affected the magnitude of the binding constant (Table 5.2). Since no correlation was found between the magnitude of V and the ionic strength, the variations observed between the different buffers are most likely linked to the nature of each buffer (phosphate is an inorganic triacid, citrate a tricarboxylic acid, MES a morpholino sulphonic acid, and bis-Tris a tertiary amine).

Table 5.2: Dependence of the nature of the buffer on the quenching of 2-phenylindole by V-BrPO.^a

Buffer	Ionic strength (mM)	V ($\times 10^5 \text{ M}^{-1}$)
Citrate	320	1.12
MES	60	0.90
Phosphate	260	0.81
Bis-Tris	75	1.78

^a Buffer concentrations 0.1 M, pH 6.00.

Discussion

2-Phenylindole was found to be a useful tool to study the binding of indoles to V-BrPO. The excitation and absorption wavelengths of 2-phenylindole were sufficiently removed from the corresponding fluorescence properties of the enzyme. It was shown in this study that V-BrPO quenches the fluorescence of 2-phenylindole (Fig. 5.1 & 5.2) and that the corresponding Stern-Volmer plot had a marked upward curvature (Fig. 5.3). Such a departure from linear behavior is generally attributed to a combination of dynamic and static quenching mechanisms (Lakowicz, 1983; Eftink, 1991). However, this model was not appropriate to describe the quenching of 2-phenylindole by V-BrPO since it resulted in a (dynamic) bimolecular collisional constant three orders of magnitude greater than the limiting diffusional constant. This result implies that the observed quenching is due to a static process that involves binding of 2-phenylindole to V-BrPO. The data was fitted to equation 5.8 and gave a static quenching constant, V , of $1.1 \times 10^5 \text{ M}^{-1}$. According to the models for static quenching described, V can be thought of as a surrounding volume element around the fluorophore or as an association constant. From this model the radius of the active sphere of action was found to match the sum of the molecular radii of 2-phenylindole and V-BrPO and suggested contact between them. Therefore it appears more reasonable to discuss the quenching phenomena in terms complex formation.

Bovine serum albumin (BSA) was used in a control experiment since it had been determined that BSA is able to bind L-tryptophan with a association

constant $0.37 \times 10^5 \text{ M}^{-1}$ (Chanut et al., 1992). However, BSA did not quench the fluorescence of 2-phenylindole, suggesting that BSA does not bind 2-phenylindole (Fig. 5.2). ^1H and ^{19}F NMR studies have shown that albumin possesses two chemically distinguishable binding sites for tryptophan. The first site interacts strongly with tryptophan and causes the amino acid to become highly immobilized whereas the other site appeared to be much weaker (Coibion & Laszlo, 1978; Gerig & Klinkenborg, 1980). The strong interactions detected suggested that binding of tryptophan is rather specific and explains why 2-phenylindole does not appear to bind to BSA

Binding of 2-phenylindole to V-BrPO was found to be independent of the active site vanadium since it occurred even with the apo enzyme (Figure 5.4). This result indicates that binding of the indole substrate is not part of the catalytic cycle of the enzyme and may occur "away" from the vanadium binding site. This observation is confirmed by the structure of the active site of V-BrPO that can be deduced from comparison with the structure of the active site of V-CIPO from *C. inaequalis* (Figure 1.5) (Messerschmidt & Wever, 1996). The hydrophobic portion of the active site channel provides a possible binding site for a hydrophobic substrate such as 2-phenylindole or other indoles. However, these results do not give further insight on the nature of the brominating species, whether it is enzyme-bound, or freely diffusible. If the substrate is being bound away from the vanadium active site, the oxidized bromine intermediate has to be released for bromination to occur, but is trapped by the bound-substrate before it can be released outside of the protein, and react in a " Br_2/HOBr -like" way.

The value of the association constant V depended also on the viscosity, the temperature, and the pH. The inward movement of a substrate to its binding site will be facilitated by fluctuations in the structure of the protein to form lattice vacancies. The frequency of these fluctuations are regulated by the intramolecular interactions which stabilize the protein structure and may involve the breaking of hydrogen bonds or salt linkages as well as the separation of oily group. Since it appears that the binding site of 2-phenylindole is located in the channel leading to the active site vanadium, the variations in the magnitude of V with the above mentioned factors could reflect how those factors affect the fluctuations required to facilitate access of 2-phenylindole to its binding site.

The association constant of 2-phenylindole to V-BrPO was found to depend on the nature of the buffer (Table 5.3). In phosphate buffer at pH 6.00, V was *ca.* $0.84 \times 10^5 \text{ M}^{-1}$. This value is in agreement with the binding constant of 2-methylindole and 3-methylindole estimated from kinetic measurements ($K_S = 1.33 \times 10^5 \text{ M}^{-1}$ and $0.45 \times 10^5 \text{ M}^{-1}$, respectively (Chapter 4)) as well as with the competition experiments that showed that 2-phenylindole is a slightly poorer substrate for V-BrPO than is 2-methylindole but a better substrate than 3-methylindole.

The exact nature of the quenching mechanism is not clear. However, photoaffinity labeling of V-BrPO with 5-azido-2-phenylindole introduced a perturbation in the tryptic digest of V-BrPO that suggested that crosslinking of the probe took place on or in the vicinity of a lysine or an arginine side-chain, both bearing amine functions (Chapter 6). In addition, it has been determined in previous studies that the $-\text{NH}_3^+$ moiety is an excellent quencher of the

fluorescence of the indole ring, and that the quenching process occurred *via* excited-state proton transfer and protonation of the indole ring (Van der Dongt, 1969; Ricci, 1970; Ricci & Nesta, 1975). In view of these observations it is possible that the quenching step may not involve production of a non-fluorescent complex through static interactions and but solely proton transfer. Since this transfer would take place inside of the protein it is not expected to be diffusion limited in the way expected for transfer "in the bulk solvent". The "limiting step" would then be the binding of 2-phenylindole to V-BrPO detected in the fluorescence quenching experiment.

Chapter 6
Photoaffinity Labeling of Vanadium-Bromoperoxidase
with Azidoindoles

Introduction

Understanding enzymatic reaction mechanisms often requires locating the active site and identifying the amino acids involved either in binding of the substrate(s) or in catalytic activity. Photoaffinity labeling has become a method of choice in determining, by derivitization, the characteristics of a specific site for ligand interaction (Bayley & Knowles, 1977; Bayley, 1983; Guillory, 1989).

Photoaffinity labeling is a special category of general affinity labeling in which the label can be activated by photoexcitation after binding to the receptor site. It is a technique far more powerful and specific than the classical electrophilic labeling procedures. Electrophilic reagents require the presence of a reactive nucleophilic function at the generalized ligand binding site and are also likely to react, with varying degrees, with other protein nucleophiles not necessarily situated at the binding site under study (Guillory, 1989). On the other hand, photogenerated reagents such as carbenes or nitrenes, are much less selective towards covalent bond formation, are very reactive, and are capable of carbon-hydrogen bond insertion (Doering & Buttery, 1956). In addition, covalent insertion of an active-site-bound photogenerated reagent is expected to be first-order, whereas reactions at secondary sites would not be dependent upon binding

potential and therefore would more likely to be second-order processes (Guillory, 1980).

The design of a suitable photoaffinity label must meet certain requirements for successful labeling:

- The precursor should be chemically stable and susceptible to photoactivation at wavelengths remote from protein damaging regions.
- The photogenerated reagents should be highly reactive and short lived, and should form a stable adduct after irradiation.

Arylazides are currently the most widely used photoprobes for biochemical applications (Guillory & Jeng, 1983). They are generally relatively easy to make and handle, and they are chemically stable in the absence of light. Upon photoactivation they produce mainly singlet state nitrenes that are converted to triplet state nitrenes *via* intersystem crossing. Singlet nitrenes have half lives on the order of 100 nsec (Reiser & Wagner, 1977), and react preferentially by insertion into oxygen-hydrogen, nitrogen-hydrogen or carbon-hydrogen bonds. Insertion into carbon-hydrogen bonds is a unique reaction characteristic of aryl nitrenes that does not readily occur with other known chemical agents and allows them to react with the otherwise unreactive amino-acid side chain residues containing only hydrocarbon functions (Ala, Gly, Leu, Ile, Val, Phe). Due to their radical nature, triplet state nitrenes engage in hydrogen abstraction reactions generating two radicals. In some cases these two radicals can combine to form a covalent linkage. The lifetime of the triplet nitrenes are longer than the lifetime of singlet nitrenes, and therefore they are less specific in the reactions they undergo. Fortunately, singlet nitrene insertion reactions are generally faster than the

conversion to the triplet state (Lwowski, 1970), and loss of reactivity of the probe due to spin conversion is generally minimal.

However, there are limitations to the use of photoaffinity labels. Nitrenes have the potential to insert in almost any amino acid side chain, and as is the case with electrophilic labeling, it is not always possible to distinguish between non-specific labeling and labeling at the active site. Photogenerated nitrenes can also undergo multiple forms of degradation that depend on the type and the time of the irradiation used. The intermediates formed in the activation process can all have different reactivities and complicate the labeling experiment (Guillory, 1980). Photoaffinity label insertion reactions usually give low yields, but they can be improved by using a probe having a close structural relationship with the natural ligand (Bayley, 1983).

Photoaffinity labeling was used to further investigate the binding of indoles to V-BrPO. Azidoindoles were obvious photoreactive structural analogues of indoles. A fluorescent photoprobe (5-azido-2-phenylindole) and a radioactive photoprobe ($[^3\text{H}]$ 5-azido-1,2-dimethylindole) were synthesized and tested for insertion into the enzyme.

Materials and Methods

Materials. 1,2-Dimethylindole, deuterium oxide (99.9 %) and cyanogen bromide were purchased from Aldrich (Milwaukee, MI). [^3H]-Water (5 Ci/mL) was purchased from American Radiolabeled Chemicals (St. Louis, MO). DEAE Sepharose CL-6B was obtained from Pharmacia Biotech and sequencing grade trypsin was purchased from Sigma (St. Louis, MO). HPLC was carried out on a Waters system with Waters 510 pumps and Waters 484 UV detector using Vydac C-4 (4.6 mm x 25 cm, 5 mm particle size) and C-18 (4.6 mm x 25 cm, 5 mm particle size) columns (gradients are described in figure legends). Proton NMR spectra were obtained at 500 MHz on a General Electric GN-500 instrument. Infrared spectra were recorded on a Perkin-Elmer 1330 infrared spectrophotometer. UV-Vis spectra were obtained on a Hewlett-Packard HP8452A diode-array spectrophotometer. Fluorescence spectra were obtained with a Perkin-Elmer LS 50 luminescence spectrophotometer. Scintillation counts were recorded on a LKB Wallac 1219 Rackbeta spectral liquid scintillation counter using BioSafe II counting cocktail from RPI (Mount Prospect, IL).

Synthesis of 5-Azido-2-Phenylindole. A solution of NaNO_2 (1.40 g, 20.3 mmol) in 50 mL conc. H_2SO_4 cooled to 5 °C was added over 5 min to a solution of 2-phenylindole (3.00 g, 15.5 mmol) in 100 mL conc. H_2SO_4 cooled to 5°C in an ice-bath. The reaction mixture was stirred for 30 min and poured over 200 g of ice. The resulting yellow precipitate was collected by filtration, washed repeatedly with water and dried in a dessicator under vacuum for 3 days to give 3.45 g of 5-nitro-2-phenylindole as a yellow powder (93 %). ^1H NMR (CDCl_3 ,

500 MHz) δ 6.96 (d, $J = 1.5$ Hz, 1H), 7.38 (t, $J = 7.5$ Hz, 1H), 7.41 (d, $J = 9$ Hz, 1H), 7.47 (t, $J = 7.5$ Hz, 2H), 7.67 (d, $J = 7.5$ Hz, 2H), 8.09 (dd, $J = 1.5$ Hz and $J = 9$ Hz, 1H), 8.56 (d, $J = 1.5$ Hz, 1H) 8.75 (s, 1H); EIMS m/z (rel int) 238 (M^+ , base), 208 (40), 192 (68), 165 (29).

5-Nitro-2-phenylindole (270 mg, 1.13 mmol) was dissolved in 45 mL of 10 % (v/v) ethanol. Zinc (1 g) and 1 mL of conc HCl were then added, and the mixture was refluxed for 1.5 h. After cooling to room temperature and addition of 50 mL of water, 2 N NaOH was added dropwise until precipitation occurred. The precipitate could not be easily filtered and was extracted 3 times with ethyl acetate. The organic phases were combined, dried over $MgSO_4$ and evaporated to dryness to give 47 mg (20 %) of 5-amino-2-phenylindole as a pale brown solid. 1H NMR (Acetone- d_6 , 500 MHz) δ 2.95 (s, 2H), 6.60 (dd, $J = 2.5$ Hz and $J = 8$ Hz, 1H), 6.65 (d, $J = 1$ Hz, 1H), 6.82 (d, $J = 2.5$ Hz, 1H), 7.14 (d, $J = 8$ Hz, 1H), 7.25 (t, $J = 7.5$ Hz, 1H), 7.40 (t, $J = 7.5$ Hz, 2H), 7.80 (d, $J = 7.5$ Hz, 2H), 10.26 (s, 1H).

5-Amino-2-phenylindole (47 mg, 0.23 mmol) was dissolved in 4 mL of 80 % (v/v) acetic acid and cooled to 0 °C in an ice-salt bath. To this was first added sodium nitrite (18.5 mg, 0.27 mmol) and, after 5 min, sodium azide (17.5 mg, 0.27 mmol), each dissolved in 100 mL of ice-cold water. After 3 h of continuous stirring at 0 °C, the mixture was evaporated to dryness, to give a dark brown solid residue. Ethanol (10 mL) was added and the mixture treated with activated charcoal, refluxed for 5 min and filtered through celite. Water was added to the filtrate which was then refrigerated. 5-azido-2-phenylindole crystallized as small brownish plates and was collected by suction filtration (50 mg, 93 %). 1H NMR

(CDCl₃, 500 MHz) δ 6.75 (s, 1H), 6.85 (dd, $J = 8.5$ Hz and $J = 1.7$ Hz, 1H), 7.26 (d, $J = 1.7$ Hz, 1H), 7.32 (t, $J = 7$ Hz, 1H), 7.34 (d, $J = 8.5$ Hz, 1H), 7.34 (t, $J = 7$ Hz, 2H), 7.63 (d, $J = 7$ Hz, 2H), 8.33 (s, 1H); IR (KBr) ν 3420, 3040, 2098, 1465, 1300, 1260, 765.

Synthesis of [³H] 5-Azido-1,2-Dimethylindole. All glassware, syringes and needles were flame dried and cooled down in a dessicator. 1,2-dimethylindole (102.2 mg, 0.779 mmol) was dissolved in 0.5 mL of dry THF in a sealed vial flushed with argon. *n*-Butyllithium (1.5 M, 0.5 mL, 0.750 mmol) was added *via* syringe to the solution. The mixture rapidly turned red and after 5 min. was transferred *via* syringe into another sealed vial containing [³H] water (5mL, 0.275 mmol, 5 Ci/mL, 25 mCi). The reaction mixture was allowed to stand at room temperature for 10 min, quenched with 1 mL of water and extracted 4 times with 3 mL of ether. The organic phases were combined, dried over MgSO₄ and evaporated to dryness to give [³H]-1,2-dimethylindole as a yellow solid. The solid was immediately dissolved in 0.6 mL of conc H₂SO₄ and cooled in an ice-bath. A solution of NaNO₃ (67 mg, 0.79 mmol) in 0.5 mL of cold conc H₂SO₄ was then added dropwise in 5 min, and the reaction was stirred for 5 more min. The mixture was then poured on 20 g of ice. The precipitate formed was extracted 5 times with ether. The organic layers were combined, dried over MgSO₄ and evaporated to dryness to give [³H]-5-nitro-1,2-dimethylindole as yellow solid. [³H] 5-nitro-1,2-dimethylindole was immediately dissolved in 2 mL of ethanol. 250 mg of zinc and 0.8 mL of 48 % HBr were then added, and the mixture was gently refluxed for 2 h. The mixture was then neutralized with 10 % NaHCO₃, and extracted 4 times with ethyl acetate. The organic layers were combined, dried

over MgSO_4 and evaporated to dryness. The solid residue was purified by silica gel chromatography (hexanes/ethyl acetate 75:25). $[^3\text{H}]$ 5-amino-1,2-dimethylindole (5.0 mg) was obtained as a white solid. This compound (0.027 mmol) was quickly dissolved in 1 mL of 80 % acetic acid and cooled down to 0 °C by immersion in a salt-ice bath. To this solution was first added NaNO_2 (1.96 M, 16.5 mL, 0.032 mmol) and 5 min later NaN_3 (2.03 M, 16.5 mL, 0.033 mmol). The reaction mixture was stirred for 2 h at 0 °C and then evaporated to dryness under vacuum. The black residue was purified by silica gel chromatography (hexanes/ethyl acetate 75:25). The title compound was obtained as a white solid: 1.7 mg (34 %, this step, 1.1 % overall). ^1H NMR (CDCl_3 , 500 MHz) δ 2.40 (s, 3H), 3.63 (s, 3H), 6.17 (s, 1H), 6.80 (dd, $J = 2$ Hz and $J = 8.5$ Hz, 1H), 7.15 (d, $J = 2$ Hz, 1H), 7.17 (d, $J = 8.5$ Hz, 1H); IR (KBr) ν 3030, 2920, 2100, 1450, 1300.

Photolysis Experiments. Irradiations were performed at 25 °C using an Oriel 6035 low pressure mercury (argon) pen lamp. Samples were placed in 0.5 mL (5 mm path length) or 3.0 mL (10 mm path length) quartz cuvettes and clamped 5 cm from the lamp. A 308 nm cut-off filter was placed between the lamp and the sample, 1 cm away from the lamp. Photoactivation assays were done in 100 mM Tris-HCl, pH 8.3 containing 10 % to 30 % ethanol. The enzyme remained fully active when photolyzed under these conditions in the absence of the photoprobes.

Labeling of V-BrPO with $[^3\text{H}]$ 5-azido-1,2-dimethylindole. V-BrPO (49 μM) was incubated with $[^3\text{H}]$ 5-azido-1,2-dimethylindole (610 μM) in 3 mL of 100 mM Tris buffer, pH 8.3, containing 30 % ethanol and irradiated for 40 min.

After irradiation, the excess reacted label was removed by binding labeled V-BrPO to a DEAE ion-exchange resin, and washing the resin with 20 mL 60 % ethanol. The enzyme was then eluted from the resin by a salt gradient 0-0.5 M KCl in 100 mM Tris buffer, pH 8.3. 4 mL fractions were collected and analyzed for enzymatic activity. Levels of radioactivity were measured by taking 100 μ L aliquots of each fractions for scintillation counts.

In-Gel Tryptic Digestion of V-BrPO (Rosenfeld et al., 1992). Reducing SDS-PAGE was run according to the method of Laemmli (Laemmli, 1970) with 12.5 % (w/v) acrylamide gels (50 x 90 x 1.5 mm). After electrophoresis, the gels were stained with 0.2 % Coomassie brilliant blue in 40:10 methanol:acetic acid and destained with 40:10 methanol/acetic acid. The protein bands were excised from the gel and washed twice with 50 % acetonitrile in 200 mM ammonium carbonate pH 8.9 for 20 min at 30 °C. The gel slices were semi-dried in air for 20 min and rehydrated with 20 μ L of 200 mM ammonium carbonate pH 8.9, containing 0.02 % Tween 20. Trypsin (50 μ L, 0.13 mg/mL) was added, followed by 30 μ L of 200 mM ammonium carbonate pH 8.9. The digestion was carried out at 37 °C for 4 h and stopped by adding 15 μ L of trifluoroacetic acid (TFA). The peptides were extracted by washing the gel slices with 200 μ L of 80 % acetonitrile containing 0.1 % TFA. The extracts were combined, concentrated to 100 μ L in a SpeedVac (Savant) and injected on the HPLC.

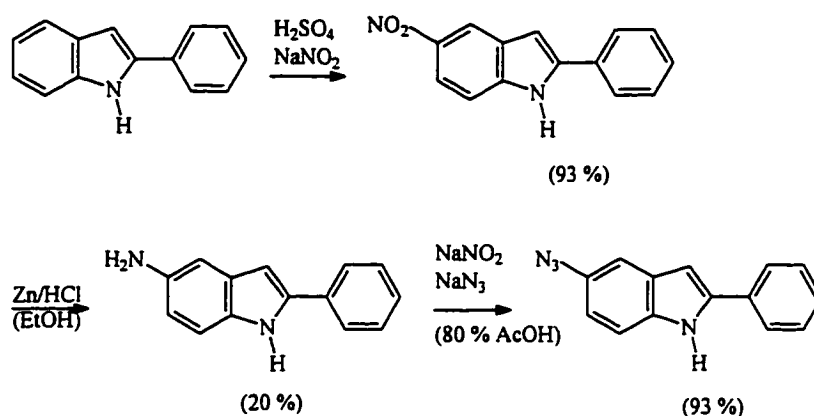
Tryptic Digestion of V-BrPO. V-BrPO was first denatured in 0.1 M Tris buffer pH 8.3, containing 6 M guanidine hydrochloride and 0.1 M dithiothreitol at 100 °C for 40 min. Trypsin was added to reach a 1:10 ratio with respect to V-

BrPO. The solution was incubated 12 h at 37 °C and injected on the HPLC for analysis.

CNBr Cleavage of V-BrPO. The buffer containing V-BrPO was exchanged with water by successive washing on a Centricon 30 (Amicon). V-BrPO was then lyophilized and dissolved in 70 % formic acid. After a few crystals of CNBr were added, the solution was flushed with argon and allowed to sit in the dark at room temperature for 12 h. The reaction mixture was then diluted with water to 7 % formic acid, and evaporated to dryness. The residue was redissolved in 0.1 M Tris buffer pH 8.3, containing 6 M guanidine hydrochloride and 0.1 M dithiothreitol, the non-soluble material filtered off, and the filtrate injected on the HPLC for peptide analysis.

Results

Photoaffinity Labeling of V-BrPO with 5-Azido-2-Phenylindole. Synthesis and Properties of 5-Azido-2-Phenylindole. 5-Azido-2-phenylindole was synthesized as a photoreactive analogue of 2-phenylindole. The synthesis involved, first, nitration of 2-phenylindole at the C-5 position, followed by reduction of the nitro group to the amine. Diazotation of the amino group and displacement by azide yielded the azido derivative almost quantitatively (Scheme 6.1) Although mass spectral analysis was not performed due to the instability of



Scheme 6.1

the compound, the presence of the azido group was confirmed by the characteristic strong IR absorption band at $\nu = 2098 \text{ cm}^{-1}$. 5-Azido-2-phenylindole was stored as a solid at room temperature in the dark, and was stable for months under these conditions. 5-Azido-2-phenylindole does fluoresce when excited at $\lambda = 314 \text{ nm}$ (Figure 6.1) and can be potentially used as a fluorescent

photoprobe for the binding site of V-BrPO. The emission spectrum had three peaks at 354 nm, 375 nm and 479 nm.

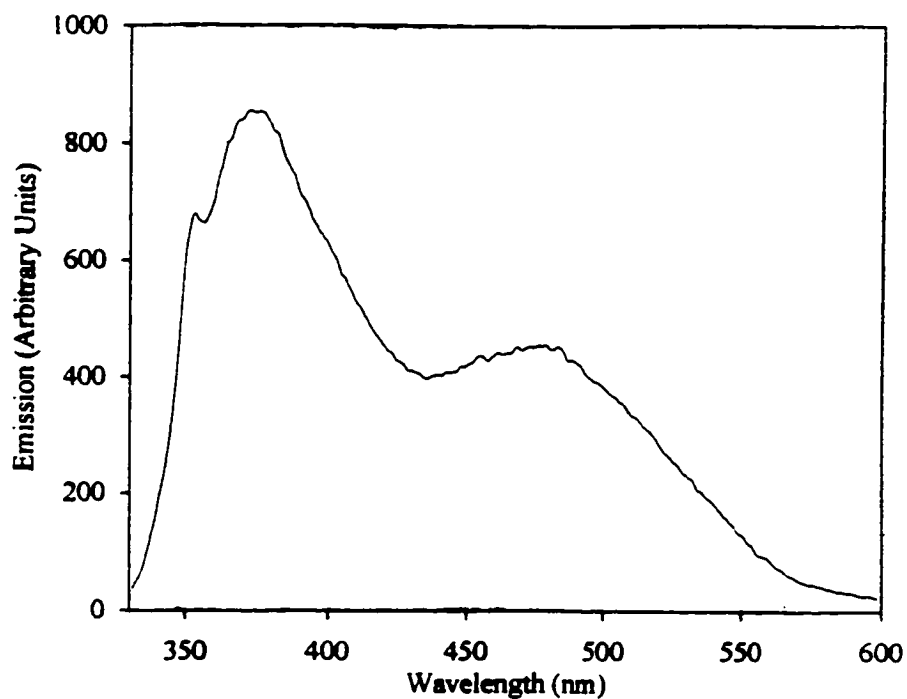


Figure 6.1: Fluorescence emission spectrum of 5-azido-2-phenylindole ($\lambda_{\text{ex}} = 314$ nm). Conditions: 100 mM Tris buffer, pH 8.3, 1 % ethanol, 0.52 μM 5-azido-2-phenylindole.

5-Azido-2-phenylindole was also a substrate for V-BrPO, but it was only *ca.* 65 % as reactive as 2-phenylindole. The decrease in reactivity can be attributed either to a mild electron withdrawing effect of the azido group or to a steric effect. The low ionic character of the azido group may also affect the binding affinity of 5-azido-2-phenylindole to a non-polar pocket in the enzyme.

Figure 6.2 shows the effect of the length of time of irradiation on the absorption spectrum of 5-azido-2-phenylindole. Although the absorptions at $\lambda = 260$ nm and at $\lambda = 320$ nm decrease as a function of the duration of the photolysis, the photolysis does not seem to follow first order kinetics. This behavior indicates a complex mechanism for photoactivation of the probe, or for the decay of the photoactivated species in which cases the formation of multiple products is generally expected (Guillory, 1989).

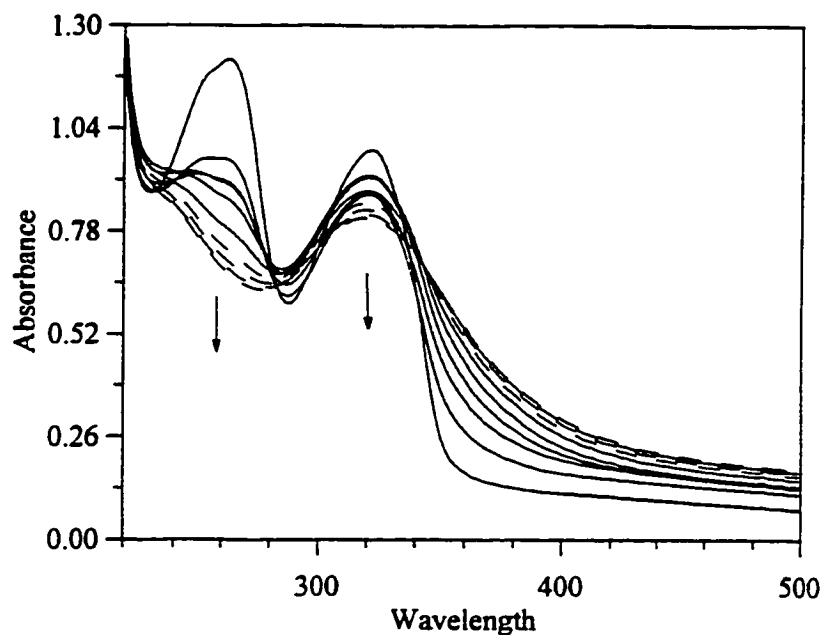


Figure 6.2: Effect of the irradiation time on the absorption spectrum of 5-azido-2-phenylindole. 5-Azido-2-phenylindole ($103 \mu\text{M}$ in 100 mM Tris pH 8.3 and 10% ethanol) was photolyzed, for 5 min time periods, with a total irradiation time of 40 min. UV-Vis spectra were recorded during the time between irradiation periods (*ca.* 30 s).

HPLC Separation of 5-Azido-2-Phenylindole-Labeled V-BrPO Tryptic Peptides. A solution of V-BrPO (9 μM) and 5-azido-2-phenylindole (207 μM) in 500 μL of 100 mM Tris buffer, pH 8.3, containing 20 % ethanol was irradiated for 40 min. Labeled V-BrPO was separated from excess reacted photoaffinity label by SDS-PAGE. V-BrPO was subsequently digested in-gel with trypsin. The tryptic fragments were separated by HPLC, analyzed by fluorescence ($\lambda_{\text{ex}} = 314$ nm, $\lambda_{\text{em}} = 370$ nm) and compared to the fragments obtained from the tryptic digest of unlabeled V-BrPO (Figure 6.3). No fluorescence could be detected for any of the fragments collected. However, the tryptic digests of unlabeled and labeled V-BrPO showed some differences, indicating that cross-linking may have occurred. Two major fragments, eluting at 42 and 48 min, present in the digest of unlabeled V-BrPO (marked (-), Figure 6.3a) are absent in the digest of labeled V-BrPO. The latter included, instead, a fragment eluting much later (at 93 min, marked (+), Figure 6.4a) that did not appear in the unlabeled V-BrPO tryptic digest. The fact that the tryptic digest of V-BrPO was perturbed by crosslinking of the photoaffinity label seems to indicate that the photoactivated 5-azido-2-phenylindole crosslinked to, or in the neighborhood of, an arginine or a lysine side chain and thus, prevented cleavage at that particular residue. The resulting tryptic peptide would then be much longer but would also include an additional fairly lipophilic group (the reacted probe), that would elute much later than the two parent fragments. The absence of fluorescence was not surprising, since V-BrPO quenches the fluorescence of 2-phenylindole (see Chapter 4). Covalent linkage of the fluorescent photoprobe to the "quenching site" could conceivably result in

enhanced quenching and therefore mask of the presence of the fluorescent probe, even after tryptic digest.

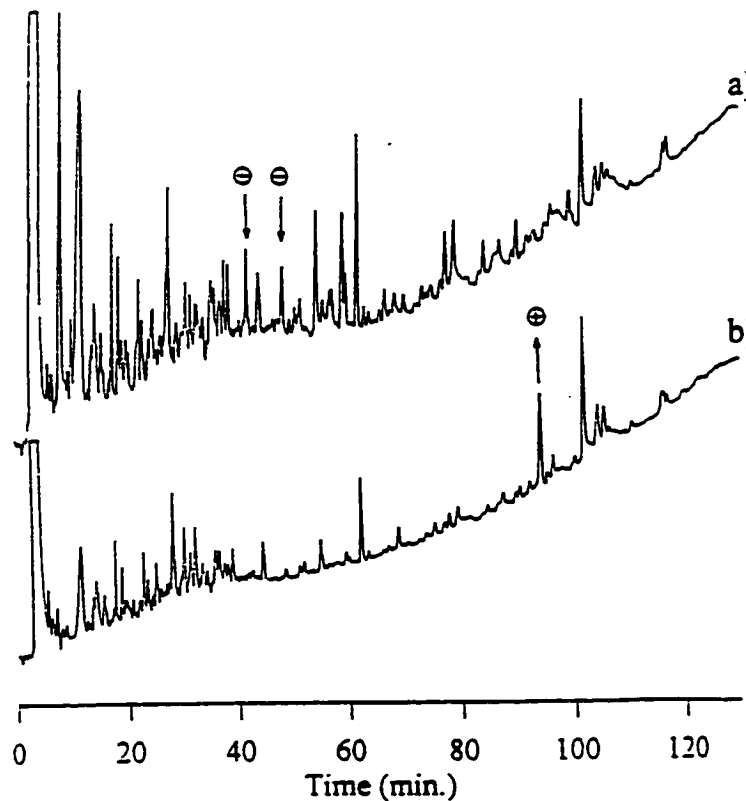
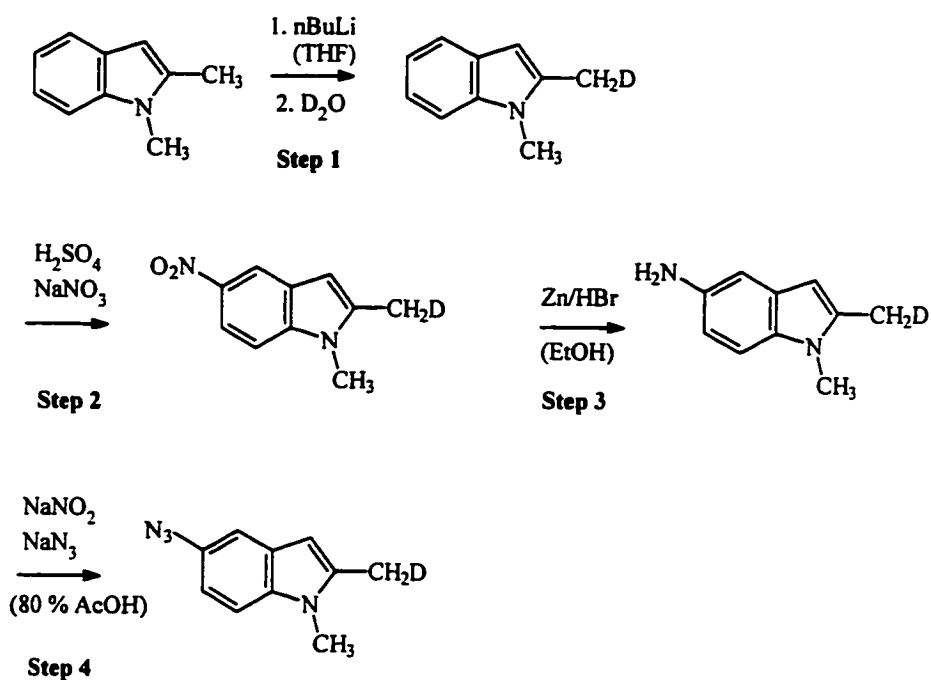


Figure 6.3 C-18 HPLC profile of tryptic peptides of a) V-BrPO and b) V-BrPO following cross-linking with 5-azido-2-phenylindole. After in-gel digestion, the tryptic peptides of V-BrPO and 5-azido-2-phenylindole labeled V-BrPO were separated on a Vydac C-18 column eluted at a flow rate of 0.8 mL/min. The profile was developed with a gradient of solvent B (80 % acetonitrile, 0.1 % TFA) into solvent A (0.1 % TFA), 0-5 min (0 % B), 5-110 min (0-100 % B), 110-125 min (100 % B), and followed at $\lambda = 218$ nm. Fractions were collected every minute and analyzed by fluorescence spectrophotometry.

Photoaffinity Labeling of V-BrPO with [³H] 5-Azido-1,2-Dimethylindole.

Synthesis of [³H] 5-Azido-1,2-Dimethylindole. [³H] 5-Azido-1,2-dimethylindole was prepared in a similar manner to 5-azido-2-phenylindole but included an additional step to add a radioactive tag (Scheme 6.2, synthetic route shown with D₂O). 1,2-Dimethylindole was easily deprotonated at the 2-methyl position by *n*-butyllithium (Step 1). The carbanion could then be reprotated using tritiated



Scheme 6.2

water.

The synthesis was first tested using D₂O. The incorporation and fate of the deuterium atom was then easily followed by proton NMR (Figure 6.4). Table 6.1 shows that there was no loss in the level of deuteration in the course of the

synthesis. When tritiated water was used, [³H]-5-azido-1,2-dimethylindole was obtained in a final 1.1 % yield with an activity of *ca* 30 mCi/mmol.

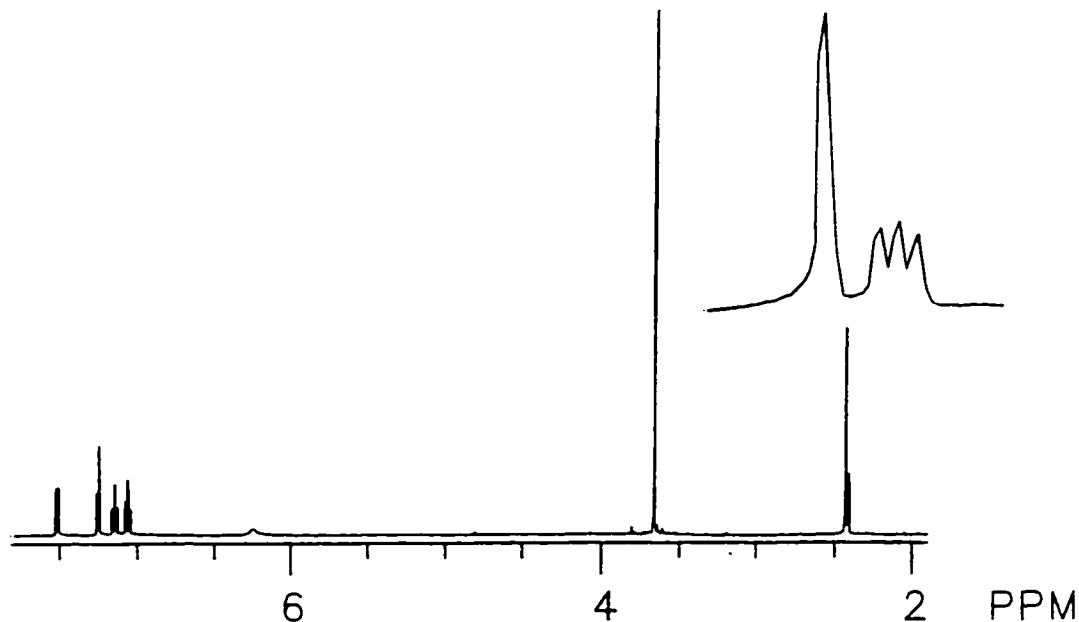


Figure 6.4: ¹H NMR of [²H] 1,2-dimethylindole.

Table 61: Percentage of deuteration as determined by ¹H NMR for each step of the synthesis of [²H] 5-azido-1,2-dimethylindole (Scheme 6.2).^a

Step #	Deuteration (%)
1	69
2	70
3	70
4	68

^a The percentage of deuteration was calculated using the following equation:

$$\% \text{ Deuteration} = \frac{(\text{Integration of } -\underline{\text{CH}}_2\text{D})/2}{(\text{Integration of } -\underline{\text{CH}}_3)/3 + (\text{Integration of } -\underline{\text{CH}}_2\text{D})/2} \times 100$$

Photolysis of [³H] 5-Azido-1,2-Dimethylindole. Figure 6.5 shows the variation of the UV-Vis spectrum of 5-azido-1,2-dimethylindole as a function of the irradiation time. The absorption at $\lambda = 248$ nm decreases as a function of time, and the rate of photolysis follows apparent first-order kinetics (Figure 6.6) with a half-life of *ca.* 1200 sec under these conditions. The products of photolysis under the nonenzymatic conditions have not been determined.

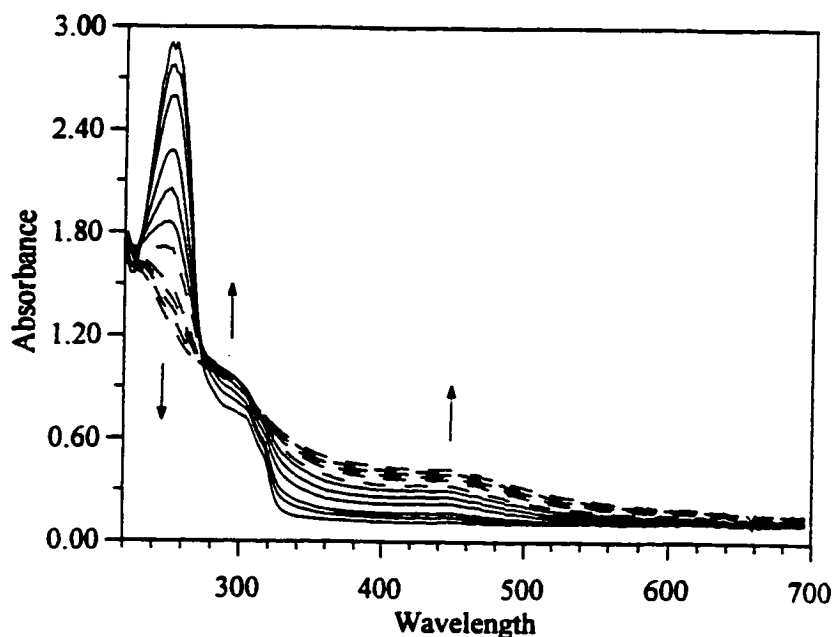


Figure 6.5: Effect of the irradiation time on the absorption spectrum of [³H] 5-azido-1,2-dimethylindole. [³H] 5-azido-1,2-dimethylindole (264 mM in 100 mM Tris pH 8.3 and 20 % ethanol) was photolyzed, for 5 min time periods, with a total irradiation time of 40 min. UV-Vis spectra were recorded during the time between irradiation periods (*ca.* 30 s).

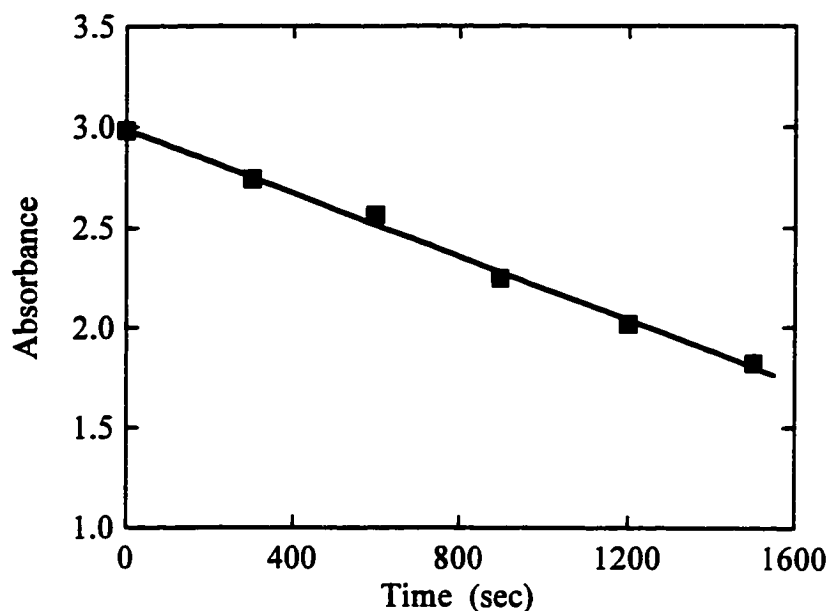


Figure 6.6: Absorbance of 5-azido-1,2-dimethylindole at 248 nm as a function of duration of photolysis.

Incorporation of [³H] 5-Azido-1,2-Dimethylindole into V-BrPO. V-BrPO was labeled with [³H] 5-azido-1,2-dimethylindole and run over a DEAE column to separate excess label. V-BrPO did bind to the resin, and the excess label was eluted by washing the column using 60 % ethanol. Labeled V-BrPO then was eluted off the resin using a salt gradient (Figure 6.7). After the 20 first fractions that contained the excess label, most of the radioactivity was confined in a narrow region that co-eluted exactly V-BrPO (determined by MCD bromination). The level of incorporation of [³H] 5-azido-1,2-dimethylindole into V-BrPO was

estimated to be around 0.2 mole of label per mole of enzyme, based on the recovered enzymatic activity and the associated radioactivity.

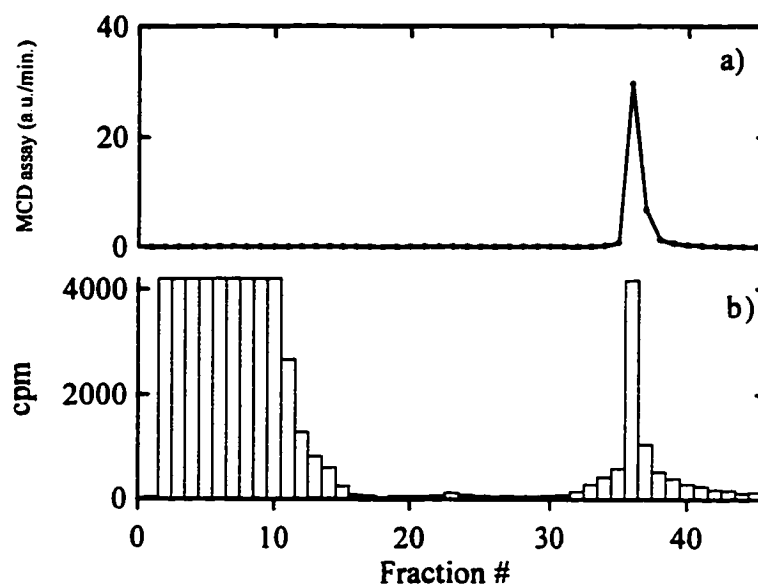


Figure 6.7: DEAE purification of V-BrPO labeled with [^3H] 5-azido-1,2-dimethylindole. a) Enzymatic activity; b) Scintillation counts.

HPLC Separation of Cyanogen Bromide and Tryptic Peptides from [^3H] 5-Azido-1,2-Dimethylindole Labeled V-BrPO. Cyanogen bromide and trypsin treated samples of [^3H] 5-azido-1,2-dimethylindole-labeled V-BrPO, purified by DEAE column, were analyzed by HPLC using C-4 and C-18 reverse phase columns, respectively. When [^3H] 5-azido-1,2-dimethylindole-labeled V-BrPO was cleaved by cyanogen bromide, the resulting peptides were highly insoluble and after filtration only 10 % of the original radioactivity of the sample could be

injected onto the HPLC column of which 75 % eluted during the run. Figure 6.8 shows the HPLC profile at $\lambda = 214$ nm and the radioactivity measured in each fraction. Although the radioactive background due to residual photolyzed label that did not crosslink was significant, a single peptide, eluting at 40 min, contained an excess of radioactivity (Figure 6.8). Two other peptides eluting at 51 and 65 min seemed to contain also smaller amounts of radioactivity.

When tryptic peptides of [^3H] 5-azido-1,2-dimethylindole-labeled V-BrPO were separated by HPLC only 50 % of the radioactivity applied to the column was recovered, of which 20 % was contained in a single fraction near 62 min of the gradient (Figure 6.9), corresponding to a major peak in the HPLC profile. The broad peak centered at 90 min of the gradient was also attributed to residual photolyzed label that could not be washed out during the DEAE purification step.

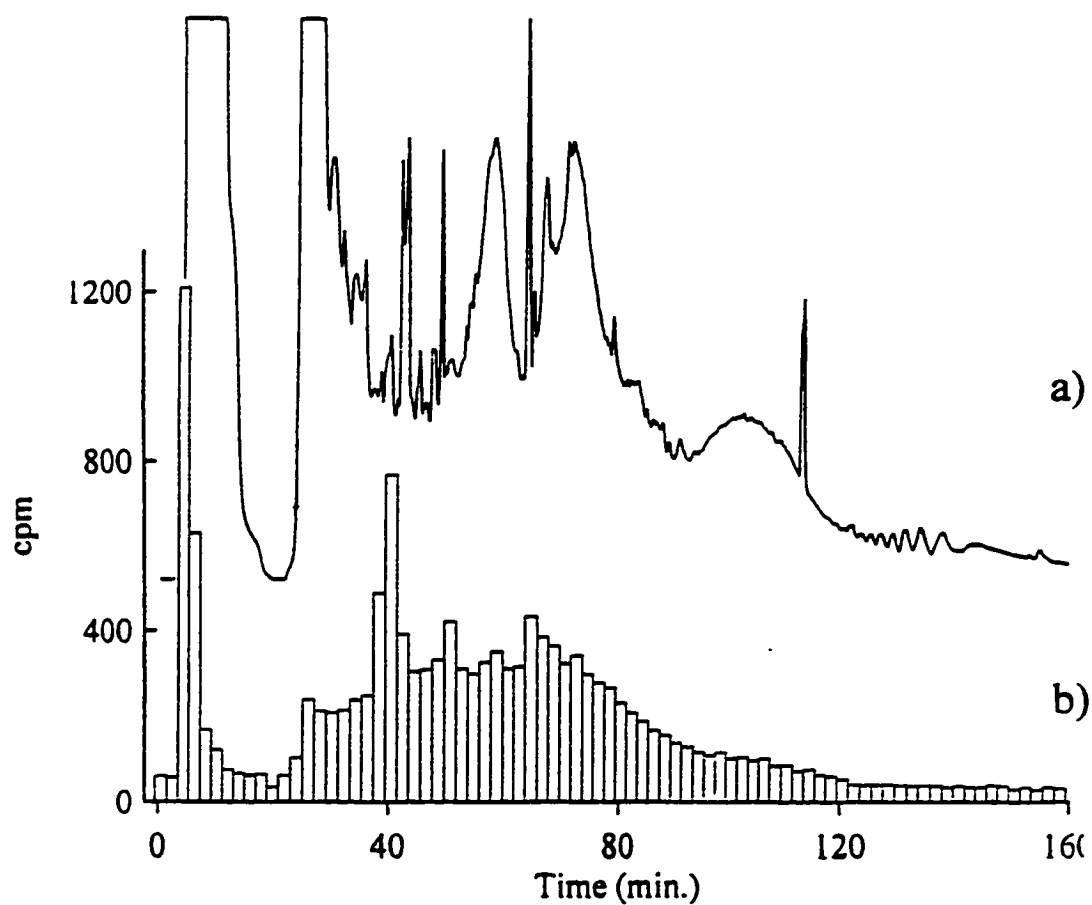


Figure 6.8: C-4 HPLC profile of cyanogen bromide peptides of [^3H] 5-azido-2-phenylindole labeled V-BrPO. After cyanogen cleavage, the peptides were separated on a Vydac C-4 column eluted at a flow rate of 0.8 mL/min. The profile was developed with a gradient of solvent B (80 % acetonitrile, 0.1 % TFA) into solvent A (0.1 % TFA), 0-5 min (0 % B), 5-140 min (0-100 % B), 140-160 min (100 % B), and followed at $\lambda = 214$ nm. Fractions were collected every 2 min and the radioactivity measured by scintillation counting. a) HPLC profile at 214 nm; b) Scintillation counts.

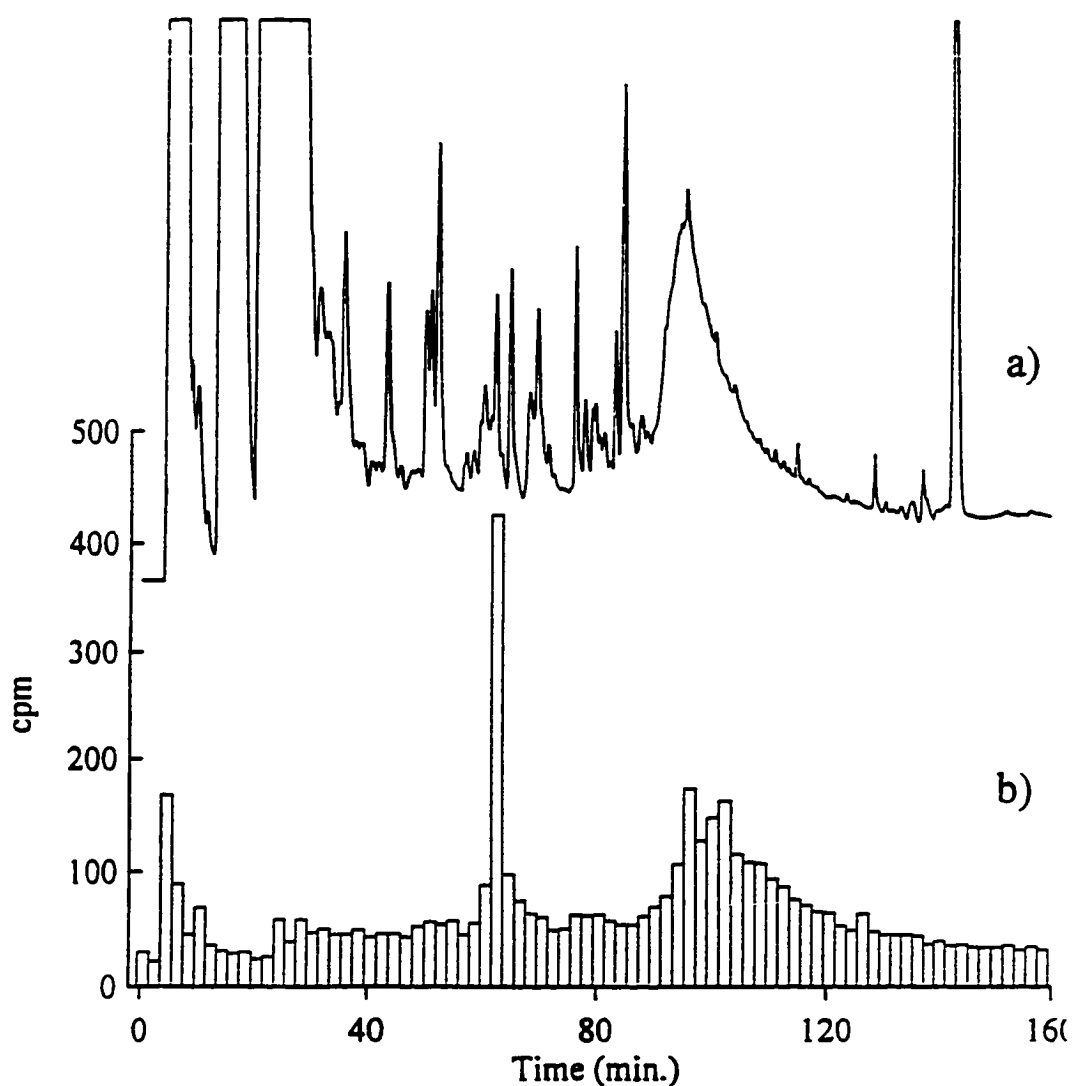


Figure 6.9: C-18 HPLC profile of tryptic peptides of [^3H] 5-azido-2-phenylindole labeled V-BrPO. After tryptic digestion, the peptides were separated on a Vydac C-18 column eluted at a flow rate of 0.8 mL/min. The profile was developed with a gradient of solvent B (80 % acetonitrile, 0.1 % TFA) into solvent A (0.1 % TFA), 0-5 min (0 % B), 5-80 min (0-30 % B), 80-135 min (30-100 % B), 135-160 min (100 % B), and followed at $\lambda = 214$ nm. Fractions were collected every 2 min and the radioactivity measured by scintillation counting. a) HPLC profile at 214 nm; b) Scintillation counts.

Discussion

It has been shown here that V-BrPO can be covalently modified by the photoaffinity indole analogs 5-azido-2-phenylindole and 5-azido-1,2-dimethylindole. The use of 5-azido-2-phenylindole as a fluorescent probe was not successful, but comparison of the tryptic digest of unlabeled and labeled V-BrPO suggested that the insertion of the probe was specific and occurred at only one site. Specific crosslinking of azidoindoles to V-BrPO was further confirmed by photoaffinity labeling of V-BrPO with [³H] 5-azido-1,2-dimethylindole. Following digestion with CNBr or digestion with trypsin and separation of the peptide fragments by HPLC, the radioactivity was associated with only one peptide peak. Those results are quite noteworthy since the use of photoaffinity labeling techniques to identify specific binding sites on proteins can potentially present a few problems (Chowdhry & Westmeister, 1979) due to their lack of specificity. The photoactivated groups, in this case nitrenes, can react with almost any amino acid side chain in the protein. This problem was not encountered when V-BrPO was probed with azidoindoles, indicating that a) non-specific binding of indoles to V-BrPO can be ruled out b) motion of the probe during the lifetime of the photoactivated intermediate was limited.

The level of incorporation at a given site is another problem often encountered with photoaffinity probes. Classical electrophilic affinity labels frequently display stoichiometric incorporation, whereas stoichiometric incorporation of photoaffinity labels is rarely achieved. When V-BrPO was irradiated with a 12-fold molar excess of [³H] 5-azido-1,2-dimethylindole, *ca.* 0.2

mol of reagent was incorporated per mol of enzyme.¹ On the other hand, when V-BrPO was covalently modified by a 23-fold molar excess of 5-azido-2-phenylindole, the incorporation appeared to be almost stoichiometric. Such a high level of insertion of an azidoindole is not unique; when the α -subunit of tryptophan synthase from *Escherichia coli* (1 mg/mL) was irradiated with 5-azidoindole, stoichiometric incorporation was achieved when the concentration of 5-azidoindole was raised above 2 mM (Brock et al., 1983).

The large shift in the HPLC retention time observed for the 5-azido-2-phenylindole modified tryptic peptide of V-BrPO is not uncommon. For example, the single modified tryptic peptide of [³H] 8-azidoadenosine-5'-triphosphate labeled *recA* protein from *E. coli* eluted more than 7 min earlier than the unmodified one, due to the hydrophilic character of the inserted probe (Knight & McEntee, 1985). The length of the tryptic peptide was not affected by the cross-linking of the probe. In the case of V-BrPO and 5-azido-2-phenylindole, however, it appeared that labeling had occurred in such a way that it inhibited cleavage at tryptic site, suggesting that labeling had taken place near (or at) a arginine or lysine. The X-ray structure of V-CIPO from *C. inaequalis* revealed that the active-site vanadium was at the bottom of a well that was composed of a hydrophilic half and a hydrophobic half (Messerschmidt & Wever, 1996). The hydrophilic surface included carbonyl oxygens and two arginine side chains. If the active site of V-BrPO resembles the active site of V-CIPO, a binding site for

¹ The value given here must be taken with some precaution since it has not been determined yet whether there was loss of radioactivity following irradiation. The actual level of label incorporation may, therefore, be higher than 0.2 mole of probe per mole of V-BrPO.

the hydrophobic substrate, and nearby nucleophilic residues (i.e. arginines) that can react with the photogenerated intermediate (Figure 6.10).

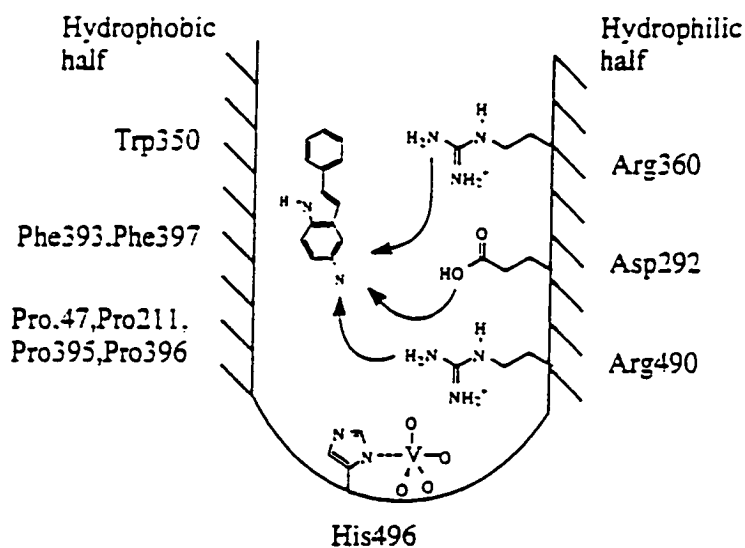


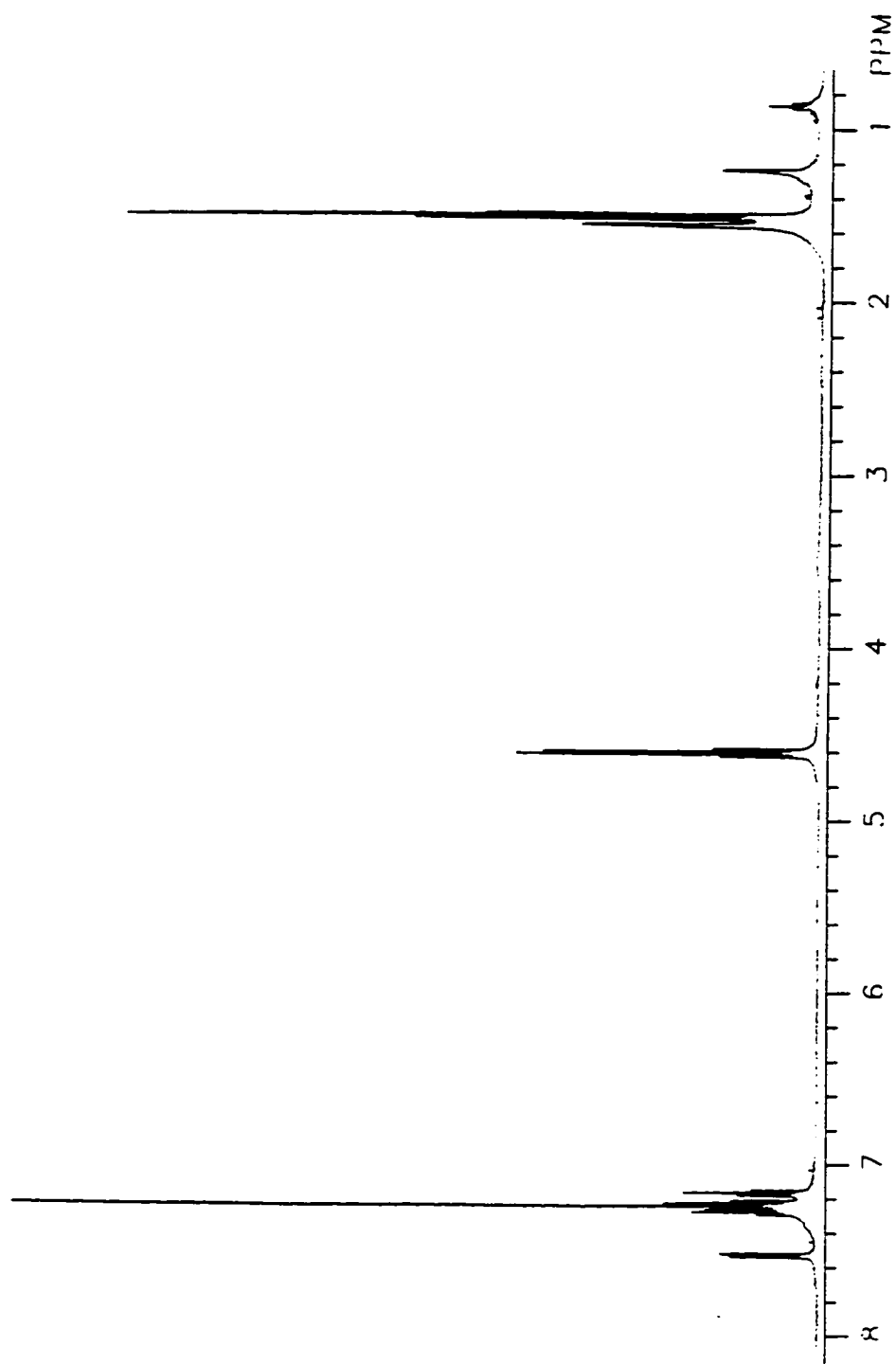
Figure 6.10: Schematic view of the channel leading to the vanadium binding site of V-CIPO from *C. inaequalis* with the photoactivated 5-azido-2-phenylindole bound to the hydrophobic surface of the channel (adapted from Messerschmidt & Wever, 1996).

Although the exact cross-linking site of 5-azidoindoles to V-BrPO has not been determined yet, the data presented here confirm the results obtained by kinetic measurements (Chapt. 4) or fluorescence quenching measurements (Chapt. 5) in that the high selectivity observed with V-BrPO for indoles is likely due to specific binding of this class of compounds to the enzyme. It is unclear at this time why V-BrPO from *A. nodosum* shows such a high affinity for indoles over other substrates since, to this date, no brominated indolic secondary

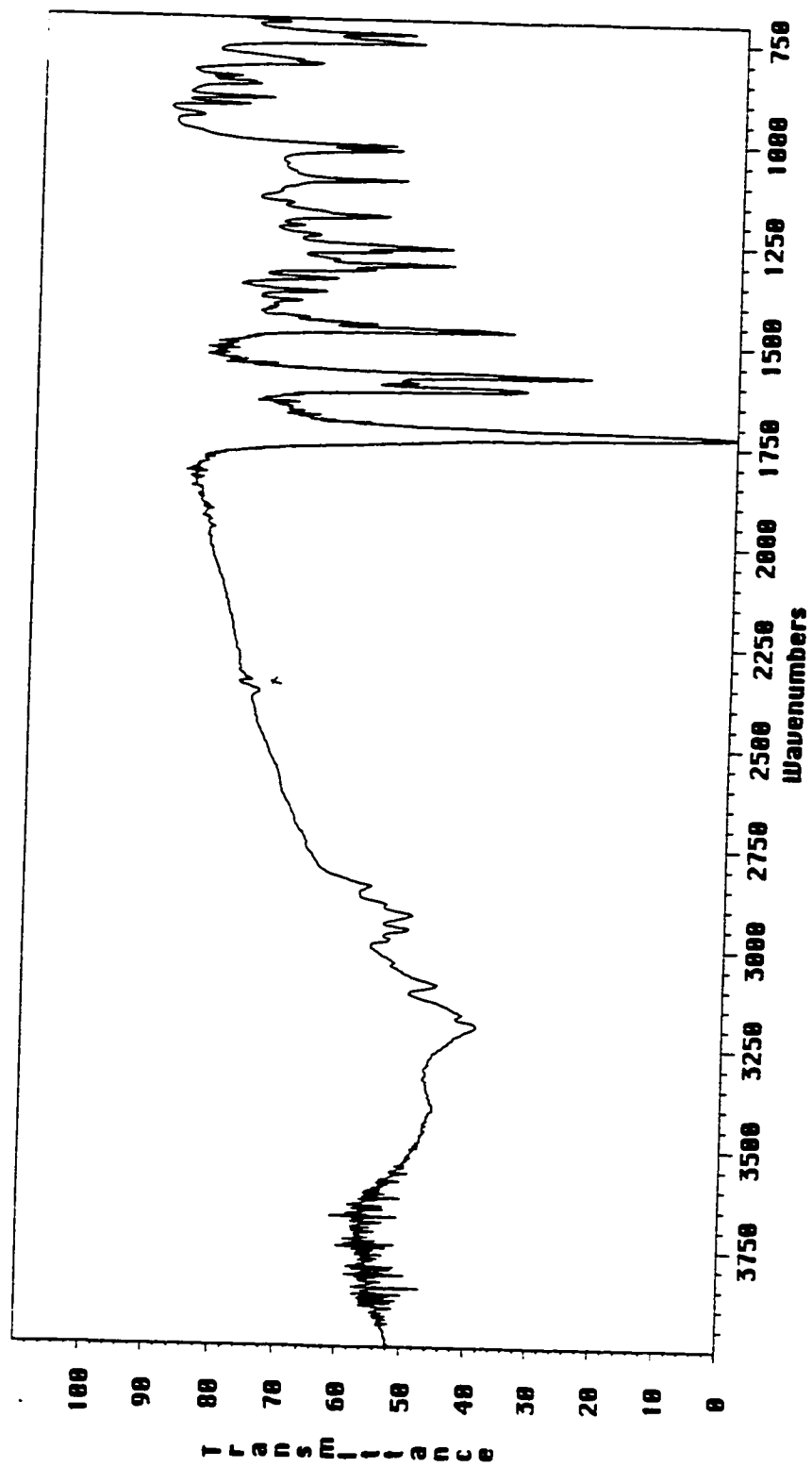
metabolites have been isolated from *A. nodosum*. In any case, the discovery of a binding site in V-BrPO is of importance, and further characterization of this particular site should greatly enhance the understanding of the mechanism of action of this enzyme.

Appendix

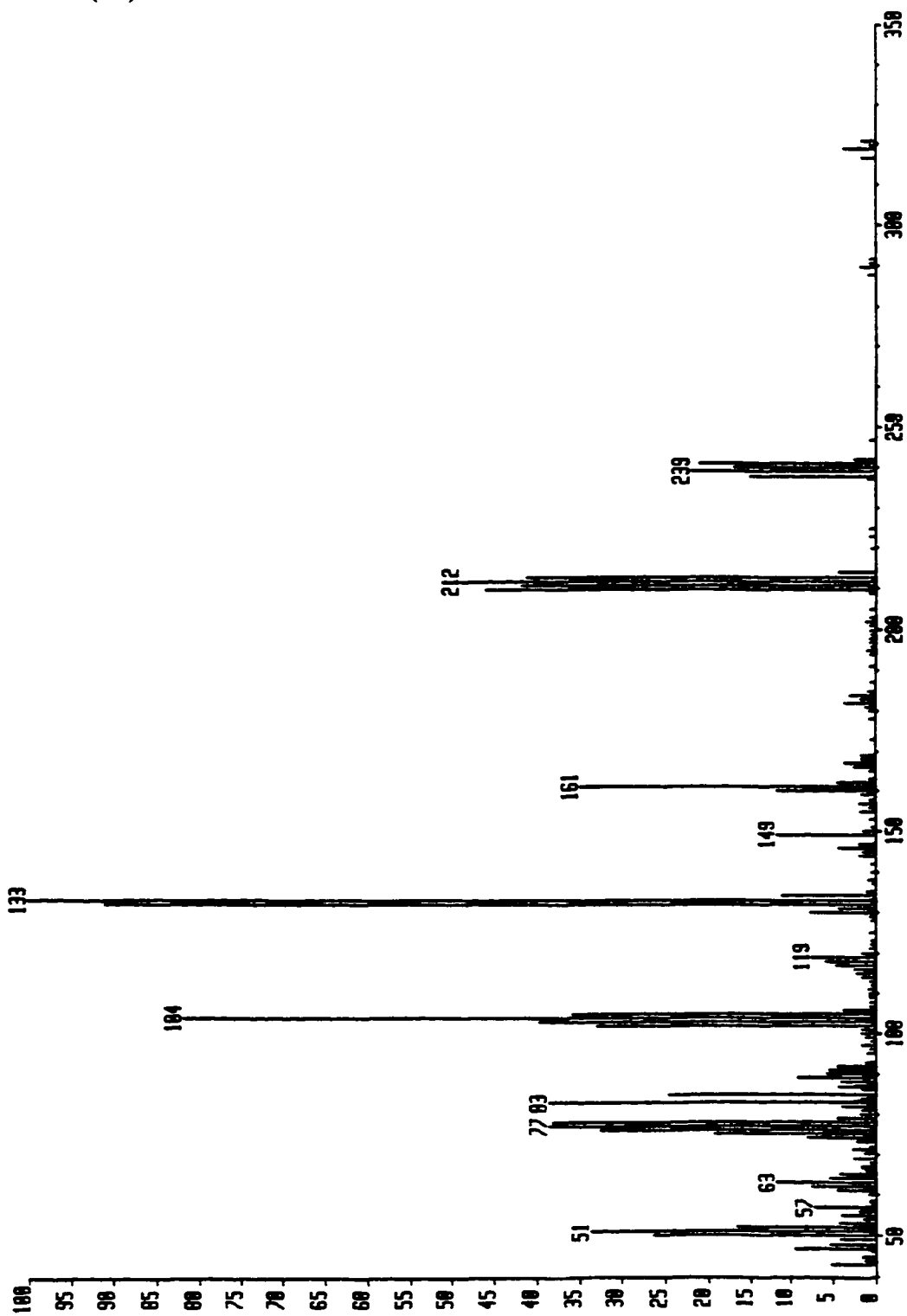
	Page
¹ H NMR of 3,3-dibromo-2-ethoxy-3 <i>H</i> -indole (19)	185
IR of (19)	186
EIMS of (19)	187
¹ H NMR of 1,3-dihydro-3-ethoxy-1-methyl-2 <i>H</i> -indol-2-one (26)	188
IR of (26)	189
EIMS of (26)	190
¹ H NMR of 1,3-dihydro-1-methyl-3-(1-methyl 1 <i>H</i> -indol-3-yl)- 2 <i>H</i> -indol-2-one (28)	191
IR of (28)	192
EIMS of (28)	193
¹ H NMR of 3-bromo-1-methyl-3-(1-methyl 1 <i>H</i> -indol-3-yl)-1 <i>H</i> -indole (29)	194
IR of (29)	195
EIMS of (29)	196
¹ H NMR of 3-3'-diphenyl-2,2'-bi-1 <i>H</i> -indole (44)	197
IR of (44)	198
EIMS of (44)	199
¹ H NMR of 3-phenyl-2-(3-phenyl-3 <i>H</i> -indol-2-yl)-1 <i>H</i> -indole (45)	200
IR of (45)	201
EIMS of (45)	202
¹ H NMR of 3-phenyl-2-(3-ethoxy-3-phenyl-3 <i>H</i> -indol-2-yl)-1 <i>H</i> -indole (46)	203
IR of (46)	204
EIMS of (46)	205
¹ H NMR of 1,3-dihydro-3-ethoxy-3-phenyl-2 <i>H</i> -indol-2-one (48)	206
IR of (48)	207
EIMS of (48)	208
¹ H NMR of (20)	209
¹³ C NMR of (20)	210
IR of (20)	211
EIMS of (20)	212

¹H NMR of 3,3-dibromo-2-ethoxy-3*H*-indole (19)

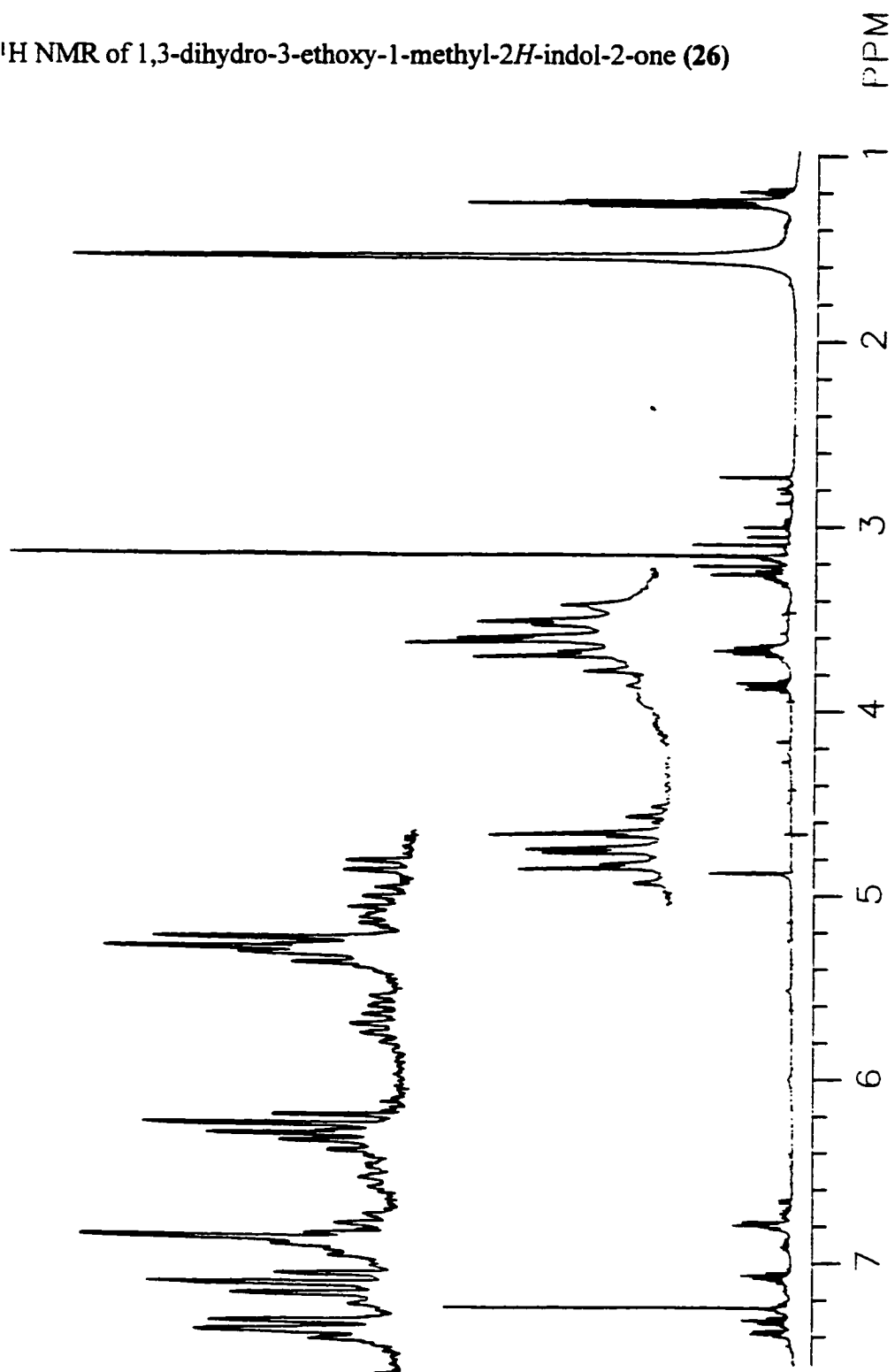
IR of (19)



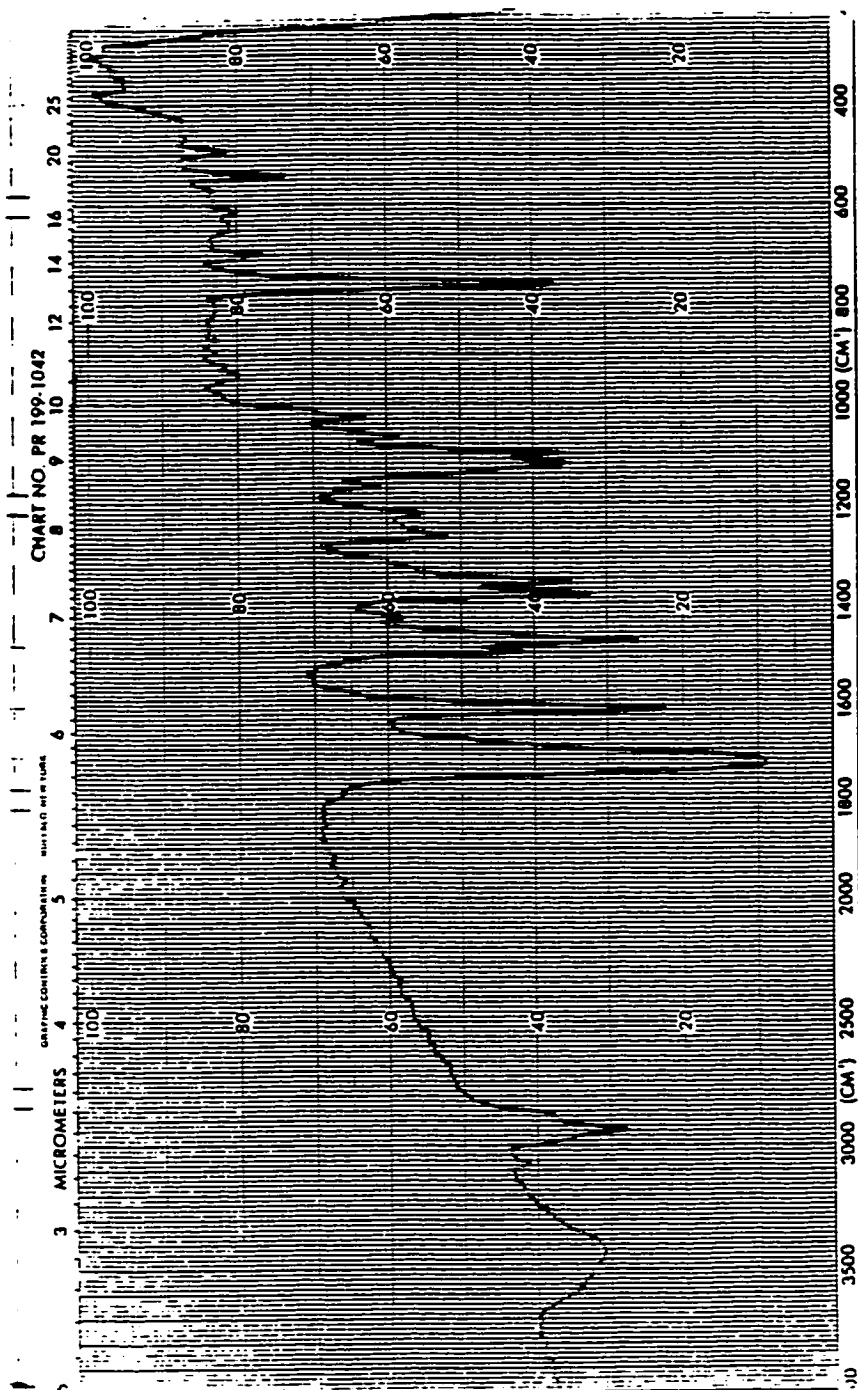
EIMS of (19)



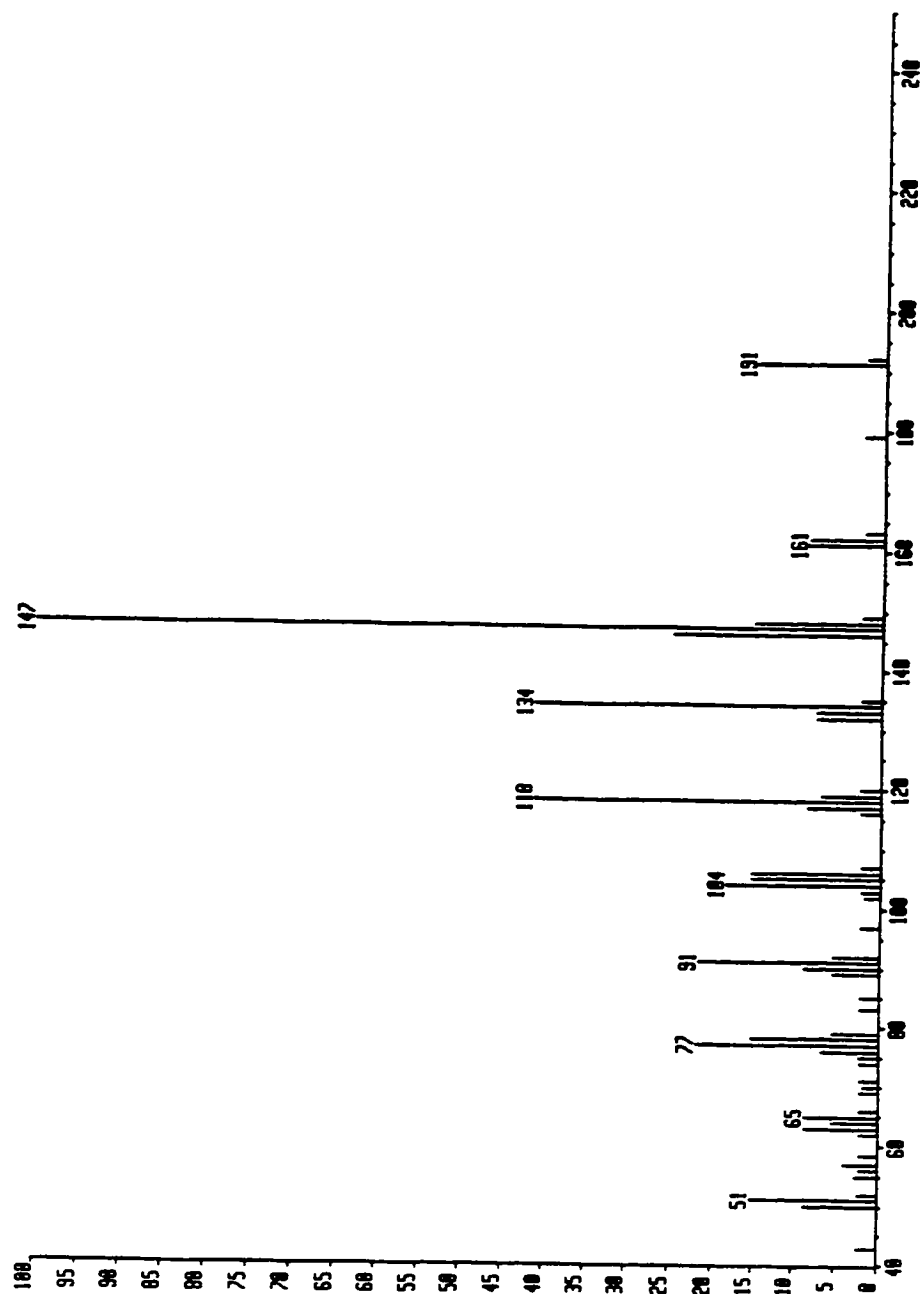
¹H NMR of 1,3-dihydro-3-ethoxy-1-methyl-2*H*-indol-2-one (26)



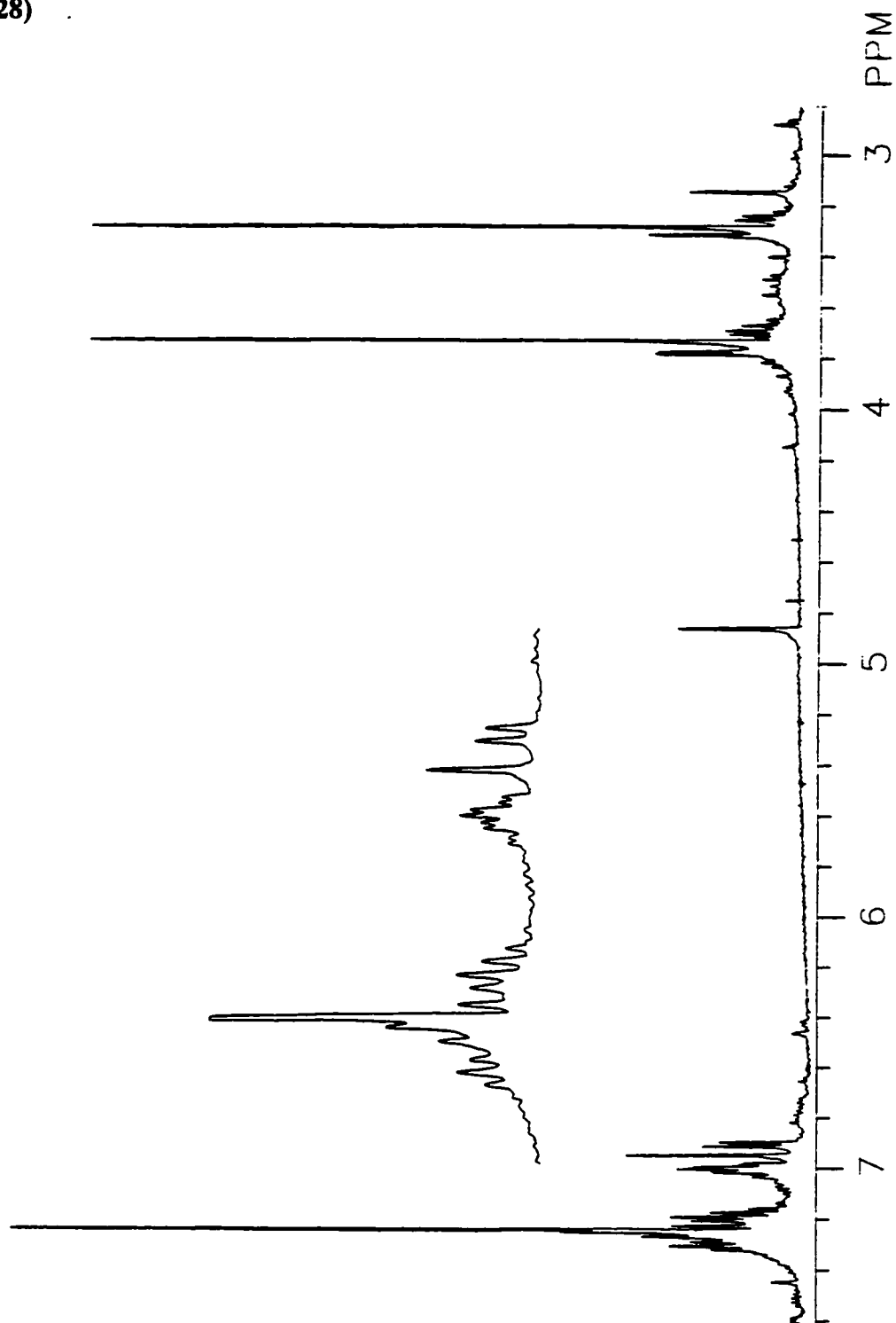
IR of (26)



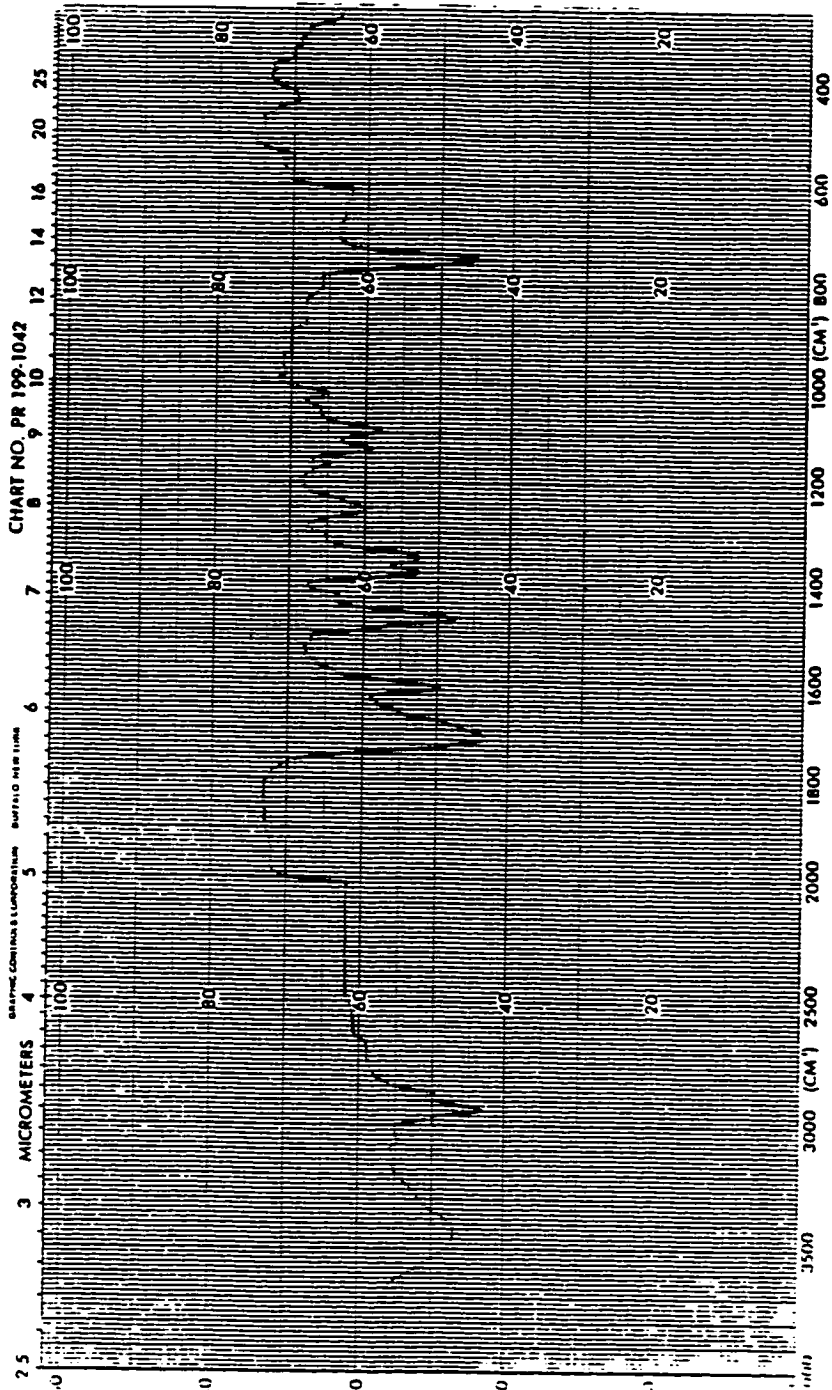
EIMS of (26)



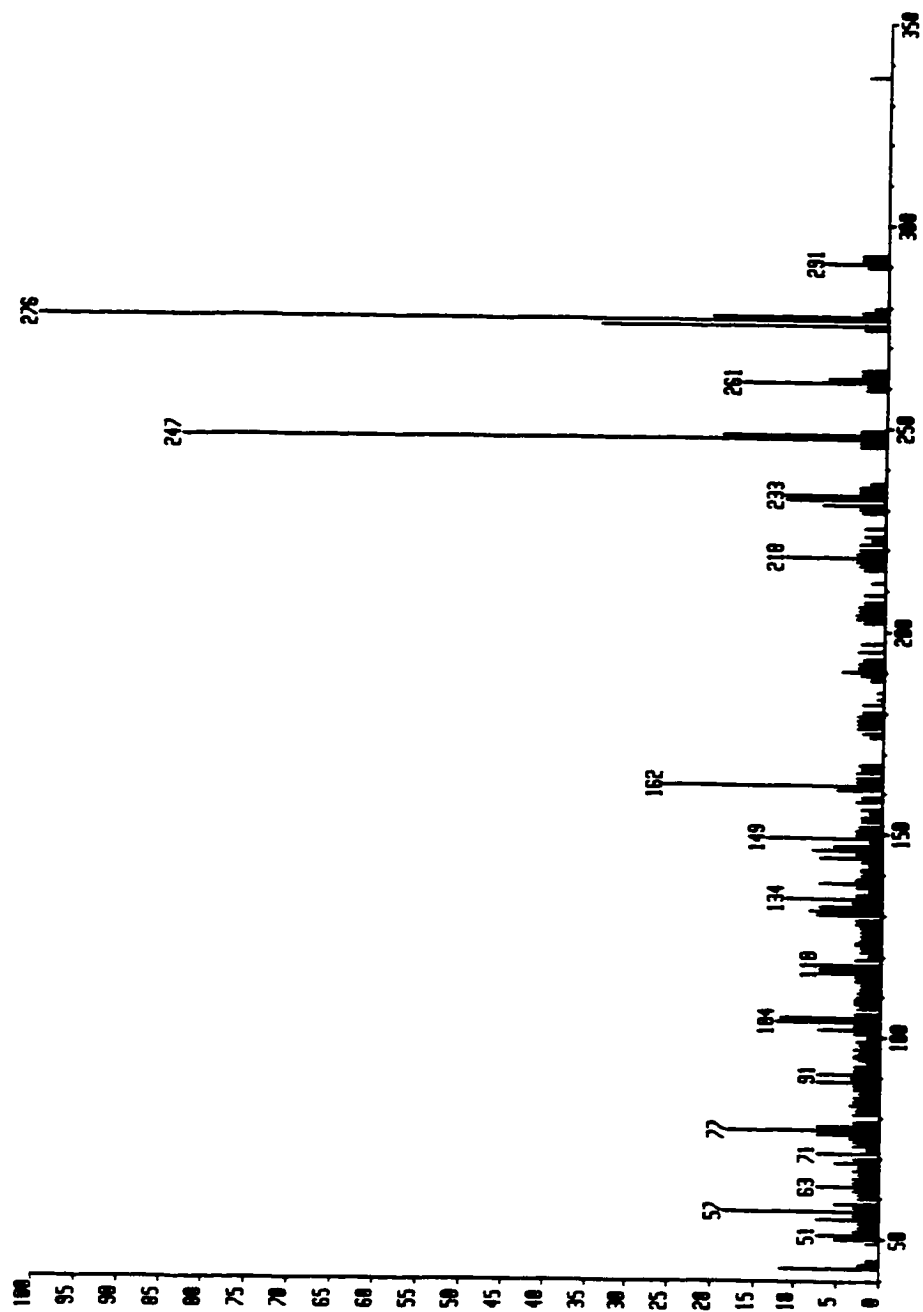
^1H NMR of 1,3-dihydro-1-methyl-3-(1-methyl-1*H*-indol-3-yl)-2*H*-indol-2-one
(28)



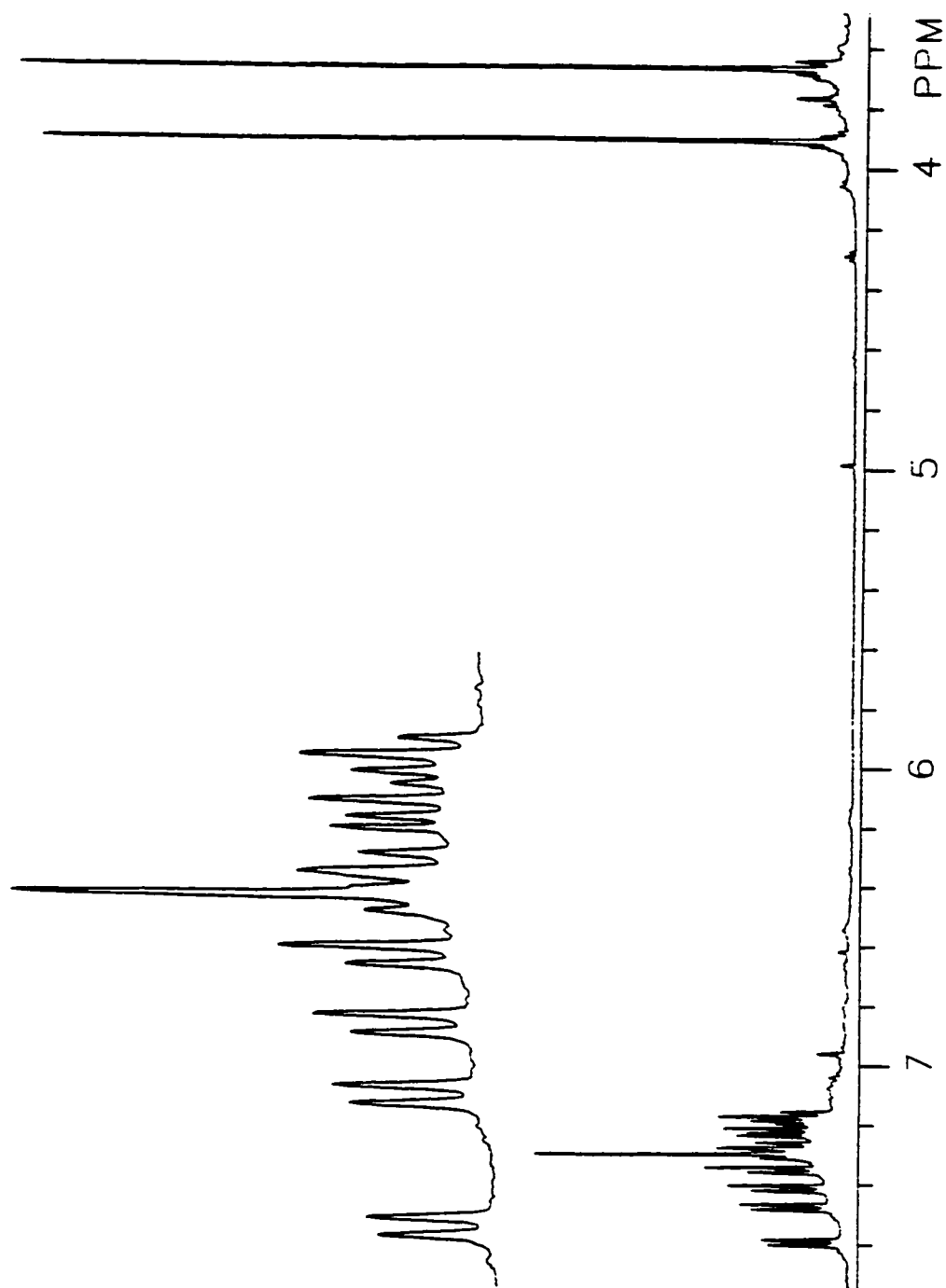
IR of (28)



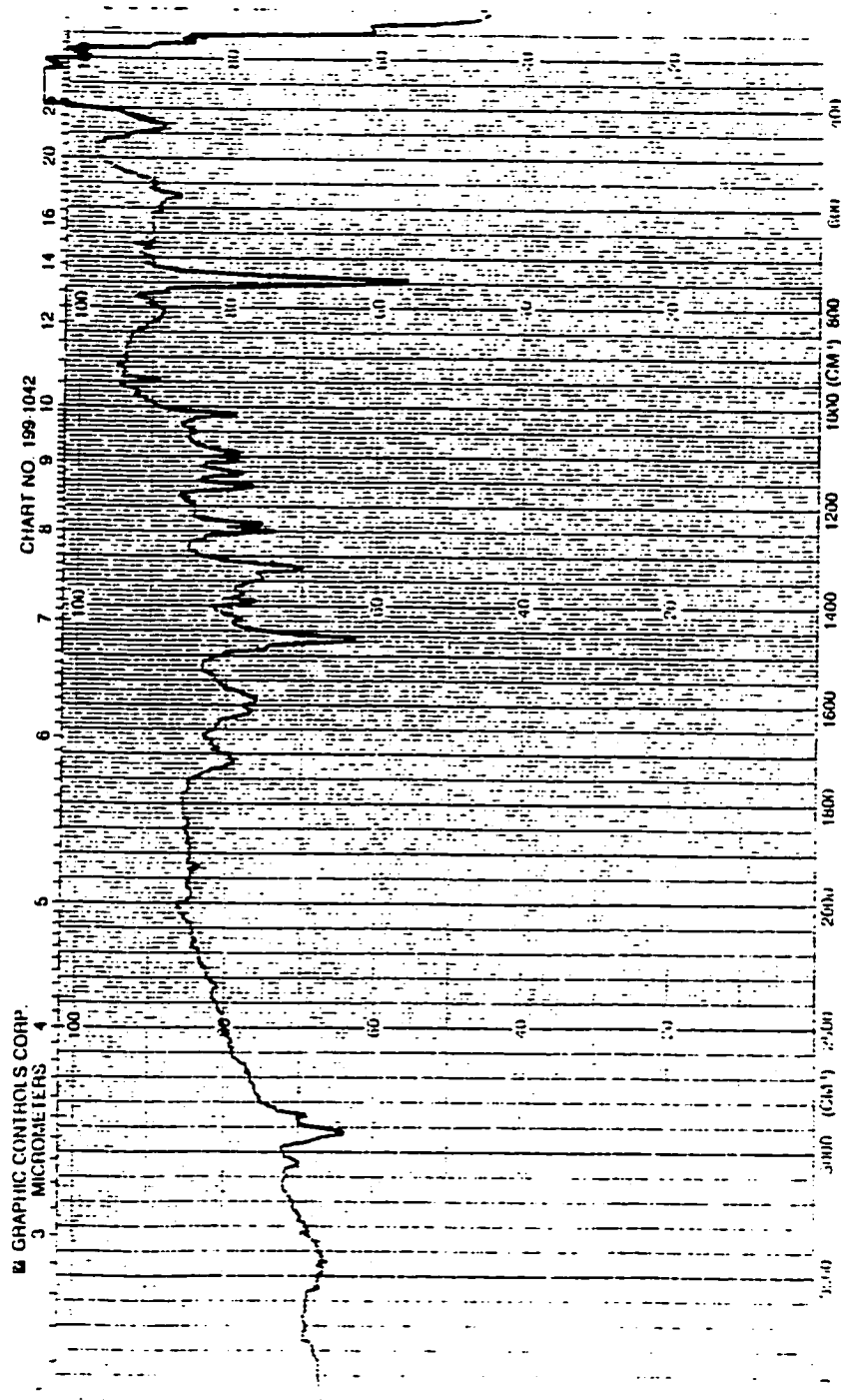
EIMS of (28)



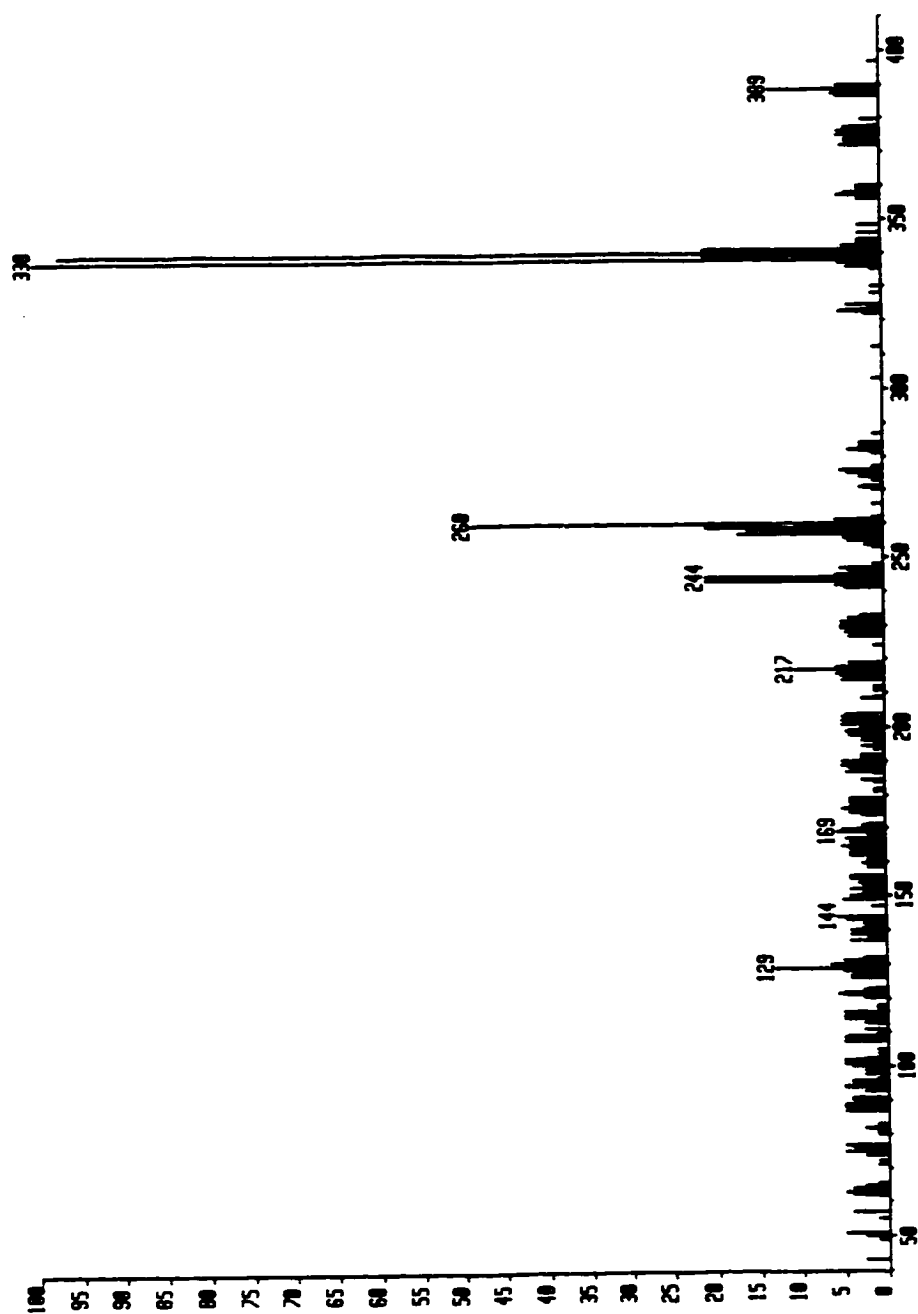
¹H NMR of 3-bromo-1-methyl-3-(1-methyl-1*H*-indol-3-yl)-1*H*-indole
(29)

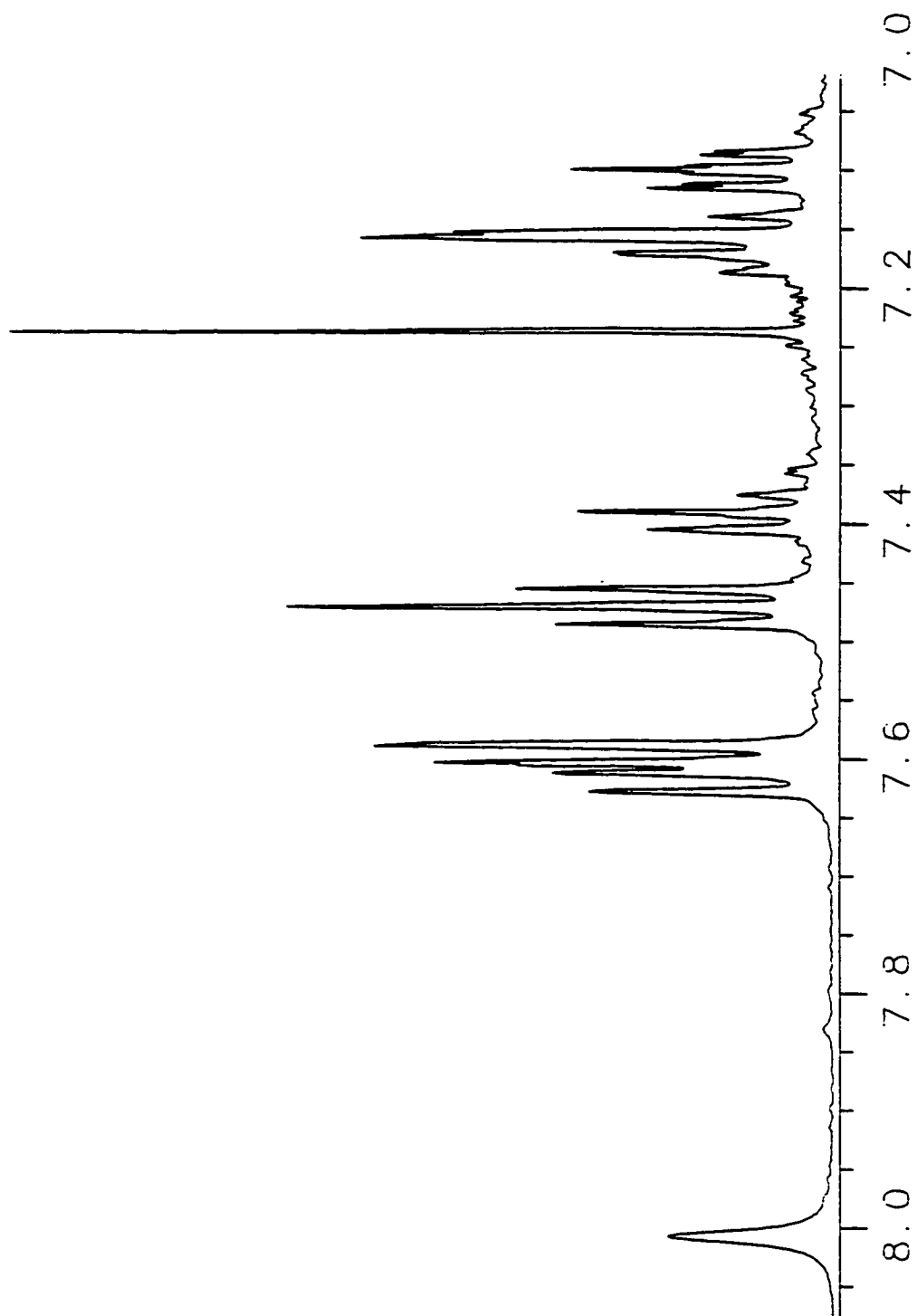


IR of (29)

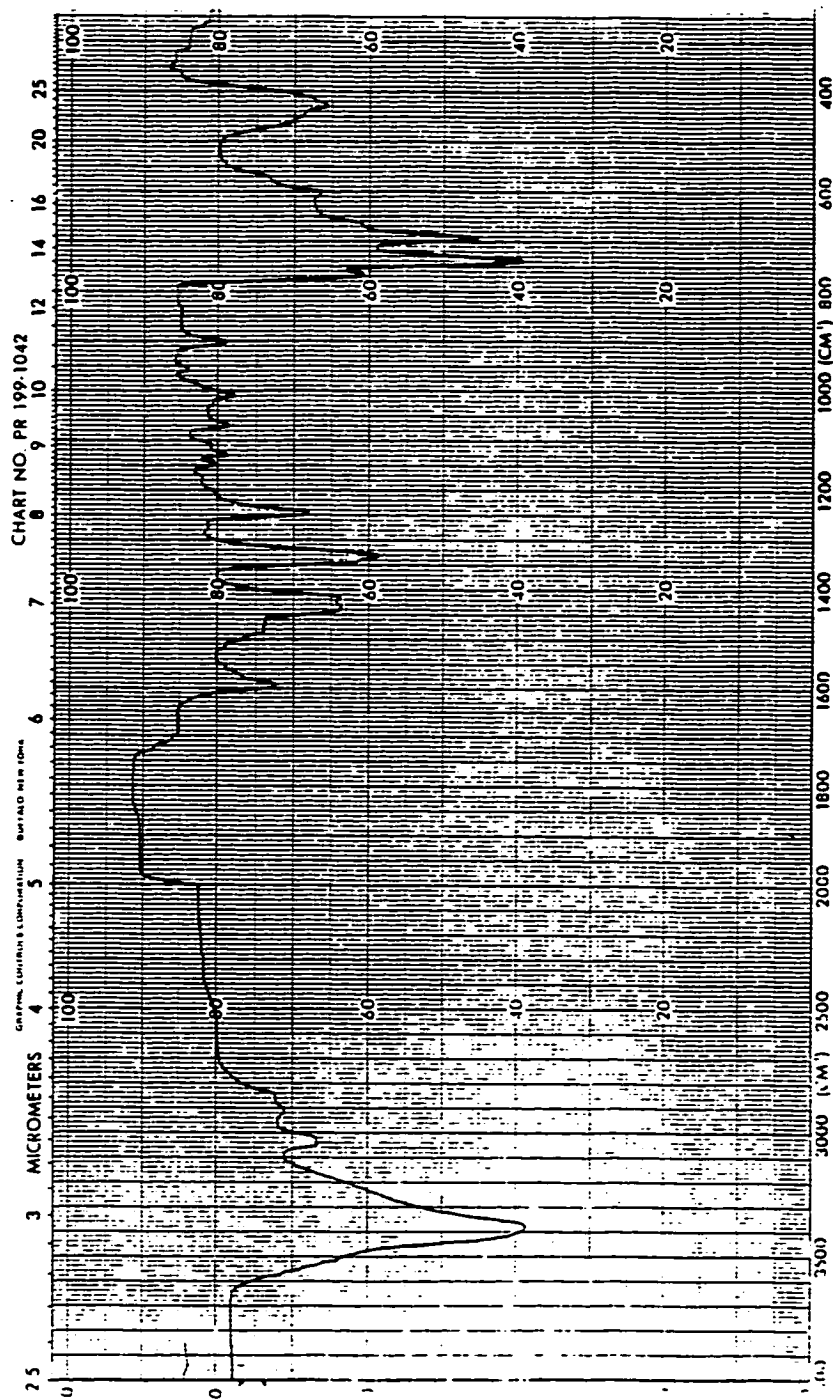


EIMS of (29)

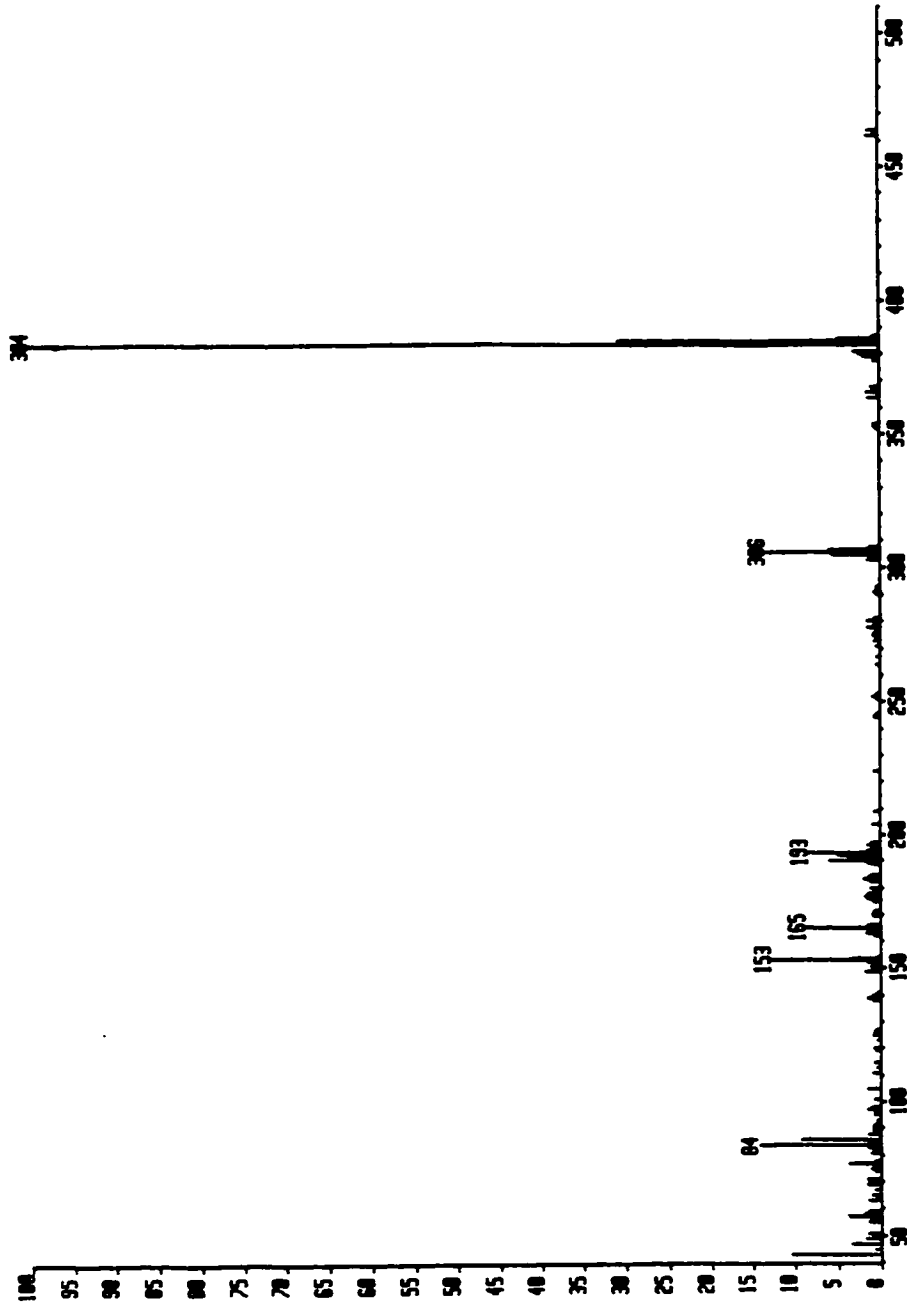


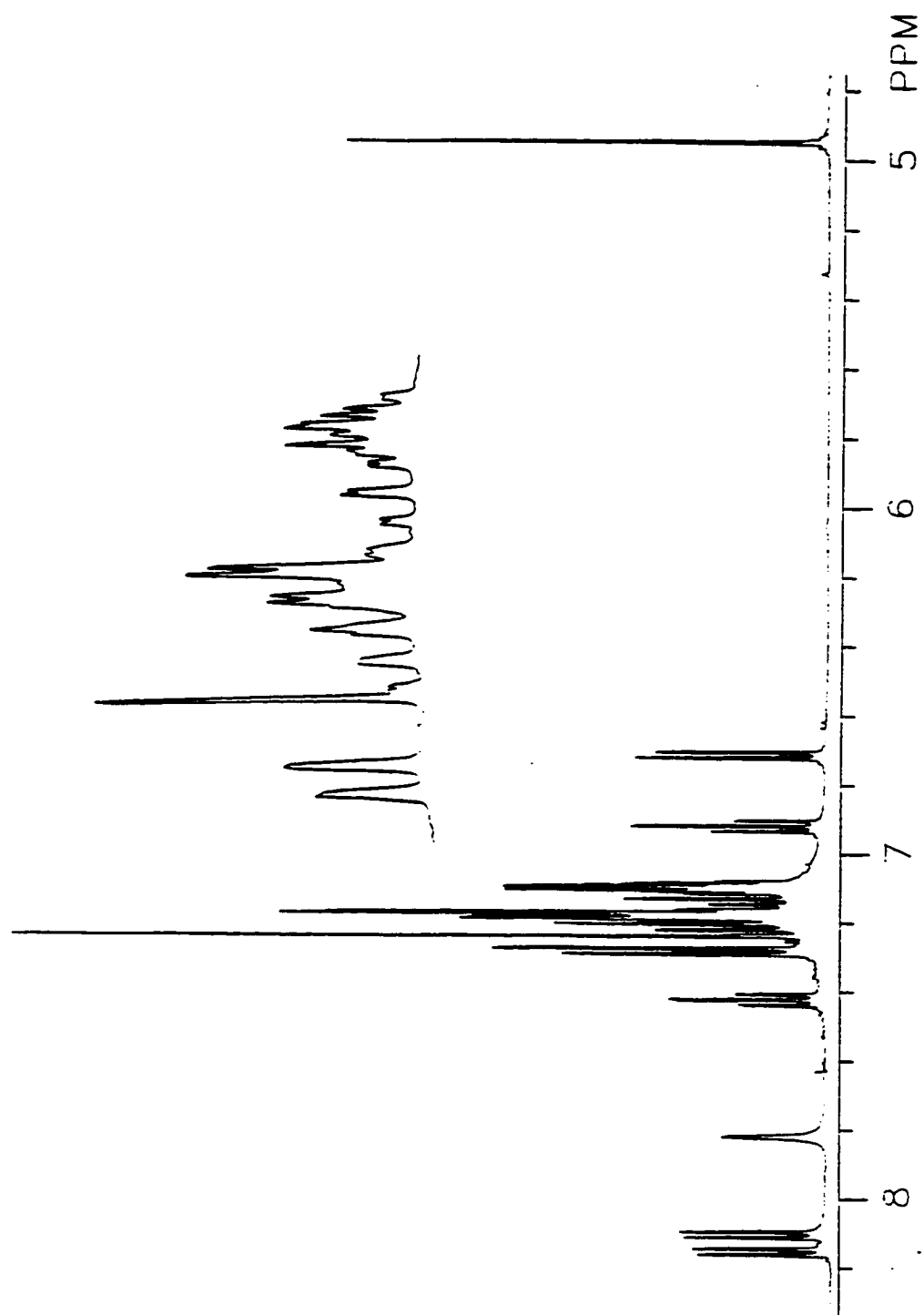
¹H NMR of 3-3'-diphenyl-2,2'-bi-1*H*-indole (44)

IR of (44)

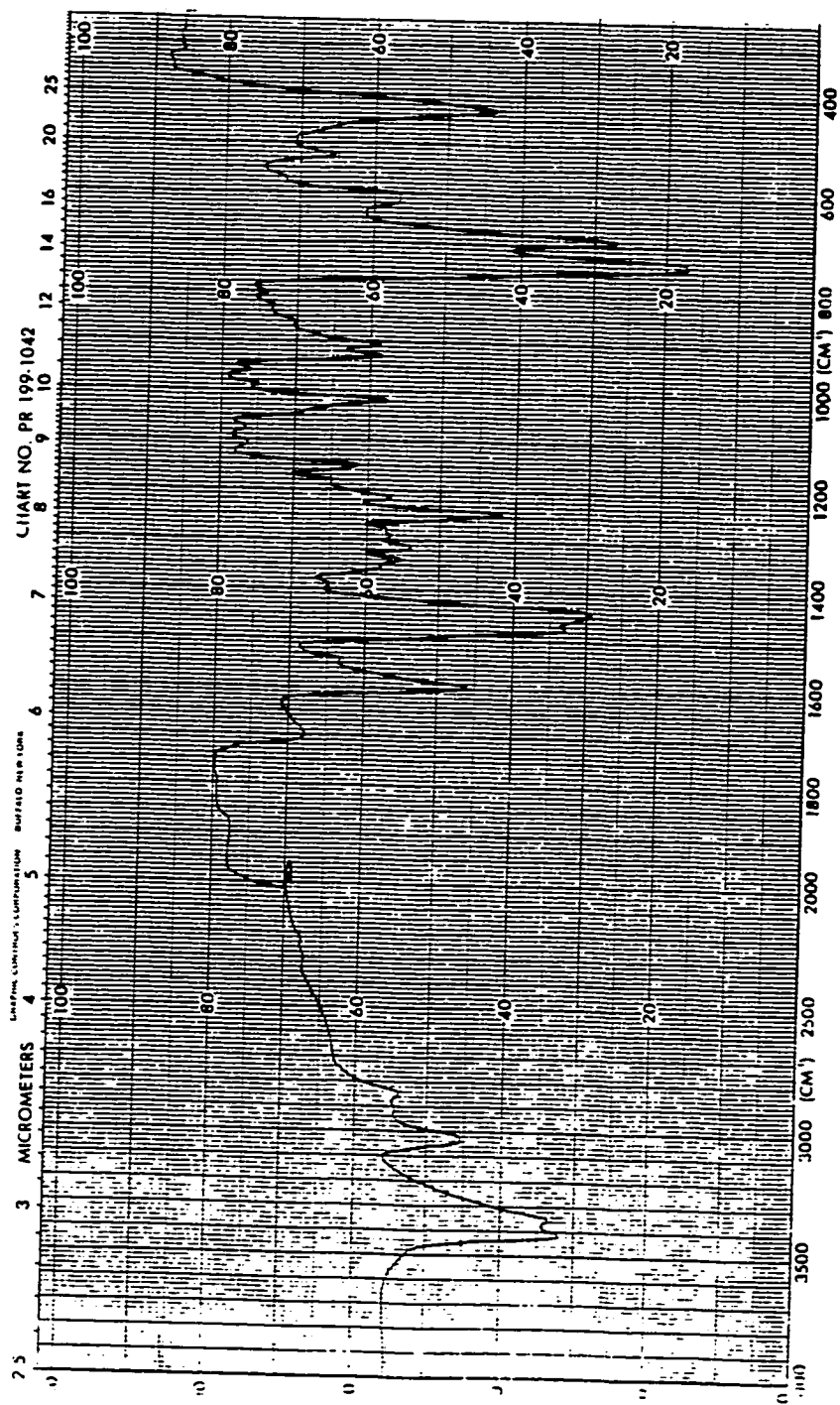


EIMS of (44)

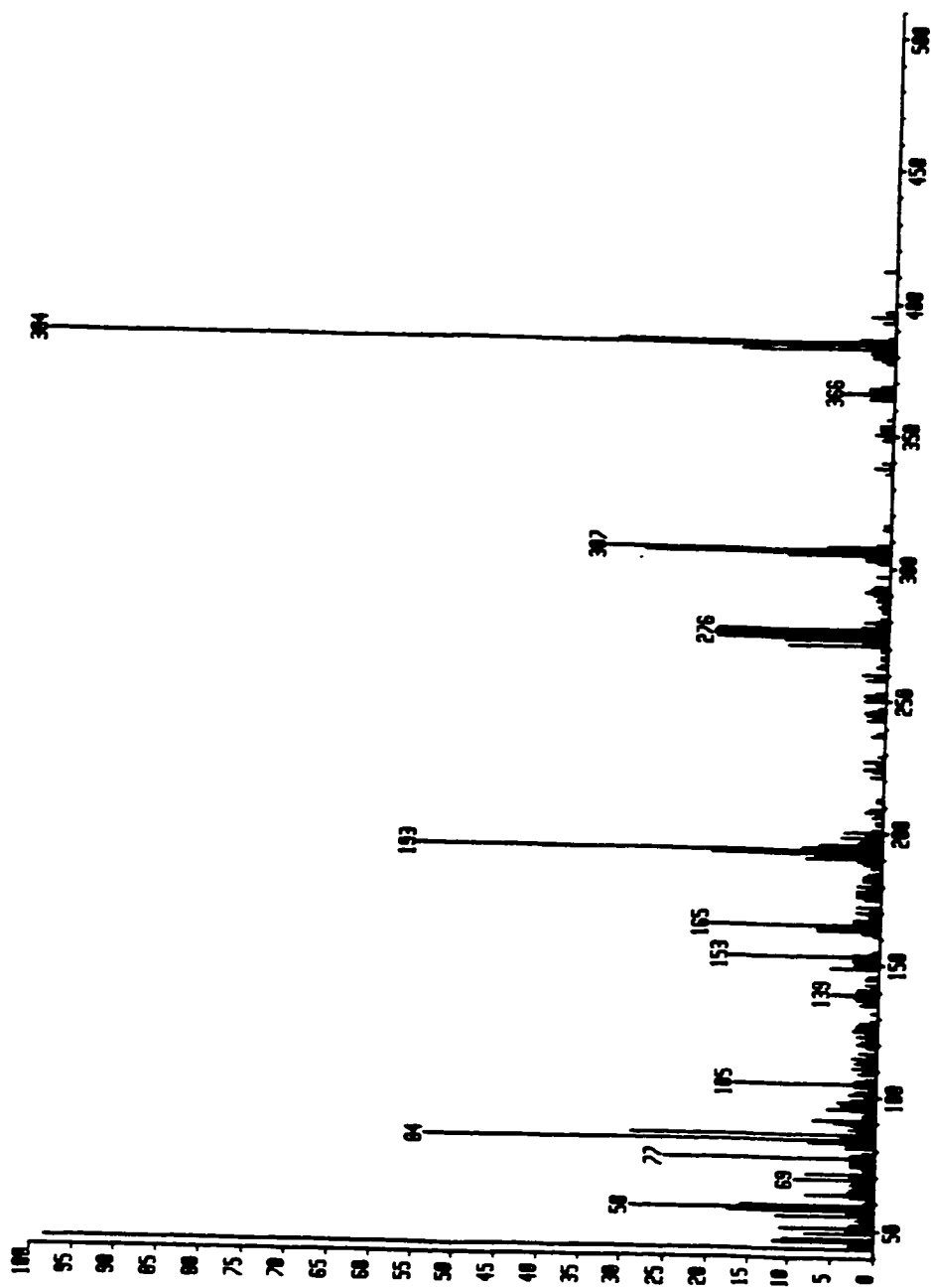


^1H NMR of 3-phenyl-2-(3-phenyl-3*H*-indol-2-yl)-1*H*-indole (45)

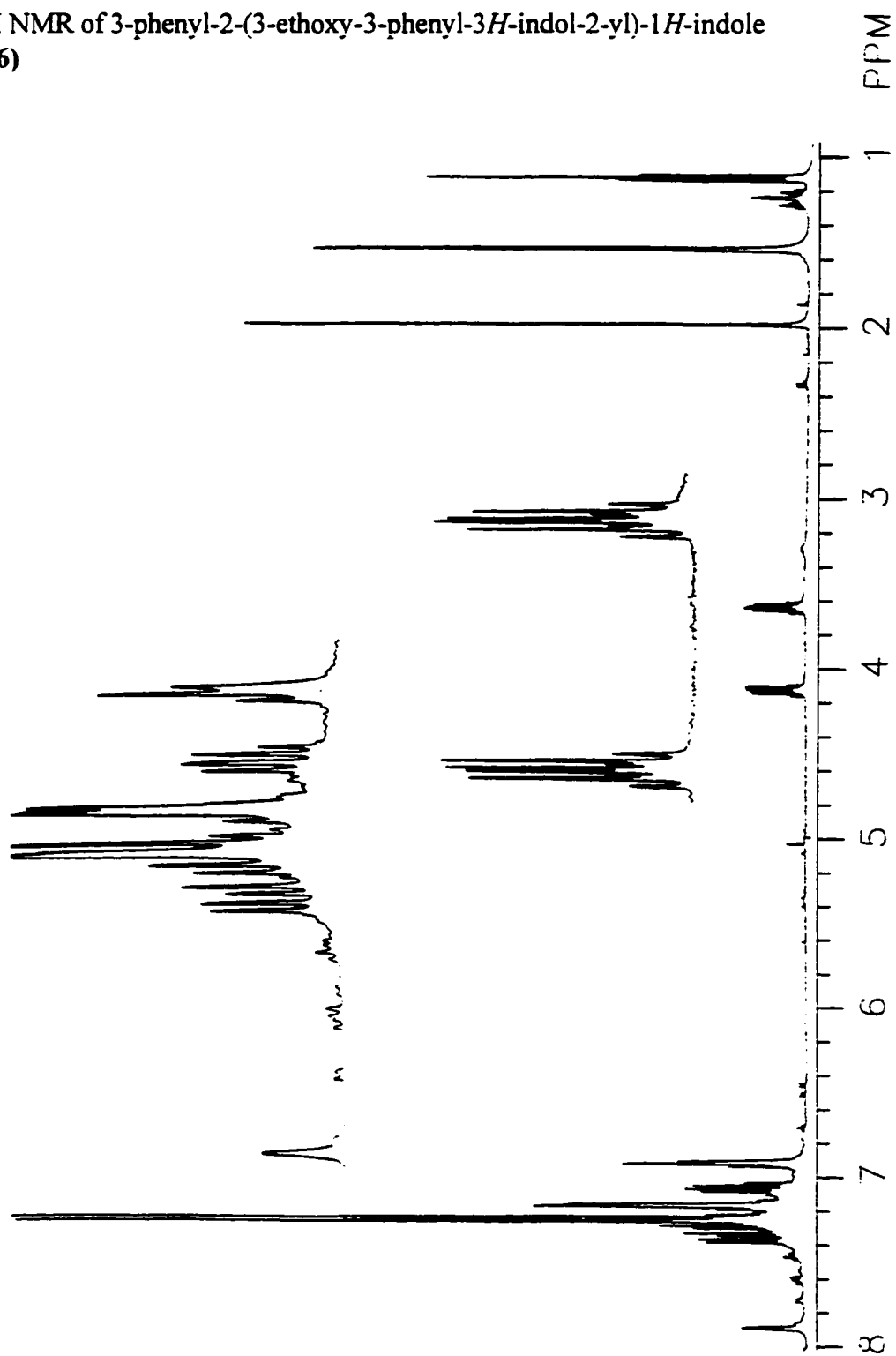
IR of (45)



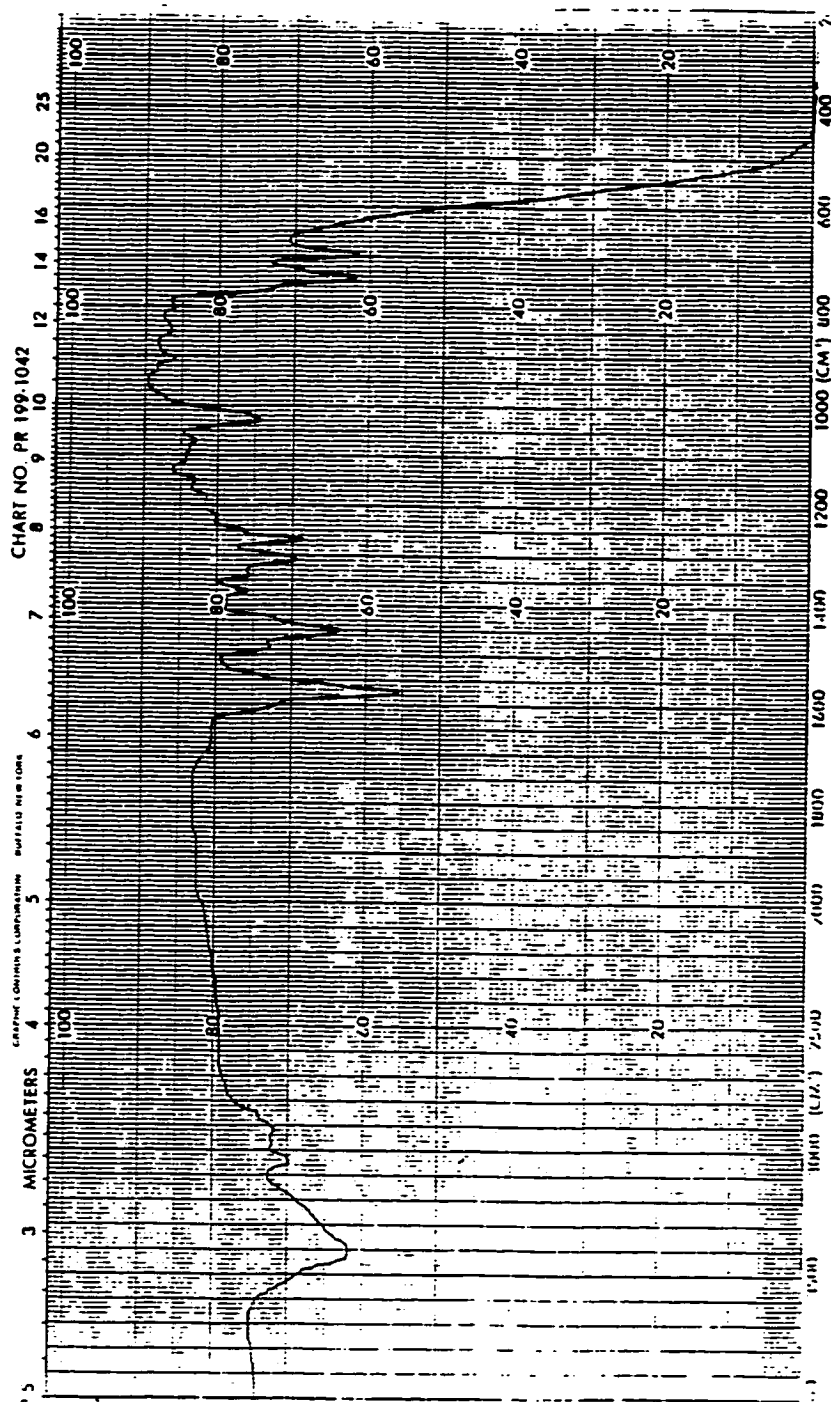
EIMS of (45)



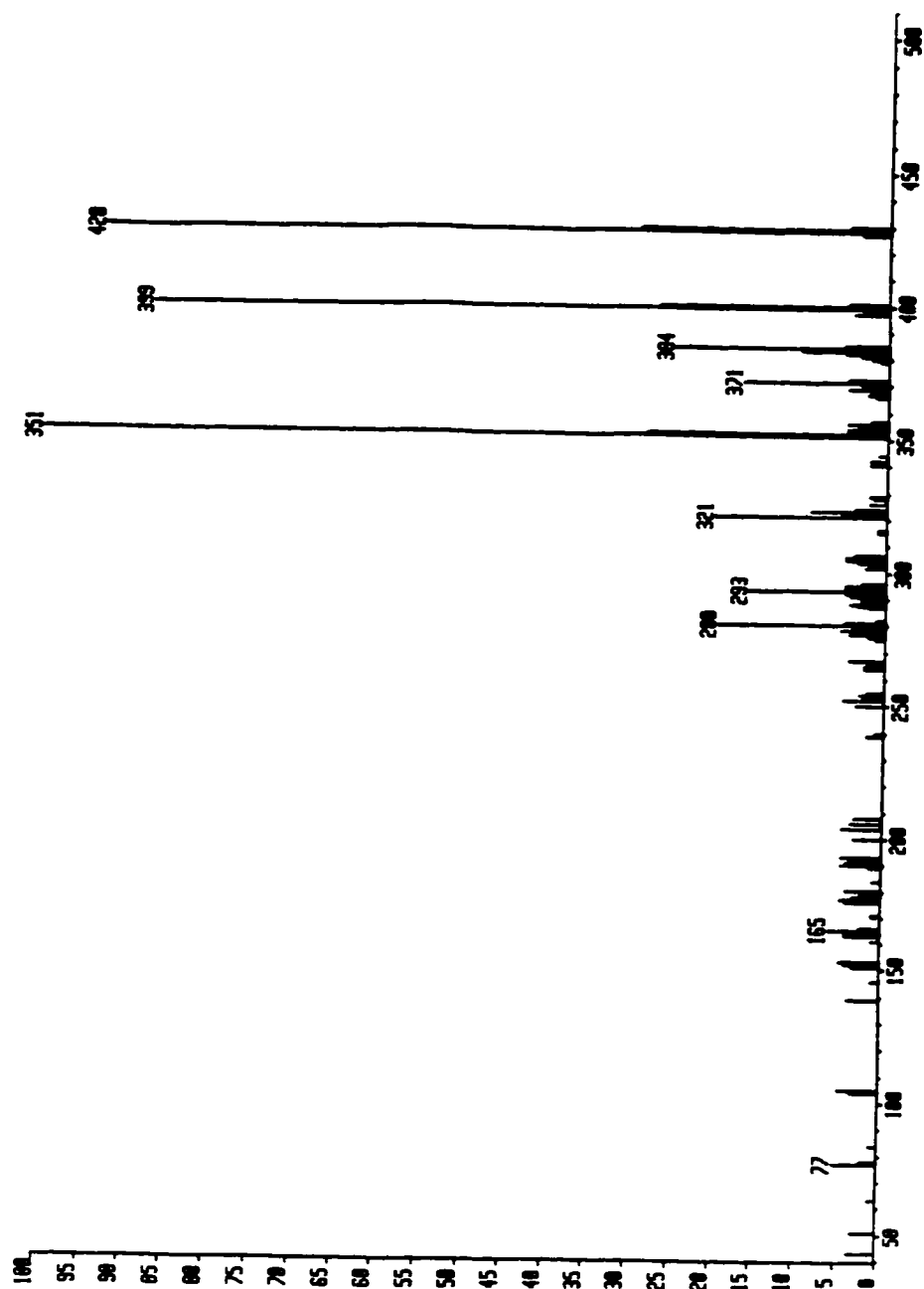
¹H NMR of 3-phenyl-2-(3-ethoxy-3-phenyl-3*H*-indol-2-yl)-1*H*-indole
(46)



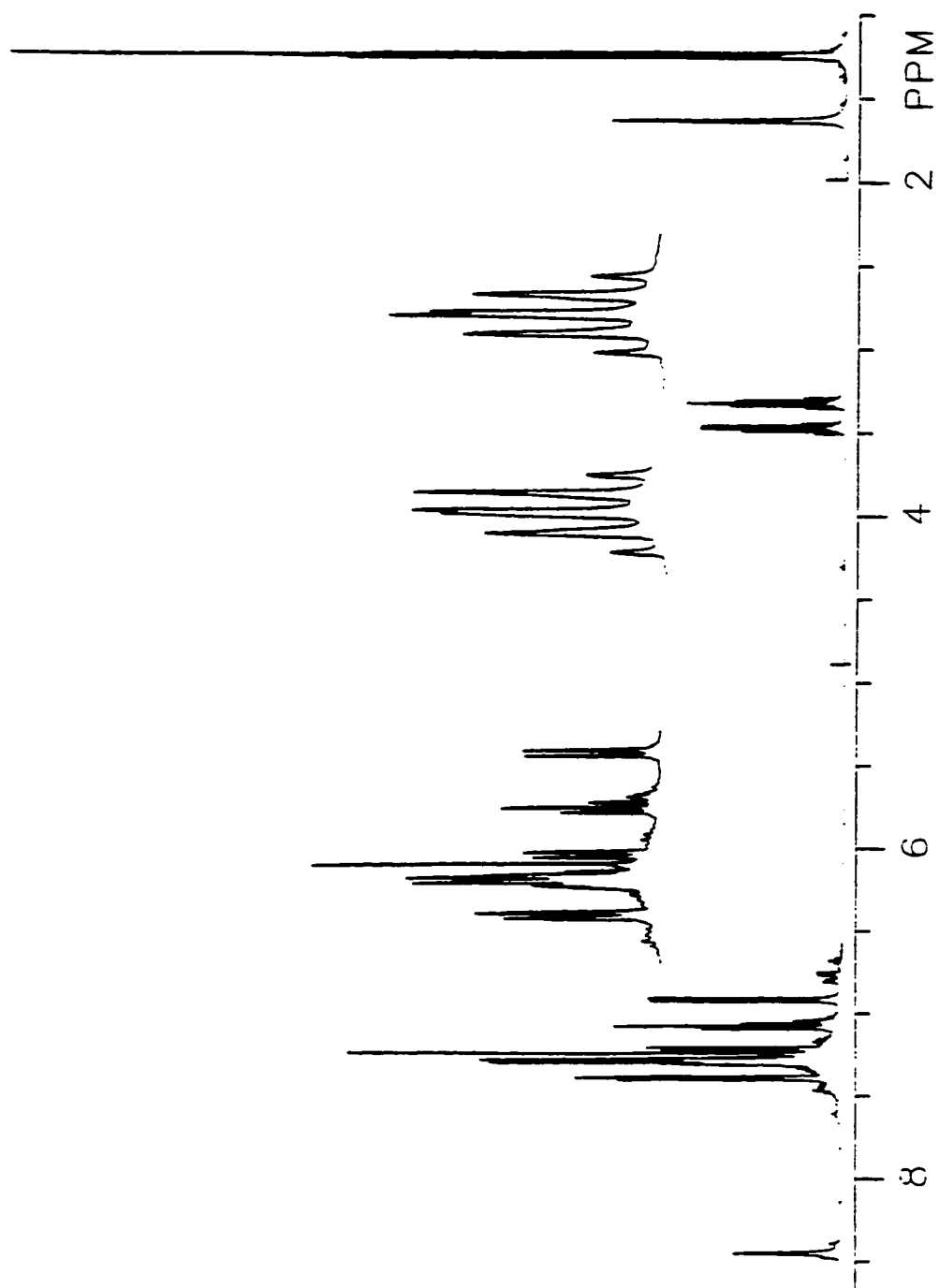
IR of (46)



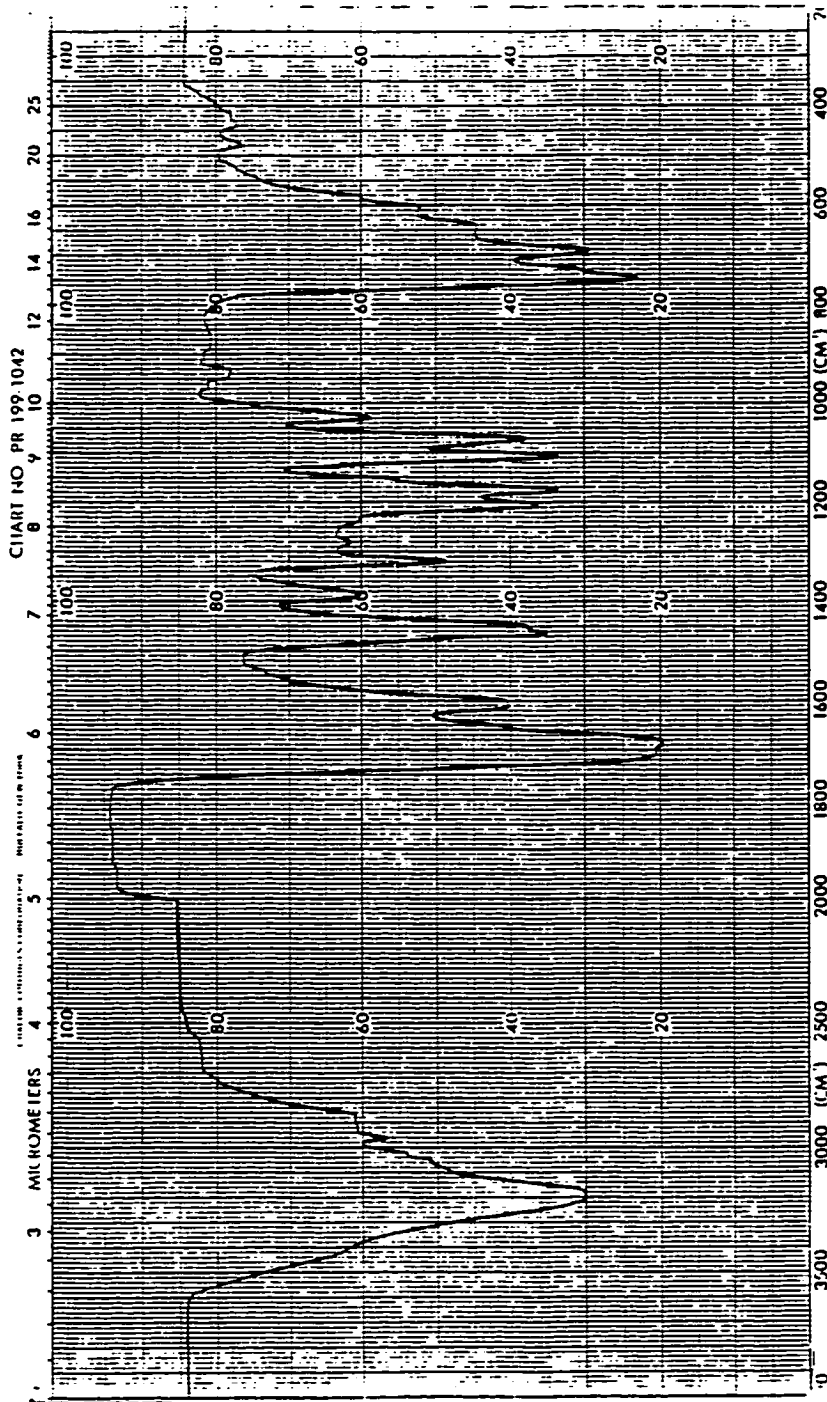
EIMS of (46)



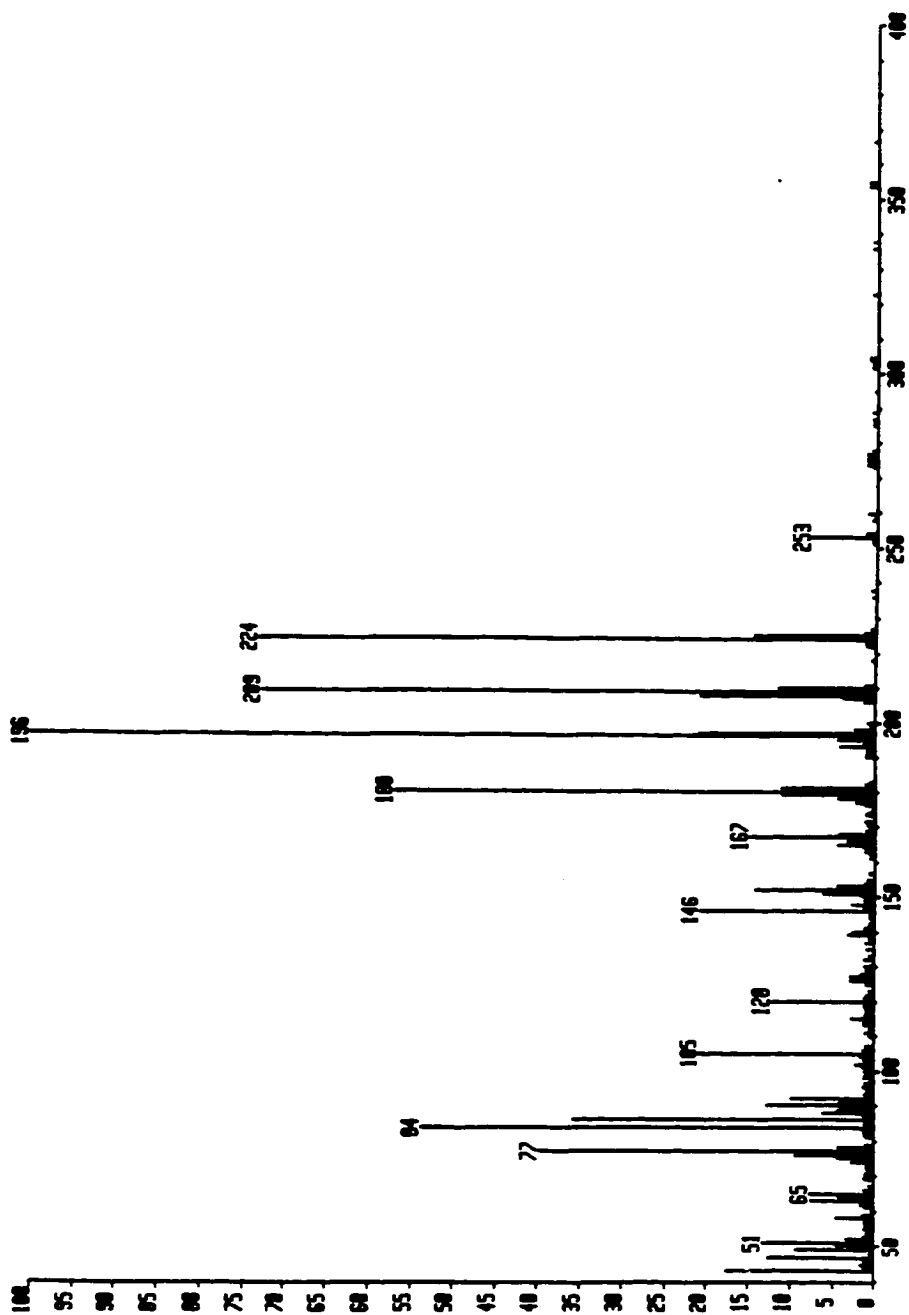
¹H NMR of 1,3-dihydro-3-ethoxy-3-phenyl-2*H*-indol-2-one (48)

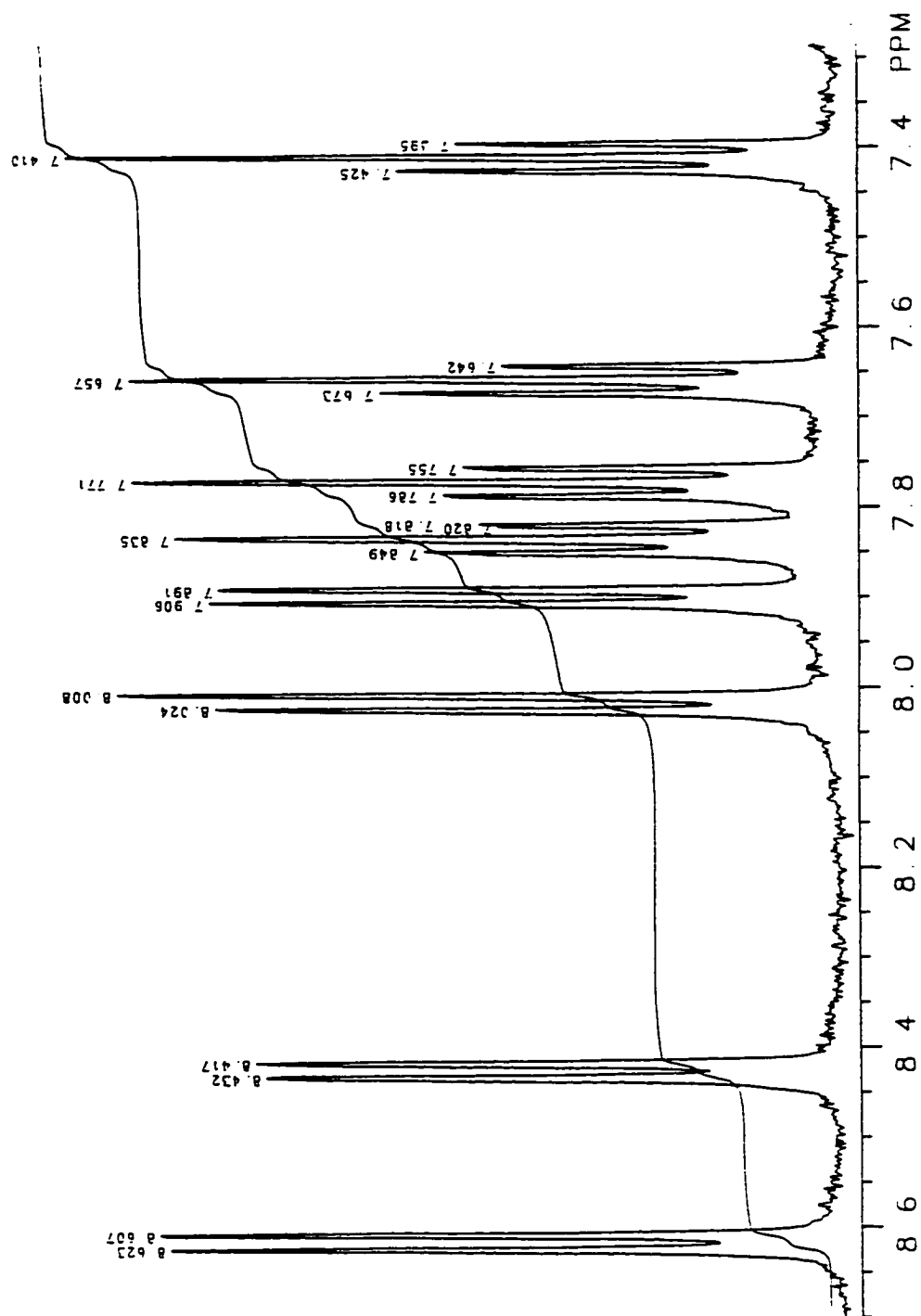


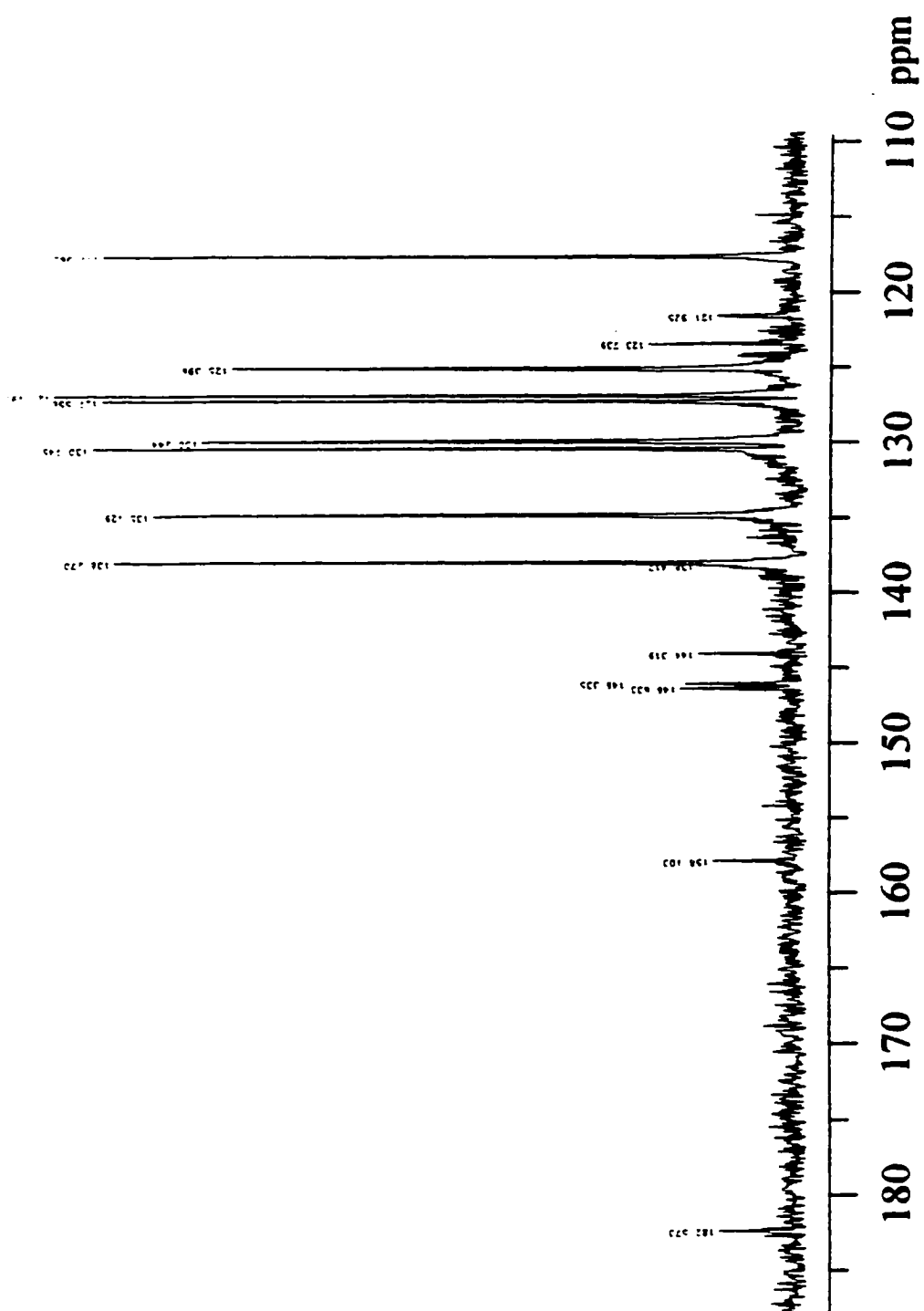
IR of (48)



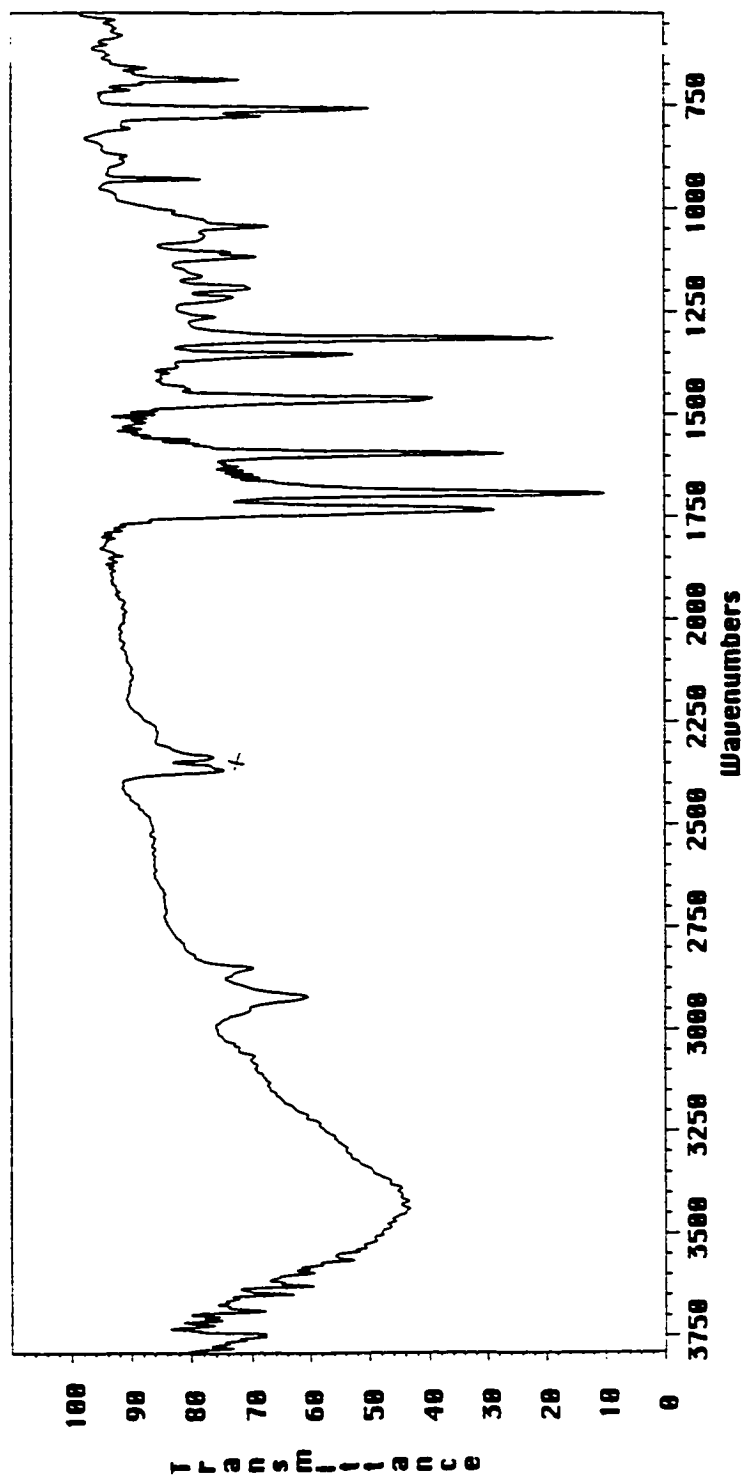
EIMS of (48)



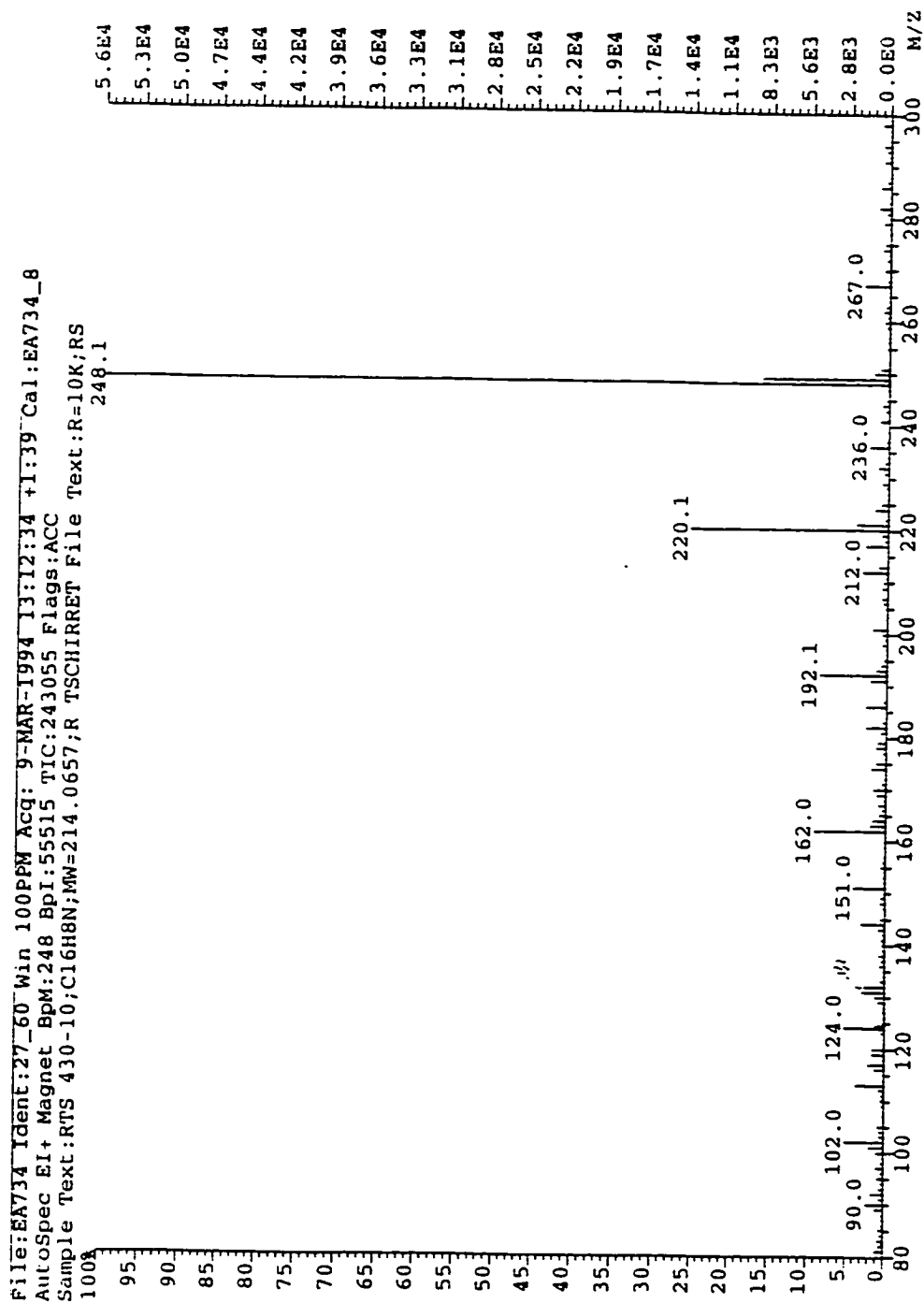
^1H NMR of (20)

^{13}C NMR of (20)

IR of (20)



EIMS of (20)



References

- Arber, G.M., de Boer, E., Garner, C.D., Hasnain, S.S., & Wever, R. (1989) *Biochemistry* 28, 7968-7973.
- Badea, M.G., & Brand, L. (1970) *Methods Enzymol.* 61, 378-425.
- Baker, J.T. (1974) *Endeavor* 33, 11-17.
- Bayley, H., & Knowles, J.R. (1977) *Methods in Enzymology* 46, 69-114.
- Bayley, H. (1983) "*Photogenerated Reagents in Biochemistry and Molecular Biology*", Elsevier, Amsterdam.
- Beecham, J., & Brand, L. (1985) *Annu. Rev. Biochem.* 9, 4723-4729.
- Beer, R.J.S., McGrath, L., & Robertson, A. (1950) *J. Chem. Soc.* 2118-2123.
- Beissner, R.S., Guilford, W.J., Coates, R.M. & Hager, L.P. (1981) *Biochemistry* 13, 3724-3731.
- Bergman, J., & Eklund, N. (1980) *Tetrahedron* 36, 1445-1450.
- Biggs, W.R., & Swinehart, J.H. (1976) in "*Metal Ions in Biological Systems*" Vol. VI (Sigel, H., Ed.) Ch. 2, Marcel Dekker, New-York.
- Blanke, S.R., & Hager, L.P. (1988) *J. Biol. Chem.* 263, 18739-18743.
- Blanke, S.R., & Hager, L.P. (1990) *J. Biol. Chem.* 265, 12454-12461.
- Blount, J.F., Daly, J.J., & Wells, R.J. (1983) *Aust. J. Chem.*
- Bocchi, V., & Palla, G. (1982) *Synthesis*, 1096-7.
- Bocchi, V., & Palla, G. (1984) *Tetrahedron* 40, 3251-3256.
- Brennan, M.R., & Erickson, K.L. (1978) *Tetrahedron* 26, 1637-1640.

- Bridges, J.W., & Williams, R.T. (1968) *Biochem. J.* 107, 225-237.
- Butler, A., Soedjak, H.S., Polne-Fuller, M., Gibor, A., Boyen, C., Kloareg, B. (1990) *J. Phycol.* 26, 589-592.
- Butler, A. (1993) in "Bioinorganic Catalysis" (Reedjik, J. Ed.) Chapt. XIII, Marcel Dekker Inc., New-york.
- Butler, A. & Walker, J.V. (1993) *Chem. Rev.* 93, 1937-1944.
- Calviou, L.J., Collison, CD., Garner, C.D., Mabbs, E., Passand, M.A., & Pearson, M. (1989) *Polyhedron* 8, 1835-1837.
- Carter, G.T., Rinehart, K.L., Li, H.L., Kuentzel, S.L., & Connor, J.L. (1978) *Tetrahedron Lett.* 4479-4482.
- Chanut, E., Zini, R., Trouvin, J.H., Riant, P., Tillement, J.P>, & Jacquot, C. (1992) *Biochem. Pharm.* 44, 2082-2085.
- Chowdhry, V., & Westmeister, F.H. (1979) *Annu. Rev. Biochem.* 48, 293-325.
- Clark, R.J.H., Cooksey, C.J., Daniels, M.A.M., & Withnall, R. (1993) *Endeavour* 17, 191-199.
- Coibion, C., Laszlo, P. (1978) *Nouv. J. Chim.* 2, 309-316.
- Collier, R.W. (1984) *Nature* 309, 441-444.
- Corbett, M.D., & Chipko, B.R. *Biochem. J.* 183, 269-276.
- Cotson, S., & Holt, S.J. (1958) *Proc. Roy. Soc., Ser. B*, 148, 506-510.
- Creed, D. (1984) *Photochem. Photobiol.* 39, 537-562.
- Dawson, J.H. (1988) *Science* 240, 433-439.
- Da Settimo, A., Saettone, M.F., Nannipieri, E., & Barili, A. (1967) *Gazz. Chim. Ital.* 97, 1304-1309.
- Da Settimo, A. & Nannipieri, E. (1970) *J. Org. Chem.* 35, 2546-2551.

- Da Settimo, A., Santerini, V., Giampaolo, P., Biagi, G., & Veneziano, C. (1977) *Gazz. Chim. Ital.* 107, 367-372.
- de Boer, E., van Kooyk, Y., Tromp, M.G.M., Plat, H., & Wever, R. (1986a) *Biochim. Biophys. Acta* 869, 48-53.
- de Boer, E., Tromp, M.G.M., Plat, H., Krenn, B.E., & Wever, R. (1986b) *Biochim. Biophys. Acta* 872, 104-115.
- de Boer, E., Tromp, M.G.M., Plat, H., van der Plas, H.C., Wever, R., Meijer, E.M., & Schoemaker, H.E. (1987a) *Biotech. Bioeng.* 30, 607-610.
- de Boer, E., Plat, H., & Wever, R. (1987b) in "*Biocatalysis in Organic Media*" (Lane, C., Tramper, J., & Lilly, M.D., Eds.) pp. 317-323, Elsevier, Amsterdam.
- de Boer, E., Boon, K., Wever, R. (1988a) *Biochem.* 27, 1629-1635.
- de Boer, E., Keijzers, C.P., Klaassen, A.A.K., Reijerse, E.J., Collison, D., Garner, C.D., & Wever, R. (1988b) *FEBS Lett.* 235, 93-97.
- de Boer, E., & Wever, R. (1988) *J. Biol. Chem.* 263, 12326-12332.
- De Fabrizio, C.R. (1968) *Ann. Chim.* 58, 1435-1445.
- De Rosa, M., Carbognani, L., & Febres, A. (1981) *J. Org. Chem.* 46, 2054-2059.
- Doering, W.V.E., & Buttery, R.C. (1956) *J. Am. Chem. Soc.* 78, 3224.
- Dugad, L.B., Wang, X., Wang, X.-X., Lukat, G.S., & Goff, H. (1992) *Biochemistry* 31, 1651-1655.
- Eftink, M.R. (1991) in "*Fluorescence Spectroscopy*" (Lakowick, J.R. Ed.), Vol. II, Plenum Press, New-York.
- Eftink, M.R. (1991a) in "*Methods of Biochemical Analysis: Protein Structure determination*" (Suelter, Ed.) Vol. 35, pp 127-205, John Wiley, New-York.

- Eftink, M.R., Selva, T.J., and Wasylewski, Z. (1987) *Photochem. Photobiol.* 46, 23-30.
- Eftink, M.R., & Ghiron, C.A. (1977) *Biochem.* 16, 5546-5551.
- Ensley, B.D., Ratzkin, B.J., Osslund, T.D., & Simon, M.J. (1983) *Science* 222, 167-169.
- Everett, R.R., & Butler, A. (1989) *Inorg. Chem.* 28, 393-395.
- Everett, R.R., Kanofsky, J.R., & Butler, A. (1990a) *J. Biol. Chem.* 265, 4908-4914.
- Everett, R.R., Soedjak, H.S., & Butler, A. (1990b) *J. Biol. Chem.* 265, 15671-15679.
- Everett, R.R. (1990) "A Novel Vanadium Bromoperoxidase: Investigation of Enzyme Kinetics and Reaction Mechanism" Ph.D. Thesis, Department of Chemistry, University of California, Santa Barbara.
- Franssen, M.C.R., Jansma, J.D., van der Plas, H.C., de Boer, E., & Wever, R. (1988) *Biorg. Chem.* 16, 352-363.
- Geigert, J., Neidleman, S.L., & Dalietos, D.J. (1989) *J. Biol. Chem.* 258 2273-2277.
- Gerig, J.T., & Klinkenborg, J.C. (1980) *J. Am. Chem. Soc.* 102, 4267-4268.
- Griffin, B.W., & Haddox, R. (1985) *Arch. Biochem. Biophys.* 239, 305-309.
- Griffin, B.W. (1991) in *Peroxidases in Chemistry and Biology* (Everse, J., Everse, K.E., & Grisham, M.B., Eds.) Vol II, pp. 85-137, CRC Press, Boca Raton, Fl.
- Gschwend, P.M., MacFarlane, J.K., & Newman, K.A. (1985) *Science* 227, 1003-1035.
- Guillory, R.J. (1989) *Pharmac. Ther.* 41, 1-25.

Guillory, R.J. (1990) in "*Frontiers in Protein Chemistry*" (Liu, T.Y., Mamiya, G., & Yasubonu, K.T., Eds.) pp 211-243, Elsevier, New-York.

Hager, L.P., Morris, D.R., Brown, F.S., & Eberwein, H. (1966) *J. Biol. Chem.* 241, 1769-1777.

Hashimoto, A., & Pickard M. (1984) *J. Gen. Microbiology* 130, 2051-2058.

Hino, T., Tonozuka, M., & Nakagawa, M. (1974) *Tetrahedron* 30, 2123-2133.

Hino, T., Tonozuka, M., Ishii, Y., & Nakagawa, M. (1977) *Chem. Pharm. Bull.* 25, 354-358.

Hormes, J., Kuetgens, U., Chauvistre, R., Schreiber, W., Anders, N., Vilter, H.,

Houlihan, W.J., Parrino, V.A. & Yasuyuki, U. (1981) *J. Org. Chem.* 46, 4511-4515.

Itoh, N., Izumi, Y., & Yamada, H. (1985) *Biochem. Biophys. Res. Commun.* 131, 428-435.

Itoh, N., Izumi, Y., & Yamada, H. (1986) *J. Biol. Chem.* 261, 5194-5200.

Itoh, N., Izumi, Y., & Yamada, H. (1987a) *Biochemistry* 26, 282-289.

Itoh, N., Hasan Q., Izumi, Y., & Yamada, H., (1987b) *Eur. J. Biochem.*, 477-484.

Itoh, N., Izumi, Y., & Yamada, H. (1986) *J. Biol. Chem.* 261, 5194-5200.

Kanofsky, J.R. (1984) *J. Biol. Chem.* 259, 5596-5600.

Kato, T., Ichinose, I., Kamoshida, A., & Kitahara, Y. (1976) *J. C. S. Chem. Comm.* 518-519.

Keilin, D., & Hartree, E.F. (1951) *Biochem J.* 49, 88.

Knight, K.L., & McEntee, K. (1985) *J. Biol. Chem.* 260, 867-872.

- Krenn, B.E., Tromp, M.G.M., & Wever, R. (1989) *J. Biol. Chem.* 264, 19287-19292.
- Krenn, B.E., & Wever, R. (1993) in "*Vanadium in Biological Systems; Physiology and Biochemistry*" (Chasteen N.D., Ed.) Chapt. V, Kluwer Academic Publishers, Dordrecht, The Netherlands.
- Kunori, M. (1962) *Nippon Kagaku Zasshi* 83, 836-838.
- Laemmli, U.K. (1970) *Nature* 227, 680-685.
- Lakowicz, J.R. (1983) *Principles of Fluorescence Spectroscopy*, Plenum Press, New-York.
- Lambier, A.-M., & Dunford, H.B. (1983) *J. Biol. Chem.* 258 13558-13563.
- Lehrer, S.S. (1971) *Biochemistry* 10, 3254-3263.
- Libby, R.D., Thomas, J.A., Kaiser, L.W., & Hager, L.P. (1980) *J. Biol. Chem.* 257, 5030-5037.
- Lwowski, W. (1970) *Nitrenes*, Interscience, New-York.
- McGovern, P.E., & Michel, R.H. (1990) *Acc. Chem. Res.* 23, 152-158.
- McAdara, J., (1991) UC Santa Barbara, Personal communication.
- Madelung, W., & Siegert, P. (1924) *Chem. Ber.* 57, 228-32.
- Maier, W., Schumann, B., & Gröger, D. (1990) *Phytochemistry* 29, 817-823.
- Mermod, N., Harayama, S., & Timmis, K.N. (1986) *BioTechnology* 4, 321.
- Messerschmidt, A., & Wever, R. (1996) *Proc. Natl. Acad. Sci.* 93, 392-396.
- Michel, R.H., & McGovern, P.E. (1987) *Archeomaterials* 4, 97-104.
- Morris, D.R., & Hager, L.P. (1966) *J. Biol. Chem.* 241, 1763-1768.
- Newman, K.A., & Gschwend, P.M. (1987) *Limnol. Oceanogr.* 32, 702-708.

- Norton, R.S., & Wells, R.J. (1982) *J. Am. Chem. Soc.* 104, 3628-3635.
- Ortiz de Montellano, P.R., Choe, Y.J., De Phillis, G., & Catalano, C.E. (1987) *J. Biol. Chem.* 262, 11641-11646.
- Oshima, T., Kawai, S., & Egami, F. (1965) *J. Biochem.* 58, 259-263.
- Palou, J. (1994) *Chem. Soc. Rev.* 357-361.
- Parrick, J., Yahya, A., & Yizun, J. (1984) *Tet. Lett.* 25, 3099-3100.
- Parrick, J., Yahya, A., Ijaz, A.S., & Yizun, J. (1989) *J. Chem. Soc. Perkin Trans. I*, 2009-2015.
- Plummerer, R., & Göttler, M. (1910) *Berichte* 43, 1376-1383.
- Prota, G. (1980) in "Marine Natural Products: Chemical and Biological Perspectives" (Scheuer, P.J. Ed.) Vol. III, pp. 159-164, Academic Press, New-York, NY.
- Rehder, D., & Weidemann, C. (1988) *Biochim. Biophys. Acta* 956, 293-299.
- Reiser, A., & Wagner, H.M. (1977) in "The chemistry of the Azido Group" (Patai, S. Ed.) 441-501, Interscience, New-York.
- Ricci, R.W. (1970) *Photochem. Photobiol.* 12, 67-75.
- Ricci, R.W., & Nesta, J.M. (1976) *J. Phys. Chem.* 80, 974-980.
- Rosenfeld, J., Capdevielle, J., Guillemot, J.C., & Ferrara, P. (1992) *Anal. Biochem.* 203, 173-179.
- Russell, G. A., & Kaupp, G. (1969) *J. Am. Chem. Soc.* 91, 3851-3859.
- Sakai, R., Higa, T., Jefford, C.W., & Bernardinelli, G. (1986) *Helv. Chim. Acta* 69, 91-105.
- Schaudolf, A. (1968) *Naturforsch.* 23b, 572-576.

- Sitter, A.J., & Turner, J. (1985) *J. Labelled Compounds and Radiopharmaceuticals* 22, 461-465.
- Smith, G.F., & Waters, A.E. (1961) *J. Chem. Soc.* 940.
- Soedjak, H.S., & Butler, A. (1990) *Biochemistry* 29, 7974-7981.
- Soedjak, H.S., & Butler, A. (1991) *Biochim. Biophys. Acta* 1079, 1-7.
- Soedjak, H.S., Everett, R.R., & Butler, A. (1991) *J. Indust. Microbiol.* 8, 37-44.
- Soedjak, H.S. (1991) Ph.D. Dissertation, UC Santa Barbara.
- Soedjak, H.S., Walker, J.V., & Butler, A. (1995) *Biochemistry*, in press.
- Squire, P.G., & Himmel, M.E. (1979) *Arch. Biochem. Biophys.* 196, 165-177.
- Sun, H.H. (1983) in "Marine Natural Products: Chemical and Biological Perspectives" (Scheuer, P.J. Ed.) Vol. V, pp. 223, Academic Press, New-York, NY.
- Tanaka, J., Higa, T., Bernardinelli, G., & Jefford, C.W. (1988) *Tetrahedron Lett.* 29, 6091-6094.
- Tanaka, J., Higa, T., Bernardinelli, G., & Jefford, C.W. (1989) *Tetrahedron* 45, 7301-7310.
- Tanasescu, I., & Georgescu, A. (1932) *Bull. Soc. Chim. Fr.* 51, 234-240.
- Theiller, R., Cook, C., & Hager, L.P. (1978) *Science* 202, 1094-1097.
- Thomas, J.A., Morris, D.R., & Hager, L.P. (1970a) *J. Biol. Chem.* 245, 3129-3134.
- Thomas, J.A., Morris, D.R., & Hager, L.P. (1970b) *J. Biol. Chem.* 245, 3135-3142.
- Tromp, M.G.M., Olafsson, G., Krenn, B., & Wever, R. (1990) *Biochim. Biophys. Acta* 1040, 192-198.

- Tromp, M.G.M., Van, T.T., & Wever, R. (1991) *Biochim. Biophys. Acta* 107,3 53-56.
- van der Donckt, E. (1969) *Bull. Soc. Chim. Belg.* 78, 69-75.
- van Schijndel, J.W.P.M., Vollenbroek, E.G.M., & Wever, R. (1993) *Biochim. Biophys. Acta* 1161, 249-256..
- van Tamelen, E.E., & Hessler, E.J. (1966) *Chem. Comm.* 411-413.
- Vilter, H., Glombitza, K.-W., & Grawe, A. (1983) *Bot. Mar.* 26, 331-340.
- Vilter, H. (1983a) *Bot. Mar.* 26, 429-435.
- Vilter, H. (1983b) *Bot. Mar.* 26, 451-455.
- Vilter, H. (1984) *Phytochemistry* 23, 1387-1390.
- Vilter, H., & Rehder, D. (1987) *Inorg. Chim. Acta* 136, L7-L10.
- von Baeyer, A. (1879) *Berichte* 12, 456-467.
- von Baeyer, A. (1883) *Berichte* 16, 188-197.
- von Baeyer, A. (1888) DP 11857.
- Wahl, A., & Bagard, P. (1910) *Bull. Soc. Fr.* 7, 1090-1095.
- Weissgerber, R. (1913) *Ber.* 46, 651-659.
- Welfle, H., Misselwitz, R., Welfle, K., Groch, N., & Heinemann, U. (1992) *Eur. J. Biochem.* 204, (1049-1055).
- Wever, R., Plat, H., & de Boer, E. (1985) *Biochim. Biophys. Acta* 830, 181-186.
- Wever, R., Krenn, B.E., de Boer, E. Offenbergh, H., & Plat, H. (1988a) in "Oxidases and Related Redox Systems" (King, T.E., Morrison, H.S., & Morrison, M., Eds.), pp 477-493, Alan R. Liss, Inc., New-york, NY.

Wever, R., Krenn, B.E., de Boer, E. Offenberg, H., & Plat, H. (1988b) *Prog. Clin. Biol. Res.* 274, 477-493.

Wiesner, W., van Pee, K.-H., & Lingens, F. (1986) *F.E.B.S.* 209, 321-324.

Witkop, B., & Patrick, J.B. (1951) *J. Am. Chem. Soc.* 73, 713-718.

Wolinsky, L.E., & Faulkner, D.J. (1976) *J. Org. Chem.* 41, 597-600.

Xia, Z.-Q., & Zenk, M.H. (1992) *Phytochemistry* 31, 2695-2697.

Ziderman, I. (1972) *Isr. J. Chem.* 11, 7-20.